AT A SNAIL'S PACE:

SUITABILITY OF *Cornu aspersum* AND *Theba pisana* AS BIOINDICATORS FOR HEAVY METALS IN MALTA

Nathanael Schembri

A dissertation submitted in partial fulfilment of the requirements for the degree of Master of Science at the Institute of Earth Systems

Master of Science (Rural and Environmental Sciences)

Institute of Earth Systems

University of Malta

March 2024

L-Università ta' Malta

FACULTY/INSTITUTE/CENTRE/SCHOOL Institute of Earth Systems

DECLARATIONS BY POSTGRADUATE STUDENTS

(a) Authenticity of Dissertation

I hereby declare that I am the legitimate author of this Dissertation and that it is my original work.

No portion of this work has been submitted in support of an application for another degree or qualification of this or any other university or institution of higher education.

I hold the University of Malta harmless against any third party claims with regard to copyright violation, breach of confidentiality, defamation and any other third party right infringement.

(b) Research Code of Practice and Ethics Review Procedures

I declare that I have abided by the University's Research Ethics Review Procedures. Research Ethics & Data Protection form code IES-2022-00002.

As a Master's student, as per Regulation 77 of the General Regulations for University Postgraduate Awards 2021, I accept that should my dissertation be awarded a Grade A, it will be made publicly available on the University of Malta Institutional Repository.

Abstract

Heavy metals are a cause for great concern in the environment due to their toxic and bioaccumulative effects and therefore monitoring their prevalence is considered greatly important. One way of doing this is by using a bioindicator such as terrestrial snails. This study set out to determine the suitability of both the soft part and the shell of two snail species *Cornu aspersum and Theba pisana*, for monitoring the heavy metals arsenic (As), zinc (Zn), cadmium (Cd), copper (Cu), nickel (Ni), lead (Pb), chromium (Cr), aluminium (Al), manganese (Mn), barium (Ba), and vanadium (V) in Malta. Snails were sampled from various environmental situations from around Malta, acid digested, and analysed using MP-AES to identify and quantify the selected heavy metals. It was determined through ordination plots that individual samples had enough variation to constitute calling them effective bioindicators and that there was significant variation between shell and soft part samples. PERMANOVA tests showed statistically significant differences between the soft parts of the two species, with *T. pisana* soft parts being found to be the better bioindicator for arsenic (p=0.046), cadmium (0.032), nickel (0.008), lead (0.012), chromium (0.007), and aluminium (0.014). The soft parts of *C. aspersum* were shown to be the most effective bioindicator for barium (0.004). In the case of vanadium, it was only detected in shell samples, meaning that shells (especially those of *T. pisana*) must be used as bioindicators for this metal, making it the only time analysing shells was preferential to soft parts. For zinc, copper, manganese, and vanadium there was no statistically significant difference between the two species. The most abundant metals found in *T. pisana* was Arsenic > Cadmium > Chromium, while in *C. aspersum* this was Arsenic > Cadmium > Barium.

TABLE OF CONTENTS

List Of Tables

List Of Figures

List Of Equations

List Of Abbreviations

ATSDR	Agency for Toxic Substances and Disease Registry
ERA	Environment and Resources Authority
FAAS	Flame Atomic Absorption Spectroscopy
ICP-MS	Inductively Coupled Plasma Mass Spectroscopy
ICP-OES	Inductively Coupled Plasma Optical Emission Spectroscopy
LOD	Limit of Detection
LOQ	Limit of Quantification
MDS	Multidimensional Scaling
MP-AES	Microwave Plasma Atomic Emission Spectroscopy
MT(s)	Metallothionein(s)
OEC	Oxygen-evolving Complex
PCA	Principal Component Analysis
PERMANOVA	Permutational Multivariate Analysis of Variance
ppm	Parts-Per-Million
SIMPROF	Similarity Profile Routine
WRB	World Reference Base for Soil Resources
XAFS	X-ray Absorption Fine Structure
XPS	X-ray Photoelectron Spectroscopy

ACKNOWLEDGEMENTS

First and foremost, I want to express my gratitude to my principal supervisor, Professor Everaldo Attard, whose support and guidance have been instrumental throughout this dissertation journey. Professor Attard's constant presence, invaluable insights, and encouragement have truly shaped the course of my research.

I would also like to thank my co-supervisor Dr. Anthony Sacco for his enthusiasm and insightful corrections and constructive feedback having significantly enriched the quality of this work.

Special thanks are also due to Dr. Julian Evans for his invaluable assistance and expert advice in navigating the complexities of statistical analysis, ensuring the robustness and accuracy of my findings.

To Enya Maria Haber, I extend my heartfelt appreciation for her unwavering support, understanding, and patience throughout this endeavour. Her encouragement and words of wisdom have been a constant source of motivation.

I am grateful to Emma Cutajar for generously providing me with a number of snail samples, which were crucial for its successful completion.

I would also like to thank Mr. Renato Camilleri for allowing me to use the Junior College chemistry labs and some equipment in order to conduct my study, as well as providing some much-needed advice with regards to the results of the MP-AES.

I would also like to express my gratitude to my father, Professor Patrick Schembri. Not only was he the driving force behind starting my masters, but he was also a constant source of advice, support, and encouragement who made this journey far easier and smoother than it would have been.

Finally, I want to thank the rest of my family, for their unwavering love, encouragement, and support throughout this journey.

1. Introduction

The levels of heavy metals in the environment have become a cause of concern in recent years due to the toxic effects of heavy metals in humans and other animals and plants living in the environment. The concern with heavy metal poisoning comes from the cumulative build-up of these metals in the body's tissue meaning that continuous intake of small doses of such metals can eventually result in harmful effects. This effect is known as chronic toxicity (Jaishankar et al., 2014). For this reason, methods of reliably monitoring heavy metals in the environment have attracted special interest as a way to limit possible intake of heavy metals in humans and reduce stresses on the environment before the situation becomes untenable.

In order to reliably monitor an area in a complete way, one must take multiple samples from different media, such as soil, water, vegetation, and air. However, this proves to be a cumbersome method as each medium requires its own unique sampling and processing method which in turn may add subtle variations in the results. A somewhat better way of doing this is by analysing the environment as a whole by using a bioindicator which integrates these different sources. Bioindicators are organisms that are used to detect or measure pollutants or contaminants in the environment (Plafkin et al., 1989). Since these are organisms that live in the environment, they can be assumed to coalesce the pollutants and contaminants that are present in their environment by the intake of food, water, and air. The bioindicator retains a certain percentage of the pollutants in their bodies either by depositing them in their soft parts (such as organs) or by sequestering them in external structures such as shells or hairs. However, not all organisms can be used as bioindicators and in addition, certain bioindicators are better suited for specific pollutants or specific concentrations of contaminants (Posudin, 2014). Therefore, before any organism can be used as a bioindicator, limit of the species' ability to be a bioindicator must first be assessed.

This study seeks to determine the suitability of two terrestrial snail species, *Cornu aspersum* (previously known as *Cantareus aspersus* or *Helix aspersa)* ***and Theba pisana***, as

bioindicators for monitoring heavy metals in Malta. As described by several studies (Itziou & Dimitriadis, 2011; Larba & Soltani, 2013; Tardugno et al., 2023), terrestrial snails such as those considered in this study make for ideal bioindicators due to their unique trophic level position, physiology, sensitivity to pollutants, and several other factors. Unlike certain other studies (Itziou & Dimitriadis, 2011), the suitability of these snails as bioindicators was not determined by testing for biochemical markers such as haemocytes, acetylcholinesterase, and metallothionines or by variations in physiology. On the contrary, this was assessed by variations in the metal profiles between snails collected from different areas, with the principal assumption being that any variation is coming from the environment and hence would show that the snails are able to represent these differences. As determined by Ćirić et al. (2018), the levels of heavy metals in snail tissues changes slightly with seasons, due to particular physiological reasons such as aestivation, but not to a significant degree. For this study, this phenomenon is further disregarded due to the fact that the organisms sampled were adults and thus variations in seasonality would not have contributed in any significant way to the overall concentrations of heavy metals.

The microwave plasma-atomic emission spectrophotometer (MP-AES) was used to rapidly burn the analyte (acid digested soft parts or shells) in order to determine the presence and concentration of selected heavy metals. The heavy metals considered in this study are arsenic (As), zinc (Zn), cadmium (Cd), copper (Cu), nickel (Ni), lead (Pb), chromium (Cr), aluminium (Al), manganese (Mn), barium (Ba), and vanadium (V). These metals were selected due to their prevalence in the environment as pollutants and their toxicity (Borg & Attard, 2020; Alloway, 2013; Jaishankar et al., 2014). Through the analysis of both the soft parts and the shells of these two snail species, this study hopes to determine:

1. The general suitability of *Cornu aspersum* and *Theba pisana* as bioindicators for heavy metals,

2. Which heavy metals (if any) *C. aspersum* and *T. pisana* are appropriate bioindicators for,

3. Any statistically significant difference between the heavy metal profiles of the shell and soft parts,

4. Which heavy metals (if any) are best suited to be analysed using the soft parts or shells as a bioindicator.

2. Literature Review

2.1 Heavy Metals

Pollutants pose significant stresses to organisms living in the contaminated habitats and hence poses stresses on the environment as a whole. One such class of pollutants that has gained an increased focus in recent years are heavy metals. This is a term with no formal definition and hence different authors may use different definitions depending on the context and field of research. For this reason, certain metals may be included in studies of heavy metals while they may be omitted in others. As stated by Duffus (2002), the term has been used so widely and ambiguously as to render it almost entirely meaningless and its issues are widespread and fundamental. When used in the context of toxicity, it is often assumed that all salts and compounds of said heavy metal are highly toxic and ecotoxic to a similar degree which is very often not the case. To further stress this inadequacy, even the term metal is sometimes misused and authors often include metalloids such as antimony and arsenic (the latter of which this study also includes), and nonmetals such as selenium in their studies. Due to the ambiguity of the term used to group together these toxic and polluting elements and their salts, this study continues to use the term ‘heavy metal' in line with the typical usage in the field of research. In environmental toxicology, researchers are oftentimes more interested in the bioavailability and relative toxicity of metals and their salts on organisms and their environment rather than their specific chemical properties. Therefore, in this context (and by extension in this study), heavy metals are most adequately described and considered on the basis of:

1. toxicity even at low concentrations,
2. persistence as an environmental pollutant,
3. mobility and ease of deposition and accumulation in body tissues.

Therefore, this study operates with the understanding that if an element or its salts satisfies one or more of the criteria above it can be described as a heavy metal, rather than basing the term on specific chemical properties or densities.

Although the terminology is yet to find a consensus, the dangers and effects of these heavy metals is widely agreed upon. When these metal compounds are in a biologically active form (i.e., can interfere with biological processes) they can affect normal bodily functions and cause a number of symptoms such as fatigue, headaches, nausea, vomiting, cramps, diarrhoea, fever, and in high enough concentrations can even lead to cancer and mass organ damage or failure (Jaishankar et al., 2014). These symptoms and the exact quantity required to produce them is highly dependent on the specific heavy metal and the state in which it was absorbed by the individual, with concentrations varying wildly. The most concerning issue however is their ability to bioaccumulate. This is when substances deposit in the body's tissues and build-up over a long period of time, meaning that continuous intake of small doses can eventually result in harmful effects. This effect is known as chronic toxicity. Another issue with heavy metal toxicity is the wide range in the mechanisms of their effect. For instance, as investigated by Stohs and Bagchi (1995), many heavy metals place oxidative stress on the body and cause lipid peroxidation, however the target organs and biological macromolecules differ. For example, chromium (III) and (VI) ions (Cr^{3+} & CrO_4^{2-}) work directly in the cell nucleus and have genotoxic effects by reacting with thiols and ascorbate forming highly reactive oxygen species such as superoxides, peroxides, and hydroxyl radicals which place oxidative stress on the cell, resulting in protein and DNA damage which also makes them carcinogenic chemicals (DesMarias & Costa, 2019). Meanwhile, lead salts mostly target the vascular endothelium and central nervous system by disrupting calcium homeostasis thereby impairing neurotransmitter release and calcium dependent enzymes like nitric oxide synthase which limits nitric oxide availability and hence impairs nitric oxide signalling (Nemsadze et al., 2009). This wide variety of toxicity pathways and target organs make heavy metal toxicity difficult to identify and treat as there is no universal medical treatment, with effects being permanent, or may appear too late to do anything about them.

2.1.1 Sources of Heavy Metal Contamination

As clearly seen from above, heavy metals pose a serious concern to the health of the environment and people. It is for this reason that possible sources of heavy metal contamination have been studied and investigated substantially. As specified by Alloway

(2013), the sources of these heavy metals can be divided into two major groups: lithogenic (originating naturally from nature) and anthropogenic (originating from human activity). When investigating heavy metals, it is important to keep in mind that their presence does not automatically prove contamination in the area. The ten most abundant elements in the earth's crust are oxygen, silicon, aluminium, iron, calcium, sodium, potassium, magnesium, phosphorus, and titanium and these constitute over 99% of the total element content with other elements comprising about 1% collectively. However, soils can have a significant concentration of elements not listed above due to their particular geological and geographic situation. Therefore, soil analysis could contain a relatively large percentage of these elements even though some of them are considered heavy metals. These are called lithogenic sources of heavy metals and should not be considered as pollutants. The more concerning type of heavy metal sources however are those coming from anthropogenic sources, this is because they are found in much greater quantities or in far more dangerous forms. Table 2.1 shows some anthropogenic sources and the heavy metals they have been known to contaminate their surroundings with.[1]

Table 2.1: Heavy metals and their typical anthropogenic source (Adapted from Alloway, 2013).

Anthropogenic Source	Associated Heavy Metal Contaminant
Ceramic Works	Al, Cd, Cr, Cu, Pb, Ni, Zn
Electrical Components	Al, Cr, Cu, Pb
Steel Works	Al, As, Cr, Pb, Ni, Zn, Mn, V
Pesticides	As, Cr, Cu, Pb, Zn, V
Printing, Graphics, Pigments, and Paints	Al, As, Cd, Cr, Pb, Zn, Ba
Plastic Works	Cd, Pb, Sn, Zn, Ba
Livestock	Cd, Cr, Pb, Ni, Zn
Waste Disposal	Al, As, Cd, Cu, Pb, Ni, Zn

[1] *It is important to note that there are more heavy metals and other pollutants associated with these sources but have not been included in the table as they are not being investigated in this study.*

2.1.2 Heavy Metals in Soils of Malta

Apart from the aforementioned sources, there are other sources of heavy metal contamination that may be of more relevance to the Maltese context. It has been found that bullets and shot from sport shooting can increase the concentrations of lead, arsenic, and tin in the surrounding areas (Alloway, 2013), which is of particular relevance due to Malta's game shooting culture. However, measuring contamination from this source type proves to be difficult as shot does not spread over an area homogeneously. Therefore, the exact level of heavy metal contamination is dependent on whether or not the sample had any shot in it.

Another source of heavy metals is from traffic, which has been shown to increase the concentrations of cadmium, lead, and zinc in areas surrounding roads (Viard et al., 2004). This is due to the wear and tear of car components, mostly breaks, which flake off and release these metals into the environment. Due to Malta's incredibly high traffic, road density, and relatively small size, it could be assumed that heavy metal contamination from this source is both significant and widespread.

Finally, fireworks may be another source of heavy metal pollution as they release vast quantities of metal oxides into the atmosphere that eventually settles on soil and water (Fu et al., 2020). Various metals are used in these pyrotechnics to create vibrant colours, loud bangs, and/or shimmering effects. Copper and zinc show a substantial increase after firework shows with arsenic, chromium, lead, and nickel showing a slight increase also. Malta is well known for its extravagant fireworks and pyrotechnic displays, especially in the summer months, and therefore this source is of particular interest.

A study by Briffa (2020) showed the persistence and general situation of heavy metal pollution in soils across the Maltese islands. In particular, lead, cadmium, and zinc were found to contaminate soils of Malta at concentrations that exceeded threshold limits set up by Finnish and Dutch standards. In addition, aluminium, manganese, and copper (while being below threshold limits) were prevalent in all localities. Vanadium was also found to be

prevalent in three of six localities (southeastern, northern, and western). As also expressed by the Environmental Resource Authority (ERA, 2018), these contaminants could be due to the burning of fuel in power stations and ships and metal works. It was also found that areas with heavy firework usage had an increase in associated heavy metals in their soil such as aluminium, manganese, and vanadium.

2.2 Bioindicators

As stated previously, heavy metals are not only harmful pollutants but their sources are numerous and can be difficult to monitor. For example's sake, taking the case of shot from sport shooting, researchers must trust that their sample is representative of the overall situation of the area of interest. That being said the sample might be collected from a patch of no contamination (in which case the concentrations will be much lower than the true value of the area) or from a patch of significant contamination (in which case the concentrations will be much higher than the true value of the area). Therefore, researchers have to find a way to homogenise or integrate the overall heavy metal situation in the area of study. This may be done by taking multiple samples of the same area, taking samples at different times, and taking samples of different media. Unfortunately, these approaches prove to be cumbersome especially if different media are involved as sampling procedures, sample preparation, and analysis can differ significantly. By extension, the best situation would be to analyse a single sample that incorporates the heavy metal concentrations over a chosen area, over multiple periods of time, and from multiple different media. This can be achieved by using a bioindicator species.

Bioindicator species are organisms that are used to detect pollutants, contaminants, or other risks be they biological (such as diseases), physical (such as plastics), or chemical (such as heavy metals). The main purpose of bioindicator species is to provide advanced warning of any dangers or potential issues that might arise if a risk is gone untreated. Bioindicator species are typically animals, but plants, bacteria, and fungi have been used for this purpose also (Posudin, 2014). In recent years, bioindicator species have been used to

investigate the extent at which pollutants and contaminants have entered the environment to assess the effects certain industries or human impacts have had.

2.2.1 Criteria for Bioindicator Species

Not all species can be used as bioindicator species however, as they must fit certain criteria to be an effective marker. As outlined by previous studies (Plafkin et al., 1989; Regoli et al., 2006), the ideal bioindicator is an organism that has a wide distribution; a sedentary lifestyle; are easy to collect and identify; and while sensitive to the hazard being investigated, have a high tolerance to this stress. A wide distribution refers to an organism's presence over multiple areas since it is best to compare results from members of the same species in order to minimise inconsistencies. Therefore, it would be far less effective to use a species which is rare or only found in a handful of areas, thereby limiting how many areas you could sample.

A sedentary lifestyle refers to an organism's tendency to remain in a relatively small area, i.e., they do not travel large distances. This is preferable as organisms will not range too far out of the area of interest making them good analogues to the situation of the particular area that they are sampled in. This is important as researchers do not want contaminants outside of the area of interest to interfere with measurements.

As touched upon briefly, results are best compared to individuals of the same species and so an individual must be easily identifiable as a member of said species. Otherwise, researchers run the risk of comparisons being rendered void due to inconsistencies that are innately present when comparing different species to one another. For example, different species detoxify heavy metals in different ways such as certain snail and slug species such as *Littorina littorea* detoxifying metals using a special class of small proteins rich in the sulfur-containing cysteine amino acid called metallothioneins which bind to the heavy metal and render it into a biologically inactive state (Baumann et al., 2017). However, bivalves have been seen to sequester heavy metals in their shells to isolate the toxins from biological processes

(Nour, 2020). This is also highly species specific with different species having higher accumulation abilities for different heavy metals such as *Tridacna squamosa* for lead, nickel, and zinc; *Chama pacifica* for cobalt and cadmium; and *Periglypta reticulata* for copper.

A good bioindicator must also be easy to collect to facilitate sampling (preferably with little to no or inexpensive equipment required) and should not limit sampling periods due to migration patterns, lifecycles, or other behaviours. This is because being unable to sample during a period of time could introduce gaps in data and limit certain pattern analysis, such as seasonality.

Finally, a good bioindicator should obviously be sensitive to the hazard that is being investigated. If an organism is tolerant to the desired pollutant, then it would not accumulate enough of the contaminants before they are already far above the desired levels. Therefore, an organism sensitive to the pollutant would be preferable as it would show contamination even at low levels. However, while being sensitive to the hazard they must also have a high tolerance to it, otherwise the organism may expire before portraying an accurate circumstance of the area or become weakened and alter its usual behaviour, thereby interfering with the measurement. Similarly, bioindicators must be functional in the expected range of the contaminants present in the area. Even if a bioindicator was sufficient in another area with low concentration of the pollutant of interest, in another area of high contamination it may not be appropriate due to the increased stresses that organisms might face.

2.3 Terrestrial Snails

Keeping in mind the above requirements for a sentinel species, one type of organism that matches these criteria are terrestrial snails. As exemplified by Larba & Soltani (2013) and Itziou & Dimitriadis (2011), common terrestrial snail species such as *C. aspersum* and *T. pisana* make ideal bioindicators, especially for heavy metals in the environment, as they comply with all aforementioned criteria. They are two of the most common snail species in Malta and

hence any area of interest will have at least one of the two species. This allows for comparisons of different areas and to establish helpful baselines for pollutants. This also means that procedures for sample collection and sample preparation do not need to be altered due to using a different organism, adding to the repeatability and reliability of the results. Snails are also sedentary animals and hence do not tend to travel too far from their environment, this means they will represent specifically the area they are collected from with little interference due to ranging to outside areas. Their slow movement also helps with their ease of collection alongside the fact that they do not hide in difficult to reach places. In addition, *C. aspersum* and *T. pisana* do not resemble many other snails found in Malta and hence can be easily identified.[2]

The suitability of terrestrial snails as bioindicators are not the only point of interest for their use in research papers. Most snails occupy a low trophic level as a primary consumer that feeds primarily on plants, lichen, and fungi. Snails also take up significant amounts of nutrients from the soil itself from dissolving the molecules in the mucus covered foot. This means that the soil can be considered a part of their diet and has a large impact on their health and growth (Dallinger et al., 2001). Hence due to their immediate use of soil nutrients, snails provide a very good representation not only of bioactive pollutants but also of the situation in the soil specifically. In addition, due to their trophic level, snails are often prey of other animals and hence are heavily involved in the transferring of pollutants along the trophic chain (Dar et al., 2019; Hispard et al., 2008). This is an important point of interest as a hazard found to accumulate in snails will almost certainly affect the food chain as a whole and by extension the health of the environment or habitat. This effect is not so common with animals occupying higher trophic levels as they are not preyed upon as often and so the transfer of hazards will be substantially less.

[2] *T. pisana bears a slight resemblance to another terrestrial snail Eobania vermiculata but can be easily differentiated with little training. For specifics on differentiation, refer to Appendix 1: Sampling Advice.*

The term snail does not refer to any particular taxa, but rather commonly refers to any gastropod with an external shell and hence snail species can differ significantly in behaviour, distribution, and anatomy. However, on the whole these invertebrates make excellent bioindicators for heavy metals due to their ability to bioaccumulate heavy metals in their tissues and shell yet are resistant to such toxins (Viard et al., 2004). This high tolerance is due to the ability for sequestration of the metals into their tissue and shell. As touched upon previously, the heavy metals deposited in the organism are an expression of the environment as a whole through ingestion of food (plant and water), cutaneous contact (mostly from the mucus covered foot), and even the polluted air which they breath (Gomot de Vaufleury, 2000). However, their high tolerance does not make them impervious to the toxin's effects even at sublethal levels. When the rate of absorption surpasses the rate of excretory metabolic storage and detoxification, the toxic effects have been known to cause organ damage, stunt development, place strain on reproductivity due to decreased fecundity and variation in mineral composition of egg (Graveland et al., 1994), and can even cause mortality due to weakness induced starvation rather than morphological or metabolic disruptions due to poisoning (Russell et al., 1981).

2.3.1 *Cornu aspersum*

One of the snail species considered in this study is the common garden snail, *Cornu aspersum* (previously known as *Cantareus aspersus* or *Helix aspersa*; Maltese: Għakrux Raġel). This is a terrestrial snail typically with a shell height of 25-33mm and a diameter of 23-27mm in Maltese specimens (Giusti et al., 1995). The colour of the shell varies slightly but is typically dark brown to reddish-brown with streaks, stripes, or specks of yellow while the animal is yellow green in colour with a brownish head and neck. In Malta, the species is very common and has an incredibly wide distribution being present in virtually all anthropogenic and natural habitats. They are an herbivorous species feeding primarily on fleshy plants such as vegetable crops, fruit trees, and garden plants. Within these habitats they are typically found under stones, on the underside of fleshy plants, and in the cavities between rubble walls. During the summer months, *C. aspersum* has been known to aestivate by hiding deep within crevasses or underneath rocks in order to avoid the hot and dry period of the season.

An added point of interest for the selection of *C. aspersum* as a bioindicator is the use of this species as a culinary delicacy. These snails are used all over the world, including Malta, as a food item and are typically bred for this purpose. However, it is not uncommon for wild snails to be foraged and eaten in these dishes which could potentially prove to be a health risk due to this direct relationship it has with humans.

Figure 2.1: Cornu aspersum shell. Photo available via wikicommons < https://commons.wikimedia.org/wiki/File:Cornu_aspersum_f._maxima_01.jpg >.

2.3.2 *Theba pisana*

The other snail species considered in this study is the white garden snail, *Theba pisana* (Maltese: Bebbuxu tas-sajd). This is a terrestrial snail typically with a shell height of 10.6-13.9mm and diameter of 11.1-19.3mm in Maltese specimens (Giusti et al., 1995). The shell is predominantly yellowish white in colour with reddish-brown steaks or flecks or with no markings at all, however snails will practically always have a black whorl at the shell apex. As for the body, it is typically yellow grey with a slight reddishness on the head and foot and with two black lines running along the neck. In Malta, the species is very common and has an incredibly wide distribution being present in essentially all anthropogenic and natural habitats. *T. pisana* has been described as a typical example of a dune, retrodune, and coastal

dwelling snail (Giusti et al., 1995). This is due to the species being thermophilic (resistant to high temperatures) and thalassophilic (resistant to maritime conditions). *T. pisana* are herbivorous snails that can be found forming large aggregations on vegetation and have a biennial life cycle in Mediterranean habitats.

Like virtually all other snail species in Malta, *T. pisana* aestivates during hot seasons. However, unlike some other species, it does not burrow underground or hide in crevasse or under stones. Instead, *T. pisana*'s behaviour differs in that they congregate together in large clusters on vegetation, upright stems of plants, branches of trees, and on the sides of walls to avoid the hot and dry conditions of the soil during these months.

Figure 2.2: Theba pisana shell. Photo courtesy of Gargominy O., available via wikicommons <https://commons.wikimedia.org/wiki/File:Theba_pisana_pisana_(MNHN-IM-2010-13179).jpeg>.

2.4 Terrestrial Snails as Bioindicators in Malta

As exemplified in numerous studies (Larba & Soltani, 2013; Yap and Cheng, 2013; Itziou & Dimitriadis, 2011; Berger & Dallinger, 1993), terrestrial snail species are ideal bioindicator species for all the reasons mentioned previously. However, the suitability of a species to act as a bioindicator tends to be heavily dependent on the particular circumstances of the environment in question. Unfortunately, there has never been a study done to determine if the two snail species mentioned above are suitable to the Maltese context. In order to determine that a species is an appropriate bioindicator it must accurately portray the situation of their environment. Since certain areas are inherently more contaminated than others (for example industrial areas compared to rural areas), a good bioindicator species is expected to show this difference in heavy metal content between different sites. If it is found that snails collected from one area have a statistically significant heavy metal profile to snails collected from a different area it can be assumed that the snails accurately portray the difference in their situations and hence can be used as sentinel species. Building upon this, it must also be determined to what extent a sentinel species is suitable as they may be able to show a stark difference between different areas (for example between industrial and isolated areas) but not between similar areas (for example between two separate urban areas). In addition, which species is most appropriate as a bioindicator for which heavy metal must also be determined. For example, a species 'A' may be better suited for detecting and measuring lead in the environment while a species 'B' may be better suited for mercury due to the particular biology of the organisms.

2.5 Methods of pollutants Extraction and Analysis

As stated previously, snails have been used extensively to detect and monitor for pollutants in the environment. This is not simply limited to heavy metals however, other pollutants that have been measured using snails include fungicides, pesticides, herbicides, and polycyclic aromatic compounds (Baroudi et al., 2020). Each category of pollutant can have

a variety of extraction and analysis methods but since this research focuses on heavy metals, other pollutants and their associated analytical methods will not be discussed.

2.5.1 Pollutant Extraction

In the case of heavy metals, the most widely used technique is extraction via acid digestion. Most commonly nitric acid is used (Baroudi et al., 2020), however the procedures can differ significantly with some using hot concentrated nitric acid (Berger & Dallinger, 1993; Gomot de Vaufleury & Pihan, 2002; Massadeh et al., 2016), a mixture of acids such as hydrochloric (HCl) and perchloric ($HClO_4$) acid (Abdel Gawad, 2018; Dummee et al., 2012), and sometimes with the aid of microwave-assisted acid digestion technology (Lau et al., 1998; Li et al., 2013).

There exists a significant limitation with using acid digestion or microwave assisted digestion to transform samples into a state where metals can be analysed, it destroys the original form of the metal of interest. Taking the case of digestion using nitric acid, this will convert the relevant metal ions to the corresponding cation of the nitrate(IV) form. If a study is not only interested in the presence of a metal in general but rather on a specific form of said metal (for example CrO_4^{2-} or $Cr_2O_7^{2-}$ rather than just chromium in general) this would not be an appropriate method of doing so and another technique would need to be utilised, such as X-ray photoelectron spectroscopy (XPS)(Singh et al., 2022) or X-ray absorption fine structure (XAFS) (Yasoshima et al., 2001).

2.5.2 Methods of Analysis

As with extraction methods, there exists a wide variety of techniques that can be used to detect and quantify heavy metals. Historically, this was done via wet chemistry and titration, but nowadays more sensitive and reliable techniques are used. The most used technique is spectroscopy with the three most common types of analytical equipment used being flame atomic absorption spectroscopy (FAAS), microwave plasma atomic emission spectroscopy (MP-AES), and inductively coupled plasma optical emission spectroscopy (ICP-

OES) (Baroudi et al., 2020). In the case of element detection, FAAS operates on the principle that electrons in a ground state can be excited to a higher energy by a certain wavelength of light, whereas ICP-OES and MP-AES operates on the principle that an ionised sample being in a higher energy state will return to its ground state and by doing so emit light radiation in a wavelength specific to the element. In FAAS this excitation is done by a use of a torch (acetylene and/or N_2O and air, depending on elements measured) whereas plasma is used in the case of ICP-OES (argon plasma) and MP-AES (nitrogen plasma). As for determination of concentration of an element, all three techniques work on the same principle of Beer-Lambert Law which describes the relationship between light intensity and concentration of the element. Essentially, the more light that is absorbed or emitted, the more of that specific element is present in the sample. This means that the three techniques could be used to not only identify the element in a sample but also measure their prevalence.

The three techniques each have their own strengths and weaknesses and the ideal choice is highly dependent on the specific needs and circumstances of the research and availability. Table 2.2 gives a brief overview of these techniques for comparison.

Table 2.2: Comparative overview of three different analytical techniques (Adapted from Agilent Technologies, Inc., 2021b).

Category	FAAS	MP-AES	ICP-OES
Sensitivity	Moderate	Moderate	High
No. of elements that can be measured	~67	~70	~74
Detection range	~100 ppb to 1000 ppm	~100 ppb to 1000 ppm	~20 ppb – 10,000 ppm
Tolerance to solids	Moderate	Low	High
Element measurement	Sequential	Sequential	Simultaneous
Running cost	Moderate	Low	High
Maintenance requirements	Low	Low	High
Operator skill required	Low	Low	Moderate

2.5.3 Microwave Plasma — Atomic Emission Spectroscopy

As can be seen from the above, each method described can be used in this study to determine heavy metal presence and concentration in a biological matrix. However, although not as commonly used as FAAS or ICP-OES, several studies have made use of the MP-AES to analyse heavy metals in acid digested matrices (Borg and Attard, 2020; Li et al., 2013) just as this study hopes to do. Compared to FAAS, MP-AES has better instrument detection limits; a greater linear dynamic range; a simpler sample preparation procedure as there are less significant chemical and ionising interferences that would require buffers or releasing agents (Agilent Technologies, Inc., 2021a).

Generally, the ICP-OES is a better instrument than the MP-AES from an analytical point of view. It has a better detection range, is more sensitive, can analyse more elements, and is

faster as it can analyse the desired metals simultaneously. However, for this application the range and sensitivity of the MP-AES should suffice. For this reason, and the increased difficulty in operating the ICP-OES, the MP-AES was selected as the preferred instrument.

3. Methodology

3.1 Sampling

As this study aims to find and quantify potential differences in concentrations of the selected heavy metals between the two species of snails occurring in different locations, the geographical position of the sampling locations was not given much consideration, as no geographical survey was being conducted. Instead, more importance was given to the type of environment with regards to their perceived exposure to different pollutants. This phenomenon could even be observed through simple physical inspection with individuals from different areas being smaller, weaker, discoloured, and heavily infested by parasites. Figure 3.1 shows two shells of different thicknesses, this could be due to a lack of calcium in their environment which the organisms use to build their shells, or it could be due to divalent elements (such as lead ions) depositing in the shell and taking the place of calcium in the structure which weakens the shell as shown (Carbone & Faggio, 2019).

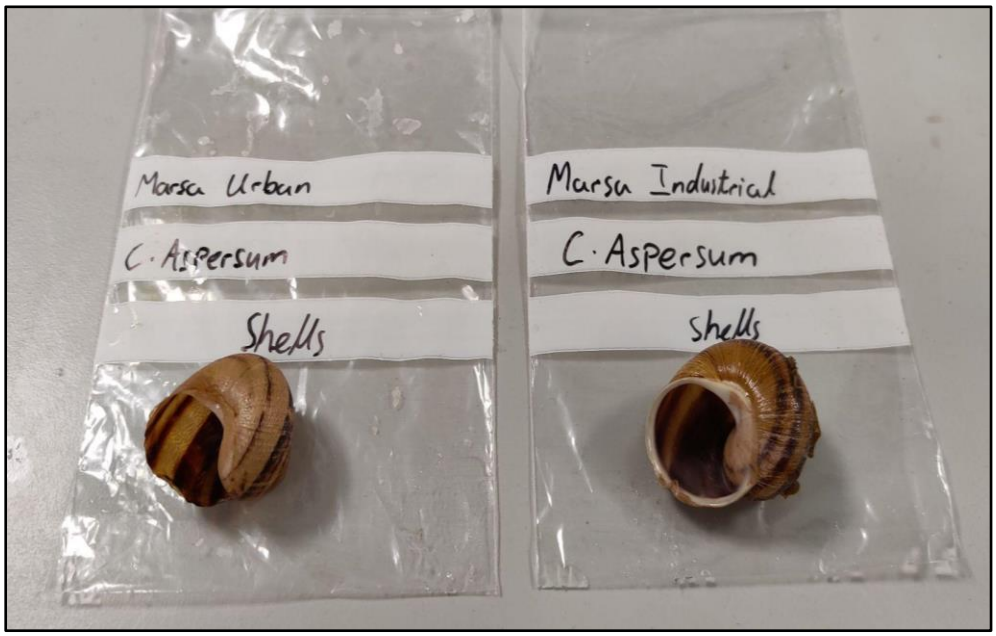

Figure 3.1: Shells from two *C. Aspersum* individuals from different locations showing a difference in shell thickness.

The location types were defined as: Industrial, Urban, Residential, Agricultural, Rural, and Isolated. For the purpose of this study:

- Industrial areas are defined as having significant industrial presence in the form of workshops, factories, refuse sites, etc. Oftentimes, these businesses will pollute the nearby area with high levels of contaminants that would not be found commonly anywhere else (Alloway, 2012). These locations often have very little in the form of vegetation and so snails were collected from roadside vegetation or fields used as scrap and dump sites.

- Urban was defined as an area with a significant human presence but not in the form of heavy industry. Snails were often sampled from roadside vegetation or fields adjacent to traffic heavy roads.

- Residential was defined as private homes of people and snails were collected from private gardens.

- Agricultural areas were defined as fields that are in active use for crops and farming.

- Rural areas were defined as areas having little human development and presence.

- Isolated was defined as areas that have minimal to no human presence for long periods of time.

After the above strata were defined and categorised, individuals were sampled randomly. Figure 3.2 shows the locations sampled.

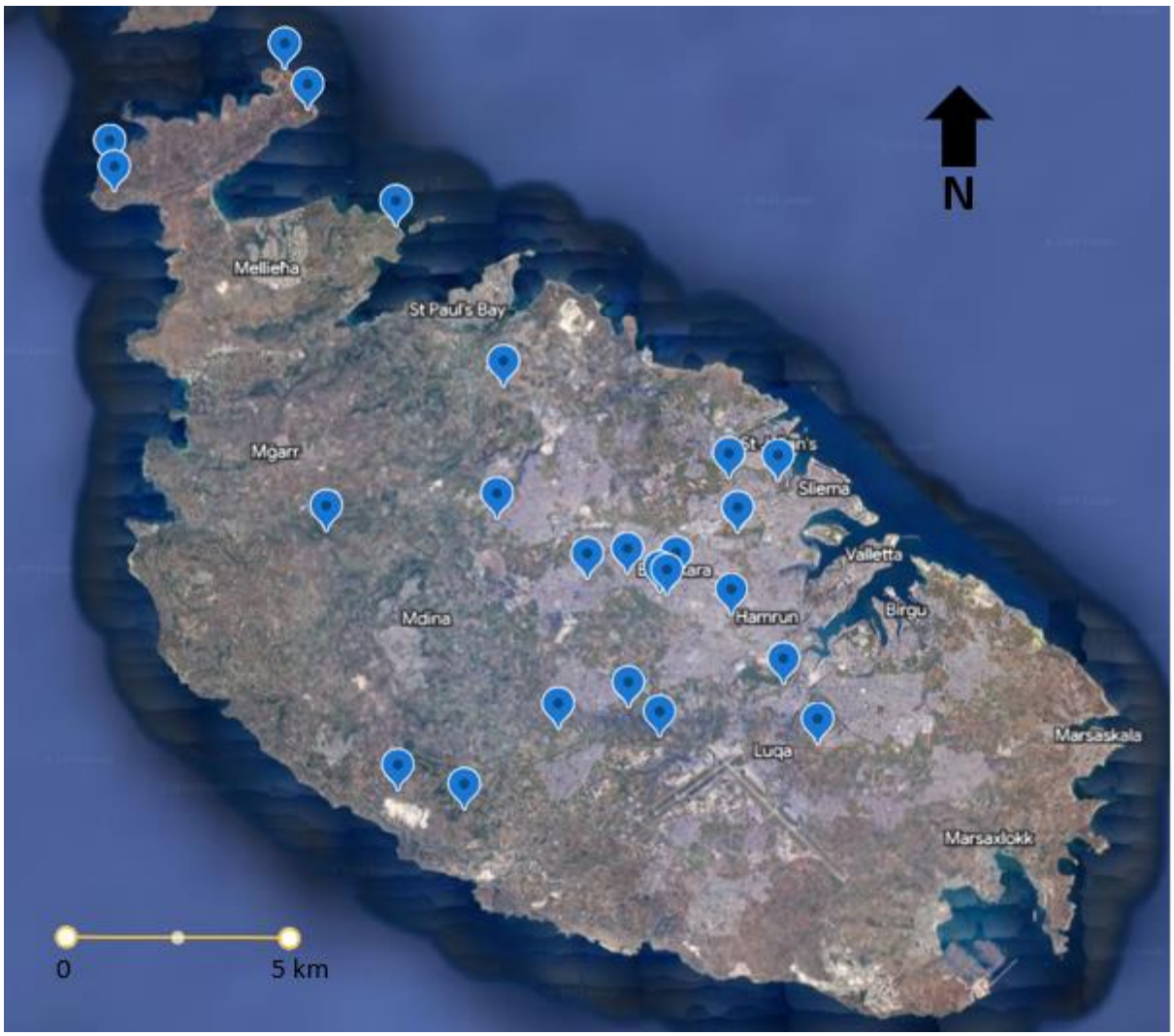

Figure 3.2: Map of Sampling Locations (base map obtained from Google Earth).

In the case of *T. pisana,* most individuals were collected between June and September due to their behaviour whilst aestivating. Due to their relatively small size, around 10 individuals had to be collected in order to have a sufficient sample for testing. For *C. aspersum*, most individuals were collected between November and April due to their relative activity during the winter months. Due to their size, around 5 individuals were considered sufficient enough for testing.

3.2 Sample Processing

The individuals collected from the same area were kept together but kept separate from individuals of different species or locations. These were then left for two weeks without food in order to starve them and remove their gut contents. This was done as not all heavy metals will be absorbed by the animal and such analysing an individual which was not properly starved would have interfered with the final inferences of the research. As some individuals were sampled in the summer months when they are known to aestivate, these individuals were activated by distilled water before starvation. After the starvation period, the snails were placed in a freezer set at -16℃ overnight to terminate them.

3.2.1 Method Validation

Acid-digestion was the method selected to convert the heavy metals into a state that allowed for their analysis. This is a widely used technique but for various reasons, procedures may differ slightly (Berger & Dallinger, 1993; Massadeh et al., 2016; Viard et al., 2004; Vranković et al., 2020). This could be due to the chemicals or quality of the labs available to the researchers, the specific analytes of interest, the analytical equipment that will be used, *et cetera*. Therefore, this research does not follow any specific procedure verbatim, and the method used was specifically crafted to the needs and situations of this researcher. Unfortunately, either due to a lack of proper refereeing in research journals or a perceived lack of usefulness or interest, researchers tend to omit certain steps from their procedure. For example, several papers listed the use of highly concentrated acids for digestion but do not specify what methods were used to neutralise the sample after digestion. It could be assumed that no neutralisation took place, but this is unlikely as most widely available analytical equipment are highly sensitive and would not be able to tolerate such corrosive chemicals without proper treatment. Therefore, before any such procedure could be applied to all samples, a validation of the method had to take place.

There exist two methods to treat such acidic and corrosive samples to render it into a less harmful state, dilution or neutralisation. As the concentration of heavy metals was

expected to be low due to the nature of the samples, dilution was not considered a good approach. This is because in order to reduce the high acidity of the sample, the amount of deionised water needed would risk diluting the concentration of heavy metals possibly below the detection limit of the MP-AES. Therefore, neutralisation was chosen.

Two methods of neutralisation were identified, by use of solid sodium carbonate or ammonia solution. Table 3.1 shows results obtained from the same sample using ammonia and sodium carbonate as neutralising agents. The test samples were neutralised to pH -0.5 (determined by use of a pH probe) using either 30% *puriss.* grade ammonia solution or analytical grade sodium carbonate and passed through a 0.45 µm nylon filter before analysis.

Table 3.1: Concentrations (ppm) of heavy metals using different neutralising agents.

Metal	Concentration (ppm) using the neutralising agent	
	Ammonia	Sodium Carbonate
Arsenic (As)	3.94	0.02
Cadmium (Cd)	5.55	0.18
Chromium (Cr)	0.17	0.00 (<LOD)
Copper (Cu)	1.12	0.11
Nickel (Ni)	0.27	0.02
Lead (Pb)	0.25	0.26
Zinc (Zn)	1.15	0.03

As can be seen from Table 3.1, the results obtained from the different neutralising agents differ significantly from each other, with the results obtained using sodium carbonate differing from what is to be expected. This could be due to the significant quantity of sodium carbonate required to neutralise the sample, the concentration of sodium ions in the sample

caused a sort of 'blow out' and interfered with the spectra readings of the other heavy metals. This was not the case with the ammonia method as the chemical contains no metal ions and hence will not interfere with other metal spectra. Hence, the ammonia neutralisation method was used. Validation of the equipment and method used can be found in Appendix 2 - Method and Equipment Validation.

3.2.2 Processing Procedure

After termination, the soft parts were separated from the shells and their masses weighed. The soft parts were then placed in an oven at 80°C for 4 days to remove the water content and a dry weight was obtained. The dry mass of the soft parts and the shells were each treated with 20cm^3 70% analytical grade nitric acid for digestion and kept until all traces of solid matter have dissolved, usually about twenty-four hours. After this, the acid-digested material was treated with 20cm^3 35% analytical grade hydrogen peroxide in order to break down any persistent organic material in the matrix and in turn reduce the viscosity of the matrix. Samples were left to react in screw-cap bottles and burped twice daily to expel gas build up. This procedure was repeated until no more gas was observed to be produced.

10cm^3 of this stock sample was then taken by use of a class AS volumetric pipette and neutralised to pH -0.5 (determined by use of a pH probe) using 30% *puriss.* grade ammonia solution. This was required to bring the sample down to the operating tolerance of the MP-AES, as the machine could not withstand the acidity of the digestive mixture (70% nitric acid and 35% hydrogen peroxide). However, samples had to be kept acidic to prevent any precipitation of heavy metals which tends to happen in non-acidic conditions. Figure 3.3 shows the setup used during this neutralisation step.

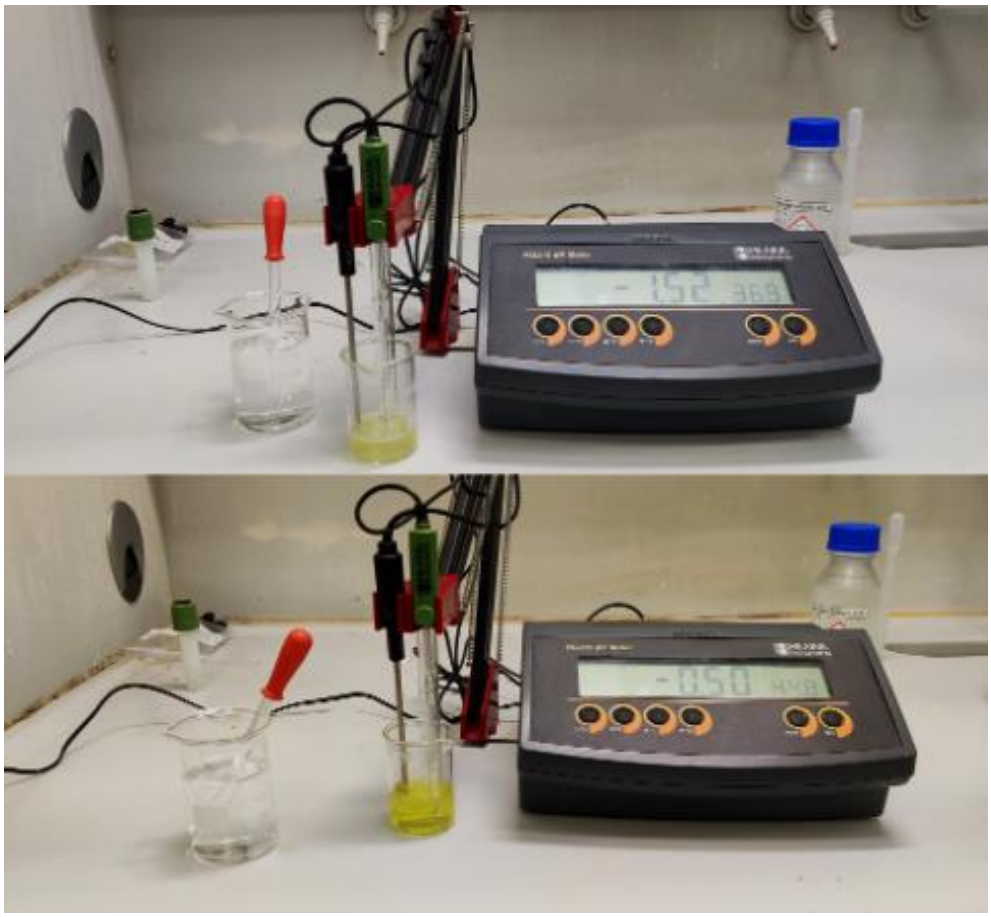

Figure 3.3: Setup of sample processing procedure showing pH and temperature probe in a sample and a beaker of ammonia. *Top:* Sample before addition of ammonia *Bottom:* Sample after addition of ammonia.

Samples were then passed through a 0.45µm nylon filter to further remove any material that was not digested or dissolved by the nitric acid and hydrogen peroxide so as not to block or damage the MP-AES. The integrity of the filter disks was verified using a standard bubble test, to confirm that the acid did not damage the pore diameter of the disks. The sample was then made up to 50cm^3 with deionised water. Deionised water was chosen as any heavy metals would be filtered out and thereby not interfere with analysis. The samples were then stored at 2°C until analysed using MP-AES to determine the concentration of the selected heavy metals.

3.3 Sample Analysis

Samples were analysed using a MP-AES Agilent 4100 series, with the running conditions being shown in Table 3.2. The MP-AES utilises a high-energy plasma of an inert gas (in this case the gas used is Nitrogen) to rapidly burn an analyte. The resulting emission of the burnt analyte is detected, the wavelength of which directly corresponds to a specific element and so the presence of said element is determined. Similarly, the intensity of the spectral signal emitted by the burnt analyte directly corresponds to the concentration of specified elements in the sample (Jankowski & Reszke, 2011). Therefore, the MP-AES can both detect and quantify the presence of the different elements in a sample making a highly efficient and useful analytical technique. The heavy metals chosen for this study were chosen due to their prevalence in the environment and their toxicity (Borg & Attard, 2020; Lau et al., 1998; Massadeh et al., 2016; Rota et al., 2016.)

Table 3.2: Running conditions of the MP-AES 4100 series.

Nebulizer	One-neb (concentric)
Spray Chamber	Cyclonic spray chamber, single pass
Calibration correlation coefficient limit	0.99999
Pump speed (rpm)	15
Number of replicates	3
Stabilisation time (s)	15
Uptake time (s)	15

The emission spectrum of each individual element is not only unique, but it is comprised of peaks at different wavelengths. Therefore, a number of wavelengths could theoretically be used to identify an element and one must select the most appropriate wavelength for identification. This is typically the peak with the highest intensity, resolution (i.e., the narrowness of the peak band), and lack of interference from peaks of other elements. Table 3.3 lists the wavelengths used to identify the elements listed in this study, as well as the

correlation coefficient (R^2), standard deviation, limit of detection (LOD), and the limit of quantification (LOQ).

Table 3.3: Wavelength, correlation coefficient, standard deviation, LOD and LOQ for the selected metals.

Element	Wavelength (nm)	R^2	Standard Deviation	LOD (ppm)	LOQ (ppm)
As	193.695	0.99978	61	0.4944	1.6479
Zn	213.857	0.99982	26	0.0074	0.0246
Cd	226.502	0.99996	48	0.1243	0.4145
Cu	324.754	0.99994	58	0.0015	0.0051
Ni	352.454	0.99997	60	0.0102	0.0339
Pb	405.781	0.99979	12	0.0123	0.0411
Cr	425.433	0.99987	14	0.0014	0.0047
Al	396.152	0.99993	4	0.0015	0.0049
Mn	403.076	0.99992	5	0.0011	0.0037
Ba	455.403	0.99948	9	0.0008	0.0027
V	437.923	0.99998	6	0.0026	0.0086

The machine was calibrated using a multi-elemental standard which contained an equal concentration of various metals. The sample tubes were then labelled with a simple identifier before allowing the sample to be passed through the machine. For each sample, the different metals are analysed individually by the MP-AES, and for each spectrum three readings are taken before an average is given in parts-per-million (ppm). However, results were not presented in this manner. This is because the original samples (all the individual snails collected from one area) did not amount to the same weight nor the same number of individuals and so presenting and using the data in this manner would be inaccurate and grossly misleading. Therefore, results were converted to weight-by-weight (µg/g) (Equation 3.1) to make comparisons possible.

$$Concentration\ (\mu g/g) = \frac{\bar{C} \times 40}{m}$$

Where;

$\bar{C}$= mean concentration determined experimentally (ppm)

m= dry weight of the original sample (g)

40 a volumetric constant

Equation 3.1: Conversion from ppm to w/w.

3.4 Data Analysis

After standardisation, the data was organised into charts for preliminary visual analysis of possible patterns before analysis was performed. The methods used in this study were Principal Component Analysis (PCA), Multidimensional Scaling (MDS), and Cluster Analysis.

Both MDS and PCA are methods used to group samples together in order to determine any patterns in the data set and, to a degree, could be used interchangeably. However, both methods were utilised in this study in order to verify that any potential patterns found would not be due to the differences between the two methods but are indeed present in the data set, i.e., if both produce similar results then those results can be trusted unequivocally. It is important to note that neither MDS nor PCA are statistical tests but rather a means of visualising a dataset as each point relates to one another.

A cluster analysis was performed to determine any groupings, and thereby correlations and/or patterns, in the dataset which was then used to overlay on the ordination

plots. A similarity profile (SIMPROF) test was also performed in conjunction to the cluster analysis to determine if the clusters formed are statistically significant.

A permutational multivariate analysis of variance (PERMANOVA) test was also carried out. This is typically used to compare groups and test for equivalence between them and is typically used when a dataset has multiple variables that interact with each other, such as in the case of this study. That being said, PERMANOVA was also used as a univariate test to determine any statistically significant differences between location type or species of each individual metal at a time. While this is not the intended use of this test, there is a president to use it in such a way (Anderson, 2017) and due to inherent limitations of this research no alternative, such as ANOVA, was possible. The two main assumptions of ANOVA are that data is normally distributed and there is homogeneity of variance. The Shapiro-Wilk test was used to test for normality and the Levene test was used to test for homogeneity of variance, and it was determined that for most datasets these assumptions were not met. Therefore, PERMANOVA was still selected as the p-value is obtained by permutation (unlike in ANOVA) and therefore avoids the assumption of normality and homogeneity of variance.

4. Results

4.1 Results of the Analysis

Before analysis, samples were given a unique number. The species, location type, and sample type (whether they were soft parts or shells) of each sample and their corresponding number can be seen in Table 4.1.

Table 4.1: Sample numbers.

Soft Parts		Shells	
Sample No	Species & Location Type	Sample No	Species & Location Type
1	*T. pisana* Urban	25	*T. pisana* Industrial
2	*C. aspersum* Agriculture	26	*T. pisana* Residential
3	*C. aspersum* Residential	27	*T. pisana* Isolated
4	*C. aspersum* Isolated	28	*C. aspersum* Agriculture
5	*T. pisana* Rural	29	*C. aspersum* Residential
6	*T. pisana* Agriculture	30	*C. aspersum* Urban
7	*C. aspersum* Agriculture	31	*C. aspersum* Isolated
8	*C. aspersum* Isolated	32	*T. pisana* Isolated
9	*T. pisana* Industrial	33	*T. pisana* Agriculture
10	*C. aspersum* Rural	34	*T. pisana* Residential
11	*C. aspersum* Urban	35	*C. aspersum* Residential
12	*T. pisana* Urban	36	*T. pisana* Rural
13	*C. aspersum* Residential	37	*T. pisana* Industrial
14	*C. aspersum* Urban	38	*C. aspersum* Agriculture
15	*T. pisana* Industrial	39	*T. pisana* Agriculture
16	*T. pisana* Residential	40	*C. aspersum* Industrial
17	*T. pisana* Isolated	41	*C. aspersum* Rural
18	*T. pisana* Agriculture	42	*C. aspersum* Isolated
19	*T. pisana* Rural	43	*C. aspersum* Rural
20	*T. pisana* Isolated	44	*T. pisana* Urban
21	*C. aspersum* Industrial	45	*C. aspersum* Urban
22	*C. aspersum* Industrial	46	*T. pisana* Rural
23	*C. aspersum* Rural	47	*T. pisana* Urban
24	*T. pisana* Residential	48	*C. aspersum* Industrial

Samples were then analysed using MP-AES whereby three replicate readings were taken to present an average of the concentration of specific metals in ppm. These results were standardised according to Equation 3.1 and can be found presented in Appendix 3 - Summarised Data as edited results according to location type. However, in the interest of transparency and the free unfettered access to data, the unedited raw data can be found in its entirety in Appendix 3 - Raw Data.

Using the summarised results, clustered bar graphs were drawn for each location type illustrating what percentage of individual heavy metals contributed to the samples (Figures 4.1-4.6). All metals selected for analysis in this study were found to be present in all samples except for vanadium in the soft parts of both *C. aspersum* and *T. pisana* which was not present in concentrations significant enough for the MP-AES to detect. For samples of soft parts, arsenic was found to be the most dominant metal for both species followed by either barium or cadmium, however, there was a single exception in sample 2 (agricultural, *C. aspersum*) where barium was the predominant metal followed by cadmium and then arsenic. For samples of shells, arsenic was found to be the most dominant metal by far.

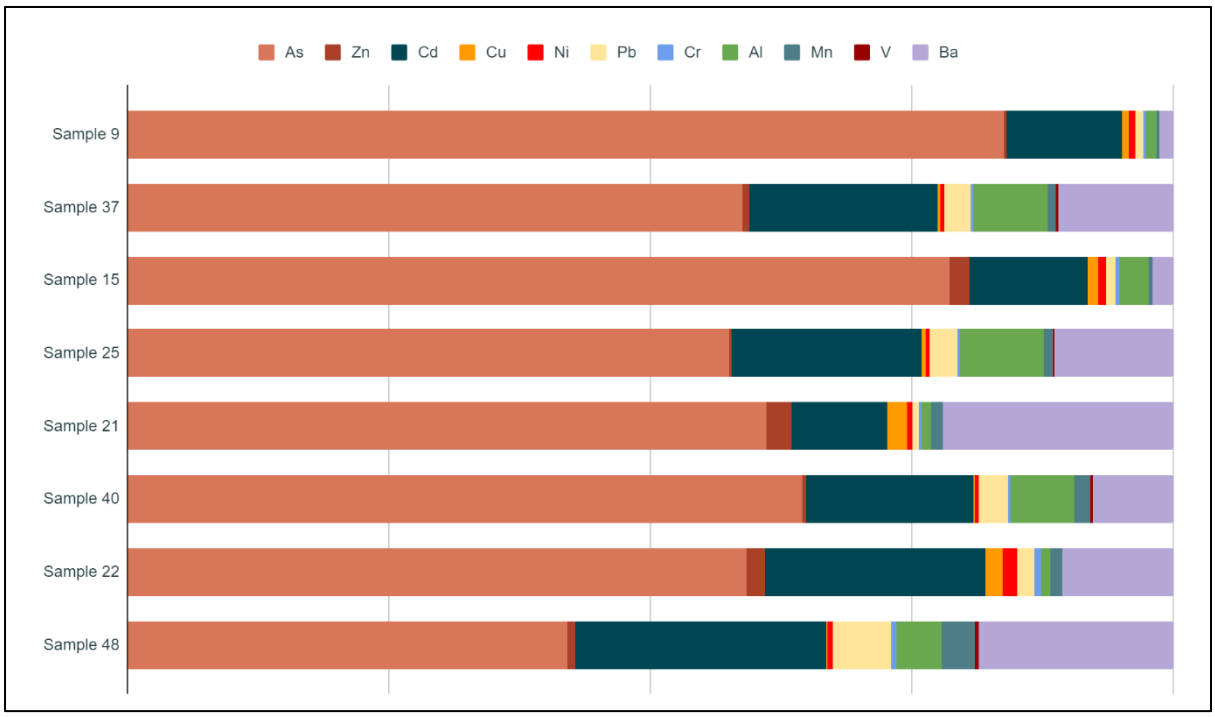

Figure 4.1: Percentage of Heavy Metals found in each Sample for Industrial Location Type.

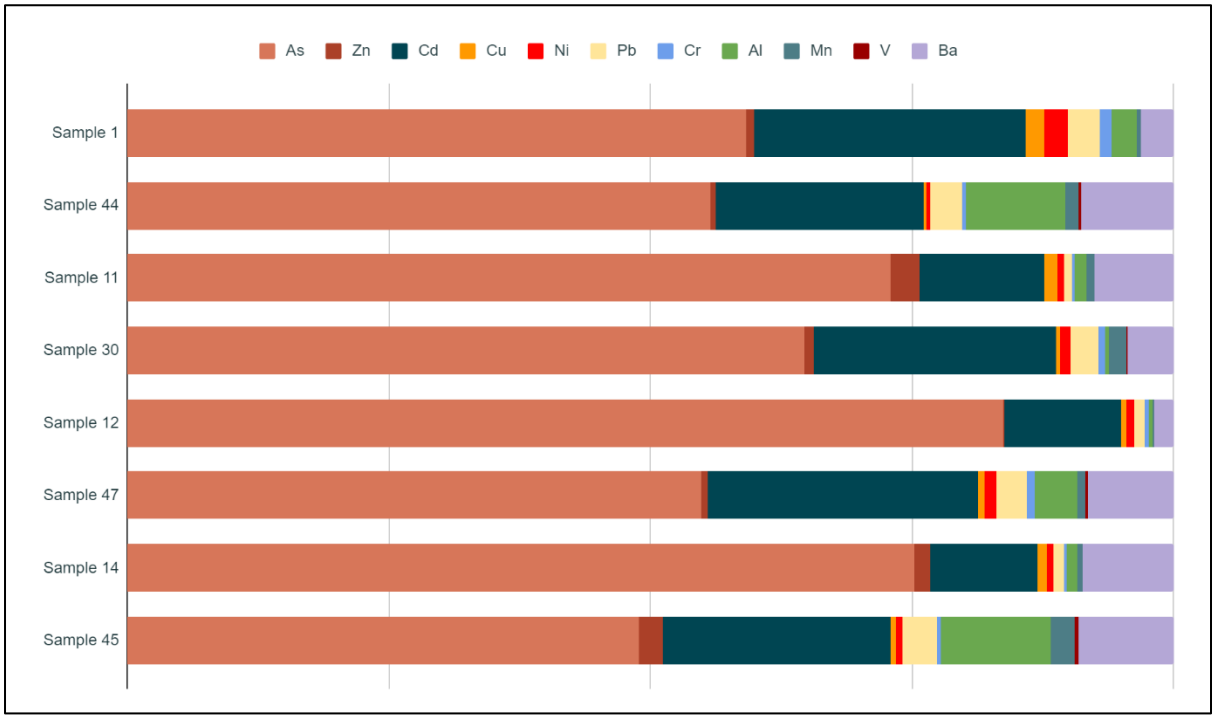

Figure 4.2: Percentage of Heavy Metals found in each Sample for Urban Location Type.

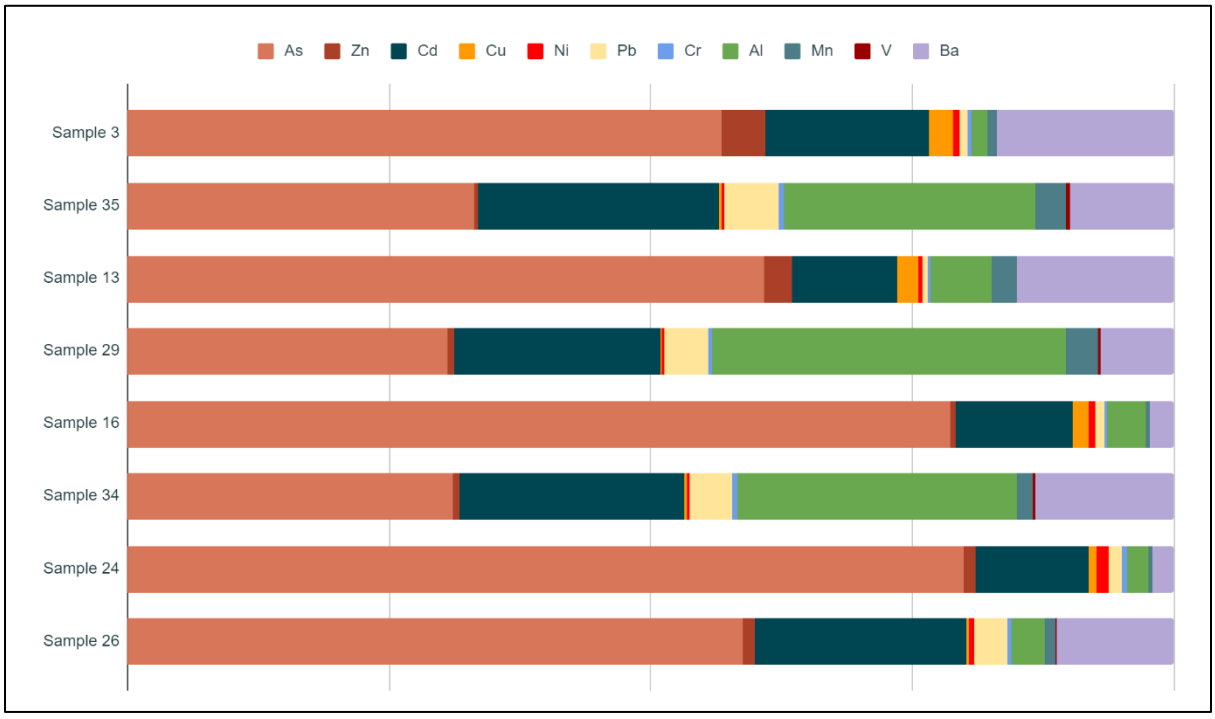

Figure 4.3: Percentage of Heavy Metals found in each Sample for Residential Location Type.

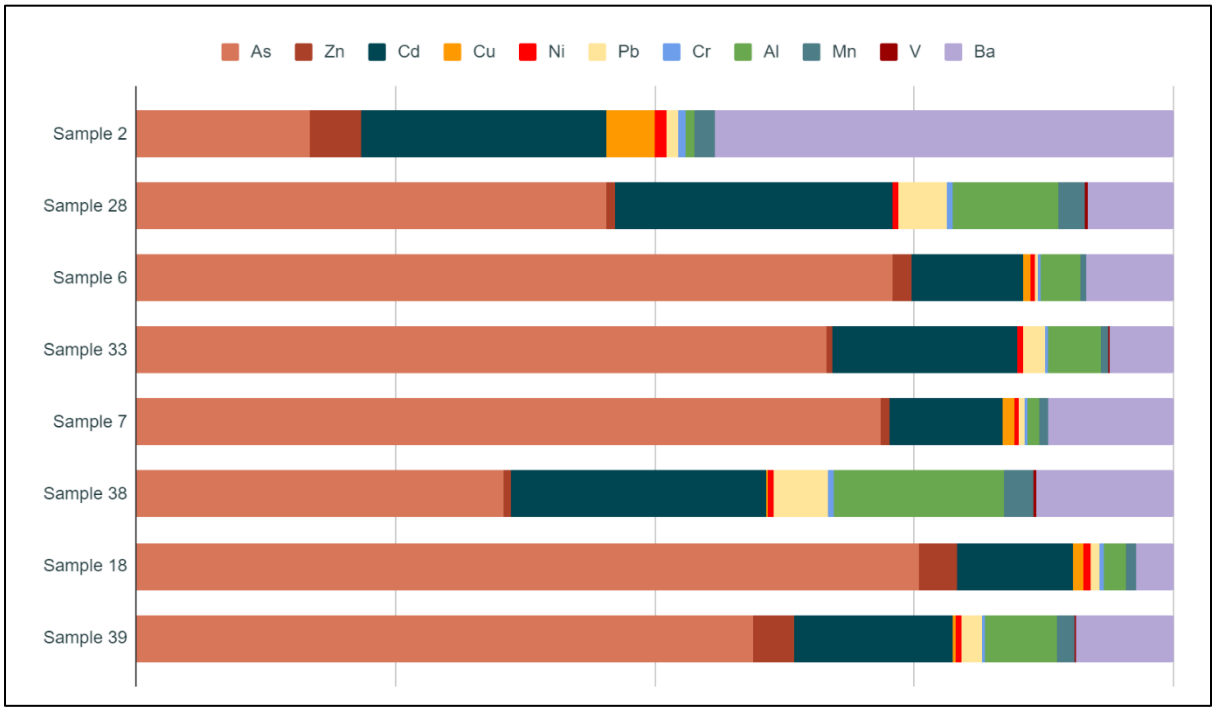

Figure 4.4: Percentage of Heavy Metals found in each Sample for Agricultural Location Type.

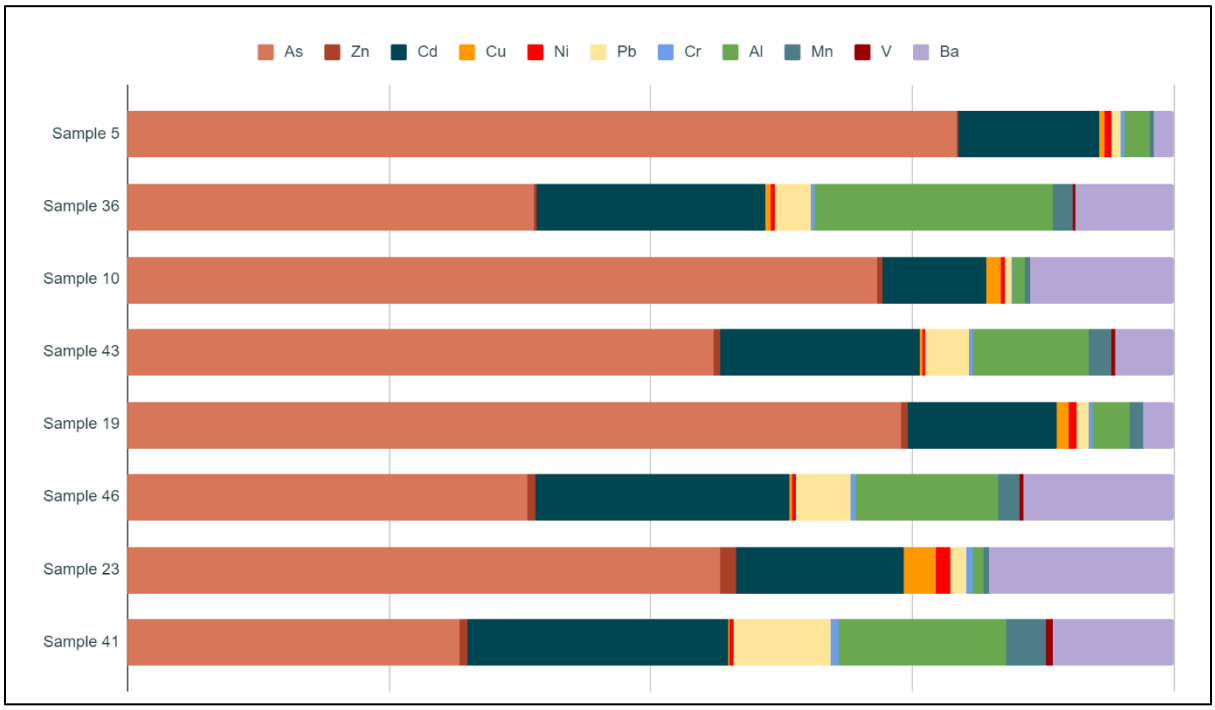

Figure 4.5: Percentage of Heavy Metals found in each Sample for Rural Location Type.

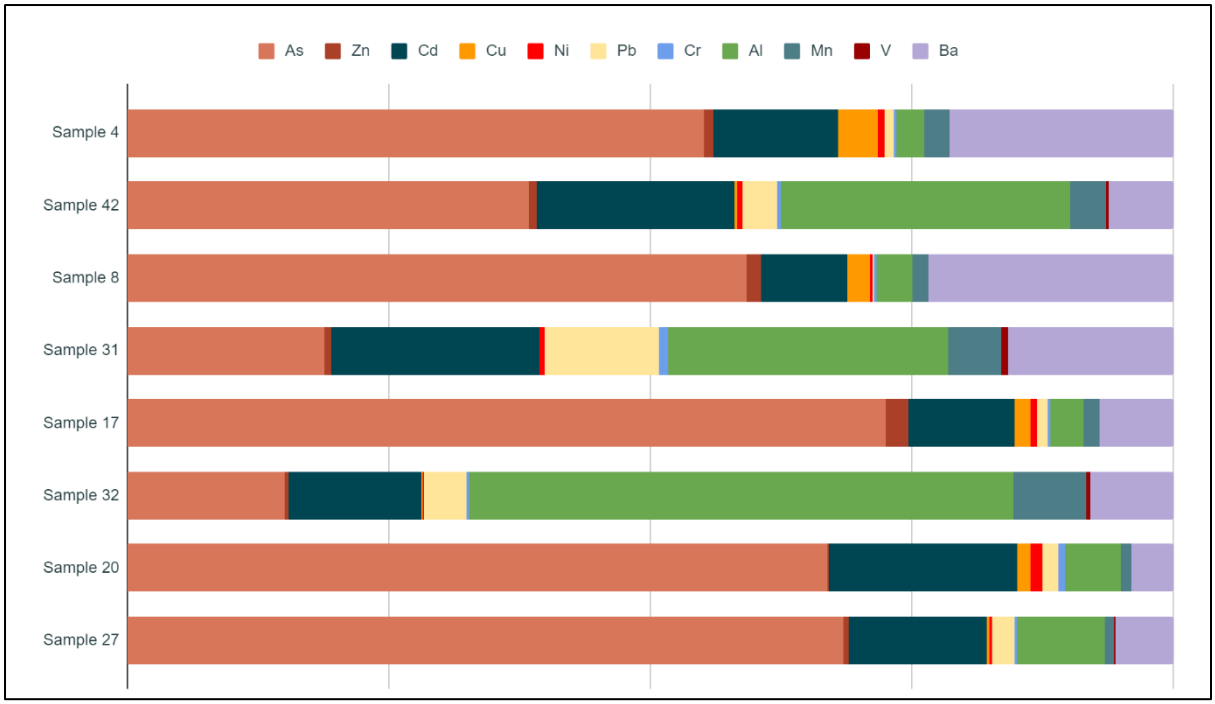

Figure 4.6: Percentage of Heavy Metals found in each Sample for Isolated Location Type.

4.2 Collective Analysis

In order to determine any patterns and correlations that these variables have with/on each other, data was analysed collectively.

4.2.1 Visual Analysis

Firstly, a visual analysis was performed by drawing cluster bar charts for all metals showing their distribution across location types (Figures 4.7-4.10).

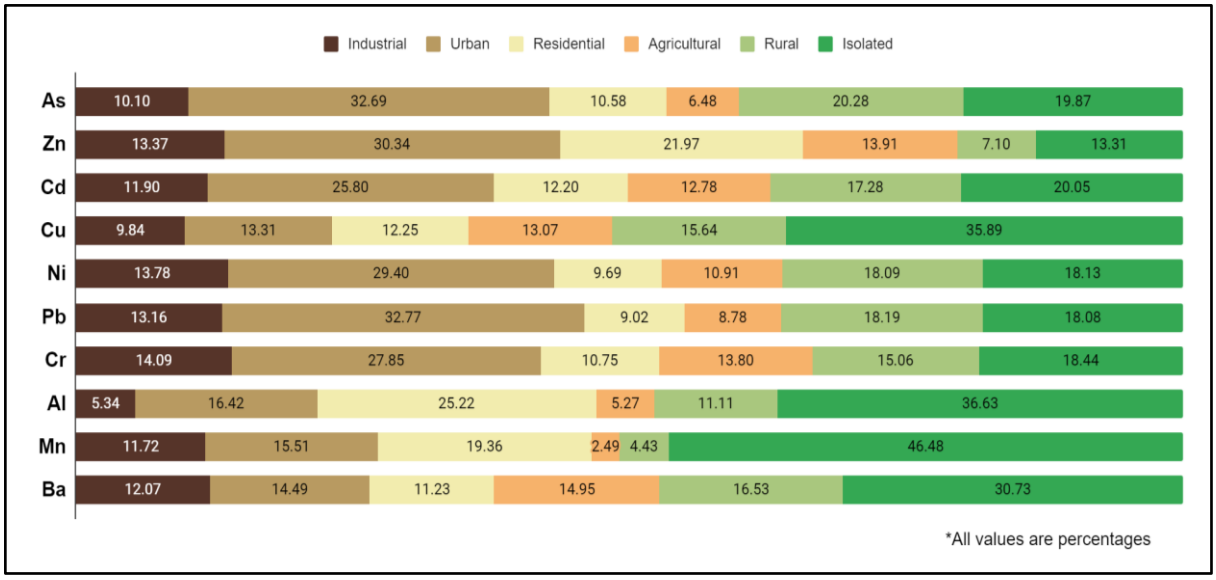

Figure 4.7: Percentage of individual heavy metals in *C. aspersum* soft parts according to location type.

Figure 4.7 shows the percentage of each heavy metal across all the location types for the soft parts of *C. aspersum.* Urban locations were found to have the highest percentage for six out of ten metals (arsenic, zinc, cadmium, nickel, lead, chromium) making it the location type with the highest concentration of metals overall, followed by isolated locations which was the location type for the remaining four metals. Note that vanadium was not included due to the fact that concentrations in soft parts were too low to detect.

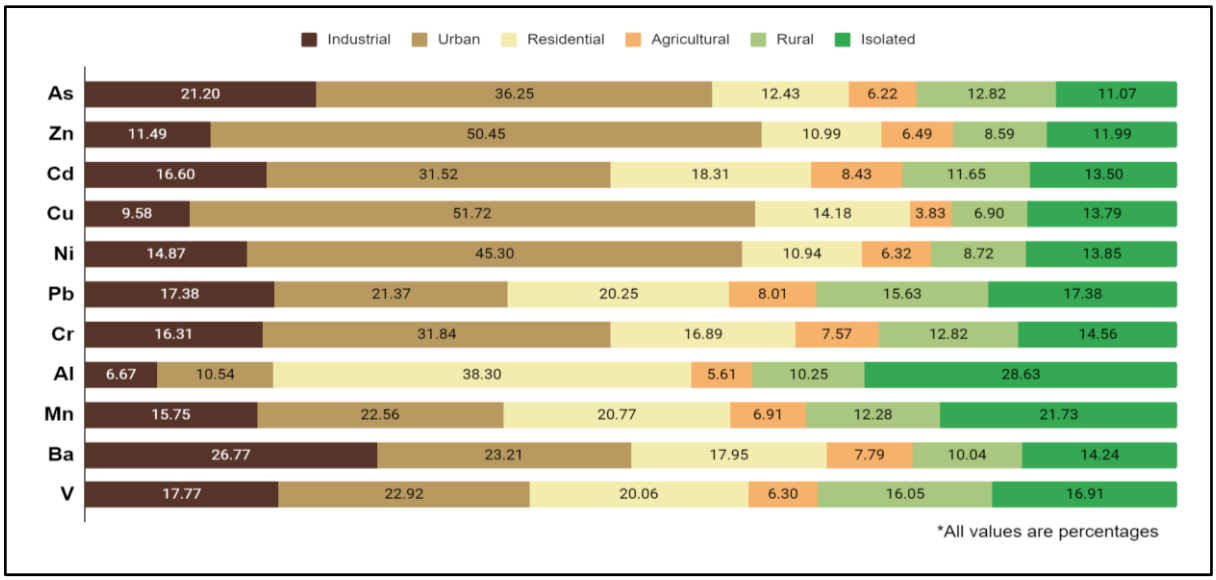

Figure 4.8: Percentage of individual heavy metals in *C. aspersum* shells according to location type.

Figure 4.8 shows the percentage of each heavy metal across all the location types for the shells of *C. aspersum.* Urban locations were found to have the highest percentage for nine out of eleven metals (arsenic, zinc, cadmium, copper, nickel, lead, chromium, manganese, vanadium) making it the location type with the highest concentration of metals overall. This was followed by both residential and industrial locations which were the predominant location type for one metal each, aluminium and barium respectively.

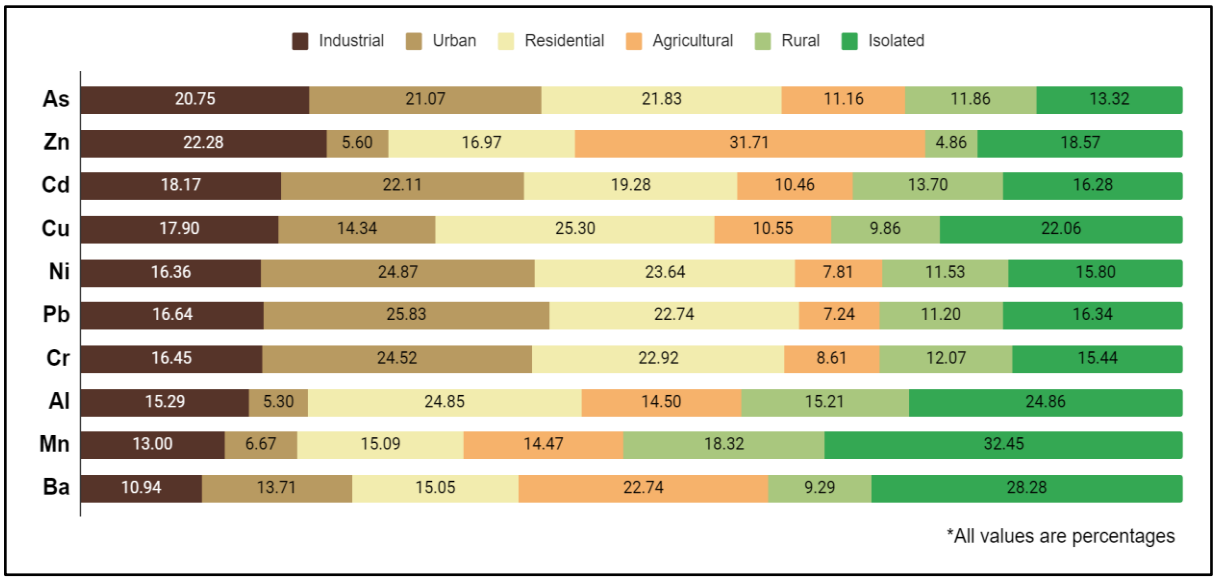

Figure 4.9: Percentage of individual heavy metals in *T. pisana* soft parts according to location type.

Figure 4.9 shows the percentage of each heavy metal across all the location types for the soft parts of *T. pisana.* Urban locations were found to have the highest percentage for four out of ten metals (cadmium, nickel, lead, chromium) making it the location type with the highest concentration of metals overall. This was followed by isolated locations which was the predominant location type for three metals, aluminium, manganese, and barium. Residential was the predominant location type for two metals, arsenic and copper, followed by agricultural which was the predominant location type for zinc. Note that vanadium was not included due to the fact that concentrations in soft parts were too low to detect.

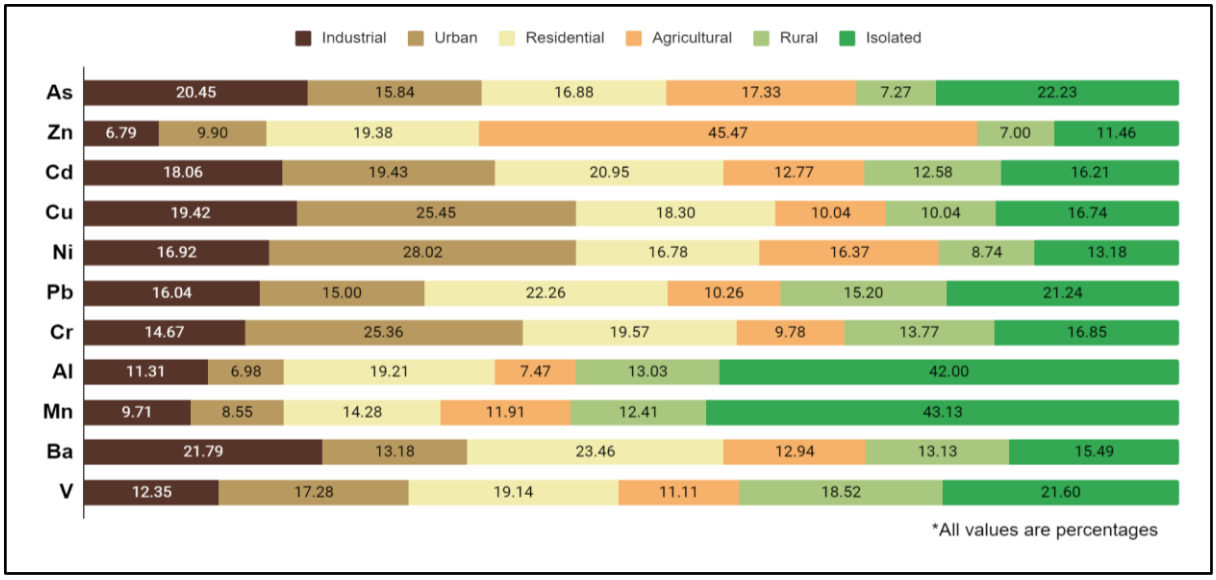

Figure 4.10: Percentage of individual heavy metals in *T. pisana* shells according to location type.

Figure 4.10 shows the percentage of each heavy metal across all the location types for the shells of *T. pisana.* Isolated locations were found to have the highest percentage for four out of eleven metals (arsenic, aluminium, manganese, vanadium) making it the location type with the highest concentration of metals overall. This was followed by both urban and residential locations which was the predominant location type for three metals, copper, nickel, and chromium for urban and cadmium, lead, and barium for residential. Finally, agricultural was the predominant location type for the remaining metal, zinc.

4.2.2 Ordination Plots

Using the results obtained and standardised from the analysis, PRIMER v7 was used to run several statistical methods, namely PCA, MDS, and Cluster Analysis. It is important to note that only ordination plots from MDS are presented as the plots were virtually identical to the ones obtained from PCA and hence were not presented for the sake of legibility. Both MDS and PCA could be used for pattern recognition, and, to a degree, both present the same answer but do so using different methods. Therefore, the reason both methods were utilised was as a verification that the patterns obtained was in fact due to correlations and patterns within the data set rather than due to some variation innately present in the individual methods.

Before analysis could be performed, the data was transformed with a Log(x+1) transformation to reduce the skewness as certain metals are inherently found at higher concentrations than others and could have an unfair effect on the metal profile as a whole. For the sake of these analyses, the Euclidean distance is a similarity measure (similarity referring to how similar the concentrations of all metals, or metal profile as it can be referred to, are from one sample to another).

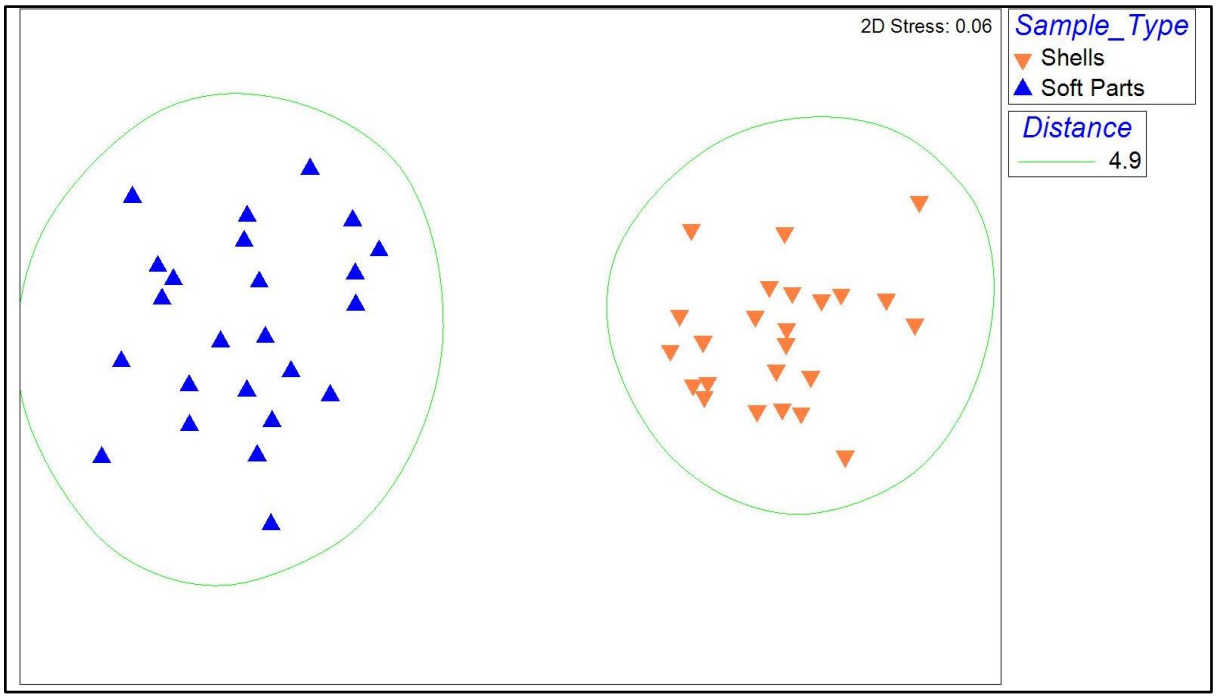

Figure 4.11: Ordination plot of all samples together.

Figure 4.11 shows an ordination plot of all samples collectively. As can be seen, two clusters clearly form separating soft part samples from shell samples. This implies that the metal profile present in the shells and that present in the soft parts differ significantly from each other and hence, further analysis can be performed treating the datasets separately.

A hierarchical cluster analysis was performed to determine any clusters of similarity between data and presented in Figure 4.12 and Figure 4.15 for soft part and shell samples respectively. A SIMPROF test was also performed which can be seen in the dendrograms with bold black lines representing statistical significance. The results of the cluster analysis were then overlaid on the respective ordination plots to visualise any similarities between samples.

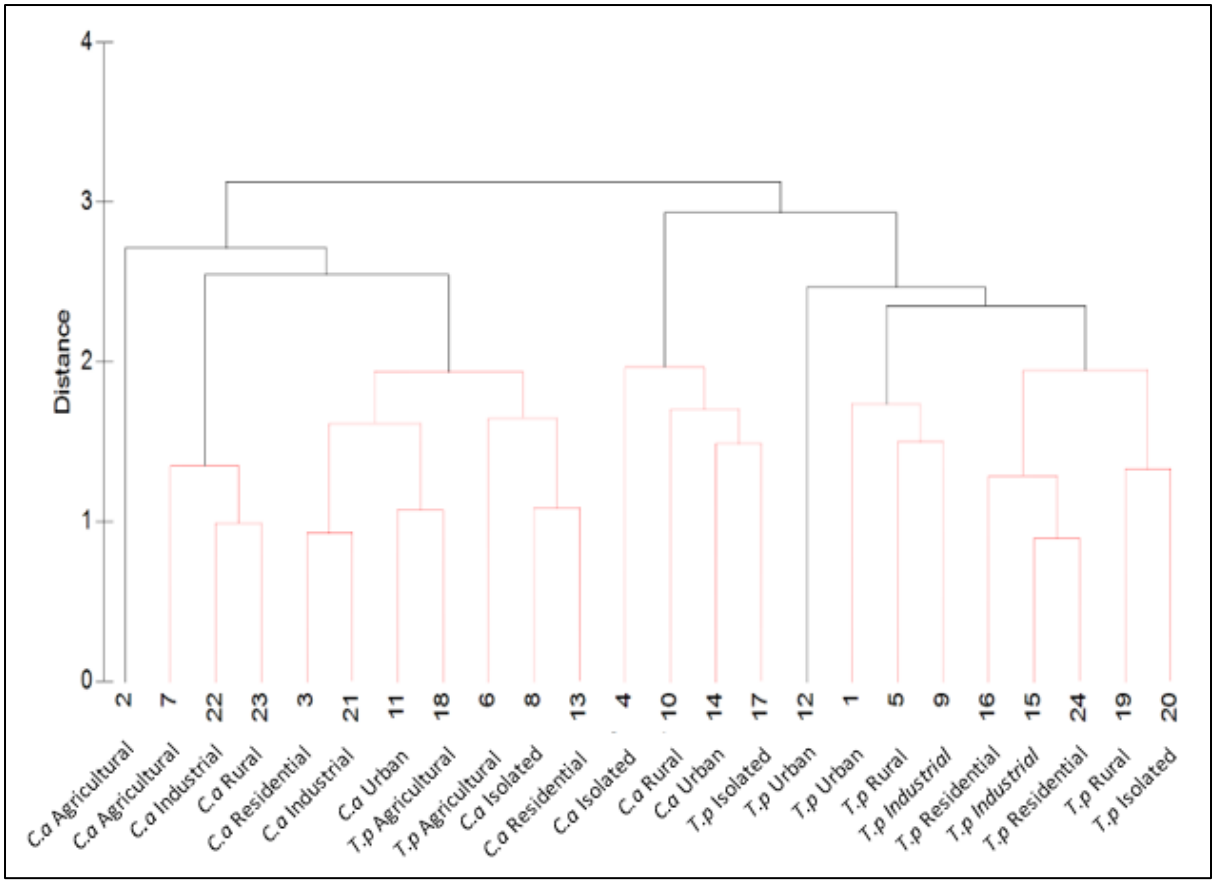

Figure 4.12: Hierarchical cluster analysis dendrogram of soft part samples with SIMPROF test.

The dendrogram in Figure 4.12 shows the possible clustering present in the soft part samples. As can be seen from the SIMPROF test, most clusters are not seen to be statistically significant until at least a Euclidean distance of about 2.5. This may be interpreted as clusters below this distance level are not significant and hence are not similar in metal profile.

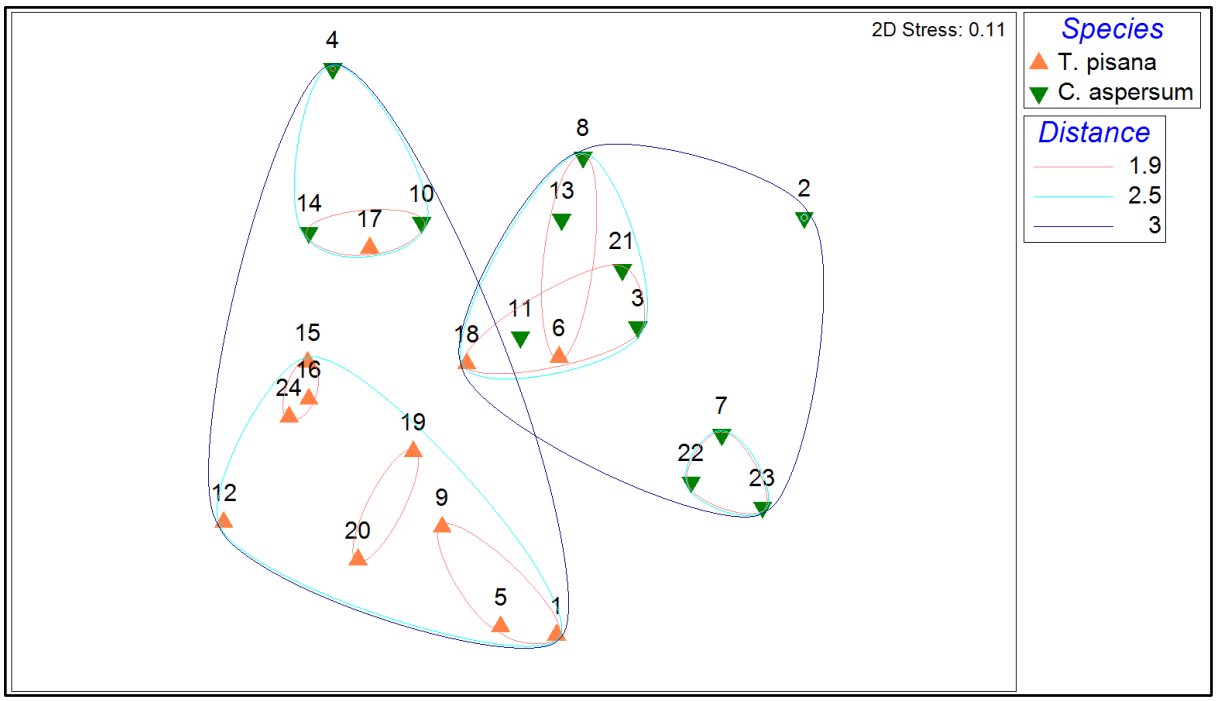

Figure 4.13: Ordination plots of soft part samples with species highlighted.

Figure 4.13 shows an ordination plot for the soft part samples, labelled according to their species. As can be observed, samples form two major groups which split the data set well according to species with some exemptions, namely samples 4, 6, 10, 14, and 18[3]. Therefore, it can be stated that there is variation between the metal profiles of the two snail species.

[3] *In Figure 4.13, sample 18 appears to be in both the T. pisana and C. aspersum clusters however in reality this is not the case. As can be seen from Figure 4.12, sample 18 is in the C. aspersum dominated cluster.*

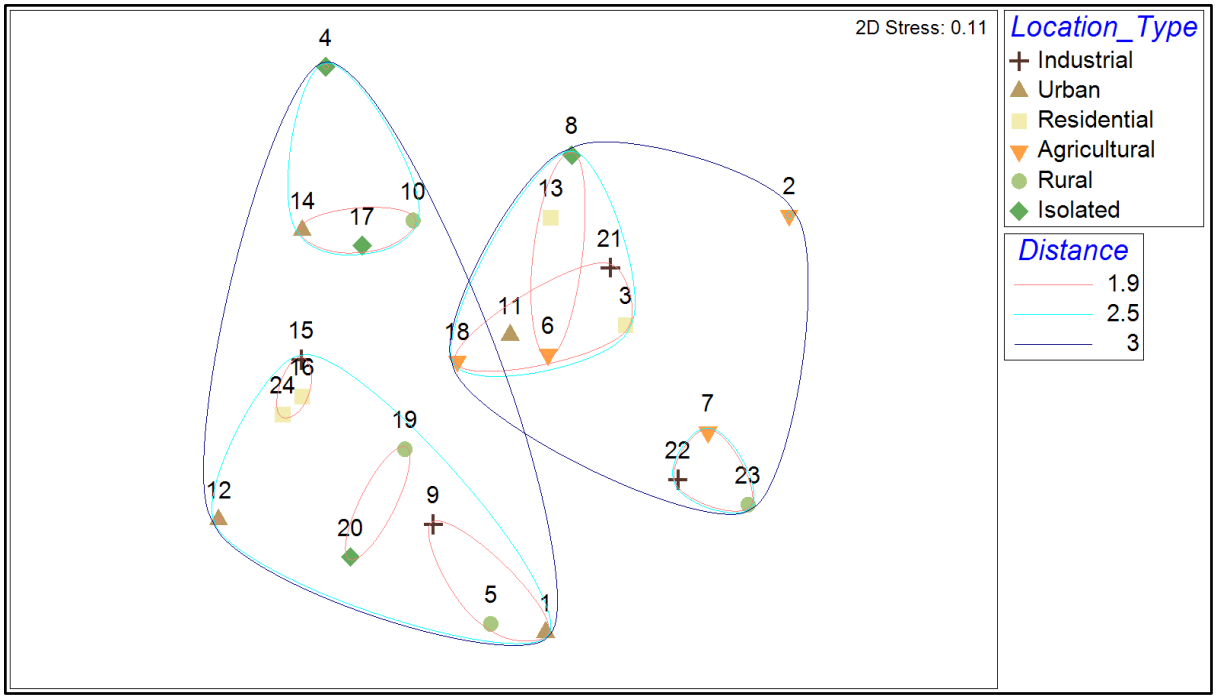

Figure 4.14: Ordination plots of soft part samples with location type highlighted.

Figure 4.14 shows the same ordination plot for the soft part samples, but this time labelled according to their location type. As can be observed, while major clusters are present, they do not correspond in any significant way to location type. In simpler terms, soft part samples from the six location types do not show variation between their metal profiles. However, the presence of these multiple clusters shows that samples are not all similar with regards to their metal profile and hence, generally speaking, samples can be considered to be significantly different to each other.

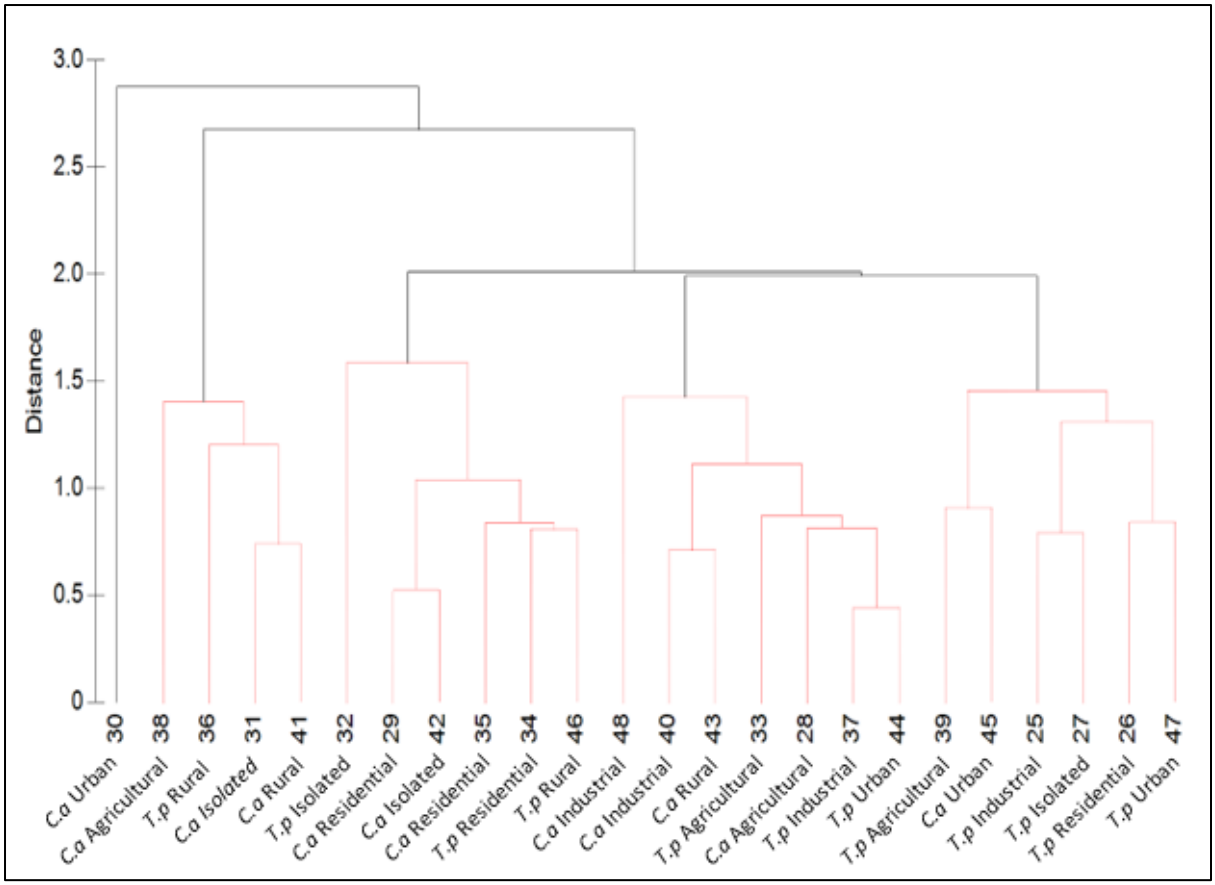

Figure 4.15: Hierarchical cluster analysis dendrogram of shell samples with SIMPROF test.

The dendrogram in Figure 4.15 shows the possible clustering present in the shell samples. As can be seen from the SIMPROF test, most clusters are not seen to be statistically significant until at least a Euclidean distance of about 2. This may be interpreted as clusters below this distance level are not significant and hence are not similar in metal profile.

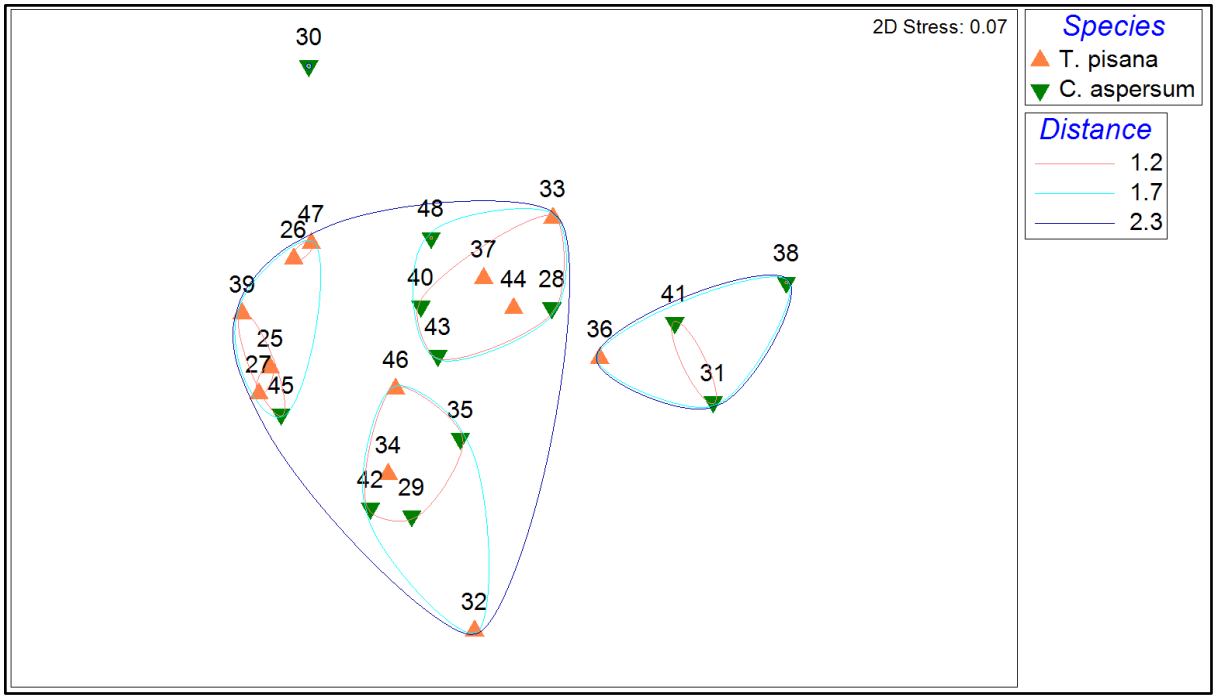

Figure 4.16: Ordination plots of shell samples with species highlighted.

Figure 4.16 shows the ordination plot for the shell samples, labelled according to their species. As can be observed, while some major clusters are present, they do not correspond in any significant way to species. I.e. there is no significant variation between the two species with regards to their metal profile. However, the presence of these multiple clusters shows that samples are not all similar with regards to their metal profile and hence, generally speaking, samples can be considered to be significantly different to each other.

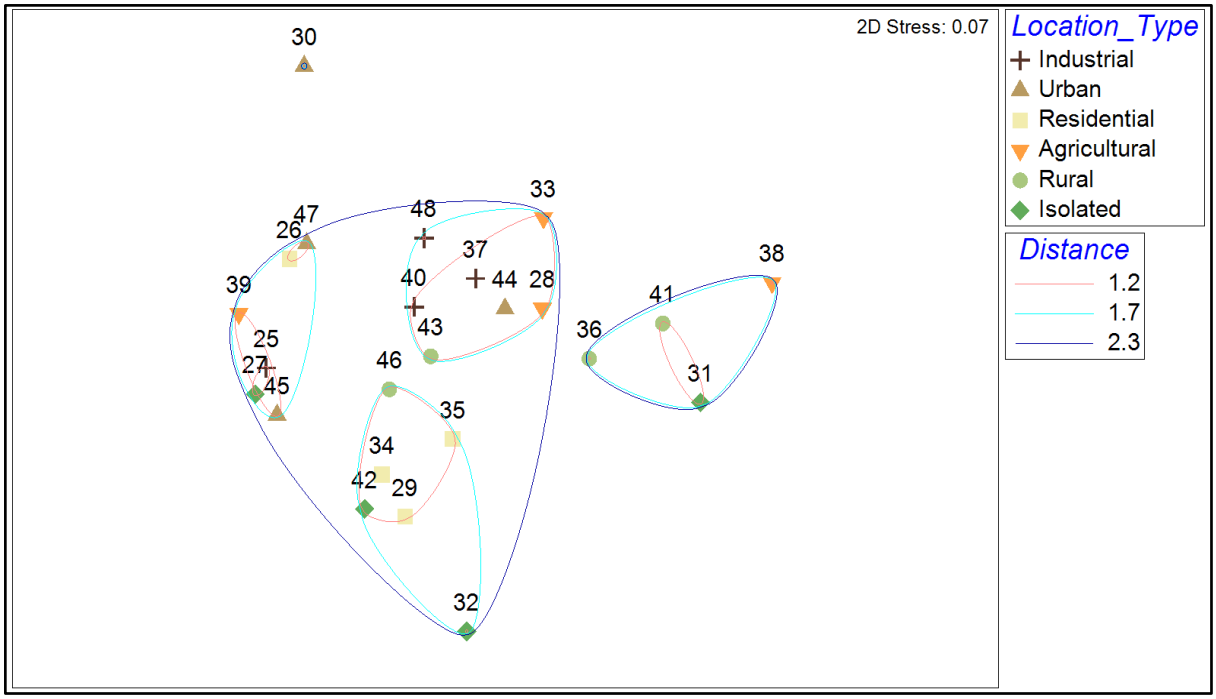

Figure 4.17: Ordination plots of shell samples with location type highlighted.

Figure 4.17 shows the same ordination plot for the shell samples, but this time labelled according to their location type. As was the case with species, while major clusters are present, they do not correspond in any significant way to location type. I.e. shell samples from the six location types do not show variation between their metal profiles. However, the presence of these multiple clusters shows that samples are not all similar with regards to their metal profile and hence, generally speaking, samples can be considered to be significantly different to each other.

4.2.3 PERMANOVA

After visual analysis and ordination plots, a statistical test was performed in the form of a PERMANOVA test using PRIMER v7 with the PERMANOVA add-on. Table 4.2 shows the results of these PERMANOVA tests with the cells highlighted showing a statistically significant difference.

Table 4.2: Results for PERMANOVA tests, highlighted cells show a statistically significant difference (α=0.05).

Metal	Soft Parts			Shells		
	Location Type	Species	Combination (Location x Species)	Location Type	Species	Combination (Location x Species)
Arsenic	0.504	0.046	0.674	0.639	0.21	0.622
Zinc	0.4763	0.5574	0.2355	0.578	0.576	0.16
Cadmium	0.303	0.032	0.778	0.181	0.367	0.803
Copper	0.182	0.187	0.415	0.13	0.149	0.879
Nickel	0.083	0.008	0.379	0.082	0.526	0.867
Lead	0.096	0.012	0.577	0.121	0.967	0.822
Chromium	0.12	0.007	0.404	0.128	0.781	0.981
Aluminium	0.03	0.014	0.5	0.89	0.635	0.739
Manganese	0.038	0.307	0.816	0.173	0.619	0.538
Barium	0.276	0.004	0.656	0.23	0.042	0.816
Vanadium				0.23	0.645	0.76
All (metal profile)	0.516	0.041	0.698	0.517	0.176	0.652

The results from the table above verify what was determined in the ordination plot of Figure 4.13 in that there is a statistically significant difference between the different species when it comes to the metal profile of soft part samples. The PERMANOVA test further revealed that this difference between species is most likely due to the metals: arsenic, cadmium, nickel, lead, chromium, aluminium, and barium. The results of Table 4.2 also verified the findings of Figure 4.14 that there is no statistically significant difference between the location types and the metal profile of soft part samples. However, there was a statistically significant difference between the location types for soft part samples for two metals, aluminium and manganese. In the case of shells, the PERMANOVA tests show that there is no statistically significant difference between the metal profile and species or location type. However, barium showed a statistically significant difference between species. The combination of both variables location type and species showed no statistically significant difference for soft part nor shell samples. For both shell and soft part samples, there was no statistical difference between any individual metal or metal profile and location type and species when considered together. In simpler terms, it could be assumed that the two species

are not affected by the particular location type they are in, with regards to metal uptake or accumulation.

4.3 Arsenic

Results were organised to show the concentration of arsenic in soft parts (Figure 4.18) and shells (Figure 4.19) for both species in each location type.

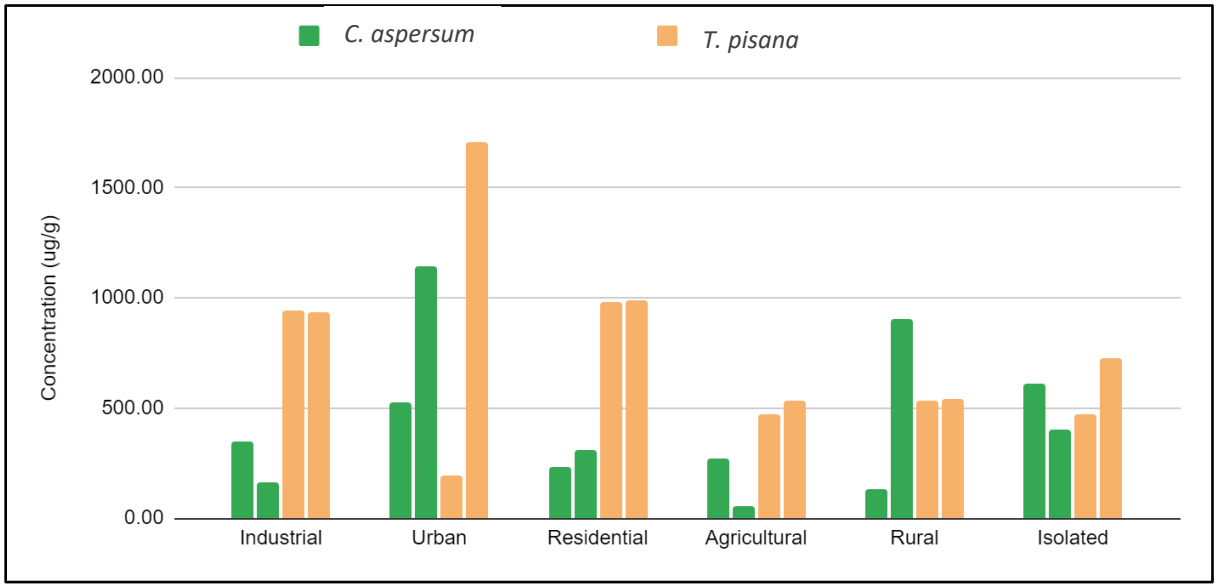

Figure 4.18: Concentration of Arsenic (µg/g) in soft parts according to species and location type. Each bar represents one sample.

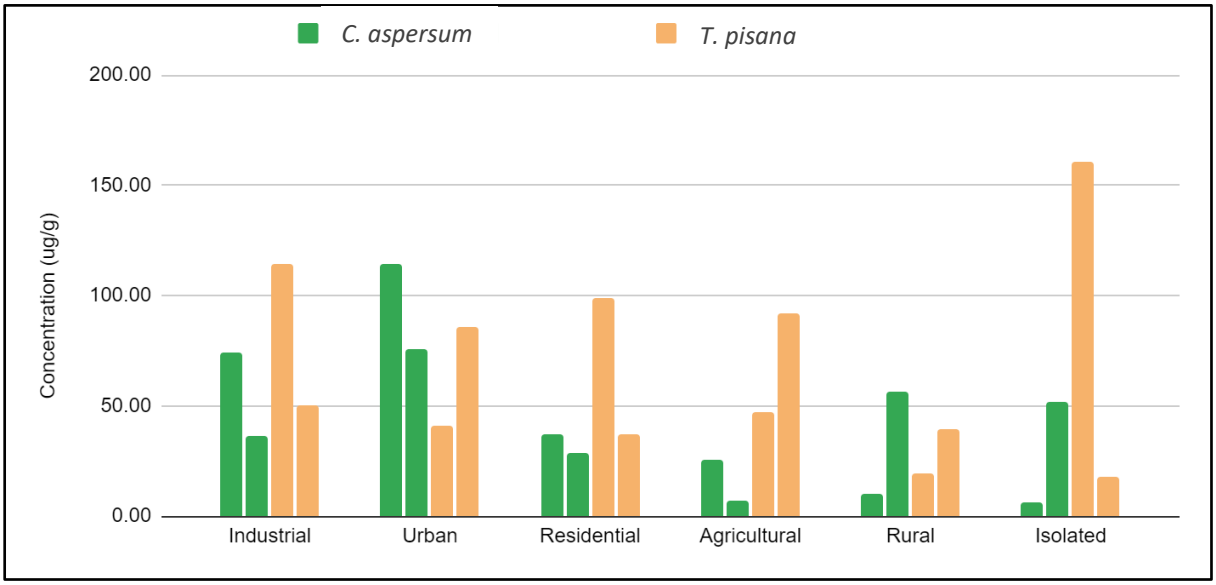

Figure 4.19: Concentration of Arsenic (µg/g) in shells according to species and location type. Each bar represents one sample.

For *C. aspersum* soft parts, the lowest value was found to be 55.65 µg/g while the highest value was 1705.28 µg/g. For *T. pisana* soft parts, the lowest value was found to be 197.38 µg/g while the highest value was 1705.28 µg/g. For *C. aspersum* shells, the lowest value was found to be 5.97 µg/g while the highest value was 114.37 µg/g. For *T. pisana* shells, the lowest value was found to be 17.99 µg/g while the highest value was 160.87 µg/g. Generally speaking, results for soft parts are approximately one order of magnitude greater than that of shells, implying that arsenic is found predominantly in the soft parts.

The PERMANOVA test determined that there was a statistically significant difference in concentration of arsenic between the two species for soft part samples. However, Figure 4.18 shows that in general, *T. pisana* samples had a higher concentration than *C. aspersum* and therefore it could be stated that arsenic uptake or accumulation is more dominant in the former species

4.4 Zinc

Results were organised to show the concentration of zinc in soft parts (Figure 4.20) and shells (Figure 4.21) for both species in each location type.

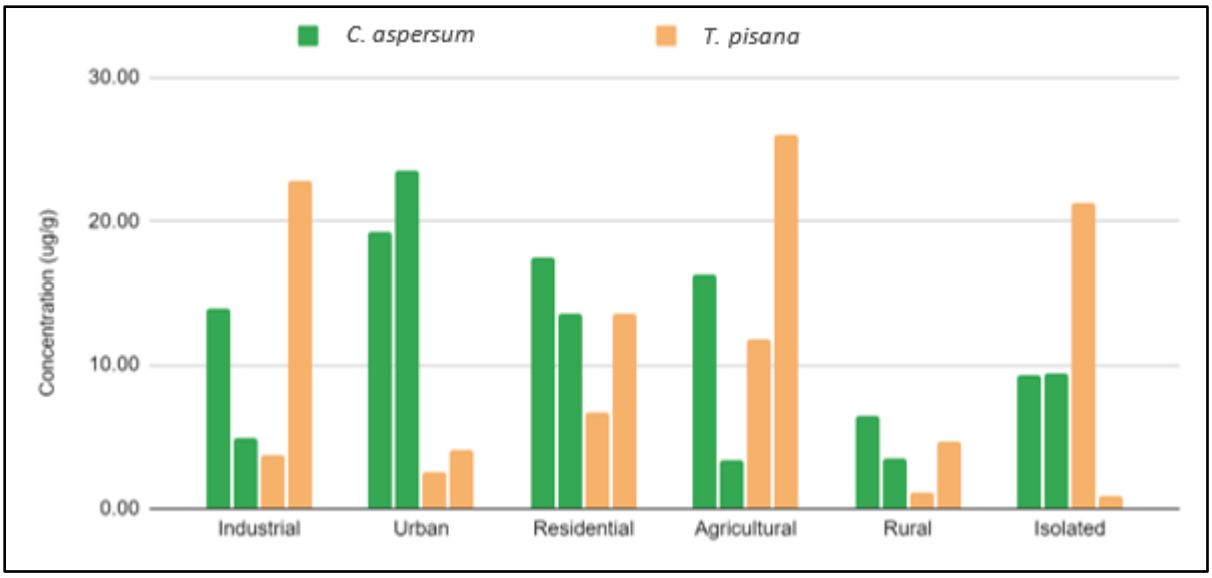

Figure 4.20: Concentration of Zinc (µg/g) in soft parts according to species and location type. Each bar represents one sample.

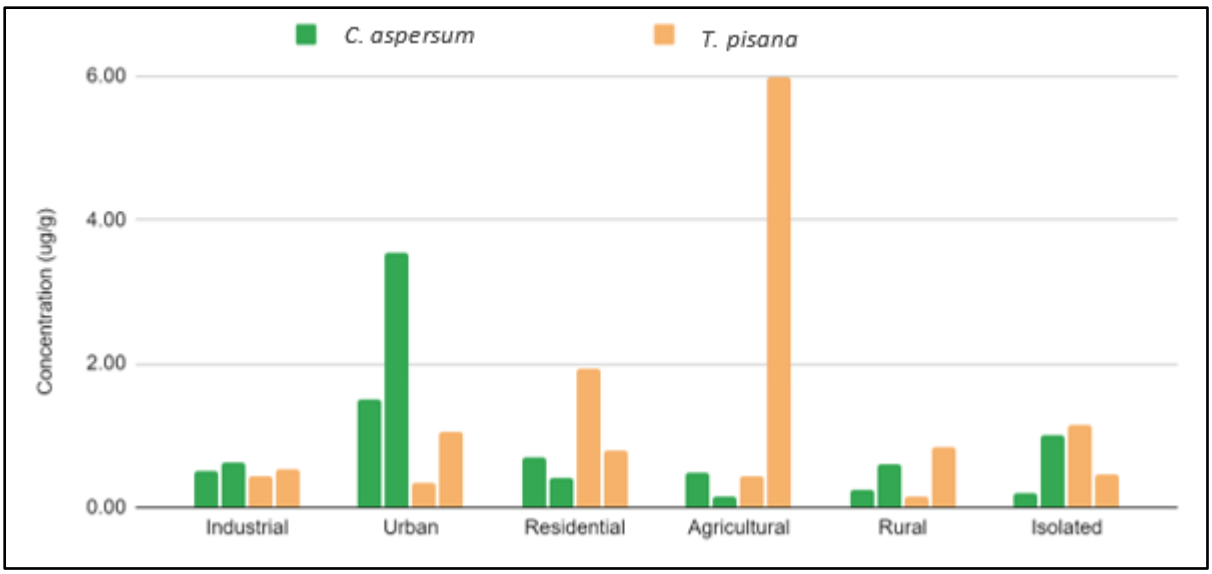

Figure 4.21: Concentration of Zinc (µg/g) in shells according to species and location type. Each bar represents one sample.

For *C. aspersum* soft parts, the lowest value was found to be 3.54 µg/g while the highest value was 23.50 µg/g. For *T. pisana* soft parts, the lowest value was found to be 0.88 µg/g while the highest value was 25.98 µg/g. For *C. aspersum* shells, the lowest value was found to be 0.16 µg/g while the highest value was 3.54 µg/g. For *T. pisana* shells, the lowest value was found to be 0.15 µg/g while the highest value was 5.99 µg/g. Generally speaking, results for soft parts are greater than that of shells, implying that zinc is found predominantly in the soft parts.

As was seen in the PERMANOVA test of Table 4.2 and further supported from the bar graphs of Figure 4.20 and Figure 4.21, there was no statistically significant difference in concentration of zinc between the two species for soft part or shell samples. Therefore, it cannot be stated whether one species is more dominant to the uptake or accumulation of zinc than the other.

4.5 Cadmium

Results were organised to show the concentration of cadmium in soft parts (Figure 4.22) and shells (Figure 4.23) for both species in each location type.

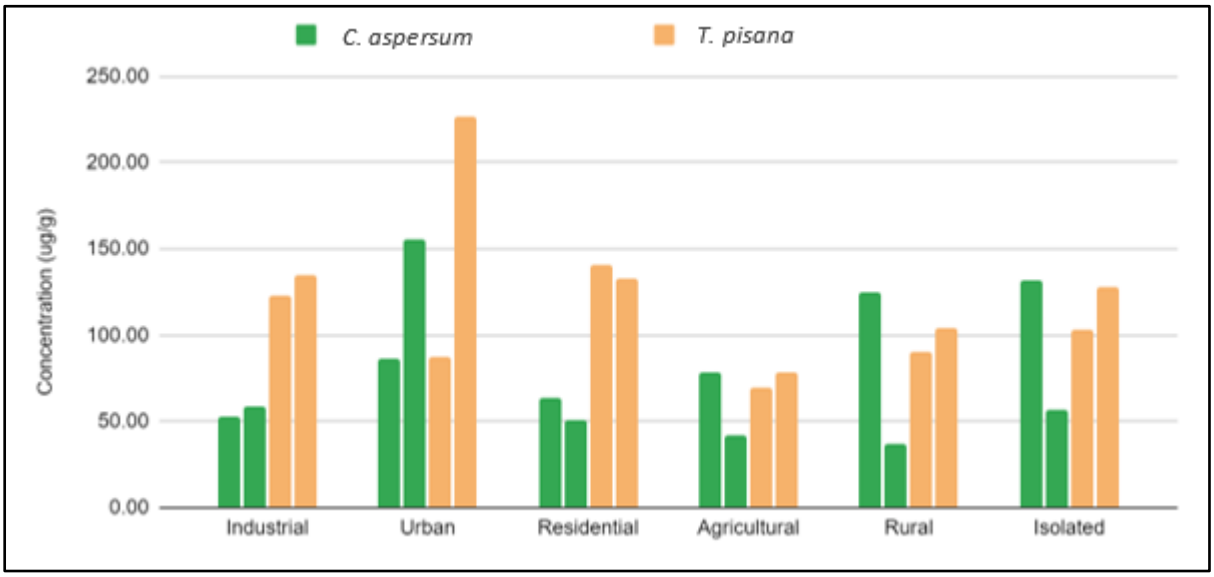

Figure 4.22: Concentration of Cadmium (µg/g) in soft parts according to species and location type. Each bar represents one sample.

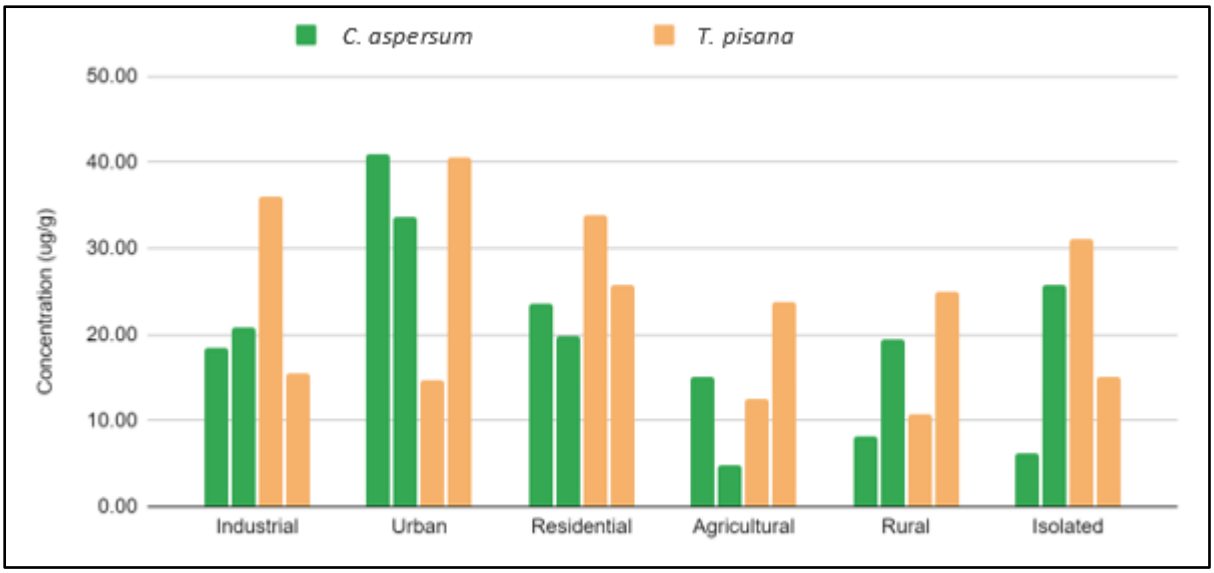

Figure 4.23: Concentration of Cadmium (µg/g) in shells according to species and location type. Each bar represents one sample.

For *C. aspersum* soft parts, the lowest value was found to be 37.20 µg/g while the highest value was 155.56 µg/g. For *T. pisana* soft parts, the lowest value was found to be 69.94 µg/g while the highest value was 226.43 µg/g. For *C. aspersum* shells, the lowest value was found to be 4.82 µg/g while the highest value was 41.04 µg/g. For *T. pisana* shells, the lowest value was found to be 10.83 µg/g while the highest value was 40.54 µg/g. Generally speaking, results for soft parts are greater than that of shells, implying that cadmium is found predominantly in the soft parts.

The PERMANOVA test determined that there was a statistically significant difference in concentration of cadmium between the two species for soft part samples. However, Figure 4.22 shows that in general, *T. pisana* samples had a higher concentration than *C. aspersum* and therefore it could be stated that cadmium uptake or accumulation is more dominant in the former species.

4.6 Copper

Results were organised to show the concentration of copper in soft parts (Figure 4.24) and shells (Figure 4.25) for both species in each location type.

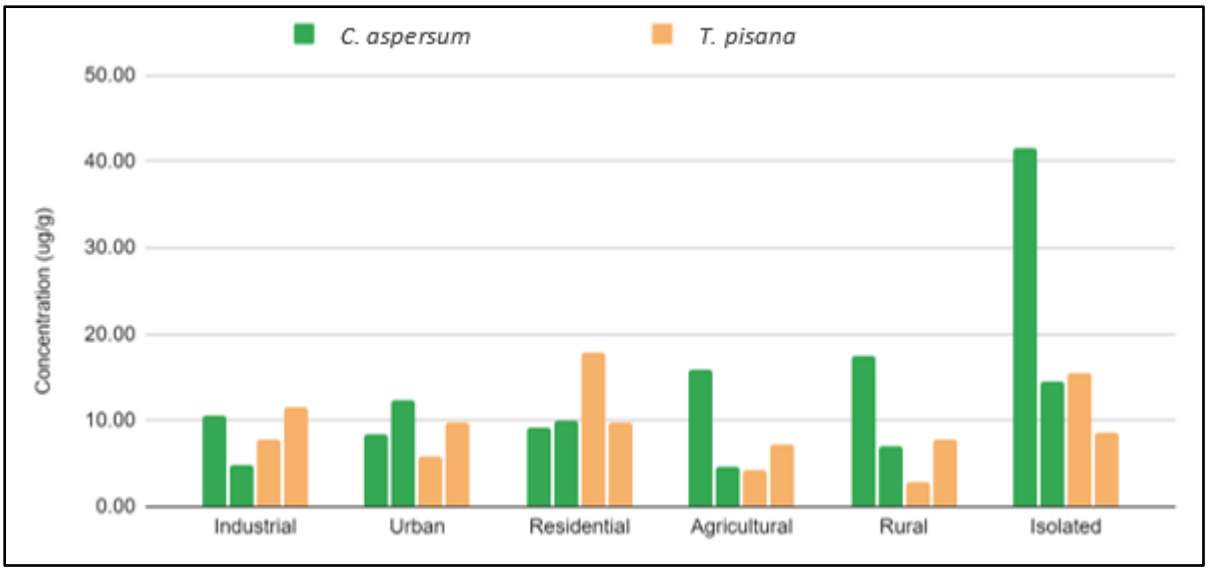

Figure 4.24: Concentration of Copper (µg/g) in soft parts according to species and location type. Each bar represents one sample.

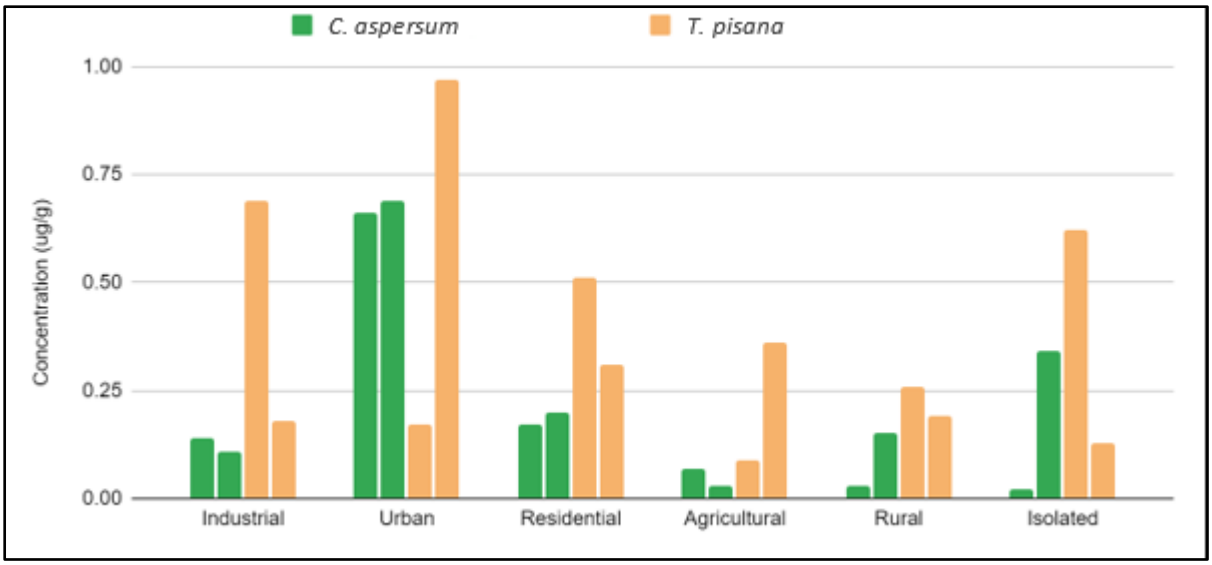

Figure 4.25: Concentration of Copper (µg/g) in shells according to species and location type. Each bar represents one sample.

For *C. aspersum* soft parts, the lowest value was found to be 4.58 µg/g while the highest value was 41.58 µg/g. For *T. pisana* soft parts, the lowest value was found to be 2.82 µg/g while the highest value was 17.78 µg/g. For *C. aspersum* shells, the lowest value was found to be 0.02 µg/g while the highest value was 0.69 µg/g. For *T. pisana* shells, the lowest value was found to be 0.09 µg/g while the highest value was 0.97 µg/g. Generally speaking, results for soft parts are greater than that of shells, implying that copper is found predominantly in the soft parts.

As was seen in the PERMANOVA test of Table 4.2 and further supported from the bar graphs of Figure 4.24 and Figure 4.25, there was no statistically significant difference in concentration of copper between the two species for soft part or shell samples. Therefore, it cannot be stated whether one species is more dominant to the uptake or accumulation of copper than the other.

4.7 Nickel

Results were organised to show the concentration of nickel in soft parts (Figure 4.26) and shells (Figure 4.27) for both species in each location type.

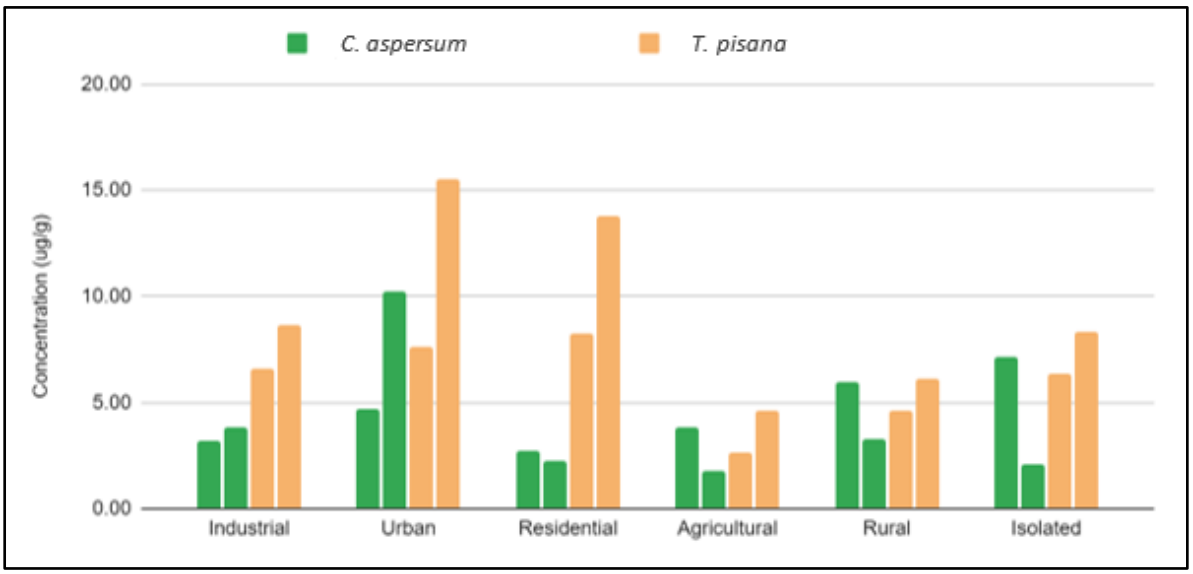

Figure 4.26: Concentration of Nickel (µg/g) in soft parts according to species and location type. Each bar represents one sample.

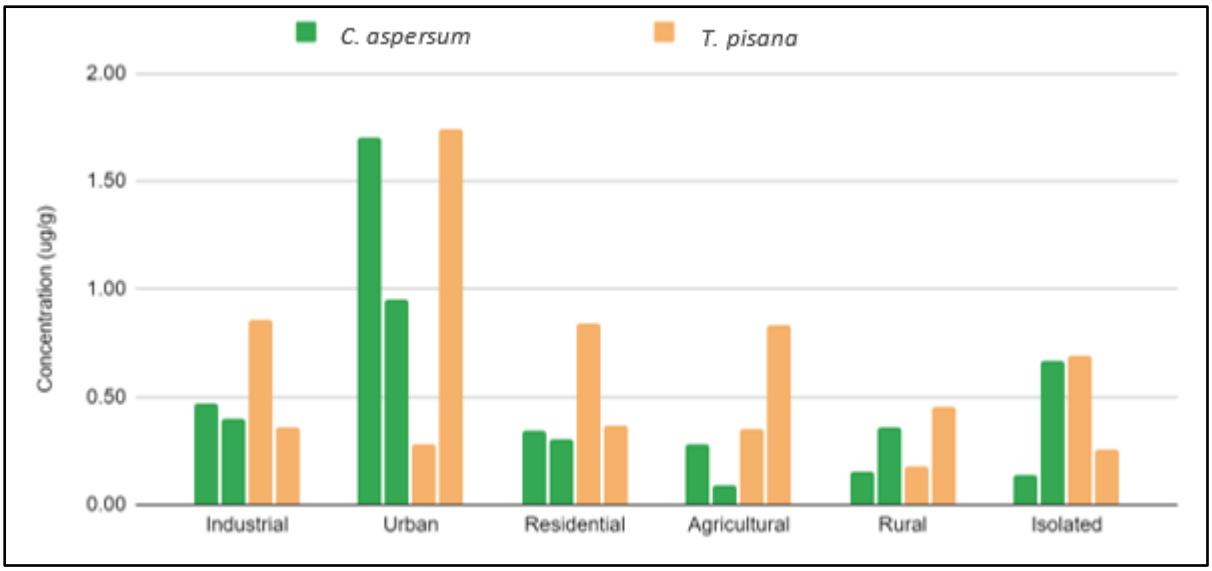

Figure 4.27: Concentration of Nickel (µg/g) in shells according to species and location type. Each bar represents one sample.

For *C. aspersum* soft parts, the lowest value was found to be 1.75 µg/g while the highest value was 10.26 µg/g. For *T. pisana* soft parts, the lowest value was found to be 2.66 µg/g while the highest value was 15.54 µg/g. For *C. aspersum* shells, the lowest value was found to be 0.09 µg/g while the highest value was 1.70 µg/g. For *T. pisana* shells, the lowest value was found to be 0.18 µg/g while the highest value was 1.74 µg/g. Generally speaking, results for soft parts are greater than that of shells, implying that nickel is found predominantly in the soft parts.

The PERMANOVA test determined that there was a statistically significant difference in concentration of nickel between the two species for soft part samples. However, Figure 4.26 shows that in general, *T. pisana* samples had a higher concentration than *C. aspersum* and therefore it could be stated that nickel uptake or accumulation is more dominant in the former species.

4.8 Lead

Results were organised to show the concentration of lead in soft parts (Figure 4.28) and shells (Figure 4.29) for both species in each location type.

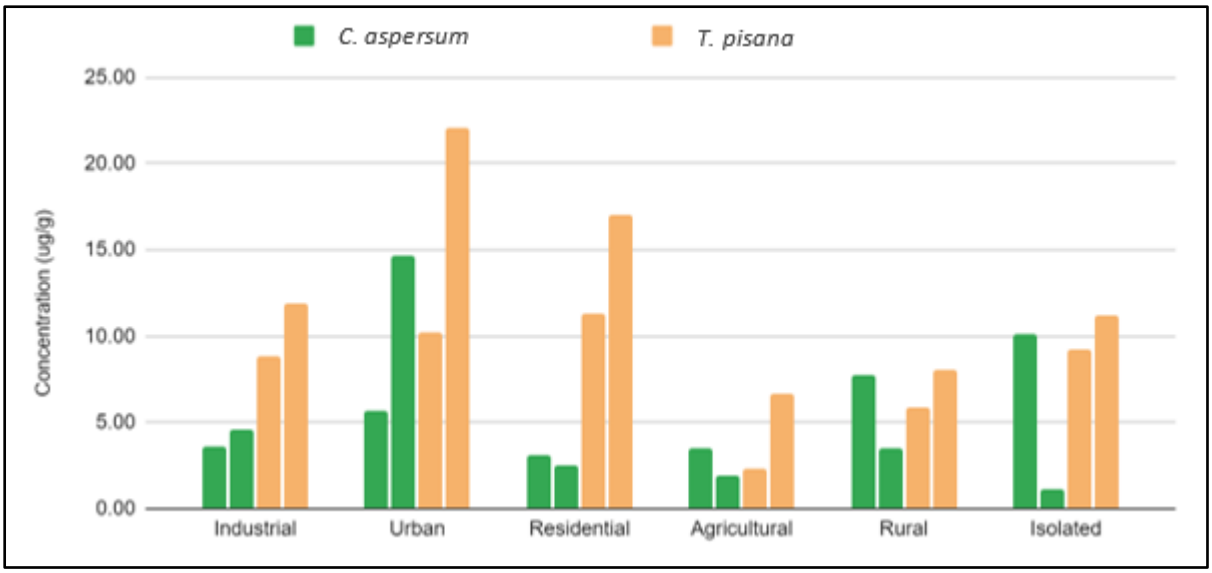

Figure 4.28: Concentration of Lead (µg/g) in soft parts according to species and location type. Each bar represents one sample.

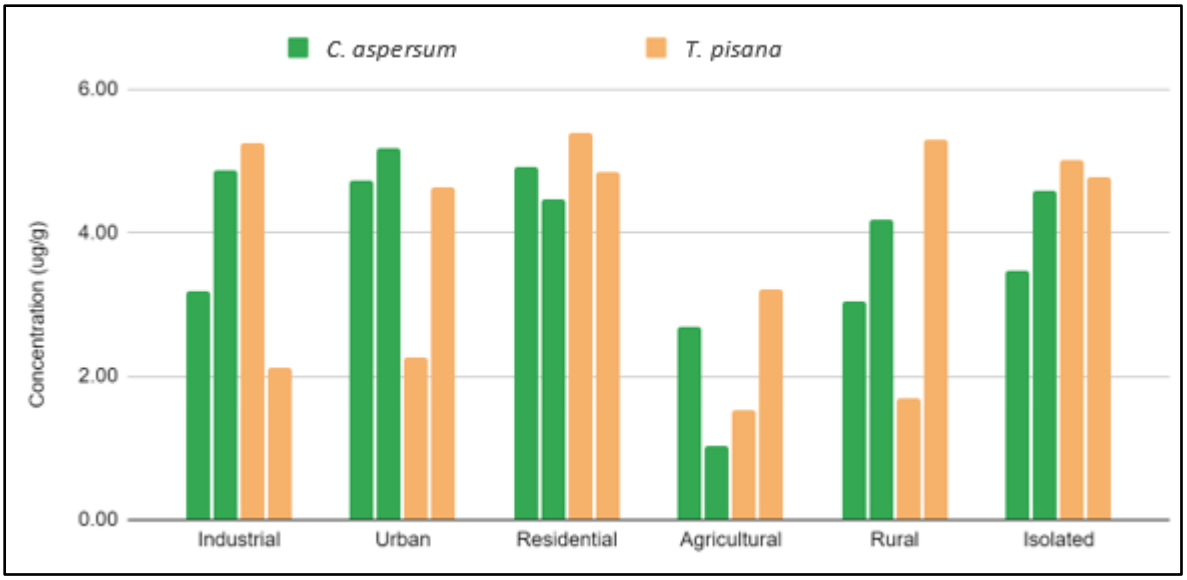

Figure 4.29: Concentration of Lead (µg/g) in shells according to species and location type. Each bar represents one sample.

For *C. aspersum* soft parts, the lowest value was found to be 1.15 µg/g while the highest value was 14.70 µg/g. For *T. pisana* soft parts, the lowest value was found to be 2.35 µg/g while the highest value was 22.02 µg/g. For *C. aspersum* shells, the lowest value was found to be 1.03 µg/g while the highest value was 5.18 µg/g. For *T. pisana* shells, the lowest value was found to be 1.52 µg/g while the highest value was 5.25 µg/g. Generally speaking, results for soft parts are greater than that of shells, implying that lead is found predominantly in the soft parts.

The PERMANOVA test determined that there was a statistically significant difference in concentration of lead between the two species for soft part samples. However, Figure 4.28 shows that in general, *T. pisana* samples had a higher concentration than *C. aspersum* and therefore it could be stated that lead uptake or accumulation is more dominant in the former species.

4.9 Chromium

Results were organised to show the concentration of chromium in soft parts (Figure 4.30) and shells (Figure 4.31) for both species in each location type.

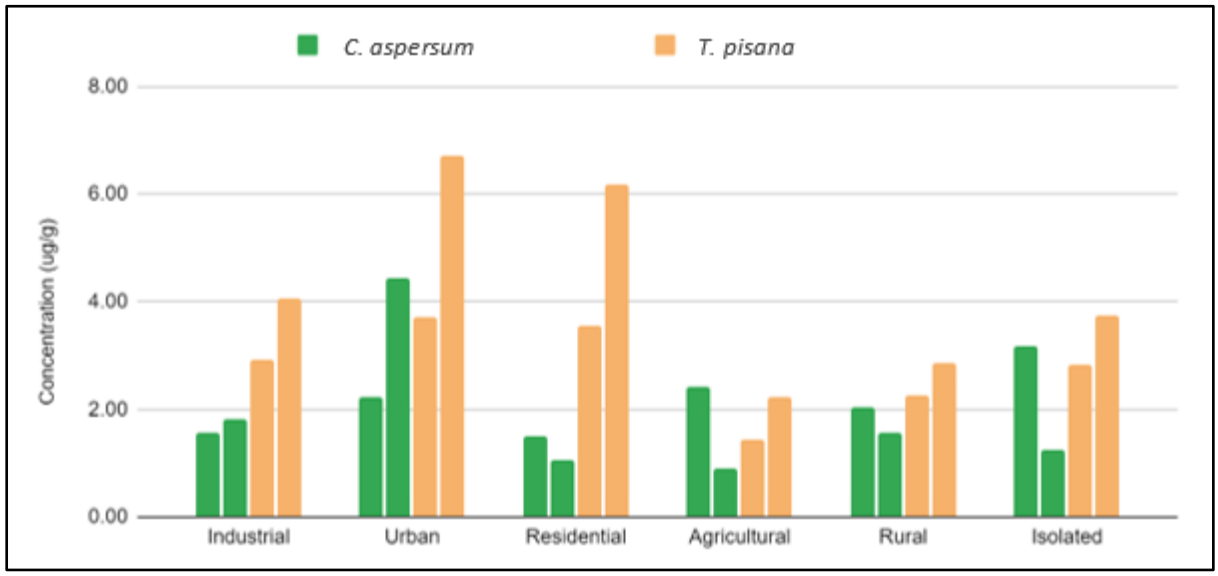

Figure 4.30: Concentration of Chromium (µg/g) in soft parts according to species and location type. Each bar represents one sample.

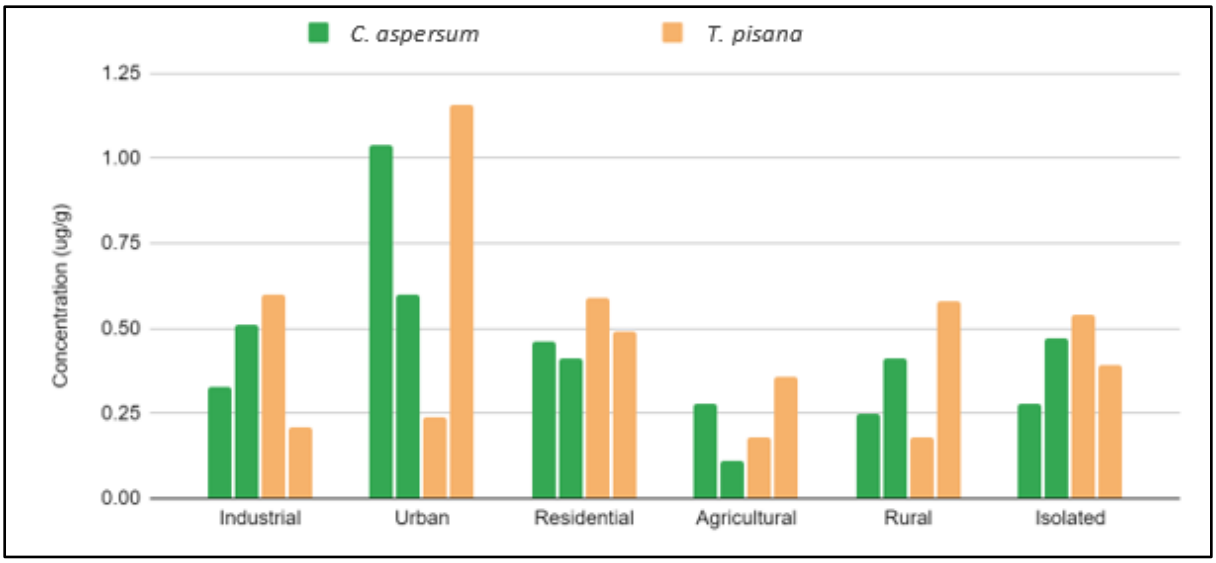

Figure 4.31: Concentration of Chromium (µg/g) in shells according to species and location type. Each bar represents one sample.

For *C. aspersum* soft parts, the lowest value was found to be 0.90 µg/g while the highest value was 4.44 µg/g. For *T. pisana* soft parts, the lowest value was found to be 1.43 µg/g while the highest value was 6.71 µg/g. For *C. aspersum* shells, the lowest value was found to be 0.11 µg/g while the highest value was 1.04 µg/g. For *T. pisana* shells, the lowest value was found to be 0.18 µg/g while the highest value was 1.16 µg/g. Generally speaking, results for soft parts are greater than that of shells, implying that chromium is found predominantly in the soft parts.

The PERMANOVA test determined that there was a statistically significant difference in concentration of chromium between the two species for soft part samples. However, Figure 4.30 shows that in general, *T. pisana* samples had a higher concentration than *C. aspersum* and therefore it could be stated that chromium uptake or accumulation is more dominant in the former species.

4.10 Aluminium

Results were organised to show the concentration of aluminium in soft parts (Figure 4.32) and shells (Figure 4.33) for both species in each location type.

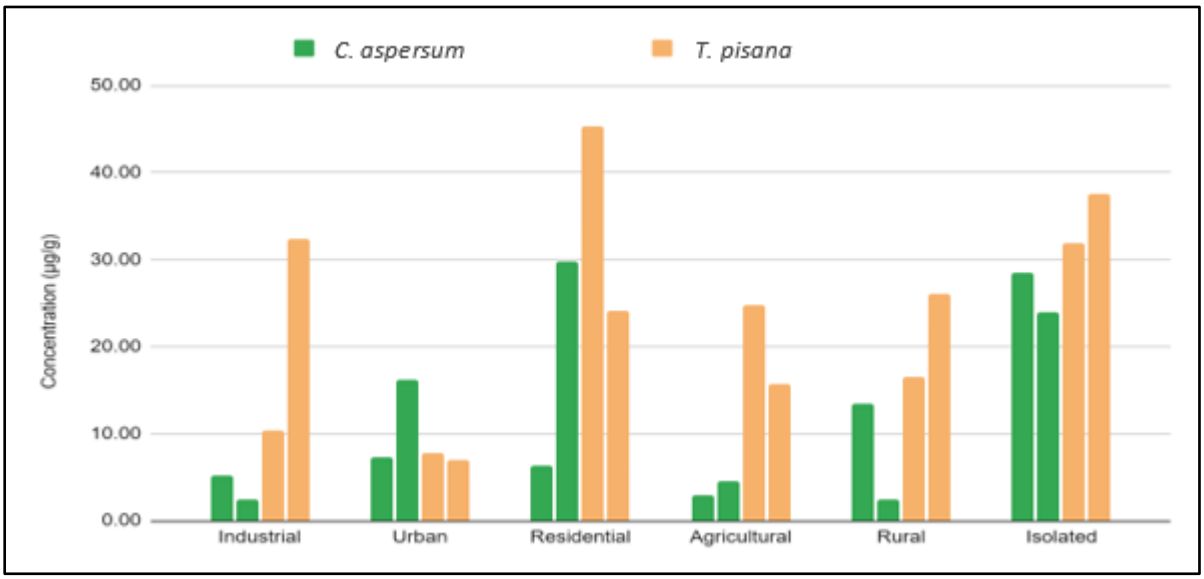

Figure 4.32: Concentration of Aluminium (µg/g) in soft parts according to species and location type. Each bar represents one sample.

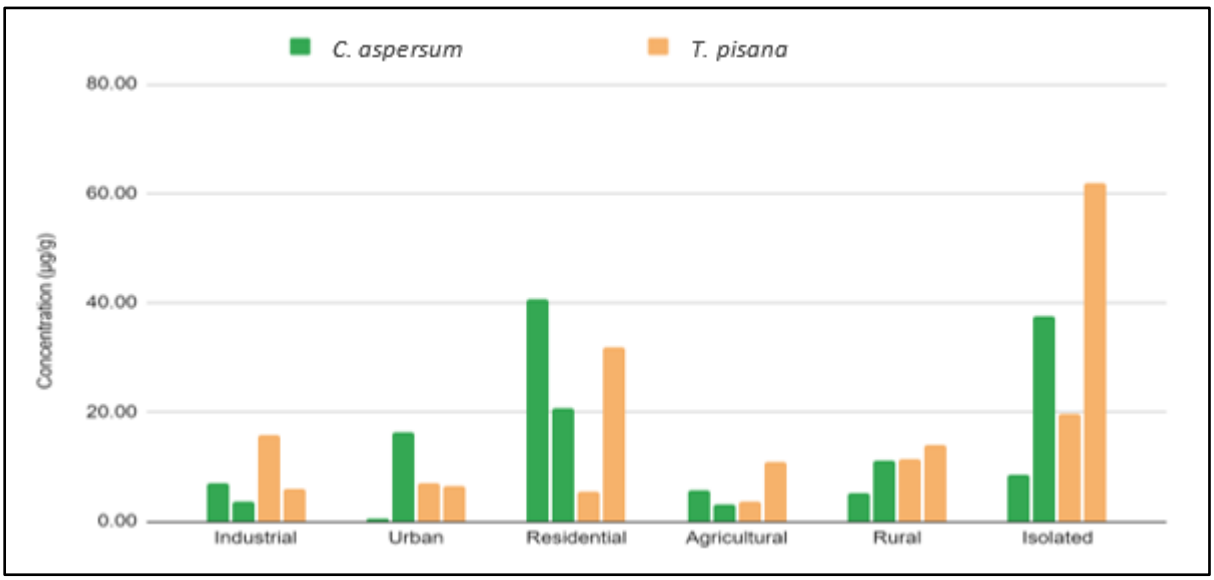

Figure 4.33: Concentration of Aluminium (µg/g) in shells according to species and location type. Each bar represents one sample.

For *C. aspersum* soft parts, the lowest value was found to be 2.39 µg/g while the highest value was 29.80 µg/g. For *T. pisana* soft parts, the lowest value was found to be 7.04 µg/g while the highest value was 45.33 µg/g. For *C. aspersum* shells, the lowest value was found to be 0.66 µg/g while the highest value was 40.69 µg/g. For *T. pisana* shells, the lowest value was found to be 3.68 µg/g while the highest value was 61.94 µg/g. Generally speaking, results for soft parts are greater than that of shells, implying that aluminium is found predominantly in the soft parts.

The PERMANOVA test determined that there was a statistically significant difference in concentration of aluminium between the two species for soft part samples. However, Figure 4.32 shows that in general, *T. pisana* samples had a higher concentration than *C. aspersum* and therefore it could be stated that aluminium uptake or accumulation is more dominant in the former species.

The PERMANOVA test also determined that there was a statistically significant difference in concentration of aluminium between the location types. However, it does not indicate where this difference is coming from. For that, a Dunn's post-hoc test[4] was conducted (Table 4.3).

Table 4.3: Dunn's post-hoc test for aluminium soft part samples. Highlighted cells show a statistically significant difference (α=0.05).

Location Type	Industrial	Urban	Residential	Agricultural	Rural	Isolated
Industrial		0.9203	0.1770	0.8808	0.8026	0.0512
Urban	0.9203		0.1471	0.9601	0.7263	0.0404
Residential	0.1770	0.1471		0.1336	0.2713	0.5485
Agricultural	0.8808	0.9601	0.1336		0.6892	0.0357
Rural	0.8026	0.7263	0.2713	0.6892		0.0891
Isolated	0.0512	0.0404	0.5485	0.0357	0.0891	

This shows that the difference is between isolated locations with urban and agricultural locations.

[4] *It is important to note that the Dunn test is not being used for its traditional role as, for the reasons mentioned in section 3.4, an ANOVA test cannot be run on this dataset.*

4.11 Manganese

Results were organised to show the concentration of manganese in soft parts (Figure 4.34) and shells (Figure 4.35) for both species in each location type.

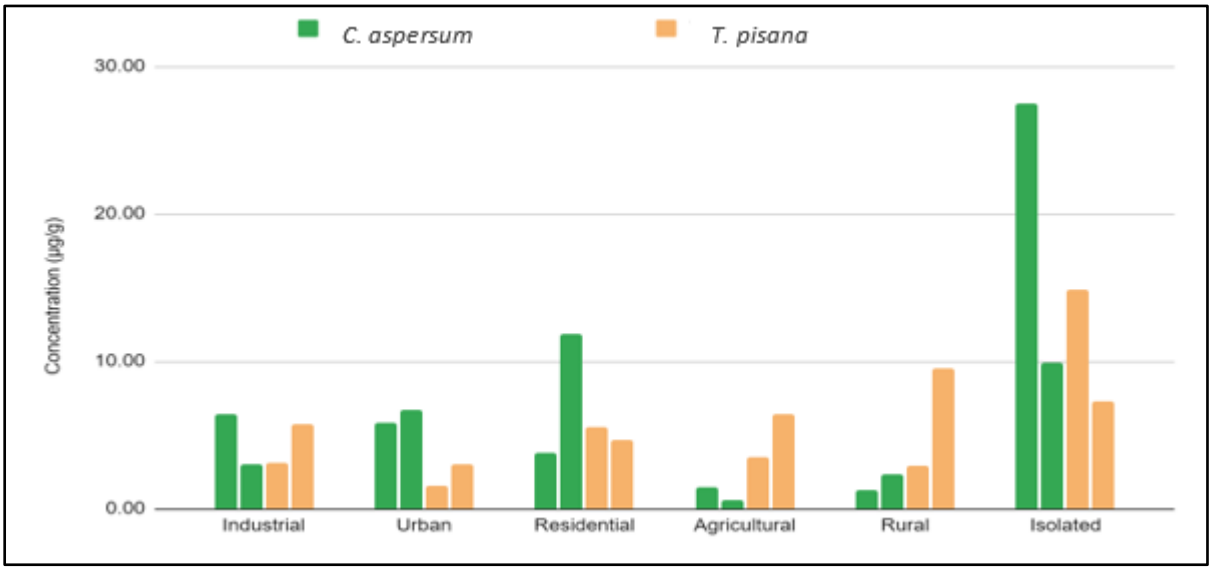

Figure 4.34: Concentration of Manganese (µg/g) in soft parts according to species and location type. Each bar represents one sample.

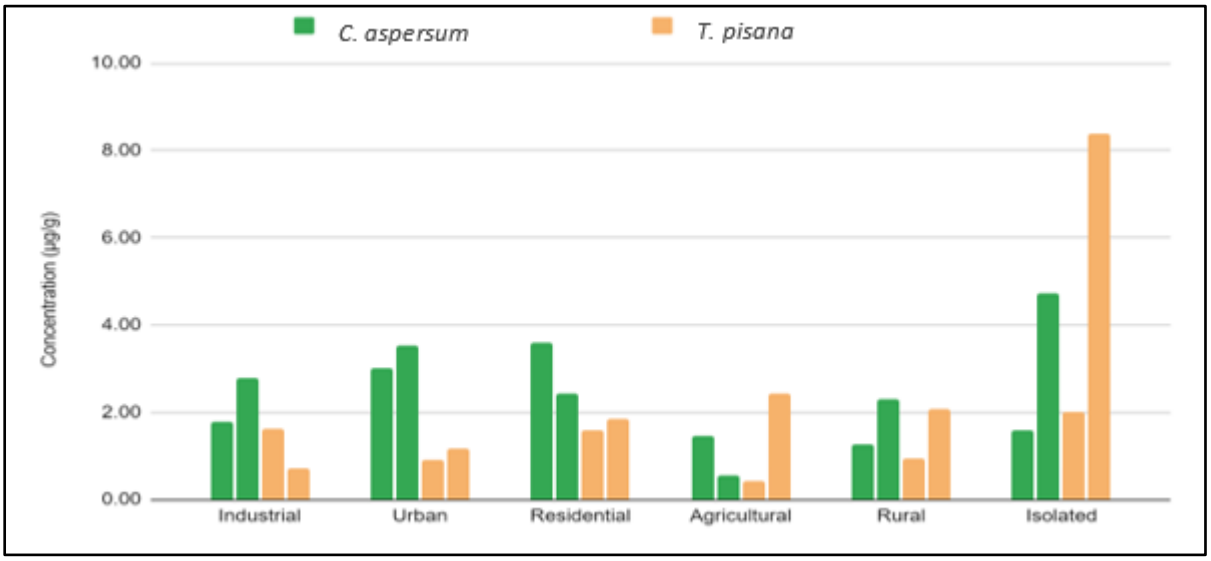

Figure 4.35: Concentration of Manganese (µg/g) in shells according to species and location type. Each bar represents one sample.

For *C. aspersum* soft parts, the lowest value was found to be 0.55 µg/g while the highest value was 27.52 µg/g. For *T. pisana* soft parts, the lowest value was found to be 1.52 µg/g while the highest value was 14.84 µg/g. For *C. aspersum* shells, the lowest value was

found to be 0.55 µg/g while the highest value was 4.72 µg/g. For *T. pisana* shells, the lowest value was found to be 0.44 µg/g while the highest value was 8.39 µg/g.

As was seen in the PERMANOVA test of Table 4.2 and further supported from the bar graphs of Figure 4.34 and Figure 4.35, there was no statistically significant difference in concentration of manganese between the two species for soft part or shell samples. Therefore, it cannot be stated whether one species is more dominant to the uptake or accumulation of manganese than the other.

The PERMANOVA test also determined that there was a statistically significant difference in concentration of manganese between the location types. However, it does not indicate where this difference is coming from. For that, a Dunn's post-hoc test[5] was conducted (Table 4.4).

Table 4.4: Dunn's post-hoc test for manganese soft part samples. Highlighted cells show a statistically significant difference (α=0.05).

Location Type	Industrial	Urban	Residential	Agricultural	Rural	Isolated
Industrial		0.8415	0.6171	0.3681	0.4533	0.0512
Urban	0.8415		0.4839	0.4839	0.5823	0.0316
Residential	0.6171	0.4839		0.1615	0.2113	0.1471
Agricultural	0.3681	0.4839	0.1615		0.8808	0.0044
Rural	0.4533	0.5823	0.2113	0.8808		0.0069
Isolated	0.0512	0.0316	0.1471	0.0044	0.0069	

This shows that the difference is between isolated locations with urban, agricultural, and rural locations.

[5]*It is important to note that the Dunn test is not being used for its traditional role as, for the reasons mentioned in section 3.4, an ANOVA test cannot be run on this dataset.*

4.12 Barium

Results were organised to show the concentration of barium in soft parts (Figure 4.37) and shells (Figure 4.38) for both species in each location type.

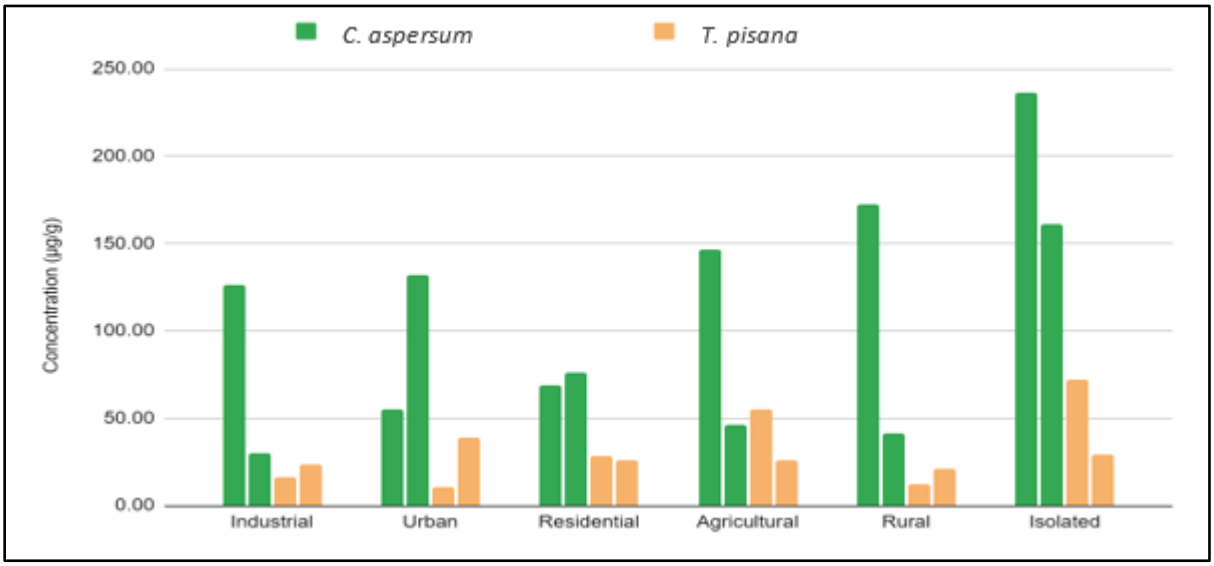

Figure 4.36: Concentration of Barium (µg/g) in soft parts according to species and location type. Each bar represents one sample.

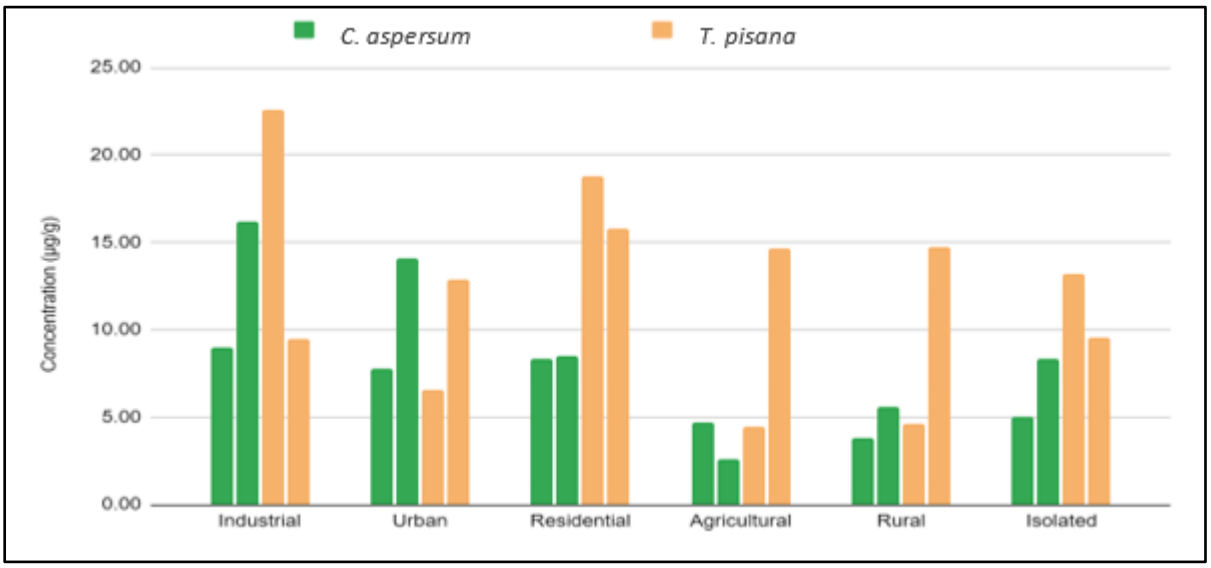

Figure 4.37: Concentration of Barium (µg/g) in shells according to species and location type. Each bar represents one sample.

For *C. aspersum* soft parts, the lowest value was found to be 29.97 µg/g while the highest value was 236.04 µg/g. For *T. pisana* soft parts, the lowest value was found to be 10.47 µg/g while the highest value was 72.11 µg/g. For *C. aspersum* shells, the lowest value

was found to be 2.58 µg/g while the highest value was 16.17 µg/g. For *T. pisana* shells, the lowest value was found to be 4.43 µg/g while the highest value was 22.62 µg/g. Generally speaking, results for soft parts are greater than that of shells, implying that barium is found predominantly in the soft parts.

The PERMANOVA test determined that there was a statistically significant difference in concentration of barium between the two species for soft part samples. However, Figure 4.37 shows that in general, *T. pisana* samples had a lower concentration than *C. aspersum* and therefore it could be stated that barium uptake or accumulation is more dominant in the latter species.

4.13 Vanadium

Results were organised to show the concentration of vanadium in shells (Figure 4.36) for both species in each location type. Concentrations of vanadium in soft parts for both species were not found at concentrations significant enough for detection and analysis and hence were excluded.

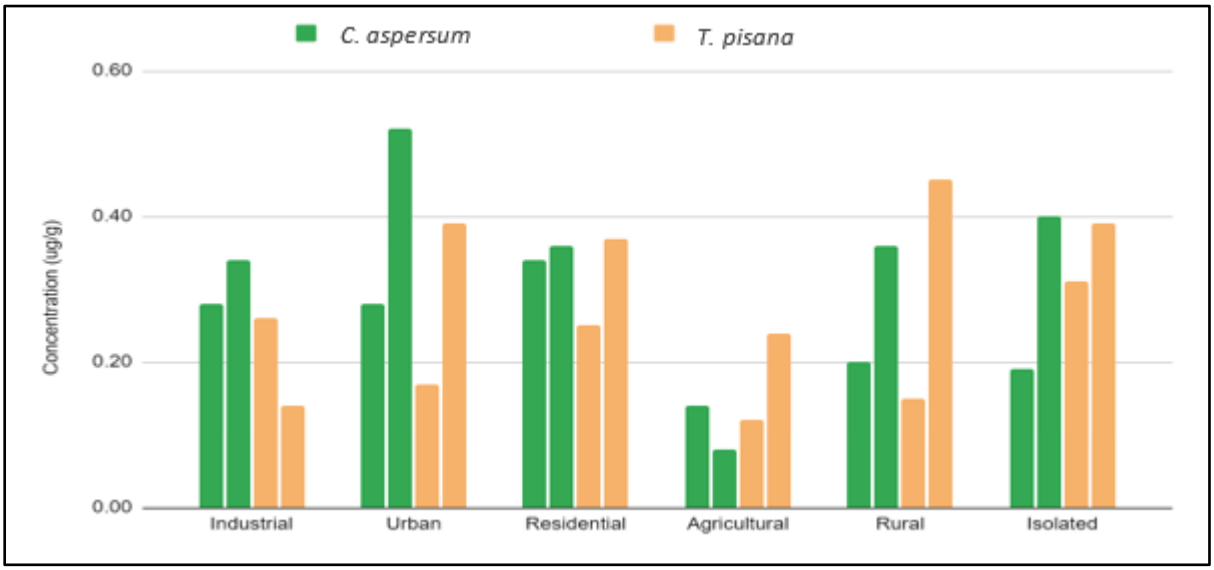

Figure 4.38: Concentration of Vanadium (µg/g) in shells according to species and location type. Each bar represents one sample.

For *C. aspersum* shells, the lowest value was found to be 0.08 µg/g while the highest value was 0.52 µg/g. For *T. pisana* shells, the lowest value was found to be 0.12 µg/g while

the highest value was 0.45 µg/g. Since concentrations of vanadium in soft parts were not present in concentrations significant enough for the MP-AES to detect but were in shells, it can be assumed that vanadium is found predominantly in the shells.

5. Discussion

5.1 Preamble

Building up from the results presented in the previous chapter, some preliminary statements should be addressed before discussing the results in further detail. Firstly, due to the significant difference exemplified between soft part samples and shell samples (Figure 4.11), the two sample types will be treated as their own separate groups. Conversely, there was no evidence to suggest any grouping or statistical significance between the location types (Figures 4.14 and 4.16 as well as in Table 4.2). Therefore, it could be stated that the classification of each location type was arbitrary to the data and hence results will not be discussed in relation to location type unless pertinent.

Results of this study will be compared to mainly two studies, Briffa (2020) and Tardugno et al. (2023) due to their similarities with this study. However, it would be remiss to not also highlight the inherent differences. Briffa (2020) focused on heavy metals in Maltese agricultural soils which would influence snails directly due to soil being considered a part of the snail's diet and has a large impact on their health and growth (Dallinger et al., 2001). However, in this study snails were collected from a variety of situations, some without any soil present in their immediate surroundings. In addition, this study collected snails from localities that were not sampled by Briffa (2020), namely Birkirkara, Marsa, and Msida, due to no agricultural soil being present, which was a limitation this study did not share. Regardless of these differences, this was the most comprehensive and modern soil analysis for heavy metal content in Malta which could be found and due also to the fact of Malta's small size, for comparison's sake results were assumed to be analogous to the overall situation of soils in Malta.

In the case of Tardugno (2023), the study bears some striking similarities with this study. Both studies investigate total heavy metal concentrations in the soft parts and shells of the same two snail species, *T. pisana* and *C. aspersum* (or *Helix aperta* as the paper named it). Both samples are concerned with Mediterranean countries with one being based in Malta and the other in Sicily. Finally, both use acid digested samples analysed with AES techniques.

However, there are fundamental differences in the two studies. Firstly, in this study each sample is a combination of a number of individuals while in the other study each sample is made up of a single individual. The fieldwork in this study consisted of directly sampling snails in their environment while Tardugno et al. (2023) purchased snails from a local market (it is unclear whether they were foraged or farmed). It is also important to note that while the study purchased snails from Sicily, *C. aspersum* samples originated from Tunisia and hence this will be the geographic location considered for the study, while *T. pisana*'s location of origin remains unknown. This present study made use of simple acid digestion while Tardugno et al. (2023) made use of a microwave-assisted digestion which is known to produce more complete results (Bizzi et al., 2011). Apart from the differences in methodology, one cannot forget the inherent differences present in the two countries (Malta and Tunisia) from which these snails originated. Malta is far smaller and has a far denser and larger urban sprawl which translates to higher road density, automobile reliance, and other anthropogenic sources of these heavy metals.

5.2 Arsenic

Arsenic was found to be the predominant metal of all the metals analysed in both soft part and shell samples with very few exceptions (namely samples 29, 31, 32 for shells and only sample 2 for soft parts) and in most cases made up more than 50% of the total metal mass for samples (Figures 4.1-4.6). This would imply that arsenic, in the form of its allotropes and/or salts, is either widespread in the environment or is taken up readily by snails. Briffa (2020) found an average concentration of arsenic in agricultural soils of Malta of 5.37 µg/g (mg/kg) making it significantly less than the concentrations of arsenic found in soft part and shell samples of this study with the average value being of shell samples being 110.74 µg/g and in soft parts being 1177.68 µg/g. There could be a number of reasons for this ranging from physiological to chemical to environmental and will be discussed collectively later on in this chapter. However, one possible explanation is the ease at which arsenic compounds bioaccumulate and biotransform. This means that snails could be constantly taking up arsenic from their environment, not only from soil but also from air, water, and vegetation. This would thereby increase the concentration within themselves by comparison, they would then

biotransform these arsenic compounds to eliminate them from their body by depositing them into their shells. This could also explain why more shell samples didn't have arsenic as the majority metal than soft part samples as it would not have biotransformed or deposited in their shells for some physiological reason.

When comparing the results of this study with those reported by Tardugno et al. (2023) for arsenic in the soft part and shells of the snails, there is a significant difference with concentrations of arsenic in snails of this study being significantly greater than that found in the aforementioned study (Table 5.1).

Table 5.1: Arsenic concentrations found in this study and Tardugno et al. (2023). Values are in ppm.

	Soft parts		Shells	
	T. pisana	*C. aspersum*	*T. pisana*	*C. aspersum*
This study	752.48	425.18	67.03	43.70
Tardugno et al. (2023)	0.02	0.046	0.015	0.07

This would imply that the Maltese samples have higher concentrations of heavy metals than those found in the Sicilian study.

Arsenic is a notorious poison, but studies have shown that it may in fact be a vital micronutrient in animals in due its role in the metabolism of the amino acid methionine and in gene silencing (Uthus, 2003) and has a positive interaction with the important micronutrient selenium (Zeng et al, 2005). Arsenic has a variety of uses in agriculture with one of its main uses being as an herbicide, pesticide, and fungicide. Historically, this was in the form of arsoric acid (H_3AsO_4) and calcium ($Ca_3(AsO_4)_2$) or lead arsenates ($PbHAsO_4$), however since the 1940s with the introduction of organic pesticides such as dithiothreitol (DTT) these forms of arsenic diminished in use and have been all but phased out by now (Alloway & Wenzel, 2013), although the accumulation in soils from this source is still a major anthropogenic source in some areas (Frank et al., 1976; Peryea & Creger, 1994; Woolson et al., 1971). In addition, organoarsenic compounds such as the ammonium and sodium salts of

methanearsonate and dimethylarsinic acid have been in use since the 1970s and are another source of arsenic in the environment (Wenzel, 2013). Another use of arsenic in agriculture is as a feed additive, such as roxarsone ((4-Hydroxy-3-nitrophenyl)arsonic acid) and nitarsone ((4-Nitrophenyl)arsonic acid), to increase weight gain, improve feed efficiency, and prevent disease. This has not only shown to increase the levels of arsenic in the tissues of the fed animals but also increases the levels of arsenic in fertilisers produced from their excrements which in turn increases the level of arsenic in soils (Wenzel, 2013). Moving away from agriculture, arsenic is also used in alloy smelting. It is added in small quantities (about 0.2%) to lead to provide resistance to bending and creep such as in car components (such as breaks) and ammunition, to brass to reduce dezincification, and, most importantly to modern applications, in gallium arsenide; a III-V direct band gap semiconductor (Carapella, 2002). In the past, arsenic was also used as a component in fireworks in order to produce a blue colour, a coveted and rare colour in pyrotechnics, but due to its toxicity this has been phased out globally. However, there is evidence that Maltese pyrotechnic enthusiasts still make use of arsenic as samples of soil taken recently after firework displays had elevated concentrations of arsenic in them (Briffa, 2020). Finally, as reported by ERA (2018), a major source for arsenic in Malta occurs from road transport tyre and brake wear and public electricity production, this again harks back to the previous point that high arsenic concentrations could be due to Malta's significant road density.

5.3 Zinc

Zinc was the 6th most prominent metal of all the metals analysed in soft part samples, and the 7th most prominent metal for shell samples (Figures 4.1-4.6). This would imply that zinc, while definitely present in the environment, is not widespread in the environment or is not taken up readily by snails. Briffa (2020) found an average concentration of zinc in agricultural soils of Malta of 174.09 µg/g (mg/kg) making it significantly larger than the concentrations of zinc found in soft part and shell samples of this study with the highest value being only 25.98 µg/g in *T. pisana* soft parts. There could be a number of reasons for this ranging from physiological to chemical to environmental and will be discussed collectively later on in this chapter.

When comparing the results of this study with those reported by Tardugno et al. (2023) for zinc in the soft part and shells of the snails, there is a significant difference with concentrations of zinc in snails of this study being less than that found in the aforementioned study, with the exception being in *T. pisana* shells (Table 5.2).

Table 5.2: Zinc concentrations found in this study and Tardugno et al. (2023). Values are in ppm.

	Soft parts		Shells	
	T. pisana	*C. aspersum*	*T. pisana*	*C. aspersum*
This study	9.92	11.76	1.18	0.83
Tardugno et al. (2023)	126.78	176.58	1.04	2.89

This would imply that the Maltese samples have lower concentrations of heavy metals than those found in the Sicilian study.

Zinc is an essential nutrient for healthy nucleic acid and protein synthesis and is only harmful to humans in large quantities. Prolonged exposure to zinc can lead to a reduced uptake of copper and hence can lead to copper deficiency in humans (ATSDR, 2005). Zinc is incredibly important and common in manufacturing processes. More than half of the zinc that is mined, processed, and recycled annually is used in galvanisation, one of the most fundamental and important processes in metalworking. The remainder is used in the manufacture of zinc-based alloys (such as brass), rubber (such as zinc oxide in motor vehicle tyres), and cosmetics (such as the use of zinc pyrithione in anti-dandruff shampoo) (Mertens & Smolders, 2013b). Possibly the most relevant source of zinc in the environment for the context of this study is that originating from tyre debris which typically contain 1–2% zinc oxide, with more than 4,000 tonnes of zinc being released via tyre debris in the EU per year (Blok, 2005). ERA (2018) further supports this by stating that road transport tyre and brake wear is the sole source for atmospheric zinc in Malta. Also discussed in the ERA (2018) report is heavy metal contamination originating from landfills and spoil grounds. Malta used to have three landfills at Magħtab, Qortin, and Wied Fulija and while these are no longer in use, they

could still present as a source of contamination either directly or from leaching into the soil and groundwater. Zinc can also originate from volcanic activities and forest fires (Mertens & Smolders, 2013b) and due to the close proximity of Malta to the active stratovolcano Mount Etna and the recent global increase in forest fires, zinc could be coming to Malta blown in on winds, a point shared by Scerri et al. (2016). Due to its role as a vital nutrient, zinc also has an agricultural use as a supplement in feed given to livestock. This, and zinc originating from other sources such as drinking water (e.g., corrosion of galvanised drinking facilities) are major zinc sources in manure which could lead to zinc entering soils if used as fertiliser (Mertens & Smolders, 2013b).

5.4 Cadmium

Cadmium was found to be the second most predominant metal of all the metals analysed in both soft part and shell samples with few exceptions in samples 2, 4, 8, and 10 (Figures 4.1-4.6). However, these are all *C. aspersum* soft part samples which have an affinity to barium which will be discussed later in section 5.11: Barium. This would imply that cadmium, in the form of its allotropes and/or salts, is either widespread in the environment or is taken up readily by snails. Briffa (2020) found an average concentration of cadmium in agricultural soils of Malta of 23.51 μg/g (mg/kg) making it somewhat comparable with the values found in shells which has an average of 43.47 μg/g, while for soft part samples the average was 196.38 μg/g, a fair deal greater than that found in soils. This would imply that cadmium is easily bioaccumulated and biotransformed by snails. This means that snails could be constantly taking up cadmium from their environment, not only from soil but also from air, water, and vegetation. This would thereby increase the concentration within themselves by comparison, they would then biotransform these cadmium compounds to eliminate them from their body by depositing them into their shells.

When comparing the results of this study with those reported by Tardugno et al. (2023) for cadmium in the soft part and shells of the snails, there is a significant difference with concentrations of cadmium in snails of this study being greater than that found in the aforementioned study (Table 5.3).

Table 5.3: Cadmium concentrations found in this study and Tardugno et al. (2023). Values are in ppm.

	Soft parts		Shells	
	T. pisana	*C. aspersum*	*T. pisana*	*C. aspersum*
This study	118.14	78.23	23.72	19.76
Tardugno et al. (2023)	0.0035	0.016	—	0.01

Most of the results for cadmium in shell samples of Tardugno et al. (2023) were found below the limit of quantification while values in soft parts were not found to be much higher. This would imply that the Maltese samples have higher concentrations of heavy metals than those found in the Sicilian study.

Cadmium is a notoriously toxic metal with no known biological function in humans and other higher organisms, although there is evidence that some marine diatoms make use of it in cadmium-dependent carbonic anhydrase enzymes (Alterio et al., 2015). In the recent past, one of the major uses of cadmium was in the production of nickel-cadmium rechargeable batteries but due to the toxicity of cadmium this form of rechargeable battery has been severely reduced and replaced by nickel–metal hydride and lithium-ion batteries (Mertens & Smolders, 2013a). Similarly, other major uses of cadmium as PVC stabilisers, pigments, and plating have declined sharply due to the toxic nature of the metal. However, these could still prove to be a significant source of cadmium today from their use in the past, especially if products were not disposed of properly (Mertens & Smolders, 2013a). A source of cadmium in agriculture is in the use of phosphorus-based fertilisers and sewage sludge, the latter of which is often used in agriculture to bolster soils due to being a rich source of organic matter and nutrients such as nitrogen and phosphorus (Mertens & Smolders, 2013a). As reported by ERA (2018), a major source of cadmium in Malta occurs from road transport tyre and brake wear and public electricity production. Keeping in mind Malta's significant road density, this could explain the high levels of cadmium found in this study. Similar to zinc, cadmium could also find a source in the landfills and spoil grounds and while these are no longer in use, they

could still present as a source of contamination either directly or from leaching into the soil and groundwater (ERA, 2018).

5.5 Copper

Copper was the 5th most prominent metal of all the metals analysed in soft part samples, and the 10th most prominent metal for shell samples (Figures 4.1-4.6). This would imply that copper is present in the environment to a reasonable degree, although may not be deposited in shells as significantly. Briffa (2020) found an average concentration of copper in agricultural soils of Malta of 95.15 µg/g (mg/kg) making it significantly larger than the concentrations of copper found in soft part and shell samples of this study with the highest value being only 41.58 µg/g in *C. aspersum* soft parts. One possible explanation is that the two snail species do not bioaccumulate copper as readily for some physiological reason. However, as several studies have shown before (Berger and Dallinger, 1993; Viard et al., 2004; and Vrankovic et al., 2020) copper bioaccumulates up to ten times higher in the tissues of snails living in polluted soil habitats than it did in snails inhabiting unpolluted areas. There could be a number of reasons for these phenomena ranging from physiological to chemical to environmental and will be discussed collectively later on in this chapter.

When comparing the results of this study with those reported by Tardugno et al. (2023) for copper in the soft part and shells of the snails, there is a significant difference with concentrations of copper in snails of this study being smaller than that found in the aforementioned study (Table 5.4).

Table 5.4: Copper concentrations found in this study and Tardugno et al. (2023). Values are in ppm.

	Soft parts		Shells	
	T. pisana	*C. aspersum*	*T. pisana*	*C. aspersum*
This study	9.05	13.01	0.37	0.22
Tardugno et al. (2023)	23.475	38.778	1.42	1.88

This would imply that the Maltese samples have lower concentrations of heavy metals than those found in the Sicilian study.

Copper is an essential nutrient in all eukaryotes due to the diverse nature of copper proteins and their role in aerobic respiration and electron & oxygen transportation. Copper is also a component in many superoxide dismutase proteins that play a major role in reducing oxidative stresses in cells by catalysing the decomposition of superoxides. Copper is especially important in molluscs, such as those investigated in this study, due to being a principal component in the hemocyanin protein, a copper-based oxygen carrier that is analogous to the iron-based haemoglobin protein found in most vertebrates (Vest et al., 2012). Copper is incredibly important and common in electrical components with it being the preferred material for almost all wiring and cables and is also used extensively in alloy smelting being a component of many alloys such as brass, bronze, and cupronickel to name a few (Oorts, 2013). Copper has a variety of uses in agriculture with one of its main uses being as a fungicide in the form of mixtures of copper salts (a common one being the Bordeaux mixture, a mix of copper(II) sulphate ($CuSO_4$) and quicklime (CaO)) that has been in use since the 19th century. It is a very widely used fungicide for many agriculturally relevant crops such as hops, grapes, orchard fruits (such as apples and avocados), coffee, and several vegetables (such as tomatoes, potatoes, and carrots) (Oorts, 2013). Another use of copper in agriculture is as an additive to feed, especially for growing pigs, and hence tends to be present in fertilisers and sewage sludge (Oorts, 2013). Copper can also originate from volcanic activity and forest fires (Oorts, 2013) which, for the reasons discussed earlier, is of particular concern in Malta. As reported by ERA (2018), a major source for copper in Malta occurs from road transport tyre and brake wear as well as contamination originating from landfills and spoil grounds.

5.6 Nickel

Nickel was found to be the 9th most predominant metal of all the metals analysed in soft part samples and 8th most predominant metal in shell samples (Figures 4.1-4.6). This would imply that nickel, while definitely present in the environment, is not widespread in the environment or is not taken up readily by snails. Briffa (2020) found an average concentration of nickel in agricultural soils of Malta of 13.10 µg/g (mg/kg) making it on the whole within the same range as that of this study that had an average value for soft parts of 12.01 µg/g while the concentrations in shells are less at 1.02 µg/g, which is to be expected of shell samples as the metal would have to be biotransformed. This may be interpreted that the snails represent the situation of nickel in their environment well. The PERMANOVA test (Table 4.2) indicates that there is a statistically significant difference with regards to the concentrations of nickel between the two species, and when looking at the two species separately and how they relate to the results of Briffa (2020) the *T. pisana* samples have distribution more similar to the aforementioned study (average of 15.54 µg/g) than that of *C. aspersum* (average of 8.49 µg/g). One possible interpretation of this is that *T. pisana* is better at representing the situation of nickel in their environment than *C. aspersum*.

When comparing the results of this study with those reported by Tardugno et al. (2023) for nickel in the soft part and shells of the snails, there is a significant difference with concentrations of nickel in snails of this study being larger than that found in the aforementioned study except for *C. aspersum* shells (Table 5.5).

Table 5.5: Nickel concentrations found in this study and Tardugno et al. (2023). Values are in ppm.

	Soft parts		Shells	
	T. pisana	*C. aspersum*	*T. pisana*	*C. aspersum*
This study	7.77	4.25	0.60	0.49
Tardugno et al. (2023)	0.09	0.121	0.007	0.64

This would imply that the Maltese samples have higher concentrations of heavy metals than those found in the Sicilian study. Another point of difference is that in the Sicilian study the concentration of nickel in *C. aspersum* shells was greater than that in soft parts, while this was not the case in this study.

Nickel is not known to play a role in any biological function in humans and other animals, although it does play an important role in the biology of some plants, fungi, bacteria, and archaea in nickel-based enzymes. For this reason, it may be considered to play a role of an essential nutrient in humans indirectly due to its vital role in bacteria living in the large intestine and thereby acts as a prebiotic (Zambelli & Ciurli, 2013). Nickel is an incredibly common component in many widely used alloys such as stainless steel and cupronickel (Gonnelli & Renella, 2013). As mentioned previously, nickel was also used in nickel-cadmium rechargeable batteries and while cadmium is no longer used for this purpose, the use of nickel remains in nickel–metal hydride batteries (Mertens & Smolders, 2013a). Nickel is also found in phosphorus-based fertilisers and sewage sludge, making them a main source in agricultural soils (Gonnelli & Renella, 2013), a point supported in ERA's (2018) state of the environment report. This source of nickel is especially pertinent to bioaccumulation as the nickel is present mainly in organic chelated forms making it readily available to living organisms such as plants and snails (Gonnelli & Renella, 2013). As reported by ERA (2018), major sources of nickel in Malta come from urban wastewater (which becomes sewage sludge), from contamination originating from landfills and spoil grounds, and public electricity production.

5.7 Lead

Lead was found to be the 7th most predominant metal of all the metals analysed in soft part samples and 5th most predominant metal in shell samples (Figures 4.1-4.6). This would imply that lead is present in the environment to a reasonable degree. Briffa (2020) found an average concentration of lead in agricultural soils of Malta of 125.58 µg/g (mg/kg) making it far greater than the concentrations of lead found in the soft part and shell samples with the largest value being only 22.02 µg/g in *T. pisana* soft parts. There could be a number of reasons for this ranging from physiological to chemical to environmental and will be

discussed collectively later on in this chapter. One possible explanation is that the two snail species do not bioaccumulate lead readily. However, as several studies have shown before (Berger and Dallinger, 1993; and Vrankovic et al., 2020) lead bioaccumulated in the tissues and even shells of snails living in polluted soil habitats, and is known to affect snails' reproductive tissues, shell health, and eggs due to bioaccumulative effect (Carbone & Faggio, 2019).

When comparing the results of this study with those reported by Tardugno et al. (2023) for lead in the soft part and shells of the snails, there is a significant difference with concentrations of lead in snails of this study being larger than that found in the aforementioned study (Table 5.6).

Table 5.6: Lead concentrations found in this study and Tardugno et al. (2023). Values are in ppm.

	Soft parts		Shells	
	T. pisana	*C. aspersum*	*T. pisana*	*C. aspersum*
This study	10.41	5.18	3.83	3.86
Tardugno et al. (2023)	0.003	0.018	0.015	0.26

This would imply that the Maltese samples have higher concentrations of heavy metals than those found in the Sicilian study. Another point of difference is that in the Sicilian study the concentrations of lead in shells was, on average, greater than that in soft parts while the reverse was true in this study.

Lead is a notoriously toxic metal with no known biological function in humans or any other organism. There are no safe limits of lead in the body with even levels considered to pose little to no risk showing signs of causing adverse health effects (ATSDR, 2019). Until recently lead salts were used extensively. As mentioned previously, lead in the form of lead arsenate was used as an insecticide (Alloway & Wenzel, 2013). In the past lead in the form of tetraethyllead was used as an additive in petrol to prevent engine knocking and hadn't been

phased completely till 2021 making it a significant source of lead in the environment (Steinnes, 2013; UNEP, 2021). As discussed previously in section 2.1.2, Malta has a major sport and game shooting culture with lead being used as ammunition and hence could be a major source of lead in the environment. As reported by ERA (2018), major sources of lead in Malta come from urban wastewater, from contamination originating from landfills and spoil grounds, and from tyre and brake wear. Like many other metals, lead salts are used extensively as pigments especially in paint with yellow lead(II) chromate ($PbCrO_4$), red lead(II,IV) oxide, (Pb_3O_4), white lead(II) carbonate ($PbCO_3$) being the most common. The use of lead for pigments has severely reduced but as with many cases the improper handling and disposal of these products could have devastating effects years after they have been phased out (Steinnes, 2013).

5.8 Chromium

Chromium was found to be the 10th most predominant metal of all the metals analysed in soft part samples (i.e., the least dominant metal in soft parts bar vanadium which could not be detected) and 9th most predominant metal in shell samples (Figures 4.1-4.6). This would imply that chromium is present in the environment but not to any significant level. Briffa (2020) found an average concentration of chromium in agricultural soils of Malta of 22.29 µg/g (mg/kg) making it far greater than the concentrations of chromium found in the soft part and shell samples with the largest value being only 6.71 µg/g in *T. pisana* soft parts. There could be a number of reasons for this ranging from physiological to chemical to environmental and will be discussed collectively later on in this chapter.

When comparing the results of this study with those reported by Tardugno et al. (2023) for chromium in the soft part and shells of the snails, there is a significant difference with concentrations of chromium in snails of this study being larger than that found in the aforementioned study (Table 5.7).

Table 5.7: Chromium concentrations found in this study and Tardugno et al. (2023). Values are in ppm.

	Soft parts		Shells	
	T. pisana	*C. aspersum*	*T. pisana*	*C. aspersum*
This study	3.54	1.99	0.46	0.43
Tardugno et al. (2023)	0.025	0.056	0.03	0.39

This would imply that the Maltese samples have higher concentrations of heavy metals than those found in the Sicilian study. Another point of difference is that in the Sicilian study the concentrations of chromium in shells was, on average, greater than that in soft parts while the reverse was true in this study.

The nutritional role of chromium is debated but chromium(III) may play a vital role in the action of insulin and thereby in the metabolism and storage of carbohydrates, lipids, and proteins. However, its mechanism has not yet been defined and so its essentiality is debatable, in point of fact while the U.S. National Institutes of Health (NIH) classify it as an essential nutrient, the European Food Safety Authority (EFSA) does not (NIH, 2022; EFSA, 2014). Chromium has a variety of uses and therefore a variety of potential sources in the environment. Chromium(III) sulfate ($(Cr_2(SO_4)_3$) is used extensively in leather tanning as the chromium(III) stabilises the leather by cross linking the collagen fibres. Chromium is also a major component in many common alloys such as stainless steel and is a common electroplating metal and is used to prevent corrosion while retaining the characteristic metallic lustre. A variety of chromium salts are used in pigments for paints, inks, and glazes such as in molybdate red, chromium oxide green, and chromium yellow (Gonnelli & Renella, 2013). As reported by ERA (2018), major sources of chromium in Malta originate from contamination originating from landfills and spoil grounds, and from tyre and brake wear.

5.9 Aluminium

Aluminium was found to be the 4th most predominant metal of all the metals analysed in soft part samples and 3rd most predominant metal in shell samples (Figures 4.1-4.6). This would imply that aluminium is present in the environment to a significant degree. Briffa (2020) found aluminium to be the most dominant metal in agricultural soils of Malta with an average concentration of 34,998.05 µg/g (mg/kg) making it significantly larger than the concentrations of aluminium found in soft part and shell samples of this study with the highest value being 45.33 µg/g in *T. pisana* soft parts. There could be a number of reasons for this ranging from physiological to chemical to environmental and will be discussed collectively later on in this chapter.

When comparing the results of this study with those reported by Tardugno et al. (2023) for aluminium in the soft part and shells of the snails, there is a significant difference with concentrations of aluminium in snails of this study being larger than that found in the aforementioned study except for *C. aspersum* shells (Table 5.8).

Table 5.8: Aluminium concentrations found in this study and Tardugno et al. (2023). Values are in ppm.

	Soft parts		Shells	
	T. pisana	*C. aspersum*	*T. pisana*	*C. aspersum*
This study	23.29	11.93	16.20	13.36
Tardugno et al. (2023)	0.01	0.2525	3.11	514.45

This would imply that the Maltese samples have higher concentrations of heavy metals than those found in the Sicilian study. Another point of difference is that in the Sicilian study the concentrations of aluminium in shells was greater than that in soft parts. However, while this was the case in *C. aspersum*, this was not the case for *T. pisana*.

Although aluminium has a widespread occurrence in the earth's crust, it has no known nutritional role, a common occurrence in toxic metals. However, aluminium is not considered

a toxic element and therefore the salts are used as an additive in the food and beverage industry. Examples of this include sodium aluminium phosphate ($NaH_{14}Al_3(PO_4)_8$) as an emulsifier and sodium aluminosilicate ($AlNa_{12}SiO_5$) as an anti-caking agent (Alasfar & Isaifan, 2021). The global production and use of aluminium are staggering, being rivalled only by that of iron. It is used extensively as an alloy in a wide variety of industries such as aviation; transportation; packaging; building and construction; machinery; and household items. Therefore, aluminium has many anthropogenic sources in the environment such as tyre and brake wear, construction waste, and contamination originating from landfills and spoil grounds. Unfortunately, ERA does not view aluminium as a contaminant of concern and hence it is not reported upon in their state of the environment report and hence an investigation into the specific sources of aluminium in Malta is not known.

The Dunn's post-hoc test for aluminium soft part samples (Table 4.3), showed a statistically significant difference between isolated locations with urban (p=0.0404) and agricultural (p=0.0357) locations. Looking at the results (Figure 4.32), this is likely due to a higher percentage of aluminium being found in the isolated samples. Unfortunately, a good explanation for this could not be determined, however as discussed previously, aluminium is widely used and is naturally abundant in the Earth's crust.

5.10 Manganese

Manganese was found to be the 8th most predominant metal of all the metals analysed in soft part samples and 6th most predominant metal in shell samples (Figures 4.1-4.6). This would imply that manganese is present in the environment but not to a significant degree. Briffa (2020) found an average concentration of manganese in agricultural soils of Malta of 473.51 µg/g (mg/kg) making it significantly larger than the concentrations of manganese found in soft part and shell samples of this study with the highest value being 27.52 µg/g in *C. aspersum* soft parts. There could be a number of reasons for this ranging from physiological to chemical to environmental and will be discussed collectively later on in this chapter.

When comparing the results of this study with those reported by Tardugno et al. (2023) for manganese in the soft part and shells of the snails, there is a significant difference with concentrations of manganese in snails of this study being less than that found in the aforementioned study except for *T. pisana* shells (Table 5.9).

Table 5.9: Manganese concentrations found in this study and Tardugno et al. (2023). Values are in ppm.

	Soft parts		Shells	
	T. pisana	*C. aspersum*	*T. pisana*	*C. aspersum*
This study	5.67	7.78	2.01	2.42
Tardugno et al. (2023)	22.11	30.17	1.57	11.11

This would imply that the Maltese samples have lower concentrations of heavy metals than those found in the Sicilian study.

Manganese is an essential nutrient as it is used extensively in biological reactions due to being a cofactor for many classes of enzymes. To name a few, it is a major component in oxygen-evolving complex (OEC) which allows the photooxidation of water in photosynthesis; in oxidoreductase which creates electron transport chains in bacteria, chloroplasts, and mitochondria by catalysing the transfer of electrons from one molecule to another; and in transferase a massive class of enzymes that catalyse transfer functional groups from one molecule to another (Li & Yang, 2018). Due to its use in these essential biological roles, manganese is often found as an additive in fertilisers (Uren, 2013). Manganese is used extensively as an alloying component such as in steel and aluminium alloys due to its ability of sulfur-fixing and deoxidising, making it particularly well suited to removing excess oxygen, sulfur, and phosphorus from the metal matrix (Verhoeven, 2007). In Malta, manganese has anthropogenic sources from tyre and brake wear, fertilisers and sewage sludge, and contamination originating from landfills and spoil grounds. There is also evidence that points to the fact that fireworks could increase the concentration of manganese in soils (Briffa, 2020). Unfortunately, ERA does not view manganese as a contaminant of concern and hence it is not reported upon in their state of the environment report.

The Dunn's post-hoc test for manganese soft part samples (Table 4.4), showed a statistically significant difference between isolated locations with urban (p=0.0316), agricultural (p=0.0044), and rural (p=0.0069) locations. Looking at the results (Figure 4.34), this is likely due to a higher percentage of manganese being found in the isolated samples. Unfortunately, a good explanation for this could not be determined, however as discussed previously, there is evidence that points to the fact that fireworks could increase the concentration of manganese in soils, and these are often set off in isolated places for safety reasons.

5.11 Barium

Barium was found to be the 3rd most predominant metal of all the metals analysed in soft part samples and 4th most predominant metal in shell samples (Figures 4.1-4.6). This would imply that barium is present in the environment to a significant degree. Briffa (2020) found an average concentration of barium in agricultural soils of Malta of 185.43 µg/g (mg/kg) making it only marginally larger than the concentrations of barium found in *C. aspersum* soft parts with only sample 4 exceeding it with a value of 236.04 µg/g, but significantly larger than *C. aspersum* shells and *T. pisana* samples (both soft part and shell) with the largest value being 72.11 µg/g in *T. pisana* soft parts. This implies that *C. aspersum* has a particular affinity to barium that *T. pisana* does not. There could be a number of reasons for this ranging from physiological to chemical to environmental and will be discussed collectively later on in this chapter.

When comparing the results of this study with those reported by Tardugno et al. (2023) for barium in the soft part and shells of the snails, there is a significant difference with concentrations of barium in snails of this study being greater than that found in the aforementioned study, with only a marginal difference in *C. aspersum* shell values (Table 5.10).

Table 5.10: Barium concentrations found in this study and Tardugno et al. (2023). Values are in ppm.

	Soft parts		Shells	
	T. pisana	*C. aspersum*	*T. pisana*	*C. aspersum*
This study	29.80	107.66	12.28	7.83
Tardugno et al. (2023)	0.88	0.66	2.64	8.42

This would imply that the Maltese samples have higher concentrations of heavy metals than those found in the Sicilian study. Another noteworthy point is that in Tardugno et al. (2023), the levels of barium in shells was found to be greater than in soft parts while the reverse was true in this study.

Barium is a toxic metal with no known biological function in humans or any other organism. However, one order of single-celled algae, *desmidiales*, has shown to have cavities that contain crystals of barium sulfate ($BaSO_4$), the purpose of which is unclear but may play a role in maintaining orientation. Regardless, for this order barium seems essential as a deficiency in diet will stunt growth (Wilcock et al., 1989). Due to this toxicity, uses of barium tend to be scarce or niche and so to its anthropogenic sources. Its main use is as barium sulfate as a drilling fluid in oil and gas wells as a densifying agent (Madejón, 2013). Barium sulfate is also used as a radiocontrast agent due to its low toxicity (due to its insolubility) and high density which makes it opaque to X-rays (Madejón, 2013). Barium sulfate is also used in the white pigment lithopone, a very common pigment in paints and plastics (O'Brien, 1915). Barium borate ($Ba(BO_2)_2$) is used as a strong bactericide and fungicide, sometimes added directly to soil but most often added to paints, plastics, and paper products to prevent the growth of bacteria and fungus (Nikogosyan, 1991). Barium nitrate ($Ba(NO_3)_2$) and barium dichlorate ($Ba(ClO_3)_2$) are used in fireworks to impart an apple green or brilliant green colour (Russell, 2008), making it a source of barium in the environment especially in Malta. Not much else is known of barium contamination in Malta, however a report by ERA (2016) found that public sewers contributed to barium contamination.

5.12 Vanadium

Vanadium proved to be an interesting result as it was the only metal that wasn't found in both soft part and shell samples, but only found in the latter as the 11th (least) most prominent metal of all the metals analysed in shell samples (Figures 4.1-4.6). This would imply that vanadium is present in the environment but not to a significant degree. Briffa (2020) found an average concentration of vanadium in agricultural soils of Malta of 32.75 µg/g (mg/kg) making it significantly larger than the concentrations of vanadium found in soft part and shell samples of this study with the highest value being 0.52 µg/g in *C. aspersum* shells. There could be a number of reasons for this ranging from physiological to chemical to environmental and will be discussed collectively later on in this chapter.

Comparing the results of this study with those reported by Tardugno et al. (2023) for vanadium, the Sicilian study found no concentration within the limit of detection of the equipment for *T. pisana* soft part or shells. In addition, for *C. aspersum* results this study found lower values of vanadium (Table 5.11).

Table 5.11: Vanadium concentrations found in this study and Tardugno et al. (2023). Values are in ppm.

	Soft parts		Shells	
	T. pisana	*C. aspersum*	*T. pisana*	*C. aspersum*
This study	—	—	0.27	0.29
Tardugno et al. (2023)	—	0.003	—	1.61

This would imply that the Maltese samples have lower concentrations of heavy metals than those found in the Sicilian study. Another noteworthy point is that in Tardugno et al. (2023), the levels of vanadium in shells was found to be greater than in soft parts, a phenomenon shared with this study.

Vanadium is not known to have any biological importance in humans and most other animals, although it has been shown that a vanadium deficient diet stunts normal bone

growth (Korbecki, 2012). However, it is used as a cofactor in a number of enzymes such as vanadium bromoperoxidase which removes hydrogen peroxide produced during photosynthesis of several marine algae (Butler & Carter-Franklin, 2004) and in vanadium nitrogenase used in nitrogen fixing by azotobacter when molybdenum is unavailable (Robson et al., 1986). Vanadium is also present in significant quantities in tunicates (a marine invertebrate) and macromycetes (fungi forming large fruiting bodies) but these exact purposes are yet unknown although some hypotheses have been put forward such as a predation deterrent (Smith, 1989; da Silva et al., 2013). A major source of vanadium in the environment is from the petrochemical industry as it is the most abundant metallic constituent in crude oil, which means it is often released into the environment from the extraction, refining, and use of crude oil products (Schlesinger et al., 2017). Vanadium is also released from volcanic activity and forest fires which, for the reasons discussed earlier, is of particular concern in Malta (Schlesinger et al., 2017). Unfortunately, ERA does not view manganese as a contaminant of concern and hence it is not reported upon in their state of the environment report. Although vanadium isn't used directly in fireworks, it is a common component in titanium powder which is used to produce brilliant white sparks (Ogundele et al., 2015).

5.13 Collective Discussion

5.13.1 General Considerations of Metals in Soils and Snails

As interesting and useful as it is to consider each metal individually, one cannot dismiss the general trends that emerge between the results of the individual metals and what this might mean in relation to all of them together. With the exception of nickel in soft parts, all metals had concentrations which differed from what is to be expected for heavy metals in soils as described by Briffa (2020), with results being either less than or greater than expected. Firstly, soil analysis is used to determine the full chemical composition of the soil sample of interest, regardless of what state they were originally in. This calls into question the bioavailability of the metals in the soil i.e., the extent at which the metal can enter and permeate through biological systems. For example, lead in the form of lead(II) ethanoate ($Pb(CH_3COO)_2$), lead chloride ($PbCl_2$), and lead(II) oxide (PbO) spiked in soils shows no sign of

elevating the lead content in plant shoots and roots in lettuce and wallaby grasses (De Silva et al., 2019). Therefore, it could be stated that simply having a high content of lead, or any other metal, in soil samples does not necessarily mean that organisms living in said soil, such as plants or snails, will have an elevated level of lead and other metals in their diets and therefore an elevated level of lead and other metals in their bodies.

Although not all metal salts are in a bioavailable state, this is not always inherently the case in all environmental systems. Plants form an integral role in most food chains and oftentimes are the entry point for many pollutants being mobilised into the food chain and thereby being converted to a bioavailable state for many organisms that feed upon them. However, given the differences between the physiology of organisms, a metal that is not taken up by a certain species of plant does not mean it cannot be taken up by any other. For example, members of the genus *Alhagi* (family *Fabaceae*) show more uptake of chromium and cadmium than *Malva sylvestris* (family *Malvaceae*) (Shojaei et al., 2021) while *Typha latifolia* (family *Typhaceae*) showed greater uptake of nickel and cadmium than *Arundo donax* (family *Poaceae*) which showed a greater uptake in manganese (Shehu et al., 2011). However, it is not simply a matter of what plant species is inhabiting the particular environment but also depends to a great degree the chemistry of the soil they are in.

Malta has very calcareous soils due to the parent rock being limestone ($CaCO_3$) and is exemplified by terra rossa, carbonate raw, and xerorendzina soils[6] and as such have rather alkaline pH (8.0-8.5) (Lang, 1960). As mentioned in an earlier chapter, as a general rule most metals tend to precipitate out in alkaline pH and rendered into insoluble states and thereby into less bioavailable states (Alloway, 2013), so this may be the case in Malta due to the calcareous nature of the soils. This could, at least in part, explain why certain metals have concentrations in soil far greater than that found in the snails. However, soil chemistry can be incredibly complex with various components and reactions and hence it is not always so simply put. For example, vanadium in calcareous soils can be converted to an inert state (Alloway, 2013) but if in the presence of iron oxides and hydroxides it will form iron(III)

[6]This is an outdated system of soil classification with the current accepted system being the World Reference Base for Soil Resources (WRB). However, the old system was quoted as is still very popular and due to the fact that this study is not on soil science the official nomenclature wasn't given much importance.

vanadate(V) ($Fe(VO_3)_2$) which is easily mobilised by soluble organic matter in soil and chelated to form bioavailable organic complexes (Madejón, 2013). However, this does not explain why for certain metals a higher concentration was found in the soft parts than what was found in soils and for that we must turn to other phenomena such as biomagnification. This describes how a pollutant increases in concentration in the tissues of organisms as it goes up trophic levels (Silvy, 2012). This could be because of the bioaccumulative nature of the pollutant building up in the tissues and having a very slow rate of excretion, therefore as the organism continues to consume food the pollutant is excreted slowly and so the rate of pollutant intake is greater than pollutant excretion. This has been seen to occur especially in mercury and arsenic (Suedel et al., 1994), the latter of which was found in significant quantities in snails but not in soils and hence supports this observation.

When metals enter the body's tissues, this does not mean they will invariably remain there permanently, as there are a number of ways to detoxify the metals. As touched upon previously one way in which this is done is by using metallothioneins (MT). These are a special class of small proteins rich in the sulfur-containing cysteine amino acid localised in the Golgi apparatus of most eukaryotic cells. These serve a function in the homeostasis of physiologically important metals such as zinc and copper and also detoxify more xenobiotic (chemical substances that are not produced or expected to be present naturally) metals such as cadmium, lead, and mercury (Dallinger et al., 2000). In terrestrial gastropods (such as those analysed in this study) MT proteins are characterised by their short chains consisting of a large percentage of hydrophilic amino acids and distinct lack of aromatic amino acids. While these hydrophilic amino acids make the protein water-soluble (an uncommon characteristic for this type of protein), it is the sulfur-rich cysteine component that actually deals with metal binding. In gastropods, these proteins show two main isoforms (or variants), MT-A and MT-B which show preference to particular metals and binding potential depending on the particular isoform, with primary structure being unique among other animal phyla and even non-terrestrial gastropods. For example, MT-A shows a bonding preference to cadmium with a stoichiometry of six Cd^{2+} ions per molar metal equivalent while MT-B shows a bonding preference to copper with a stoichiometry of twelve Cu^{+} ions per molar metal equivalent (Dallinger et al., 2000). This not only implies that metal species are not all treated the same with regards to detoxification in body tissues but also provides a mechanism for where and

how these differences arise, partially explaining the presence, or lack thereof, of certain metals in snail tissues.

As discussed in section 5.1, it is important to note that while there were a number of similarities between Tardugno et al. (2023) and this study, there are also a number of differences that may result in inherent variations in the results. Therefore, one cannot take the values of the Sicilian study and compare them directly to this study and one must keep in mind the nuances present when comparing unlike studies together, such as those outlined previously. For example, Tardugno et al. (2023) made use of ICP-MS which has a higher sensitivity and detection range than the MP-AES used in this study.

Another point that should be made about the results is that they are values of the total content of the specific metal analysed regardless of the form of their original species. As mentioned in a previous chapter, acid digestion, in this case nitric acid, will convert the relevant metal ions to the corresponding cation of the nitrate(IV) form. In some cases, this fact may seem inconsequential, however as previously shown, the presence of a metal doesn't inherently mean it is in a bioavailable state. Not to mention, while there is an assumption that all heavy metal salts and compounds are toxic and ecotoxic to a similar degree which is very often not the case. For example, chromium(III) is not seen to be particularly toxic unless in large doses and even debatably beneficial in small ones, however chromium(VI) is incredibly toxic and mutagenic in even minute concentrations (Gonnelli & Renella, 2013). Therefore, the particular species of the heavy metal can be incredibly relevant in ecotoxicology and another technique would need to be utilised such as XPS (Singh et al., 2022) or XAFS (Yasoshima et al., 2001).

5.13.2 Specific Considerations of The Results

From the results of this study, certain statements could be made. Firstly, the soft parts and shells of snails show a very different metal profile with concentrations in soft parts being, in general, larger than in shells (Figure 4.11). This is most likely due to metals being deposited in shells as a form of detoxification and so it would stand to reason for shells to have lower levels of metals as lower percentage would be biotransformed. One can discern that a number

of clusters are present for both shell and soft part samples (Figures 4.12 and 4.15) and therefore it could be stated that there is enough variation between individual samples to consider them significantly different from another and hence good bioindicators. However, it could be stated that since more clusters are present between soft part samples than shell samples, soft parts make for better bioindicators than shells in general.

With regards to location types, locations were classified in that way for sampling purposes to ensure that there was a good representation of the different situations of the environment. However, the result of this study makes it clear that the classifications chosen for the different locations (industrial, urban, residential, agricultural, rural, isolated) were arbitrary, statistically speaking (Figures 4.14 and 4.17). Therefore, it could be stated that there is no overarching pattern present for the levels of metals across Malta.

There exists a clear difference between the two species *C. aspersum* and *T. pisana* (Figure 4.13 and Table 4.2). This calls into question which species is more dominant in the uptake or accumulation of a specific heavy metal to another. For the majority of heavy metals (arsenic, cadmium, nickel, lead, chromium, aluminium) *T. pisana* was seen as the dominant species for the uptake or accumulation of these metals, and hence could be considered the better bioindicator for these metals. For barium *C. aspersum* was seen as the dominant species for the uptake or accumulation, and hence could be considered the better bioindicator for barium. For the remaining metals (zinc, copper, manganese) neither species was seen to be the dominant species for the uptake or accumulation, and hence neither could not be considered the better bioindicator. For vanadium, a dominant species could not be determined, however due to the fact that no vanadium could be detected in the soft parts of either species it is clear that shell samples must be used as bioindicators for that metal.

As for potential sources for these heavy metals, while this study did not in any way investigate the sources of these heavy metals, it is evident from ERA (2016) and other studies into common sources for the specified metals as outlined and summarised in sections 5.2-5.12, that the major source of these heavy metals in Malta is most likely due to the significant road density with all of the metals being a component to some degree of brake and tyre wear or automobile exhaust. Another major source for heavy metals could be those being blown

in as particulate matter from volcanic activity and forest fires as these events release large quantities of certain metals into the atmosphere. Finally, another pertinent source of heavy metals in Malta are those originating from pyrotechnic displays and fireworks as heavy metals are used to produce a variety of effects which then fall back down to the environment.

6. Conclusion

6.1 Conclusions of The Research

The biggest outcome of this study is that the two species of interest in this study, *C. aspersum* and *T. pisana*, can be used as bioindicators for the selected heavy metals. This is due to the fact that there was significant variation between the individual samples.

This study has shown that there is a difference between the levels of the selected heavy metals between the soft parts and shells of the two snail species with concentrations in soft parts being, in general, larger than in shells. The exception to this being vanadium which was not detected in soft part samples but was detected in shell samples. With this in mind, it can be recommended that soft parts be used as a bioindicator for the selected heavy metals, except in the case of vanadium where shells should be used.

This study has also shown that there is a difference between the levels of the selected heavy metals between the two snail species. *T. pisana*, in general, tends to be the dominant species for the uptake or accumulation of the metals arsenic, cadmium, nickel, lead, chromium, aluminium and hence it can be recommended that *T. pisana* soft parts be used as a bioindicator for the aforementioned heavy metals. *C. aspersum* was the dominant species for the uptake or accumulation of barium and hence it can be recommended that *C. aspersum* soft parts be used as a bioindicator for barium. For the remaining metals zinc, copper, and manganese either species can be used.

It is important to note that this study made no attempt to use the bioindicators as a tool to directly measure the concentrations of metals in the environment. Further to this point, concentrations of almost all heavy metals (excluding nickel) in snails differs to what is expected for the levels of the metals in soils as determined by previous studies (Briffa, 2020). However, they can still be used to determine the levels of the heavy metals that have actually entered the food chain. Nickel did show comparable results for what is to be expected in soils, however more research should be done to determine if this is in fact a repeatable observable phenomenon.

6.2 Recommendations for Future Research

Building upon the present study, there are a number of investigations that could be carried out to improve upon and/or confirm the present results. Such investigations may include:

1. Increasing the numbers of samples may reveal patterns that were not seen due to the relatively small sample size (12 samples per species).

2. Increasing the variation of the variables being tested. Testing for more metals may yield more conclusions for which species is best used as a bioindicator and verify if snails can be used as a bioindicator for them. Testing for more species could reveal if any other species is better suited as a bioindicator for other metals.

3. Altering the methodology. Microwave-assisted acid digestion could potentially provide more accurate results for the levels of heavy metals present in samples. Using other analytical equipment could provide better results, for example the ICP-AES is known to have better detection limits and sensitivity than the MP-AES used in this study. Alternatively, as touched upon previously in this dissertation, using analytical equipment such as XPS or XAFS can reveal not only the concentration of the particular heavy metal but also the chemical species which could be more relevant for ecotoxicological purposes.

7. List of References

Abdel Gawad, S.S., (2018). Acute toxicity of some heavy metals to the freshwater snail, *Theodoxus niloticus* (Reeve, 1856). *Egyptian J. Aquatic Res*. 44, 83–87.

Agilent Technologies, Inc. (2021a). *Microwave Plasma Atomic Emission Spectroscopy (MP-AES) Application eHandbook*. https://www.agilent.com/cs/library/applications/5991-7282EN_MP-AES-eBook.pdf

Agilent Technologies, Inc. (2021b). *Elemental Analysis using ICP-OES, Flame AAS or MP-AES*. https://www.agilent.com/en/product/atomic-spectroscopy/icp-oes-vs-flame-aas-vs-mp-aes

Alasfar, R. H., & Isaifan, R. J. (2021). 'Aluminum environmental pollution: the silent killer'. *Environmental Science and Pollution Research*, *28*(33), 44587–44597. https://doi.org/10.1007/s11356-021-14700-0

Alloway, B, ed., (2013). *Heavy metals in soils: Trace metals and metalloids in soils and their bioavailability*. 3rd ed. Dordrecht: Springer

Alterio, V., Langella, E., De Simone, G., & Monti, S. (2015). 'Cadmium-containing carbonic anhydrase CDCA1 in marine diatom *Thalassiosira weissflogii*'. *Marine Drugs*, 13(4), 1688–1697. https://doi.org/10.3390/md13041688

Anderson, M. J. (2017). 'Permutational multivariate analysis of variance (PERMANOVA)'. *Wiley StatsRef: Statistics Reference Online*, 1–15. https://doi.org/10.1002/9781118445112.stat07841

Agency for Toxic Substances and Disease Registry (ATSDR) (2005). 'Toxicological Profile for Zinc'. pp.21-84. Available at: https://www.atsdr.cdc.gov/ToxProfiles/tp60.pdf

Agency for Toxic Substances and Disease Registry (ATSDR) (2019). 'Toxicological Profile for Lead'. pp.2-9. https://www.atsdr.cdc.gov/toxprofiles/tp13.pdf

Baroudi, F., Al Alam, J., Fajloun, Z., & Millet, M. (2020). 'Snail as Sentinel organism for monitoring the environmental pollution; a review', *Ecological Indicators*, 113, p. 106-240.

Baumann, C., Beil, A., Jurt, S., Niederwanger, M., Palacios, O., Capdevila, M., Atrian, S., Dallinger, R., & Zerbe, O. (2017). 'Structural adaptation of a protein to increased metal stress: NMR structure of a marine snail metallothionein with an additional domain'. Angewandte *Chemie International Edition*, 56(16), 4617–4622. https://doi.org/10.1002/anie.201611873

Berger, B. and Dallinger, R., (1993). 'Terrestrial snails as quantitative indicators of environmental metal pollution'. *Environmental Monitoring and Assessment*, 25(1), pp.65-84.

Bizzi, C. A., Flores, E. M. M., Barin, J. S., Garcia, E. E., & Nóbrega, J. A. (2011). 'Understanding the process of microwave-assisted digestion combining diluted nitric acid and oxygen as auxiliary reagent'. *Microchemical Journal*, *99*(2), 193–196. https://doi.org/10.1016/j.microc.2011.05.002

Blok, J. (2005). 'Environmental exposure of road borders to zinc.' *Science of the Total Environment*, 348(1–3), 173–190

Borg, D. and Attard, E. (2020) 'Honeybees and their products as bioindicators for heavy metal pollution in Malta', *Acta Brasiliensis*, 4(1), p. 60.

Butler, A., & Carter-Franklin, J. N. (2004). 'The role of vanadium bromoperoxidase in the biosynthesis of halogenated marine natural products'. *Natural Product Reports*, *21*(1), 180. https://doi.org/10.1039/b302337k

Carbone, D. and Faggio, C. (2019) '*Helix aspersa* as Sentinel of development damage for biomonitoring purpose: A validation study', *Molecular Reproduction and Development*, 86(10), pp. 1283–1291. doi:10.1002/mrd.23117

Carapella, S. C. (2002). 'Arsenic and arsenic alloys.' *Kirk-Othmer Encyclopedia of Chemical Technology*. https://doi.org/10.1002/0471238961.0118190503011801.a01.pub2

Ćirić, J. et al. (2018) 'Seasonal distributions of heavy metal concentrations in different snail (Helix Pomatia) tissues from an urban environment in Serbia', *Environmental Science and Pollution Research*, 25(33), pp. 33415–33422. doi:10.1007/s11356-018-3295-1.

da Silva, J. A., Fraústo da Silva, J. J., & Pombeiro, A. J. (2013). 'Amavadin, a vanadium natural complex: Its role and applications'. *Coordination Chemistry Reviews*, *257*(15–16), 2388–2400. https://doi.org/10.1016/j.ccr.2013.03.010

Dallinger, R., Berger, B., Triebskorn-Köhler, R. and Köhler, H., (2001). 14 Soil Biology and Ecotoxicology. *The biology of terrestrial molluscs*, p.489.

Dallinger, R., Hunziker, P. E., Berger, B., Gruber, C., & Stürzenbaum, S. (2000). 'Metallothioneins in terrestrial invertebrates: Structural aspects, biological significance and implications for their use as biomarkers'. *Cellular and Molecular Biology*, 46(2), 331–346.

Dar, M., Green, I. and Khan, F., (2019). Trace metal contamination: Transfer and fate in food chains of terrestrial invertebrates. *Food Webs*, 20, p.e00116. Available at: <https://www.sciencedirect.com/science/article/pii/S2352249618300715?via%3Dihub>

De Silva, S., Bernett, C., Meaklim, J., Abeywardane, E., & Reichman, S. M. (2019). 'Probing the effects of different lead compounds on the bioavailability of lead to plants'. *Chemosphere*, *230*, 24–28. https://doi.org/10.1016/j.chemosphere.2019.04.122

Des Marais, T. L., & Costa, M. (2019). Mechanisms of Chromium-Induced Toxicity. *Current opinion in toxicology*, 14, 1–7. https://doi.org/10.1016/j.cotox.2019.05.003

Duffus, J., (2002). '"Heavy metals" a meaningless term? (IUPAC Technical Report)'. *Pure and Applied Chemistry*, 74(5), pp.793-807. Available at:<https://publications.iupac.org/pac/2002/pdf/7405x0793.pdf>

Dummee, V., Kruatrachue, M., Trinachartvanit, W., Tanhan, P., Pokethitiyook, P., & Damrongphol, P. (2012). Bioaccumulation of heavy metals in water, sediments, aquatic plant and histopathological effects on the golden apple snail in Beung Boraphet Reservoir, Thailand. *Ecotoxicology and Environmental Safety*, 86, 204–212.

Environment and Resource Authority (ERA). (2016). 'Contamination by Hazardous Substances'. In *MSFD-Initial Assessment*. Environment and Resource Authority. Retrieved December 23, 2023, from https://era.org.mt/wp-content/uploads/2019/05/MSFD-InitialAssessment-Contamination.pdf

Environment and Resources Authority (ERA) (2018), 'State of the Environment Report 2018.'

European Food Safety Authority (EFSA) (2014) 'Scientific Opinion on Dietary Reference Values for chromium'. *EFSA Journal*, 12(10), 3845. https://doi.org/10.2903/j.efsa.2014.3845

Frank, R., Braun, H. E., Ishida, K., & Suda, P. (1976). 'Persistent organic and inorganic pesticide residues in orchard soils and vineyards of Southern Ontario.' *Canadian Journal of Soil Science*, *56*(4), 463–484. https://doi.org/10.4141/cjss76-055

Fu, H., Yang, Z., Liu, Y. and Shao, P., (2020). 'Ecological and human health risk assessment of heavy metals in dust affected by fireworks during the Spring Festival in Beijing'. *Air Quality, Atmosphere & Health*, 14(1), pp.139-148. https://link.springer.com/article/10.1007/s11869-020-00920-9#citeas

Giusti, F., Manganelli, G. and Schembri, P. J., (1995). *The non-marine molluscs of the Maltese Islands*. Torino: Museo Regionale di Scienze Naturali - Torino, pp.467-472, 491-497.

Gomot de Vaufleury, A. (2000). 'Standardized growth toxicity testing (Cu, Zn, Pb, and pentachlorophenol) with *Helix aspersa*'. *Ecotoxicology and Environmental Safety*, 46(1), 41–50.

Gonnelli, C. & Renella, G. (2013). 'Chromium and Nickel.' In B. J. Alloway [Ed.], Heavy *metals in soils: Trace metals and metalloids in soils and their bioavailability* (3rd ed., Vol. 22, pp. 313–333). essay, Springer.

Gomot de Vaufleury, A. and Pihan, F. (2002) 'Methods for toxicity assessment of contaminated soil by oral or dermal uptake in land snails: Metal bioavailability and bioaccumulation', *Environmental Toxicology and Chemistry*, 21(4), p. 820.

Graveland, J., Van der Wal, R., Van Balen, J. H., & Van Noordwijk, A. J. (1994). Poor reproduction in forest passerines from decline of snail abundance on acidified soils. *Nature*, 368(6470), 446–448.

Hispard, F., de Vaufleury, A., Cosson, R., Devaux, S., Scheifler, R., Cœurdassier, M., Gimbert, F., Martin, H., Richert, L., Berthelot, A. and Badot, P., (2008). Comparison of transfer and effects of Cd on rats exposed in a short experimental snail–rat food chain or to $CdCl_2$ dosed food. *Environment International*, 34(3), pp.381-389. https://www.sciencedirect.com/science/article/pii/S0160412007001699?via%3Dihub

Itziou, A., & Dimitriadis, V. (2011). 'Introduction of the land snail *Eobania vermiculata* as a bioindicator organism of terrestrial pollution using a battery of biomarkers'. *Science Of The Total Environment*, *409*(6), 1181-1192. https://doi.org/10.1016/j.scitotenv.2010.12.009.

Jaishankar, M., Tseten, T., Anbalagan, N., Mathew, B. and Beeregowda, K. (2014). 'Toxicity, mechanism and health effects of some heavy metals', *Interdisciplinary Toxicology*, 7(2), 51 pp.60-72. https://www.ncbi.nlm.nih.gov/pmc/articles/PMC4427717/

Jankowski, K.J. and Reszke, E. (2011) *Microwave induced plasma analytical spectrometry*. Cambridge: Royal Society of Chemistry.

Korbecki J, Baranowska-Bosiacka I, Gutowska I, Chlubek D. (2012) 'Biochemical and medical importance of vanadium compounds'. *Acta Biochim Pol.* 2012; 59(2):195-200.

Lang, D.M. (1960). *Soils of Malta and Gozo*. H.M. Stationery Office. http://books.google.ie/books?id=iB5BAAAAYAAJ&q=soils+of+malta+and+gozo&dq=soils+of+malta+and+gozo&hl=&cd=1&source=gbs_api

Larbaa, R., & Soltani, N. (2013). Diversity of the terrestrial gastropods in the Northeast Algeria: spatial and temporal distribution. *European Journal of Experimental Biology*, *3*(4), 209-215.

Lau, S., Mohamed, M., Tan Chi Yen, A., & Su'ut, S. (1998). Accumulation of heavy metals in freshwater molluscs. *Science of The Total Environment*, 214(1–3), 113–121.

Li, W., Simmons, P., Shrader, D., Herrman, T. J., & Dai, S. Y. (2013). 'Microwave plasma-atomic emission spectroscopy as a tool for the determination of copper, iron, manganese and zinc in animal feed and fertilizer'. *Talanta*, 112, 43–48.

Li, L., & Yang, X. (2018). 'The Essential Element Manganese, Oxidative Stress, and Metabolic Diseases: Links and Interactions'. *Oxidative Medicine and Cellular Longevity*, *2018*, 1–11. https://doi.org/10.1155/2018/7580707

Madejón, P. (2013) 'Barium' In B. J. Alloway [Ed.], Heavy *metals in soils: Trace metals and metalloids in soils and their bioavailability* (3rd ed., Vol. 22, pp. 507–514). essay, Springer.

Madejón, P. (2013) 'Vanadium' In B. J. Alloway [Ed.], Heavy *metals in soils: Trace metals and metalloids in soils and their bioavailability* (3rd ed., Vol. 22, pp. 579–587). essay, Springer.

Massadeh, A. M., Alomary, A. A., Mir, S., Momani, F. A., Haddad, H. I., & Hadad, Y. A. (2016). Analysis of Zn, CD, As, Cu, Pb, and Fe in snails as bioindicators and soil samples near Traffic Road by ICP-OES, *Environmental Science and Pollution Research*, 23(13), pp. 13424–13431.

Mertens, J., & Smolders, E. (2013a). 'Cadmium.' In B. J. Alloway [Ed.], *Heavy Metals in Soils: Trace Metals and Metalloids in Soils and their Bioavailability* (3rd ed., Vol. 22, pp. 283–311). essay, Springer.

Mertens, J., & Smolders, E. (2013b). 'Zinc.' In B. J. Alloway [Ed.], *Heavy Metals in Soils: Trace Metals and Metalloids in Soils and their Bioavailability* (3rd ed., Vol. 22, pp. 465–493). essay, Springer.

National Institutes of Health (NIH) (2022, June 2). Chromium-Fact Sheet for Health Professionals. U.S. Department of Health & Human Services. https://ods.od.nih.gov/factsheets/Chromium-HealthProfessional/#h2

Nemsadze, K., Sanikidze, T., Ratiani, L., Gabunia, L., & Sharashenidze, T. (2009). Mechanisms of lead-induced poisoning. *Georgian medical news*, (172-173), 92–96.

Nikogosyan, D. N. (1991). 'Beta barium borate (BBO): A review of its properties and applications'. *Applied Physics a Solids and Surfaces*, *52*(6), 359–368. https://doi.org/10.1007/bf00323647

Nour, H. E. (2020). 'Distribution and accumulation ability of heavy metals in bivalve shells and associated sediment from Red Sea coast, Egypt'. *Environmental Monitoring and Assessment*, 192(6). https://doi.org/10.1007/s10661-020-08285-3

O'Brien, W. J. (1915). 'A Study of Lithopone'. *The Journal of Physical Chemistry*, *19*(2), 113–144. https://doi.org/10.1021/j150155a002

Ogundele, D. T. ., Adio, A. A. . and Oludele, O. E. (2015). 'Heavy Metal Concentrations in Plants and Soil along Heavy Traffic Roads in North Central Nigeria'. *Journal of Environmental & Analytical Toxicology*, *05*(06). https://doi.org/10.4172/2161-0525.1000334

Oorts, K. (2013) 'Copper' In B. J. Alloway [Ed.], Heavy *metals in soils: Trace metals and metalloids in soils and their bioavailability* (3rd ed., Vol. 22, pp. 367–394). essay, Springer.

Peryea, F. J., & Creger, T. L. (1994). 'Vertical distribution of lead and arsenic in soils contaminated with lead arsenate pesticide residues.' *Water, Air, & Soil Pollution*, *78*(3–4), 297–306. https://doi.org/10.1007/bf00483038

Plafkin, J. L. (1989). *Rapid bioassessment protocols for use in streams and rivers: benthic macroinvertebrates and fish*. United States Environmental Protection Agency, Office of Water.

Posudin, Y., (2014). Methods of Measuring Environmental Parameters.

Regoli, F. et al. (2006) 'Use of the land snail *helix aspersa* as Sentinel organism for monitoring ecotoxicologic effects of urban pollution: An integrated approach', *Environmental Health Perspectives*, 114(1), pp. 63–69. doi:10.1289/ehp.8397.

Robson, R. L., Eady, R. R., Richardson, T. H., Miller, R. W., Hawkins, M., & Postgate, J. R. (1986). 'The alternative nitrogenase of Azotobacter chroococcum is a vanadium enzyme'. *Nature*, *322*(6077), 388–390. https://doi.org/10.1038/322388a0

Rota, E., Barbato, D., Ancora, S., Bianchi, N., & Bargagli, R. (2016). Papillifera papillaris (O.F. Müller), a small snail living on stones and monuments, as indicator of metal deposition and bioavailability in urban environments, *Ecological Indicators*, 69, pp. 360–367.

Russell, L. K., DeHaven, J. I., & Botts, R. P. (1981). Toxic effects of cadmium on the Garden snail (helix aspersa). *Bulletin of Environmental Contamination and Toxicology*, 26, 634–640.

Russell, M. S. & Svrcula, K. (2008). 'Chemistry of Fireworks'. *Royal Society of Chemistry*. p. 110. ISBN 978-0-85404-127-5.

Schlesinger, W. H., Klein, E. M., & Vengosh, A. (2017). 'Global biogeochemical cycle of vanadium'. *Proceedings of the National Academy of Sciences*, *114*(52). https://doi.org/10.1073/pnas.1715500114

Shehu, J., Shehu, A., Mullaj, A. (2011) 'Uptake of heavy metals by different spontaneous plant species grown along Lana River, Albania'. *Asian Journal of Chemistry*, 23(4), 1771-1773.

Shojaei, S., Jafarpour, A., Shojaei, S., Gyasi-Agyei, Y., & Rodrigo-Comino, J. (2021). 'Heavy metal uptake by plants from wastewater of different pulp concentrations and contaminated soils'. *Journal of Cleaner Production*, *296*, 126345. https://doi.org/10.1016/j.jclepro.2021.126345

Silvy, N. J. (2012). 'The Wildlife Techniques Manual'. *JHU Press*. http://books.google.ie/books?id=PL2IHTdzSeAC&pg=RA1-PR4&dq=978-1-4214-0159-1&hl=&cd=1&source=gbs_api

Singh, V., Singh, J., Singh, N., Rai, S. N., Verma, M. K., Verma, M., Singh, V., Chivate, M. S., Bilal, M. & Mishra, V. (2022). 'Simultaneous removal of ternary heavy metal ions by a newly isolated Microbacterium paraoxydans strain VSVM IIT(BHU) from coal washery effluent'. *BioMetals*. https://doi.org/10.1007/s10534-022-00476-4

Smith, M. J. (1989). 'Vanadium biochemistry: The unknown role of vanadium-containing cells in ascidians (sea squirts)'. *Experientia*, *45*(5), 452–457. https://doi.org/10.1007/bf01952027

Steinnes, E. (2013). 'Lead.' In B. J. Alloway [Ed.], Heavy *metals in soils: Trace metals and metalloids in soils and their bioavailability* (3rd ed., Vol. 22, pp. 395–409). essay, Springer.

Stohs, S.J. and Bagchi, D., (1995). 'Oxidative mechanisms in the toxicity of metal ions'. *Free radical biology and medicine*, *18*(2), pp.321-336.

Suedel, B.C., Boraczek, J.A., Peddicord, R.K., Clifford, P.A. and Dillon, T.M., (1994). 'Trophic transfer and biomagnification potential of contaminants in aquatic ecosystems'. *Reviews of Environmental Contamination and Toxicology.* 136, pp. 21–89.

Tardugno, R., Virga, A., Nava, V., Mannino, F., Salvo, A., Monaco, F., Giorgianni, M., & Cicero, N. (2023). 'Toxic and potentially toxic mineral elements of edible gastropods land snails (Mediterranean escargot)'. *Toxics*, 11(4), 317. https://doi.org/10.3390/toxics11040317

UN Environment Programme (UNEP) (2021, August 30). *Era of leaded petrol over, eliminating a major threat to human and planetary health*. https://www.unep.org/news-and-stories/press-release/era-leaded-petrol-over-eliminating-major-threat-human-and-planetary

Uren, N. C. (2013) 'Cobalt and Manganese.' In B. J. Alloway [Ed.], Heavy *metals in soils: Trace metals and metalloids in soils and their bioavailability* (3rd ed., Vol. 22, pp. 335–366). essay, Springer.

Uthus, E. O. (2003). 'Arsenic essentiality: A role affecting methionine metabolism.' *The Journal of Trace Elements in Experimental Medicine*, *16*(4), 345–355. https://doi.org/10.1002/jtra.10044

Verhoeven, J. D. (2007). *Steel Metallurgy for the Non-Metallurgist*. ASM International.

Vest, K. E., Hashemi, H. F., & Cobine, P. A. (2012). 'The copper metallome in eukaryotic cells'. *Metal Ions in Life Sciences*, *12*, 451–478. https://doi.org/10.1007/978-94-007-5561-1_13

Viard, B., Pihan, F., Promeyrat, S., & Pihan, J. (2004). 'Integrated assessment of heavy metal (Pb, Zn, Cd) highway pollution: bioaccumulation in soil, Graminaceae and land snails.' *Chemosphere*, *55*(10), 1349-1359. https://doi.org/10.1016/j.chemosphere.2004.01.003

Vranković, J., Janković-Tomanić, M. and Vukov, T. (2020) 'Comparative assessment of biomarker response to tissue metal concentrations in urban populations of the land snail Helix Pomatia (pulmonata: Helicidae)', *Comparative Biochemistry and Physiology Part B: Biochemistry and Molecular Biology*, 245, p. 110-448.

Wenzel, W. W. (2013). 'Arsenic.' In B. J. Alloway [Ed.], Heavy *metals in soils: Trace metals and metalloids in soils and their bioavailability* (3rd ed., Vol. 22, pp. 241–282). essay, Springer.

Wilcock, J. R., Perry, C. C., Williams, R. J. P., and Brook, A. J. (1989) 'Biological minerals formed from strontium and barium sulphates. II. Crystallography and control of mineral morphology in desmids'. *Proceedings of the Royal Society of London. B. Biological Sciences*, *238*(1292), 203–221. https://doi.org/10.1098/rspb.1989.0077

Woolson, E. A., Axley, J. H., & Kearney, P. C. (1971). 'The chemistry and phytotoxicity of arsenic in soils: I. Contaminated Field soils.' *Soil Science Society of America Journal*, *35*(6). https://doi.org/10.2136/sssaj1971.03615995003500060047x

Yasoshima, M., Matsuo, M., Kuno, A., and Takano, B. (2001). 'Studies on intake of heavy metals by bradybaena similaris, land snails, by XAFS Measurement'. *Journal of Synchrotron Radiation*, 8(2), 969–971. https://doi.org/10.1107/s0909049500020677

Yap CK, Cheng WH (2013) 'Distributions of heavy metal concentrations in different tissues of the mangrove snail Nerita lineata (Taburan kepekatan logam berat dalam tisu yang berlainan bagi siput bakau Nerita lineata)'. *Sains Malaysiana* 42(5):597–603

Zambelli, B., & Ciurli, S. (2013). 'Nickel and human health'. *Metal Ions in Life Sciences*, *13*, 321–357. https://doi.org/10.1007/978-94-007-7500-8_10

Zeng, H., Uthus, E. O., & Combs Jr., G. F. (2005). 'Mechanistic aspects of the interaction between selenium and arsenic.' *Journal of Inorganic Biochemistry*, *99*(6), 1269–1274. https://doi.org/10.1016/j.jinorgbio.2005.03.006

Appendix 1 - Sampling Advice

As it is my hope that this research encourages the use of snails (especially *Theba pisana* and *Cornu aspersum*) as bioindicators. As such, I have decided to include advice for the sampling and processing of these species.

Theba pisana

Description: These are relatively small (about 2cm in diameter) snails appearing to be mostly white or with brown colouration on the shell. To the untrained eye they may be easily confused with the snail species *Eobania vermiculata* due to the similar colouration and patterns of their shell. However, *T. pisana* can be distinguished as most have a black whorl or 'comma' on the shell apex and the prominent umbilical line on the reverse of their shell.

Sampling: Like most snail species, *T. pisana* asevates during the hot and dry summer months. To escape from the heat of the ground they often climb on high vegetation such as the stems of wild fennel or on the sides of buildings and rubble walls. This makes it ideal to sample *T. pisana* during the summer period as they would be visible and in eyesight and often grouped up in large clusters, making it very easy to collect the required number of individuals (around 20 in the case of this study due to their small size). When choosing individuals to sample, I recommend picking large snails (of at least 1cm-1.5cm) to make separation of the soft parts

easier as well as allowing young individuals to remain in their habitat. This makes choosing older individuals both more 'ethical', logical, and practical.

Cornu aspersum

Description: These are relatively large (about 4 cm in diameter) snails appearing to be brown with dark-brown or golden-brown specks or streaks. There is no real concern that *C. aspersum* could be confused with another species in Malta as they are quite unique in appearance.

Sampling: *C. aspersum* also aestivate in the summer months to escape the hot and dry conditions of their habitat. However, unlike *T. pisana*, they do not climb on high vegetation but rather burrow under soil or squeeze into cracks between rocks. It is therefore my recommendation that *C. aspersum* is not sampled during these summer months. In the winter months *C. aspersum* is active and will often be found on plants or under rocks, especially after rainfall. They do not tend to group together like in *T. pisana*'s case, but due to their size only a small number is needed for analysis (around 4 individuals).

Conclusion:

Species	When to Sample	How many to collect	Where to look	Notes
Cornu aspersum	Winter (especially after rain)	~4	Under rocks, in rubble walls, on plants.	none
Theba pisana	Summer	~20	Clustered together on high plants and walls.	Could be confused with *Eobania vermiculata*

Appendix 2 – Method and Equipment Validation

This appendix presents the validation study conducted to analyse the heavy metal composition of different samples of *Theba pisana* and *Cornu aspersum*. The primary objective was to validate the method and equipment, ensuring accuracy and reliability in measuring the practical heavy metal concentrations using Microwave Plasma-Atomic Emission Spectroscopy (MP-AES).

Four samples were selected at random, but coverage of all sample variables was ensured. I.e. a sample for soft parts and shells of both species:

- *Theba pisana* shell (Sample 46)
- *Theba pisana* soft parts (Sample 19)
- *Cornu aspersum* shell (Sample 45)
- *Cornu aspersum* soft parts (Sample 14)

A multi-element standard solution was then diluted 1 in 10 to achieve elemental concentrations of 10 ppm or less. This dilution ensured that the concentrations were within the expected range of concentrations for the samples. 11 solutions were then prepared using all pertinent combinations of variables to validate the method and equipment, and presented in the table below:

Solution Component 1	Solution Component 2	Ratio
Standard (STD)	Deionised water (DI)	1:1
Standard (STD)	Control (CTRL)	1:1
Standard (STD)	Sample 14	1:1
Standard (STD)	Sample 19	1:1
Standard (STD)	Sample 45	1:1
Standard (STD)	Sample 46	1:1
Control (CTRL)	Deionised water (DI)	1:1
Sample 14	Deionised water (DI)	1:1
Sample 19	Deionised water (DI)	1:1
Sample 45	Deionised water (DI)	1:1
Sample 46	Deionised water (DI)	1:1

The samples were then analysed using Microwave Plasma-Atomic Emission Spectroscopy (MP-AES). For the specific conditions of the analysis, refer to Table 3.2: Running conditions of the MP-AES 4100 series. The results of the analysis were then analysed to determine whether there were any significant differences between the theoretical and practical (experimental) values. For the purpose of this validation, the theoretical values (Th) were calculated as the sum of the standard with deionised water and the sample or control with deionised water (e.g., sum of (STD/DI) and (Sample 14/DI), with the result being the theoretical value of sample 14). Meanwhile, the practical values (Pr) were the spiked sample or control with the standard (e.g. STD/Sample 14).

An Analysis of Variance (ANOVA) was conducted to compare the theoretical and practical values for each heavy metal in each sample:

Element	P-Value	Significance (α=0.05)
As	0.9917	No
Cd	<0.0001	Yes
Cr	<0.0001	Yes
Cu	<0.0001	Yes
Ni	<0.0001	Yes
Pb	<0.0001	Yes
Zn	<0.0001	Yes

However, the Bonferroni's Multiple Comparison Test results indicated that there were no significant differences between the theoretical and practical values for each element in the following comparisons:

- Control (Th) vs. Control (Pr)
- Sample 14 (Th) vs. Sample 14 (Pr)
- Sample 19 (Th) vs. Sample 19 (Pr)
- Sample 45 (Th) vs. Sample 45 (Pr)
- Sample 46 (Th) vs. Sample 46 (Pr)

Descriptive statistics for each element are provided in the table at the end of the appendix. These statistics include measures for mean, standard deviation, and range, which give a comprehensive overview of the heavy metal concentrations in each sample.

Bar graphs for each element have been included to visually represent the data. These graphs illustrate the comparison between theoretical and practical values, highlighting the consistency between the two sets of measurements.

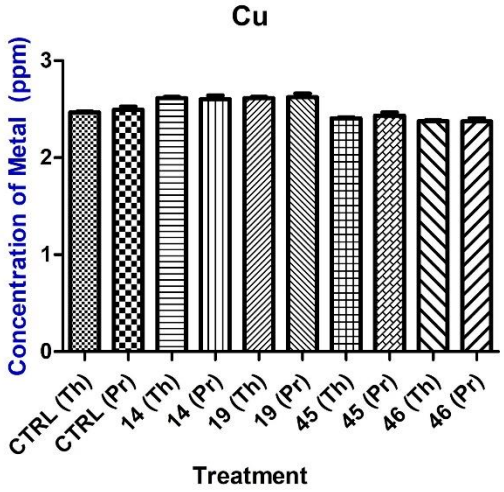

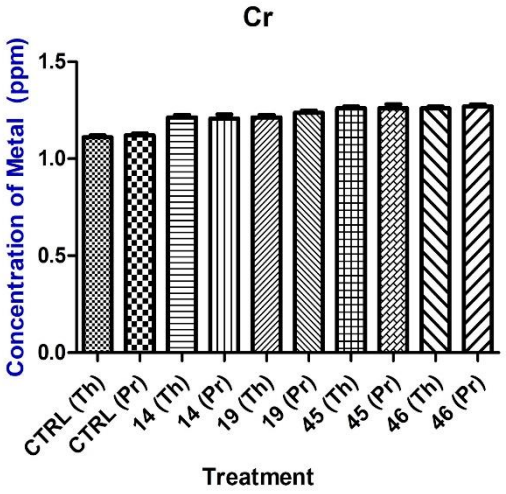

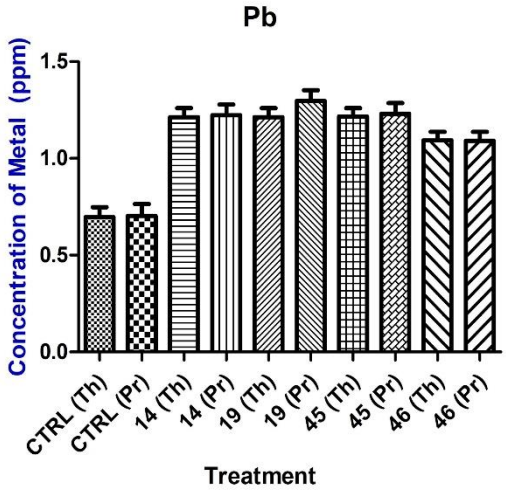

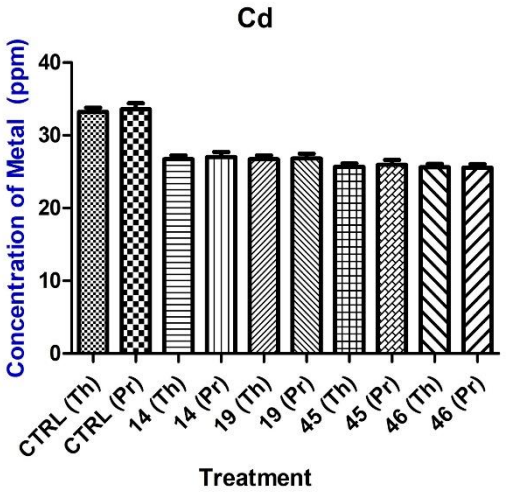

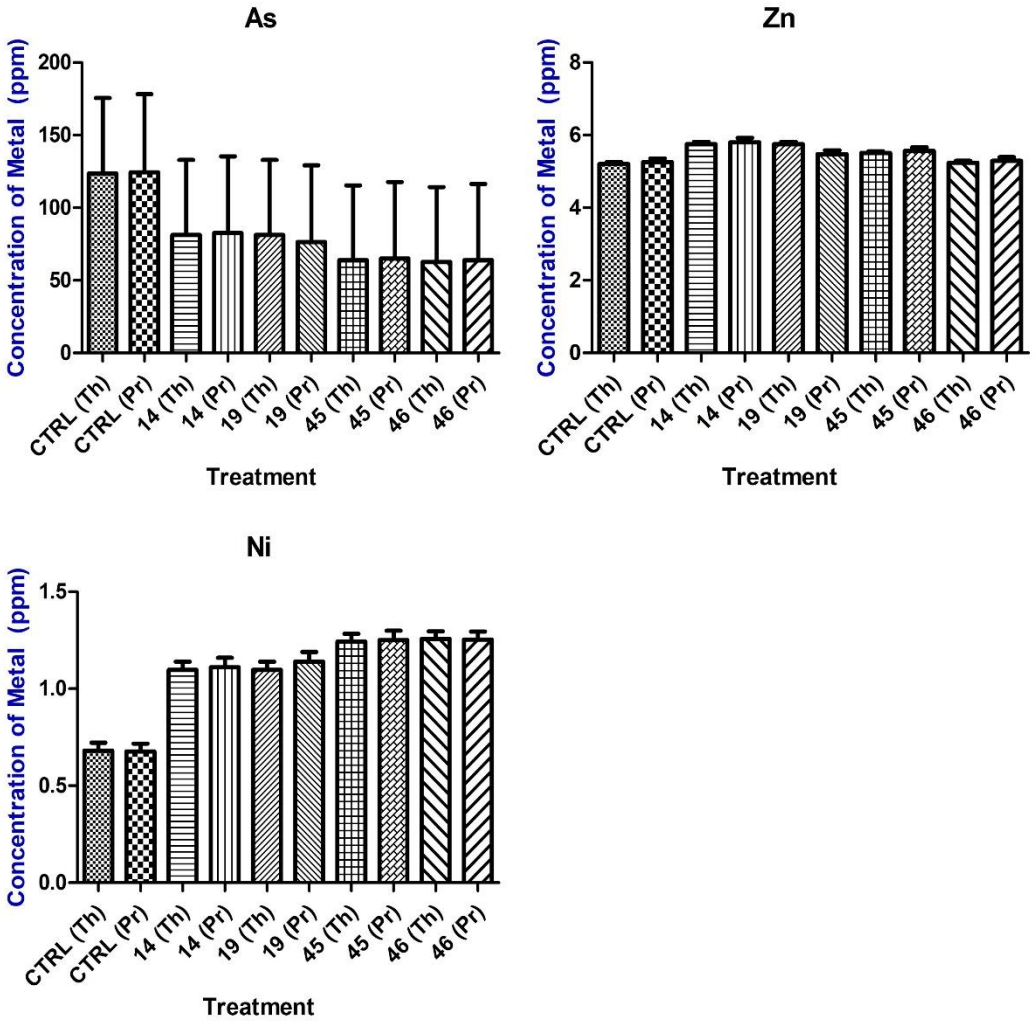

The absence of significant differences between the theoretical and practical heavy metal concentrations indicates that the analyses using MP-AES were both reliable and accurate. The detailed statistical analysis and graphical representations confirm the robustness of the methodology and the precision of the equipment used. This validation study provides confidence in the accuracy of the measurements of the heavy metal composition for *Theba pisana* and *Cornu aspersum* soft parts and shell samples.

	CTRL (Th)	CTRL (Pr)	14 (Th)	14 (Pr)	19 (Th)	19 (Pr)	45 (Th)	45 (Pr)	46 (Th)	46 (Pr)
As										
Minimum	70.83	69.410	29.330	29.640	29.330	22.730	12.170	12.050	11.090	10.980
Median	72.10	71.380	29.940	29.920	29.940	24.150	12.430	12.680	11.270	11.500
Maximum	227.7	232.30	184.60	188.300	184.600	182.200	167.000	170.300	165.800	169.100
Mean	123.6	124.40	81.290	82.610	81.290	76.350	63.860	65.020	62.700	63.850
Std. Deviation	90.23	93.480	89.460	91.510	89.460	91.650	89.300	91.200	89.240	91.120
Std. Error	52.09	53.970	51.650	52.830	51.650	52.910	51.560	52.650	51.520	52.610
Cd										
Minimum	32.50	32.180	26.130	25.860	26.130	25.780	25.110	24.860	25.100	24.600
Median	32.79	33.450	26.300	26.830	26.300	26.630	25.270	25.780	25.220	25.730
Maximum	34.40	35.090	27.750	28.310	27.750	28.040	26.630	27.160	26.560	26.300
Mean	33.23	33.570	26.730	27.000	26.730	26.820	25.670	25.930	25.630	25.540
Std. Deviation	1.024	1.459	0.890	1.234	0.890	1.142	0.835	1.158	0.811	0.865
Std. Error	0.591	0.842	0.514	0.712	0.514	0.659	0.482	0.668	0.468	0.500
Cr										
Minimum	1.090	1.110	1.190	1.180	1.190	1.220	1.240	1.230	1.240	1.260
Median	1.120	1.110	1.220	1.190	1.220	1.230	1.270	1.250	1.270	1.260

Maximum	1.120	1.140	1.230	1.250	1.230	1.260	1.270	1.300	1.270	1.290
Mean	1.110	1.120	1.213	1.207	1.213	1.237	1.260	1.260	1.260	1.270
Std. Deviation	0.017	0.017	0.021	0.038	0.021	0.021	0.017	0.036	0.017	0.017
Std. Error	0.010	0.010	0.012	0.022	0.012	0.012	0.010	0.021	0.010	0.010
Cu										
Minimum	2.450	2.430	2.590	2.540	2.590	2.550	2.390	2.370	2.360	2.320
Median	2.470	2.520	2.620	2.600	2.620	2.660	2.410	2.460	2.380	2.370
Maximum	2.480	2.530	2.630	2.670	2.630	2.660	2.420	2.470	2.390	2.430
Mean	2.467	2.493	2.613	2.603	2.613	2.623	2.407	2.433	2.377	2.373
Std. Deviation	0.015	0.055	0.021	0.065	0.021	0.064	0.015	0.055	0.015	0.055
Std. Error	0.009	0.032	0.012	0.038	0.012	0.037	0.009	0.032	0.009	0.032
Ni										
Minimum	0.620	0.610	1.040	1.030	1.040	1.060	1.190	1.170	1.200	1.180
Median	0.660	0.670	1.070	1.100	1.070	1.130	1.220	1.240	1.240	1.260
Maximum	0.760	0.750	1.180	1.200	1.180	1.230	1.320	1.340	1.330	1.320
Mean	0.680	0.677	1.097	1.110	1.097	1.140	1.243	1.250	1.257	1.253
Std. Deviation	0.072	0.070	0.074	0.085	0.074	0.085	0.068	0.085	0.067	0.070
Std. Error	0.042	0.041	0.043	0.049	0.043	0.049	0.039	0.049	0.038	0.041

Pb										
Minimum	0.610	0.600	1.140	1.130	1.140	1.200	1.140	1.130	1.020	1.000
Median	0.690	0.700	1.200	1.220	1.200	1.300	1.220	1.240	1.090	1.110
Maximum	0.790	0.810	1.300	1.320	1.300	1.390	1.290	1.320	1.170	1.160
Mean	0.697	0.703	1.213	1.223	1.213	1.297	1.217	1.230	1.093	1.090
Std. Deviation	0.090	0.105	0.081	0.095	0.081	0.095	0.075	0.095	0.075	0.082
Std. Error	0.052	0.061	0.047	0.055	0.047	0.055	0.043	0.055	0.043	0.047
Zn										
Minimum	5.120	5.070	5.630	5.580	5.630	5.280	5.430	5.370	5.150	5.100
Median	5.190	5.290	5.730	5.840	5.730	5.520	5.500	5.610	5.230	5.340
Maximum	5.300	5.410	5.880	5.990	5.880	5.630	5.600	5.710	5.330	5.430
Mean	5.203	5.257	5.747	5.803	5.747	5.477	5.510	5.563	5.237	5.290
Std. Deviation	0.091	0.172	0.126	0.207	0.126	0.179	0.085	0.175	0.090	0.171
Std. Error	0.052	0.100	0.073	0.120	0.073	0.103	0.049	0.101	0.052	0.098

Appendix 3 - Summarised Data

Results for Industrial locations

Soft parts			Shells		
Sample	Metal	Concentration (µg/g)	Sample	Metal	Concentration (µg/g)
9	As	940.27	37	As	50.34
	Zn	3.77		Zn	0.53
	Cd	123.05		Cd	15.45
	Cu	7.85		Cu	0.18
	Ni	6.63		Ni	0.36
	Pb	8.88		Pb	2.13
	Cr	2.92		Cr	0.21
	Al	10.40		Al	6.07
	Mn	3.10		Mn	0.71
	V	0.00		V	0.14
	Ba	15.88		Ba	9.48
15	As	933.41	25	As	114.15
	Zn	22.75		Zn	0.43
	Cd	134.53		Cd	35.96
	Cu	11.58		Cu	0.69
	Ni	8.62		Ni	0.86
	Pb	11.90		Pb	5.25
	Cr	4.07		Cr	0.60
	Al	32.34		Al	15.91
	Mn	5.75		Mn	1.63
	V	0.00		V	0.26
	Ba	23.23		Ba	22.62
21	As	349.17	40	As	74.57
	Zn	13.93		Zn	0.52
	Cd	52.71		Cd	18.45
	Cu	10.50		Cu	0.14
	Ni	3.23		Ni	0.47
	Pb	3.56		Pb	3.19
	Cr	1.55		Cr	0.33
	Al	5.14		Al	6.98
	Mn	6.42		Mn	1.78
	V	0.00		V	0.28
	Ba	126.02		Ba	8.99
22	As	166.30	48	As	36.63
	Zn	4.94		Zn	0.63
	Cd	58.97		Cd	20.91
	Cu	4.87		Cu	0.11
	Ni	3.79		Ni	0.40
	Pb	4.63		Pb	4.86
	Cr	1.81		Cr	0.51
	Al	2.51		Al	3.71
	Mn	3.03		Mn	2.80
	V	0.00		V	0.34
	Ba	29.97		Ba	16.17

Results for urban locations

Soft parts			Shells		
Sample	Metal	Concentration (µg/g)	Sample	Metal	Concentration (µg/g)
1	As	197.38	44	As	41.32
	Zn	2.53		Zn	0.34
	Cd	86.96		Cd	14.77
	Cu	5.74		Cu	0.17
	Ni	7.65		Ni	0.28
	Pb	10.24		Pb	2.27
	Cr	3.71		Cr	0.24
	Al	7.77		Al	7.09
	Mn	1.52		Mn	0.90
	V	0.00		V	0.17
	Ba	10.47		Ba	6.58
11	As	527.55	30	As	114.34
	Zn	19.31		Zn	1.51
	Cd	86.67		Cd	41.04
	Cu	8.47		Cu	0.66
	Ni	4.72		Ni	1.70
	Pb	5.69		Pb	4.72
	Cr	2.22		Cr	1.04
	Al	7.36		Al	0.66
	Mn	5.83		Mn	3.02
	V	0.00		V	0.28
	Ba	54.86		Ba	7.74
12	As	1705.28	47	As	86.10
	Zn	4.14		Zn	1.06
	Cd	226.43		Cd	40.54
	Cu	9.84		Cu	0.97
	Ni	15.54		Ni	1.74
	Pb	22.02		Pb	4.63
	Cr	6.71		Cr	1.16
	Al	7.04		Al	6.47
	Mn	3.02		Mn	1.16
	V	0.00		V	0.39
	Ba	38.56		Ba	12.84
14	As	1140.60	45	As	75.77
	Zn	23.50		Zn	3.54
	Cd	155.56		Cd	33.69
	Cu	12.31		Cu	0.69
	Ni	10.26		Ni	0.95
	Pb	14.70		Pb	5.18
	Cr	4.44		Cr	0.60
	Al	16.15		Al	16.24
	Mn	6.67		Mn	3.54
	V	0.00		V	0.52
	Ba	132.31		Ba	14.08

Results for residential locations

Soft parts			Shells		
Sample	Metal	Concentration (µg/g)	Sample	Metal	Concentration (µg/g)
3	As	232.28	35	As	28.47
	Zn	17.49		Zn	0.41
	Cd	63.87		Cd	19.74
	Cu	9.20		Cu	0.20
	Ni	2.70		Ni	0.30
	Pb	3.10		Pb	4.47
	Cr	1.50		Cr	0.41
	Al	6.30		Al	20.71
	Mn	3.80		Mn	2.44
	V	0.00		V	0.36
	Ba	69.07		Ba	8.53
13	As	307.47	29	As	36.74
	Zn	13.51		Zn	0.69
	Cd	50.65		Cd	23.66
	Cu	9.93		Cu	0.17
	Ni	2.24		Ni	0.34
	Pb	2.51		Pb	4.91
	Cr	1.07		Cr	0.46
	Al	29.80		Al	40.69
	Mn	11.81		Mn	3.60
	V	0.00		V	0.34
	Ba	75.97		Ba	8.34
16	As	983.11	34	As	37.17
	Zn	6.67		Zn	0.80
	Cd	140.44		Cd	25.68
	Cu	17.78		Cu	0.31
	Ni	8.22		Ni	0.37
	Pb	11.33		Pb	4.85
	Cr	3.56		Cr	0.49
	Al	45.33		Al	31.95
	Mn	5.56		Mn	1.84
	V	0.00		V	0.37
	Ba	28.22		Ba	15.79
24	As	988.24	26	As	98.61
	Zn	13.53		Zn	1.94
	Cd	132.94		Cd	33.94
	Cu	9.71		Cu	0.51
	Ni	13.82		Ni	0.84
	Pb	17.06		Pb	5.39
	Cr	6.18		Cr	0.59
	Al	24.12		Al	5.39
	Mn	4.71		Mn	1.60
	V	0.00		V	0.25
	Ba	25.59		Ba	18.78

Results for agricultural locations

Soft parts			Shells		
Sample	Metal	Concentration (µg/g)	Sample	Metal	Concentration (µg/g)
2	As	55.65	28	As	25.72
	Zn	16.24		Zn	0.49
	Cd	78.39		Cd	15.16
	Cu	15.82		Cu	0.07
	Ni	3.81		Ni	0.28
	Pb	3.53		Pb	2.68
	Cr	2.40		Cr	0.28
	Al	2.97		Al	5.79
	Mn	6.36		Mn	1.46
	V	0.00		V	0.14
	Ba	146.89		Ba	4.74
6	As	474.44	33	As	47.47
	Zn	11.76		Zn	0.44
	Cd	69.94		Cd	12.63
	Cu	4.29		Cu	0.09
	Ni	2.66		Ni	0.35
	Pb	2.35		Pb	1.52
	Cr	1.43		Cr	0.18
	Al	24.74		Al	3.68
	Mn	3.48		Mn	0.44
	V	0.00		V	0.12
	Ba	55.32		Ba	4.43
7	As	274.83	38	As	6.92
	Zn	3.38		Zn	0.16
	Cd	41.56		Cd	4.82
	Cu	4.58		Cu	0.03
	Ni	1.75		Ni	0.09
	Pb	1.93		Pb	1.03
	Cr	0.90		Cr	0.11
	Al	4.58		Al	3.21
	Mn	3.38		Mn	0.55
	V	0.00		V	0.08
	Ba	46.21		Ba	2.58
18	As	533.55	39	As	91.91
	Zn	25.98		Zn	5.99
	Cd	78.41		Cd	23.70
	Cu	7.17		Cu	0.36
	Ni	4.62		Ni	0.83
	Pb	6.69		Pb	3.20
	Cr	2.23		Cr	0.36
	Al	15.78		Al	10.84
	Mn	6.37		Mn	2.43
	V	0.00		V	0.24
	Ba	25.98		Ba	14.64

Results for rural locations

Soft parts			Shells		
Sample	Metal	Concentration (µg/g)	Sample	Metal	Concentration (µg/g)
5	As	533.29	36	As	19.26
	Zn	1.13		Zn	0.15
	Cd	90.55		Cd	10.83
	Cu	2.82		Cu	0.26
	Ni	4.65		Ni	0.18
	Pb	5.92		Pb	1.70
	Cr	2.26		Cr	0.18
	Al	16.50		Al	11.32
	Mn	2.96		Mn	0.93
	V	0.00		V	0.15
	Ba	12.41		Ba	4.64
10	As	902.59	43	As	56.78
	Zn	6.48		Zn	0.61
	Cd	125.00		Cd	19.39
	Cu	17.41		Cu	0.15
	Ni	5.93		Ni	0.36
	Pb	7.78		Pb	4.19
	Cr	2.04		Cr	0.41
	Al	13.52		Al	11.15
	Mn	7.41		Mn	2.30
	V	0.00		V	0.36
	Ba	172.41		Ba	5.63
19	As	537.76	46	As	39.23
	Zn	4.66		Zn	0.84
	Cd	103.68		Cd	24.97
	Cu	7.89		Cu	0.19
	Ni	6.10		Ni	0.45
	Pb	8.07		Pb	5.29
	Cr	2.87		Cr	0.58
	Al	26.01		Al	14.00
	Mn	9.51		Mn	2.06
	V	0.00		V	0.45
	Ba	20.81		Ba	14.71
23	As	131.93	41	As	10.46
	Zn	3.54		Zn	0.25
	Cd	37.20		Cd	8.22
	Cu	7.00		Cu	0.03
	Ni	3.29		Ni	0.15
	Pb	3.54		Pb	3.05
	Cr	1.56		Cr	0.25
	Al	2.39		Al	5.28
	Mn	1.15		Mn	1.27
	V	0.00		V	0.20
	Ba	41.15		Ba	3.81

Results for isolated locations

Soft parts			Shells		
Sample	Metal	Concentration (µg/g)	Sample	Metal	Concentration (µg/g)
4	As	608.51	42	As	52.07
	Zn	9.31		Zn	1.01
	Cd	131.49		Cd	25.70
	Cu	41.58		Cu	0.34
	Ni	7.13		Ni	0.67
	Pb	10.10		Pb	4.59
	Cr	3.17		Cr	0.47
	Al	28.51		Al	37.44
	Mn	27.52		Mn	4.72
	V	0.00		V	0.40
	Ba	236.04		Ba	8.36
8	As	405.26	31	As	5.97
	Zn	9.47		Zn	0.19
	Cd	56.75		Cd	6.30
	Cu	14.45		Cu	0.02
	Ni	2.11		Ni	0.14
	Pb	1.15		Pb	3.46
	Cr	1.24		Cr	0.28
	Al	23.92		Al	8.47
	Mn	9.95		Mn	1.60
	V	0.00		V	0.19
	Ba	160.96		Ba	5.03
17	As	730.33	32	As	17.98
	Zn	21.22		Zn	0.47
	Cd	103.10		Cd	15.05
	Cu	15.40		Cu	0.13
	Ni	6.38		Ni	0.26
	Pb	9.20		Pb	4.77
	Cr	2.82		Cr	0.39
	Al	31.92		Al	61.94
	Mn	14.84		Mn	8.39
	V	0.00		V	0.39
	Ba	72.11		Ba	9.59
20	As	472.75	27	As	160.85
	Zn	0.88		Zn	1.15
	Cd	127.69		Cd	31.08
	Cu	8.57		Cu	0.62
	Ni	8.35		Ni	0.69
	Pb	11.21		Pb	5.00
	Cr	3.74		Cr	0.54
	Al	37.58		Al	19.69
	Mn	7.25		Mn	2.00
	V	0.00		V	0.31
	Ba	29.01		Ba	13.23

Appendix 4 - Raw Data

Path: C:\Users\University Of Malta\Documents\Agilent\MP Expert\My Results\New HM01 - nathanael (Final).mpws

Date created: 20/02/2023 12:00:29

Instrument used: AU12200193 Current software: Version 1.6.2.12109

Enable EGCM for monochromator purge: Off

Notes:

Calibration Correlation Coefficient Limit: 0.9899

Standard addition: Off QC Active: Off

Reagent Blank: Off IEC: Off

Blank Subtraction: On

Reslope: Off

Common Conditions

Replicates: 3 Sample introduction: Manual

Pump Speed (rpm): 15

Sample Uptake Time (s): 15 Sample uptake fast pump: On

AVS 4 delay (s): N/A

SVS 1 delay (s): N/A Rinse time fast pump: N/A

Rinse time (s): N/A

Stabilization time (s): 15

Air Injection Mode: Off

Isomist Temperature (°C): N/A

Settings per element:

Element	Label (Wavelength nm)	Type	Background Correction	Calibration Fit	Read Time (s)	Viewing position
Ni	Ni (352.454)	Analyte	Auto	Linear Weighted	3	0
Pb	Pb (405.781)	Analyte	Auto	Rational Weighted	3	0
As	As (193.695)	Analyte	Auto	Rational Weighted	3	0
Cu	Cu (324.754)	Analyte	Auto	Linear Weighted	3	0
Zn	Zn (213.857)	Analyte	Auto	Rational Weighted	3	0
Cr	Cr (425.433)	Analyte	Auto	Rational Weighted	3	0
Cd	Cd (226.502)	Analyte	Auto	Rational Weighted	3	0

Element	Label (Wavelength nm)	Type	Nebulizer Pressure (kPa)
Ni	Ni (352.454)	Analyte	240
Pb	Pb (405.781)	Analyte	240
As	As (193.695)	Analyte	120
Cu	Cu (324.754)	Analyte	240
Zn	Zn (213.857)	Analyte	140
Cr	Cr (425.433)	Analyte	240
Cd	Cd (226.502)	Analyte	140

Calibration parameters:

Label (Wavelength nm)	Minimum Concentration	Maximum Concentration	Calibration Error
Ni (352.454)	0 ppm	11 ppm	5 %
Pb (405.781)	0 ppm	11 ppm	5 %
As (193.695)	0 ppm	11 ppm	5 %
Cu (324.754)	0 ppm	11 ppm	5 %
Zn (213.857)	0 ppm	11 ppm	5 %
Cr (425.433)	0 ppm	11 ppm	5 %
Cd (226.502)	0 ppm	11 ppm	5 %

Calibration Curves:

Ni (352.454 nm)
Intensity = 17238.29682358 * Concentration - 436.62811460
Correlation coefficient: 0.99997

Standards	Intensity	Method Concentration	Calculated Concentration	% Error
Blank	-0.82	0.00	0.03	N/A
Standard 2	10222.92	0.63	0.62	1.06
Standard 3	21150.26	1.25	1.25	0.18
Standard 4	43151.34	2.50	2.53	1.14
Standard 5	86954.56	5.00	5.07	1.39
Standard 6	176462.27	10.00	10.26	2.62

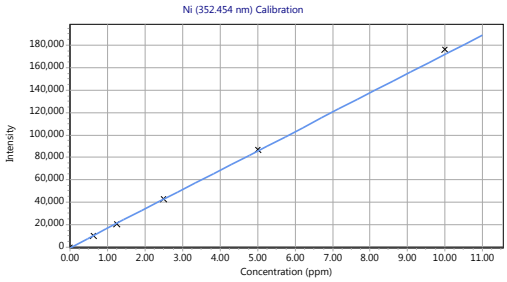

Pb (405.781 nm)
Intensity = (1854.97104367 * Concentration + 471.70838511) / (1 - 0.02928158 * Concentration)
Correlation coefficient: 0.99979

Standards	Intensity	Method Concentration	Calculated Concentration	% Error
Blank	0.16	0.00	-0.25	N/A
Standard 1	1083.57	0.31	0.32	3.78
Standard 3	2831.61	1.25	1.22	2.58
Standard 6	28250.64	10.00	10.36	3.62

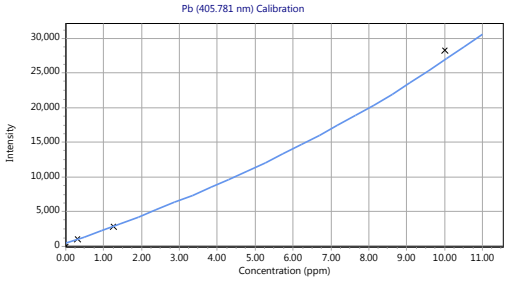

As (193.695 nm)
Intensity = (8138.48460554 * Concentration + 0.27751570) / (1 + 0.87765001 * Concentration)
Correlation coefficient: 0.99978

Standards	Intensity	Method Concentration	Calculated Concentration	% Error
Blank	0.55	0.00	0.00	N/A
Standard 4	6368.80	2.50	2.50	0.06
Standard 5	7568.91	5.00	5.06	1.21
Standard 6	8302.69	10.00	9.75	2.51

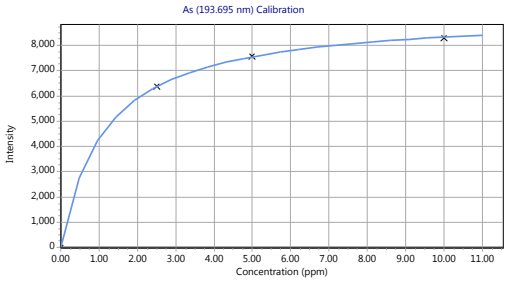

Cu (324.754 nm)
Intensity = 116275.71328419 * Concentration + 25.24847689
Correlation coefficient: 0.99994

Standards	Intensity	Method Concentration	Calculated Concentration	% Error
Blank	-0.04	0.00	0.00	N/A
Standard 1	37971.86	0.31	0.33	4.43
Standard 2	69757.51	0.63	0.60	4.05
Standard 3	146438.93	1.25	1.26	0.74
Standard 4	291147.07	2.50	2.50	0.15
Standard 5	578815.85	5.00	4.98	0.45
Standard 6	1135265.88	10.00	9.76	2.37

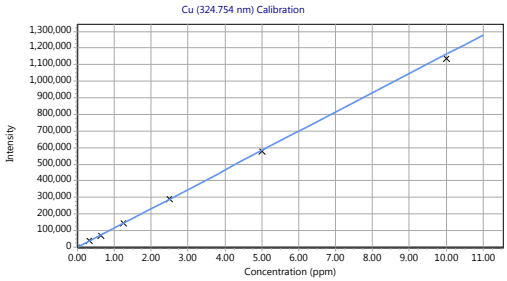

Zn (213.857 nm)
Intensity = (18603.15850360 * Concentration - 5.52508114) / (1 + 0.07603987 * Concentration)
Correlation coefficient: 0.99982

Standards	Intensity	Method Concentration	Calculated Concentration	% Error
Blank	-4.93	0.00	0.00	N/A
Standard 3	21106.55	1.25	1.24	0.64
Standard 5	68758.70	5.00	5.14	2.83
Standard 6	105288.82	10.00	9.94	0.64

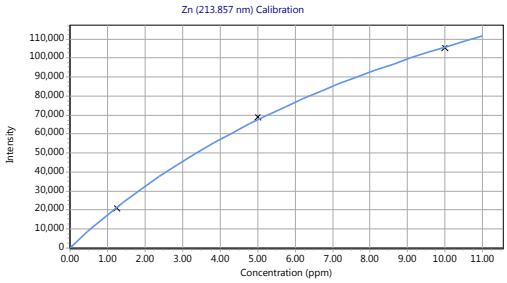

Cr (425.433 nm)
Intensity = (22109.32245124 * Concentration - 0.11222095) / (1 - 0.02739665 * Concentration)
Correlation coefficient: 0.99987

Standards	Intensity	Method Concentration	Calculated Concentration	% Error
Blank	0.39	0.00	0.00	N/A
Standard 4	57383.73	2.50	2.42	3.07
Standard 5	130211.32	5.00	5.07	1.42
Standard 6	301228.32	10.00	9.92	0.79

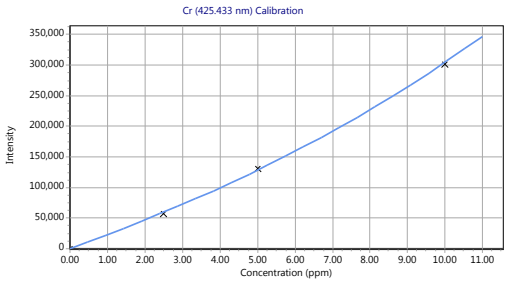

Cd (226.502 nm)
Intensity = (2247.51325447 * Concentration + 4.67772392) / (1 + 0.09077253 * Concentration)
Correlation coefficient: 0.99996

Standards	Intensity	Method Concentration	Calculated Concentration	% Error
Blank	-5.40	0.00	0.00	N/A
Standard 2	1369.45	0.63	0.64	2.85
Standard 3	2480.88	1.25	1.22	2.04
Standard 4	4602.71	2.50	2.51	0.52
Standard 5	7677.74	5.00	4.95	1.03
Standard 6	11820.61	10.00	10.06	0.60

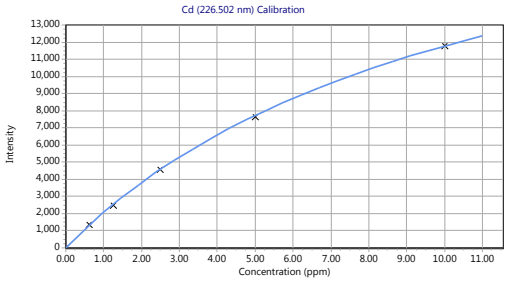

Detailed Results

Date Time	Label	Element Label (nm)	Conc	%RSD	Unadjusted Conc	Intensity	%RSD
20/02/2023 12:02:15	Blank	As (193.695 nm)	0.00 (ppm)	N/A	0.00 (ppm)	0.55	> 100.00
20/02/2023 12:02:15	Blank	Zn (213.857 nm)	0.00 (ppm)	N/A	0.00 (ppm)	-4.93	> 100.00
20/02/2023 12:02:15	Blank	Cd (226.502 nm)	0.00 (ppm)	N/A	0.00 (ppm)	-5.40	> 100.00
20/02/2023 12:02:15	Blank	Cu (324.754 nm)	0.00 (ppm)	N/A	0.00 (ppm)	-0.04	> 100.00
20/02/2023 12:02:15	Blank	Ni (352.454 nm)	0.00 (ppm)	N/A	0.00 (ppm)	-0.82	> 100.00
20/02/2023 12:02:15	Blank	Pb (405.781 nm)	0.00 (ppm)	N/A	0.00 (ppm)	0.16	> 100.00
20/02/2023 12:02:15	Blank	Cr (425.433 nm)	0.00 (ppm)	N/A	0.00 (ppm)	0.39	> 100.00
20/02/2023 12:15:59	Standard 1	As (193.695 nm)		N/A		7755.33 !	0.51
20/02/2023 12:15:59	Standard 1	Zn (213.857 nm)		N/A		3614.36 !	2.67
20/02/2023 12:15:59	Standard 1	Cd (226.502 nm)		N/A		1035.33 !	7.61
20/02/2023 12:15:59	Standard 1	Cu (324.754 nm)	0.31 ! (ppm)	N/A	0.31 ! (ppm)	37971.86 !	2.84

Date Time	Label	Element Label (nm)	Conc	%RSD	Unadjusted Conc	Intensity	%RSD
20/02/2023 12:15:59	Standard 1	Ni (352.454 nm)		N/A		5464.53 !	0.55
20/02/2023 12:15:59	Standard 1	Pb (405.781 nm)	0.31 ! (ppm)	N/A	0.31 ! (ppm)	1083.57 !	0.20
20/02/2023 12:15:59	Standard 1	Cr (425.433 nm)		N/A		5259.24 !	0.22
20/02/2023 12:17:54	Standard 2	As (193.695 nm)		N/A		7473.30 !	1.31
20/02/2023 12:17:54	Standard 2	Zn (213.857 nm)		N/A		8486.47 !	0.18
20/02/2023 12:17:54	Standard 2	Cd (226.502 nm)	0.63 ! (ppm)	N/A	0.63 ! (ppm)	1369.45 !	6.75
20/02/2023 12:17:54	Standard 2	Cu (324.754 nm)	0.63 ! (ppm)	N/A	0.63 ! (ppm)	69757.51 !	1.81
20/02/2023 12:17:54	Standard 2	Ni (352.454 nm)	0.63 ! (ppm)	N/A	0.63 ! (ppm)	10222.92 !	0.27
20/02/2023 12:17:54	Standard 2	Pb (405.781 nm)		N/A		1593.13 !	2.27
20/02/2023 12:17:54	Standard 2	Cr (425.433 nm)		N/A		11203.23 !	1.13
20/02/2023 12:08:04	Standard 3	As (193.695 nm)		N/A		6136.03	1.86
20/02/2023 12:08:04	Standard 3	Zn (213.857 nm)	1.25 (ppm)	N/A	1.25 (ppm)	21106.55	1.30
20/02/2023 12:08:04	Standard 3	Cd (226.502 nm)	1.25 (ppm)	N/A	1.25 (ppm)	2480.88	4.94
20/02/2023 12:08:04	Standard 3	Cu (324.754 nm)	1.25 (ppm)	N/A	1.25 (ppm)	146438.93	0.23
20/02/2023 12:08:04	Standard 3	Ni (352.454 nm)	1.25 (ppm)	N/A	1.25 (ppm)	21150.26	0.26
20/02/2023 12:08:04	Standard 3	Pb (405.781 nm)	1.25 (ppm)	N/A	1.25 (ppm)	2831.61	0.25
20/02/2023 12:08:04	Standard 3	Cr (425.433 nm)		N/A		25393.36	1.13
20/02/2023 12:09:53	Standard 4	As (193.695 nm)	2.50 (ppm)	N/A	2.50 (ppm)	6368.80	0.33
20/02/2023 12:09:53	Standard 4	Zn (213.857 nm)		N/A		42482.02	1.46
20/02/2023 12:09:53	Standard 4	Cd (226.502 nm)	2.50 (ppm)	N/A	2.50 (ppm)	4602.71	0.91
20/02/2023 12:09:53	Standard 4	Cu (324.754 nm)	2.50 (ppm)	N/A	2.50 (ppm)	291147.07	0.22
20/02/2023 12:09:53	Standard 4	Ni (352.454 nm)	2.50 (ppm)	N/A	2.50 (ppm)	43151.34	0.52
20/02/2023 12:09:53	Standard 4	Pb (405.781 nm)		N/A		5853.60	1.41
20/02/2023 12:09:53	Standard 4	Cr (425.433 nm)	2.50 (ppm)	N/A	2.50 (ppm)	57383.73	0.99
20/02/2023 12:11:41	Standard 5	As (193.695 nm)	5.00 (ppm)	N/A	5.00 (ppm)	7568.91	0.70
20/02/2023 12:11:41	Standard 5	Zn (213.857 nm)	5.00 (ppm)	N/A	5.00 (ppm)	68758.70	1.52
20/02/2023 12:11:41	Standard 5	Cd (226.502 nm)	5.00 (ppm)	N/A	5.00 (ppm)	7677.74	0.93
20/02/2023 12:11:41	Standard 5	Cu (324.754 nm)	5.00 (ppm)	N/A	5.00 (ppm)	578815.85	0.18
20/02/2023 12:11:41	Standard 5	Ni (352.454 nm)	5.00 (ppm)	N/A	5.00 (ppm)	86954.56	0.64
20/02/2023 12:11:41	Standard 5	Pb (405.781 nm)		N/A		12704.47	1.16
20/02/2023 12:11:41	Standard 5	Cr (425.433 nm)	5.00 (ppm)	N/A	5.00 (ppm)	130211.32	0.55
20/02/2023 12:13:29	Standard 6	As (193.695 nm)	10.00 (ppm)	N/A	10.00 (ppm)	8302.69	0.97
20/02/2023 12:13:29	Standard 6	Zn (213.857 nm)	10.00 (ppm)	N/A	10.00 (ppm)	105288.82	0.86
20/02/2023 12:13:29	Standard 6	Cd (226.502 nm)	10.00 (ppm)	N/A	10.00 (ppm)	11820.61	0.94
20/02/2023 12:13:29	Standard 6	Cu (324.754 nm)	10.00 (ppm)	N/A	10.00 (ppm)	1135265.88	1.14
20/02/2023 12:13:29	Standard 6	Ni (352.454 nm)	10.00 (ppm)	N/A	10.00 (ppm)	176462.27	0.64
20/02/2023 12:13:29	Standard 6	Pb (405.781 nm)	10.00 (ppm)	N/A	10.00 (ppm)	28250.64	1.43
20/02/2023 12:13:29	Standard 6	Cr (425.433 nm)	10.00 (ppm)	N/A	10.00 (ppm)	301228.32	0.83
21/07/2023 08:27:36	Sample 1	As (193.695 nm)	11.69 !mo (ppm)	8.04	11.69 !mo (ppm)	8468.56 !m	0.94
21/07/2023 08:27:36	Sample 1	Zn (213.857 nm)	0.15 ! (ppm)	0.30	0.15 ! (ppm)	2830.42 !	0.30
21/07/2023 08:27:36	Sample 1	Cd (226.502 nm)	5.15 !m (ppm)	2.93	5.15 !m (ppm)	7889.33 !m	2.00
21/07/2023 08:27:36	Sample 1	Cu (324.754 nm)	0.34 !m (ppm)	0.55	0.34 !m (ppm)	39697.97 !m	0.55
21/07/2023 08:27:36	Sample 1	Ni (352.454 nm)	-0.45 !mu (ppm)	1.09	-0.45 !mu (ppm)	-8276.59 !m	1.04
21/07/2023 08:27:36	Sample 1	Pb (405.781 nm)	-0.60 !mu (ppm)	0.80	-0.60 !mu (ppm)	-658.37 !m	1.36
21/07/2023 08:27:36	Sample 1	Cr (425.433 nm)	-0.22 !mu (ppm)	0.42	-0.22 !mu (ppm)	-4836.67 !m	0.42
21/07/2023 08:29:31	Sample 2	As (193.695 nm)	3.94 !m (ppm)	0.72	3.94 !m (ppm)	7193.79 !m	0.16
21/07/2023 08:29:31	Sample 2	Zn (213.857 nm)	1.15 !m (ppm)	2.30	1.15 !m (ppm)	19645.91 !m	2.11
21/07/2023 08:29:31	Sample 2	Cd (226.502 nm)	5.55 !m (ppm)	1.54	5.55 !m (ppm)	8301.61 !m	1.02
21/07/2023 08:29:31	Sample 2	Cu (324.754 nm)	1.12 !m (ppm)	1.06	1.12 !m (ppm)	130813.48 !m	1.06
21/07/2023 08:29:31	Sample 2	Ni (352.454 nm)	-0.27 !mu (ppm)	2.30	-0.27 !mu (ppm)	-5089.95 !m	2.10

Date Time	Label	Element Label (nm)	Conc	%RSD	Unadjusted Conc	Intensity	%RSD
21/07/2023 08:29:31	Sample 2	Pb (405.781 nm)	-0.25 !mu (ppm)	2.38	-0.25 !mu (ppm)	12.40 !m	88.21
21/07/2023 08:29:31	Sample 2	Cr (425.433 nm)	-0.17 !mu (ppm)	0.88	-0.17 !mu (ppm)	-3693.90 !m	0.88
21/07/2023 08:31:42	Sample 3	As (193.695 nm)	23.24 !mo (ppm)	0.64	23.24 !mo (ppm)	9451.88 !m	0.13
21/07/2023 08:31:42	Sample 3	Zn (213.857 nm)	1.75 !m (ppm)	2.10	1.75 !m (ppm)	28736.68 !m	1.85
21/07/2023 08:31:42	Sample 3	Cd (226.502 nm)	6.39 !m (ppm)	1.51	6.39 !m (ppm)	9091.54 !m	0.95
21/07/2023 08:31:42	Sample 3	Cu (324.754 nm)	0.92 !m (ppm)	1.03	0.92 !m (ppm)	107012.54 !m	1.03
21/07/2023 08:31:42	Sample 3	Ni (352.454 nm)	-0.27 !mu (ppm)	2.10	-0.27 !mu (ppm)	-5077.12 !m	1.92
21/07/2023 08:31:42	Sample 3	Pb (405.781 nm)	-0.31 !mu (ppm)	3.01	-0.31 !mu (ppm)	-108.50 !m	16.11
21/07/2023 08:31:42	Sample 3	Cr (425.433 nm)	-0.15 !mu (ppm)	0.43	-0.15 !mu (ppm)	-3393.15 !m	0.43
21/07/2023 08:33:49	Sample 4	As (193.695 nm)	30.73 !mo (ppm)	2.42	30.73 !mo (ppm)	10089.83 !m	0.63
21/07/2023 08:33:49	Sample 4	Zn (213.857 nm)	0.47 ! (ppm)	1.17	0.47 ! (ppm)	8478.52 !	1.13
21/07/2023 08:33:49	Sample 4	Cd (226.502 nm)	6.64 !m (ppm)	1.61	6.64 !m (ppm)	9317.77 !m	1.00
21/07/2023 08:33:49	Sample 4	Cu (324.754 nm)	2.10 !m (ppm)	0.54	2.10 !m (ppm)	244407.03 !m	0.54
21/07/2023 08:33:49	Sample 4	Ni (352.454 nm)	-0.36 !mu (ppm)	1.05	-0.36 !mu (ppm)	-6604.44 !m	0.98
21/07/2023 08:33:49	Sample 4	Pb (405.781 nm)	-0.51 !mu (ppm)	1.45	-0.51 !mu (ppm)	-478.30 !m	2.89
21/07/2023 08:33:49	Sample 4	Cr (425.433 nm)	-0.16 !mu (ppm)	0.32	-0.16 !mu (ppm)	-3584.15 !m	0.32
21/07/2023 08:36:06	Sample 5	As (193.695 nm)	37.81 !mo (ppm)	0.47	37.81 !mo (ppm)	10692.29 !m	0.14
21/07/2023 08:36:06	Sample 5	Zn (213.857 nm)	0.08 ! (ppm)	2.85	0.08 ! (ppm)	1516.53 !	2.85
21/07/2023 08:36:06	Sample 5	Cd (226.502 nm)	6.42 !m (ppm)	1.92	6.42 !m (ppm)	9117.98 !m	1.21
21/07/2023 08:36:06	Sample 5	Cu (324.754 nm)	0.20 !m (ppm)	0.51	0.20 !m (ppm)	23245.14 !m	0.51
21/07/2023 08:36:06	Sample 5	Ni (352.454 nm)	-0.33 !mu (ppm)	1.57	-0.33 !mu (ppm)	-6105.51 !m	1.46
21/07/2023 08:36:06	Sample 5	Pb (405.781 nm)	-0.42 !mu (ppm)	2.87	-0.42 !mu (ppm)	-314.66 !m	7.16
21/07/2023 08:36:06	Sample 5	Cr (425.433 nm)	-0.16 !mu (ppm)	0.24	-0.16 !mu (ppm)	-3558.37 !m	0.24
21/07/2023 08:38:27	Sample 6	As (193.695 nm)	46.40 !mo (ppm)	0.63	46.40 !mo (ppm)	11423.89 !m	0.22
21/07/2023 08:38:27	Sample 6	Zn (213.857 nm)	1.15 !m (ppm)	3.30	1.15 !m (ppm)	19605.35 !m	3.03
21/07/2023 08:38:27	Sample 6	Cd (226.502 nm)	6.84 !m (ppm)	1.63	6.84 !m (ppm)	9486.63 !m	1.00
21/07/2023 08:38:27	Sample 6	Cu (324.754 nm)	0.42 !m (ppm)	0.95	0.42 !m (ppm)	48678.85 !m	0.95
21/07/2023 08:38:27	Sample 6	Ni (352.454 nm)	-0.26 !mu (ppm)	2.67	-0.26 !mu (ppm)	-4976.66 !m	2.43
21/07/2023 08:38:27	Sample 6	Pb (405.781 nm)	-0.23 !mu (ppm)	0.35	-0.23 !mu (ppm)	36.61 !m	4.21
21/07/2023 08:38:27	Sample 6	Cr (425.433 nm)	-0.14 !mu (ppm)	0.55	-0.14 !mu (ppm)	-3034.50 !m	0.55
21/07/2023 08:40:39	Sample 7	As (193.695 nm)	45.56 mo (ppm)	0.32	45.56 mo (ppm)	11351.95 m	0.11
21/07/2023 08:40:39	Sample 7	Zn (213.857 nm)	0.56 (ppm)	0.80	0.56 (ppm)	10067.11	0.76
21/07/2023 08:40:39	Sample 7	Cd (226.502 nm)	6.89 m (ppm)	2.24	6.89 m (ppm)	9526.95 m	1.37
21/07/2023 08:40:39	Sample 7	Cu (324.754 nm)	0.76 m (ppm)	1.06	0.76 m (ppm)	88664.62 m	1.06
21/07/2023 08:40:39	Sample 7	Ni (352.454 nm)	-0.29 mu (ppm)	1.40	-0.29 mu (ppm)	-5422.42 m	1.29
21/07/2023 08:40:39	Sample 7	Pb (405.781 nm)	-0.32 mu (ppm)	3.35	-0.32 mu (ppm)	-129.20 m	15.59
21/07/2023 08:40:39	Sample 7	Cr (425.433 nm)	-0.15 mu (ppm)	0.66	-0.15 mu (ppm)	-3214.28 m	0.66
21/07/2023 08:42:56	Sample 8	As (193.695 nm)	42.35 mo (ppm)	1.07	42.35 mo (ppm)	11079.43 m	0.35
21/07/2023 08:42:56	Sample 8	Zn (213.857 nm)	0.99 m (ppm)	3.75	0.99 m (ppm)	17097.52 m	3.49
21/07/2023 08:42:56	Sample 8	Cd (226.502 nm)	5.93 m (ppm)	1.67	5.93 m (ppm)	8667.40 m	1.08
21/07/2023 08:42:56	Sample 8	Cu (324.754 nm)	1.51 m (ppm)	1.41	1.51 m (ppm)	175380.61 m	1.41
21/07/2023 08:42:56	Sample 8	Ni (352.454 nm)	-0.22 mu (ppm)	2.23	-0.22 mu (ppm)	-4290.90 m	2.00
21/07/2023 08:42:56	Sample 8	Pb (405.781 nm)	-0.12 mu (ppm)	7.23	-0.12 mu (ppm)	239.63 m	7.01
21/07/2023 08:42:56	Sample 8	Cr (425.433 nm)	-0.13 mu (ppm)	0.81	-0.13 mu (ppm)	-2792.71 m	0.81
21/07/2023 08:45:01	Sample 9	As (193.695 nm)	51.53 mo (ppm)	0.18	51.53 mo (ppm)	11860.55 m	0.07
21/07/2023 08:45:01	Sample 9	Zn (213.857 nm)	0.21 (ppm)	2.71	0.21 (ppm)	3804.81	2.68
21/07/2023 08:45:01	Sample 9	Cd (226.502 nm)	6.75 m (ppm)	1.34	6.75 m (ppm)	9405.97 m	0.83
21/07/2023 08:45:01	Sample 9	Cu (324.754 nm)	0.43 m (ppm)	0.64	0.43 m (ppm)	49875.42 m	0.64
21/07/2023 08:45:01	Sample 9	Ni (352.454 nm)	-0.36 mu (ppm)	1.70	-0.36 mu (ppm)	-6676.57 m	1.59
21/07/2023 08:45:01	Sample 9	Pb (405.781 nm)	-0.49 mu (ppm)	0.49	-0.49 mu (ppm)	-438.54 m	1.01

Date Time	Label	Element Label (nm)	Conc	%RSD	Unadjusted Conc	Intensity	%RSD
21/07/2023 08:45:01	Sample 9	Cr (425.433 nm)	-0.16 mu (ppm)	0.80	-0.16 mu (ppm)	-3611.03 m	0.80
21/07/2023 08:47:22	Sample 10	As (193.695 nm)	48.74 mo (ppm)	0.82	48.74 mo (ppm)	11623.05 m	0.29
21/07/2023 08:47:22	Sample 10	Zn (213.857 nm)	0.35 (ppm)	2.13	0.35 (ppm)	6301.28	2.07
21/07/2023 08:47:22	Sample 10	Cd (226.502 nm)	6.75 m (ppm)	2.80	6.75 m (ppm)	9409.89 m	1.73
21/07/2023 08:47:22	Sample 10	Cu (324.754 nm)	0.94 m (ppm)	1.34	0.94 m (ppm)	109435.06 m	1.34
21/07/2023 08:47:22	Sample 10	Ni (352.454 nm)	-0.32 mu (ppm)	1.93	-0.32 mu (ppm)	-5870.59 m	1.79
21/07/2023 08:47:22	Sample 10	Pb (405.781 nm)	-0.42 mu (ppm)	2.10	-0.42 mu (ppm)	-315.31 m	5.24
21/07/2023 08:47:22	Sample 10	Cr (425.433 nm)	-0.11 mu (ppm)	1.70	-0.11 mu (ppm)	-2375.75 m	1.70
21/07/2023 08:49:32	Sample 11	As (193.695 nm)	37.98 mo (ppm)	0.16	37.98 mo (ppm)	10707.25 m	0.05
21/07/2023 08:49:32	Sample 11	Zn (213.857 nm)	1.39 m (ppm)	3.87	1.39 m (ppm)	23376.43 m	3.49
21/07/2023 08:49:32	Sample 11	Cd (226.502 nm)	6.24 m (ppm)	2.86	6.24 m (ppm)	8953.49 m	1.82
21/07/2023 08:49:32	Sample 11	Cu (324.754 nm)	0.61 m (ppm)	0.97	0.61 m (ppm)	71090.04 m	0.97
21/07/2023 08:49:32	Sample 11	Ni (352.454 nm)	-0.34 mu (ppm)	0.63	-0.34 mu (ppm)	-6337.62 m	0.58
21/07/2023 08:49:32	Sample 11	Pb (405.781 nm)	-0.41 mu (ppm)	2.70	-0.41 mu (ppm)	-291.61 m	7.08
21/07/2023 08:49:32	Sample 11	Cr (425.433 nm)	-0.16 mu (ppm)	0.23	-0.16 mu (ppm)	-3591.70 m	0.23
21/07/2023 08:51:45	Sample 12	As (193.695 nm)	50.86 mo (ppm)	0.72	50.86 mo (ppm)	11803.95 m	0.26
21/07/2023 08:51:45	Sample 12	Zn (213.857 nm)	0.12 (ppm)	4.55	0.12 (ppm)	2204.58	4.52
21/07/2023 08:51:45	Sample 12	Cd (226.502 nm)	6.75 m (ppm)	1.72	6.75 m (ppm)	9411.56 m	1.06
21/07/2023 08:51:45	Sample 12	Cu (324.754 nm)	0.29 m (ppm)	0.66	0.29 m (ppm)	34252.22 m	0.66
21/07/2023 08:51:45	Sample 12	Ni (352.454 nm)	-0.46 mu (ppm)	1.27	-0.46 mu (ppm)	-8432.69 m	1.20
21/07/2023 08:51:45	Sample 12	Pb (405.781 nm)	-0.66 mu (ppm)	1.90	-0.66 mu (ppm)	-757.40 m	3.09
21/07/2023 08:51:45	Sample 12	Cr (425.433 nm)	-0.20 mu (ppm)	0.79	-0.20 mu (ppm)	-4398.87 m	0.79
21/07/2023 08:53:53	Sample 13	As (193.695 nm)	34.36 mo (ppm)	0.90	34.36 mo (ppm)	10398.98 m	0.25
21/07/2023 08:53:53	Sample 13	Zn (213.857 nm)	1.51 m (ppm)	3.02	1.51 m (ppm)	25241.94 m	2.71
21/07/2023 08:53:53	Sample 13	Cd (226.502 nm)	5.66 m (ppm)	1.86	5.66 m (ppm)	8407.04 m	1.23
21/07/2023 08:53:53	Sample 13	Cu (324.754 nm)	1.11 m (ppm)	0.74	1.11 m (ppm)	128629.78 m	0.74
21/07/2023 08:53:53	Sample 13	Ni (352.454 nm)	-0.25 mu (ppm)	3.35	-0.25 mu (ppm)	-4661.96 m	3.04
21/07/2023 08:53:53	Sample 13	Pb (405.781 nm)	-0.28 mu (ppm)	1.00	-0.28 mu (ppm)	-44.60 m	11.59
21/07/2023 08:53:53	Sample 13	Cr (425.433 nm)	-0.12 mu (ppm)	0.25	-0.12 mu (ppm)	-2724.51 m	0.25
21/07/2023 08:55:57	Sample 14	As (193.695 nm)	44.49 mo (ppm)	0.05	44.49 mo (ppm)	11260.84 m	0.02
21/07/2023 08:55:57	Sample 14	Zn (213.857 nm)	0.91 m (ppm)	5.81	0.91 m (ppm)	15900.32 m	5.42
21/07/2023 08:55:57	Sample 14	Cd (226.502 nm)	6.07 m (ppm)	2.31	6.07 m (ppm)	8795.69 m	1.48
21/07/2023 08:55:57	Sample 14	Cu (324.754 nm)	0.48 m (ppm)	0.88	0.48 m (ppm)	55849.44 m	0.88
21/07/2023 08:55:57	Sample 14	Ni (352.454 nm)	-0.40 mu (ppm)	1.16	-0.40 mu (ppm)	-7359.57 m	1.09
21/07/2023 08:55:57	Sample 14	Pb (405.781 nm)	-0.57 mu (ppm)	0.93	-0.57 mu (ppm)	-599.17 m	1.66
21/07/2023 08:55:57	Sample 14	Cr (425.433 nm)	-0.17 mu (ppm)	0.35	-0.17 mu (ppm)	-3867.56 m	0.35
21/07/2023 08:57:59	Sample 15	As (193.695 nm)	38.97 mo (ppm)	0.35	38.97 mo (ppm)	10791.13 m	0.11
21/07/2023 08:57:59	Sample 15	Zn (213.857 nm)	0.95 (ppm)	4.69	0.95 (ppm)	16465.10	4.38
21/07/2023 08:57:59	Sample 15	Cd (226.502 nm)	5.62 m (ppm)	1.97	5.62 m (ppm)	8365.25 m	1.31
21/07/2023 08:57:59	Sample 15	Cu (324.754 nm)	0.48 m (ppm)	0.97	0.48 m (ppm)	55933.91 m	0.97
21/07/2023 08:57:59	Sample 15	Ni (352.454 nm)	-0.36 mu (ppm)	2.17	-0.36 mu (ppm)	-6670.98 m	2.03
21/07/2023 08:57:59	Sample 15	Pb (405.781 nm)	-0.50 mu (ppm)	1.81	-0.50 mu (ppm)	-458.70 m	3.68
21/07/2023 08:57:59	Sample 15	Cr (425.433 nm)	-0.17 mu (ppm)	0.52	-0.17 mu (ppm)	-3690.50 m	0.52
21/07/2023 09:00:07	Sample 16	As (193.695 nm)	44.24 mo (ppm)	0.14	44.24 mo (ppm)	11240.24 m	0.05
21/07/2023 09:00:07	Sample 16	Zn (213.857 nm)	0.30 (ppm)	2.34	0.30 (ppm)	5428.05	2.29
21/07/2023 09:00:07	Sample 16	Cd (226.502 nm)	6.32 m (ppm)	1.58	6.32 m (ppm)	9031.16 m	1.00
21/07/2023 09:00:07	Sample 16	Cu (324.754 nm)	0.80 m (ppm)	1.52	0.80 m (ppm)	92918.33 m	1.52
21/07/2023 09:00:07	Sample 16	Ni (352.454 nm)	-0.37 mu (ppm)	1.88	-0.37 mu (ppm)	-6804.51 m	1.76
21/07/2023 09:00:07	Sample 16	Pb (405.781 nm)	-0.51 mu (ppm)	1.62	-0.51 mu (ppm)	-479.25 m	3.22
21/07/2023 09:00:07	Sample 16	Cr (425.433 nm)	-0.16 mu (ppm)	0.41	-0.16 mu (ppm)	-3597.95 m	0.41

Date Time	Label	Element Label (nm)	Conc	%RSD	Unadjusted Conc	Intensity	%RSD
21/07/2023 09:02:10	Sample 17	As (193.695 nm)	38.89 mo (ppm)	0.63	38.89 mo (ppm)	10784.68 m	0.19
21/07/2023 09:02:10	Sample 17	Zn (213.857 nm)	1.13 m (ppm)	4.11	1.13 m (ppm)	19338.62 m	3.78
21/07/2023 09:02:10	Sample 17	Cd (226.502 nm)	5.49 m (ppm)	1.75	5.49 m (ppm)	8234.42 m	1.17
21/07/2023 09:02:10	Sample 17	Cu (324.754 nm)	0.82 m (ppm)	1.53	0.82 m (ppm)	95238.61 m	1.53
21/07/2023 09:02:10	Sample 17	Ni (352.454 nm)	-0.34 mu (ppm)	1.29	-0.34 mu (ppm)	-6318.40 m	1.20
21/07/2023 09:02:10	Sample 17	Pb (405.781 nm)	-0.49 mu (ppm)	1.41	-0.49 mu (ppm)	-447.51 m	2.91
21/07/2023 09:02:10	Sample 17	Cr (425.433 nm)	-0.15 mu (ppm)	0.36	-0.15 mu (ppm)	-3413.26 m	0.36
21/07/2023 09:04:22	Sample 18	As (193.695 nm)	33.48 mo (ppm)	2.76	33.48 mo (ppm)	10323.93 m	0.76
21/07/2023 09:04:22	Sample 18	Zn (213.857 nm)	1.63 m (ppm)	3.75	1.63 m (ppm)	26958.01 m	3.33
21/07/2023 09:04:22	Sample 18	Cd (226.502 nm)	4.92 m (ppm)	0.22	4.92 m (ppm)	7649.89 m	0.16
21/07/2023 09:04:22	Sample 18	Cu (324.754 nm)	0.45 m (ppm)	2.44	0.45 m (ppm)	52309.71 m	2.44
21/07/2023 09:04:22	Sample 18	Ni (352.454 nm)	-0.29 mu (ppm)	1.81	-0.29 mu (ppm)	-5454.04 m	1.66
21/07/2023 09:04:22	Sample 18	Pb (405.781 nm)	-0.42 mu (ppm)	1.57	-0.42 mu (ppm)	-314.52 m	3.93
21/07/2023 09:04:22	Sample 18	Cr (425.433 nm)	-0.14 mu (ppm)	0.91	-0.14 mu (ppm)	-3080.72 m	0.91
21/07/2023 09:06:35	Sample 19	As (193.695 nm)	29.98 mo (ppm)	0.62	29.98 mo (ppm)	10025.95 m	0.16
21/07/2023 09:06:35	Sample 19	Zn (213.857 nm)	0.26 (ppm)	1.60	0.26 (ppm)	4691.55	1.57
21/07/2023 09:06:35	Sample 19	Cd (226.502 nm)	5.78 m (ppm)	1.57	5.78 m (ppm)	8521.74 m	1.02
21/07/2023 09:06:35	Sample 19	Cu (324.754 nm)	0.44 m (ppm)	1.47	0.44 m (ppm)	51763.05 m	1.47
21/07/2023 09:06:35	Sample 19	Ni (352.454 nm)	-0.34 mu (ppm)	1.73	-0.34 mu (ppm)	-6376.54 m	1.61
21/07/2023 09:06:35	Sample 19	Pb (405.781 nm)	-0.45 mu (ppm)	0.90	-0.45 mu (ppm)	-377.20 m	2.03
21/07/2023 09:06:35	Sample 19	Cr (425.433 nm)	-0.16 mu (ppm)	0.59	-0.16 mu (ppm)	-3540.99 m	0.59
21/07/2023 09:08:40	Sample 20	As (193.695 nm)	21.51 mo (ppm)	0.92	21.51 mo (ppm)	9304.26 m	0.18
21/07/2023 09:08:40	Sample 20	Zn (213.857 nm)	0.04 (ppm)	21.40	0.04 (ppm)	695.91	21.51
21/07/2023 09:08:40	Sample 20	Cd (226.502 nm)	5.81 m (ppm)	1.51	5.81 m (ppm)	8548.15 m	0.99
21/07/2023 09:08:40	Sample 20	Cu (324.754 nm)	0.39 m (ppm)	0.83	0.39 m (ppm)	45337.84 m	0.83
21/07/2023 09:08:40	Sample 20	Ni (352.454 nm)	-0.38 mu (ppm)	1.76	-0.38 mu (ppm)	-6988.37 m	1.65
21/07/2023 09:08:40	Sample 20	Pb (405.781 nm)	-0.51 mu (ppm)	1.24	-0.51 mu (ppm)	-483.91 m	2.45
21/07/2023 09:08:40	Sample 20	Cr (425.433 nm)	-0.17 mu (ppm)	1.04	-0.17 mu (ppm)	-3823.83 m	1.04
21/07/2023 09:10:46	Sample 21	As (193.695 nm)	35.35 mo (ppm)	0.62	35.35 mo (ppm)	10483.30 m	0.18
21/07/2023 09:10:46	Sample 21	Zn (213.857 nm)	1.41 m (ppm)	3.16	1.41 m (ppm)	23683.46 m	2.85
21/07/2023 09:10:46	Sample 21	Cd (226.502 nm)	5.33 m (ppm)	1.39	5.33 m (ppm)	8081.28 m	0.93
21/07/2023 09:10:46	Sample 21	Cu (324.754 nm)	1.06 m (ppm)	1.27	1.06 m (ppm)	123600.05 m	1.27
21/07/2023 09:10:46	Sample 21	Ni (352.454 nm)	-0.33 mu (ppm)	1.55	-0.33 mu (ppm)	-6071.94 m	1.44
21/07/2023 09:10:46	Sample 21	Pb (405.781 nm)	-0.36 mu (ppm)	1.25	-0.36 mu (ppm)	-201.76 m	4.16
21/07/2023 09:10:46	Sample 21	Cr (425.433 nm)	-0.16 mu (ppm)	0.75	-0.16 mu (ppm)	-3450.17 m	0.75
21/07/2023 09:12:53	Sample 22	As (193.695 nm)	15.92 mo (ppm)	0.43	15.92 mo (ppm)	8828.82 m	0.07
21/07/2023 09:12:53	Sample 22	Zn (213.857 nm)	0.47 (ppm)	14.00	0.47 (ppm)	8473.40	13.56
21/07/2023 09:12:53	Sample 22	Cd (226.502 nm)	5.65 m (ppm)	2.39	5.65 m (ppm)	8393.01 m	1.57
21/07/2023 09:12:53	Sample 22	Cu (324.754 nm)	0.47 m (ppm)	1.39	0.47 m (ppm)	54439.27 m	1.39
21/07/2023 09:12:53	Sample 22	Ni (352.454 nm)	-0.36 mu (ppm)	1.49	-0.36 mu (ppm)	-6673.34 m	1.39
21/07/2023 09:12:53	Sample 22	Pb (405.781 nm)	-0.44 mu (ppm)	1.17	-0.44 mu (ppm)	-349.88 m	2.76
21/07/2023 09:12:53	Sample 22	Cr (425.433 nm)	-0.17 mu (ppm)	0.33	-0.17 mu (ppm)	-3866.23 m	0.33
21/07/2023 10:13:08	Sample 23	As (193.695 nm)	16.03 !mo (ppm)	0.71	16.03 !mo (ppm)	8838.41 !m	0.11
21/07/2023 10:13:08	Sample 23	Zn (213.857 nm)	0.43 ! (ppm)	0.98	0.43 ! (ppm)	7757.56 !	0.95
21/07/2023 10:13:08	Sample 23	Cd (226.502 nm)	4.52 !m (ppm)	2.19	4.52 !m (ppm)	7207.80 !m	1.55
21/07/2023 10:13:08	Sample 23	Cu (324.754 nm)	0.85 !m (ppm)	0.92	0.85 !m (ppm)	98789.70 !m	0.92
21/07/2023 10:13:08	Sample 23	Ni (352.454 nm)	-0.40 !mu (ppm)	2.34	-0.40 !mu (ppm)	-7396.86 !m	2.21
21/07/2023 10:13:08	Sample 23	Pb (405.781 nm)	-0.43 !mu (ppm)	2.03	-0.43 !mu (ppm)	-326.81 !m	4.95
21/07/2023 10:13:08	Sample 23	Cr (425.433 nm)	-0.19 !mu (ppm)	0.28	-0.19 !mu (ppm)	-4194.43 !m	0.28
21/07/2023 10:15:07	Sample 24	As (193.695 nm)	33.60 !mo (ppm)	1.58	33.60 !mo (ppm)	10334.10 !m	0.44

Date Time	Label	Element Label (nm)	Conc	%RSD	Unadjusted Conc	Intensity	%RSD
21/07/2023 10:15:07	Sample 24	Zn (213.857 nm)	0.46 !m (ppm)	8.16	0.46 !m (ppm)	8264.48 !m	7.88
21/07/2023 10:15:07	Sample 24	Cd (226.502 nm)	4.52 !m (ppm)	2.59	4.52 !m (ppm)	7210.60 !m	1.84
21/07/2023 10:15:07	Sample 24	Cu (324.754 nm)	0.33 !m (ppm)	1.69	0.33 !m (ppm)	38699.53 !m	1.68
21/07/2023 10:15:07	Sample 24	Ni (352.454 nm)	-0.47 !mu (ppm)	0.43	-0.47 !mu (ppm)	-8604.65 !m	0.41
21/07/2023 10:15:07	Sample 24	Pb (405.781 nm)	-0.58 !mu (ppm)	2.11	-0.58 !mu (ppm)	-609.30 !m	3.74
21/07/2023 10:15:07	Sample 24	Cr (425.433 nm)	-0.21 !mu (ppm)	0.71	-0.21 !mu (ppm)	-4539.99 !m	0.71
21/07/2023 10:17:17	Sample 25	As (193.695 nm)	13.27 !mo (ppm)	1.92	13.27 !mo (ppm)	8603.05 !m	0.25
21/07/2023 10:17:17	Sample 25	Zn (213.857 nm)	-0.05 !u (ppm)	2.62	-0.05 !u (ppm)	-973.32 !	2.60
21/07/2023 10:17:17	Sample 25	Cd (226.502 nm)	4.18 !m (ppm)	1.97	4.18 !m (ppm)	6809.25 !m	1.42
21/07/2023 10:17:17	Sample 25	Cu (324.754 nm)	0.08 !m (ppm)	0.49	0.08 !m (ppm)	9201.68 !m	0.49
21/07/2023 10:17:17	Sample 25	Ni (352.454 nm)	-0.10 !u (ppm)	1.54	-0.10 !u (ppm)	-2127.79 !	1.22
21/07/2023 10:17:17	Sample 25	Pb (405.781 nm)	-0.61 !mu (ppm)	1.20	-0.61 !mu (ppm)	-660.30 !m	2.06
21/07/2023 10:17:17	Sample 25	Cr (425.433 nm)	-0.07 !u (ppm)	1.18	-0.07 !u (ppm)	-1574.54 !	1.18
21/07/2023 10:19:22	Sample 26	As (193.695 nm)	11.71 !mo (ppm)	0.94	11.71 !mo (ppm)	8470.18 !m	0.11
21/07/2023 10:19:22	Sample 26	Zn (213.857 nm)	0.23 ! (ppm)	5.04	0.23 ! (ppm)	4150.01 !	4.96
21/07/2023 10:19:22	Sample 26	Cd (226.502 nm)	4.03 !m (ppm)	1.62	4.03 !m (ppm)	6628.88 !m	1.18
21/07/2023 10:19:22	Sample 26	Cu (324.754 nm)	0.06 !m (ppm)	0.46	0.06 !m (ppm)	6984.27 !m	0.46
21/07/2023 10:19:22	Sample 26	Ni (352.454 nm)	-0.10 !u (ppm)	0.63	-0.10 !u (ppm)	-2086.20 !	0.50
21/07/2023 10:19:22	Sample 26	Pb (405.781 nm)	-0.64 !mu (ppm)	0.40	-0.64 !mu (ppm)	-723.45 !m	0.66
21/07/2023 10:19:22	Sample 26	Cr (425.433 nm)	-0.07 !u (ppm)	0.32	-0.07 !u (ppm)	-1627.25 !	0.32
21/07/2023 09:24:52	Sample 27	As (193.695 nm)	20.91 mo (ppm)	0.93	20.91 mo (ppm)	9253.69 m	0.18
21/07/2023 09:24:52	Sample 27	Zn (213.857 nm)	-0.15 u (ppm)	6.23	-0.15 u (ppm)	-2739.38	6.22
21/07/2023 09:24:52	Sample 27	Cd (226.502 nm)	4.04 m (ppm)	1.95	4.04 m (ppm)	6647.78 m	1.43
21/07/2023 09:24:52	Sample 27	Cu (324.754 nm)	0.08 m (ppm)	0.48	0.08 m (ppm)	8930.36 m	0.48
21/07/2023 09:24:52	Sample 27	Ni (352.454 nm)	-0.09 u (ppm)	0.92	-0.09 u (ppm)	-1924.14	0.71
21/07/2023 09:24:52	Sample 27	Pb (405.781 nm)	-0.65 mu (ppm)	0.66	-0.65 mu (ppm)	-737.40 m	1.09
21/07/2023 09:24:52	Sample 27	Cr (425.433 nm)	-0.07 u (ppm)	1.03	-0.07 u (ppm)	-1532.78	1.03
21/07/2023 09:26:59	Sample 28	As (193.695 nm)	7.38 m (ppm)	0.87	7.38 m (ppm)	8033.01 m	0.12
21/07/2023 09:26:59	Sample 28	Zn (213.857 nm)	-0.14 u (ppm)	0.73	-0.14 u (ppm)	-2582.11	0.73
21/07/2023 09:26:59	Sample 28	Cd (226.502 nm)	4.35 m (ppm)	1.61	4.35 m (ppm)	7014.11 m	1.15
21/07/2023 09:26:59	Sample 28	Cu (324.754 nm)	0.02 m (ppm)	0.64	0.02 m (ppm)	2747.36 m	0.64
21/07/2023 09:26:59	Sample 28	Ni (352.454 nm)	-0.08 u (ppm)	1.23	-0.08 u (ppm)	-1740.45	0.92
21/07/2023 09:26:59	Sample 28	Pb (405.781 nm)	-0.77 mu (ppm)	1.55	-0.77 mu (ppm)	-960.13 m	2.30
21/07/2023 09:26:59	Sample 28	Cr (425.433 nm)	-0.08 u (ppm)	0.74	-0.08 u (ppm)	-1735.42	0.74
21/07/2023 09:29:18	Sample 29	As (193.695 nm)	6.43 m (ppm)	1.29	6.43 m (ppm)	7877.90 m	0.19
21/07/2023 09:29:18	Sample 29	Zn (213.857 nm)	-0.12 u (ppm)	6.42	-0.12 u (ppm)	-2235.69	6.41
21/07/2023 09:29:18	Sample 29	Cd (226.502 nm)	4.14 m (ppm)	1.95	4.14 m (ppm)	6764.67 m	1.42
21/07/2023 09:29:18	Sample 29	Cu (324.754 nm)	0.03 m (ppm)	0.37	0.03 m (ppm)	3116.66 m	0.36
21/07/2023 09:29:18	Sample 29	Ni (352.454 nm)	-0.06 u (ppm)	0.75	-0.06 u (ppm)	-1548.94	0.54
21/07/2023 09:29:18	Sample 29	Pb (405.781 nm)	-0.86 mu (ppm)	0.75	-0.86 mu (ppm)	-1142.56 m	1.06
21/07/2023 09:29:18	Sample 29	Cr (425.433 nm)	-0.08 u (ppm)	1.28	-0.08 u (ppm)	-1847.09	1.28
21/07/2023 09:31:21	Sample 30	As (193.695 nm)	12.12 mo (ppm)	1.85	12.12 mo (ppm)	8505.49 m	0.23
21/07/2023 09:31:21	Sample 30	Zn (213.857 nm)	-0.16 u (ppm)	2.14	-0.16 u (ppm)	-3006.47	2.14
21/07/2023 09:31:21	Sample 30	Cd (226.502 nm)	4.35 m (ppm)	3.25	4.35 m (ppm)	7009.48 m	2.32
21/07/2023 09:31:21	Sample 30	Cu (324.754 nm)	0.07 m (ppm)	0.64	0.07 m (ppm)	7640.99 m	0.64
21/07/2023 09:31:21	Sample 30	Ni (352.454 nm)	-0.18 mu (ppm)	1.70	-0.18 mu (ppm)	-3469.32 m	1.48
21/07/2023 09:31:21	Sample 30	Pb (405.781 nm)	-0.50 mu (ppm)	1.59	-0.50 mu (ppm)	-460.66 m	3.22
21/07/2023 09:31:21	Sample 30	Cr (425.433 nm)	-0.11 mu (ppm)	0.19	-0.11 mu (ppm)	-2518.39 m	0.19
21/07/2023 09:33:31	Sample 31	As (193.695 nm)	2.54 m (ppm)	4.03	2.54 m (ppm)	6402.17 m	1.25
21/07/2023 09:33:31	Sample 31	Zn (213.857 nm)	-0.08 u (ppm)	3.82	-0.08 u (ppm)	-1438.90	3.80

Date Time	Label	Element Label (nm)	Conc	%RSD	Unadjusted Conc	Intensity	%RSD
21/07/2023 09:33:31	Sample 31	Cd (226.502 nm)	2.68 m (ppm)	2.25	2.68 m (ppm)	4842.15 m	1.81
21/07/2023 09:33:31	Sample 31	Cu (324.754 nm)	0.01 m (ppm)	1.42	0.01 m (ppm)	1438.88 m	1.40
21/07/2023 09:33:31	Sample 31	Ni (352.454 nm)	-0.06 u (ppm)	1.34	-0.06 u (ppm)	-1524.43	0.96
21/07/2023 09:33:31	Sample 31	Pb (405.781 nm)	-1.47 mu (ppm)	0.99	-1.47 mu (ppm)	-2272.09 m	1.19
21/07/2023 09:33:31	Sample 31	Cr (425.433 nm)	-0.12 u (ppm)	1.93	-0.12 u (ppm)	-2630.22	1.93
21/07/2023 09:36:11	Sample 32	As (193.695 nm)	4.18 m (ppm)	1.70	4.18 m (ppm)	7287.69 m	0.36
21/07/2023 09:36:11	Sample 32	Zn (213.857 nm)	-0.11 u (ppm)	0.42	-0.11 u (ppm)	-1992.57	0.41
21/07/2023 09:36:11	Sample 32	Cd (226.502 nm)	3.50 m (ppm)	2.12	3.50 m (ppm)	5972.30 m	1.60
21/07/2023 09:36:11	Sample 32	Cu (324.754 nm)	0.03 m (ppm)	0.46	0.03 m (ppm)	3892.69 m	0.46
21/07/2023 09:36:11	Sample 32	Ni (352.454 nm)	-0.06 u (ppm)	0.58	-0.06 u (ppm)	-1467.81	0.41
21/07/2023 09:36:11	Sample 32	Pb (405.781 nm)	-1.11 mu (ppm)	1.29	-1.11 mu (ppm)	-1608.53 m	1.67
21/07/2023 09:36:11	Sample 32	Cr (425.433 nm)	-0.09 u (ppm)	1.05	-0.09 u (ppm)	-2081.36	1.05
21/07/2023 09:38:18	Sample 33	As (193.695 nm)	16.27 mo (ppm)	3.00	16.27 mo (ppm)	8858.61 m	0.47
21/07/2023 09:38:18	Sample 33	Zn (213.857 nm)	-0.15 u (ppm)	2.67	-0.15 u (ppm)	-2868.28	2.67
21/07/2023 09:38:18	Sample 33	Cd (226.502 nm)	4.33 m (ppm)	1.47	4.33 m (ppm)	6986.04 m	1.05
21/07/2023 09:38:18	Sample 33	Cu (324.754 nm)	0.03 m (ppm)	0.45	0.03 m (ppm)	3474.67 m	0.44
21/07/2023 09:38:18	Sample 33	Ni (352.454 nm)	-0.12 u (ppm)	1.72	-0.12 u (ppm)	-2516.90	1.42
21/07/2023 09:38:18	Sample 33	Pb (405.781 nm)	-0.52 u (ppm)	1.57	-0.52 u (ppm)	-494.65	3.07
21/07/2023 09:38:18	Sample 33	Cr (425.433 nm)	-0.06 u (ppm)	0.81	-0.06 u (ppm)	-1217.70	0.81
21/07/2023 09:40:14	Sample 34	As (193.695 nm)	6.05 m (ppm)	1.07	6.05 m (ppm)	7803.79 m	0.17
21/07/2023 09:40:14	Sample 34	Zn (213.857 nm)	-0.13 u (ppm)	2.61	-0.13 u (ppm)	-2381.48	2.61
21/07/2023 09:40:14	Sample 34	Cd (226.502 nm)	4.18 m (ppm)	1.54	4.18 m (ppm)	6811.11 m	1.11
21/07/2023 09:40:14	Sample 34	Cu (324.754 nm)	0.05 m (ppm)	0.68	0.05 m (ppm)	6380.84 m	0.68
21/07/2023 09:40:14	Sample 34	Ni (352.454 nm)	-0.06 u (ppm)	0.43	-0.06 u (ppm)	-1525.79	0.31
21/07/2023 09:40:14	Sample 34	Pb (405.781 nm)	-0.79 mu (ppm)	1.06	-0.79 mu (ppm)	-998.19 m	1.56
21/07/2023 09:40:14	Sample 34	Cr (425.433 nm)	-0.08 u (ppm)	0.72	-0.08 u (ppm)	-1728.89	0.72
21/07/2023 09:42:19	Sample 35	As (193.695 nm)	5.61 m (ppm)	0.26	5.61 m (ppm)	7706.73 m	0.04
21/07/2023 09:42:19	Sample 35	Zn (213.857 nm)	-0.08 u (ppm)	7.25	-0.08 u (ppm)	-1583.13	7.22
21/07/2023 09:42:19	Sample 35	Cd (226.502 nm)	3.89 m (ppm)	2.37	3.89 m (ppm)	6465.93 m	1.75
21/07/2023 09:42:19	Sample 35	Cu (324.754 nm)	0.04 m (ppm)	0.46	0.04 m (ppm)	5036.70 m	0.45
21/07/2023 09:42:19	Sample 35	Ni (352.454 nm)	-0.06 u (ppm)	0.69	-0.06 u (ppm)	-1477.90	0.48
21/07/2023 09:42:19	Sample 35	Pb (405.781 nm)	-0.88 mu (ppm)	0.47	-0.88 mu (ppm)	-1174.43 m	0.66
21/07/2023 09:42:19	Sample 35	Cr (425.433 nm)	-0.08 u (ppm)	1.24	-0.08 u (ppm)	-1765.56	1.24
21/07/2023 09:44:14	Sample 36	As (193.695 nm)	7.47 m (ppm)	0.51	7.47 m (ppm)	8046.32 m	0.07
21/07/2023 09:44:14	Sample 36	Zn (213.857 nm)	-0.06 u (ppm)	8.12	-0.06 u (ppm)	-1195.41	8.08
21/07/2023 09:44:14	Sample 36	Cd (226.502 nm)	4.20 m (ppm)	1.27	4.20 m (ppm)	6835.38 m	0.92
21/07/2023 09:44:14	Sample 36	Cu (324.754 nm)	0.10 m (ppm)	0.70	0.10 m (ppm)	11342.09 m	0.70
21/07/2023 09:44:14	Sample 36	Ni (352.454 nm)	-0.07 u (ppm)	0.62	-0.07 u (ppm)	-1597.26	0.45
21/07/2023 09:44:14	Sample 36	Pb (405.781 nm)	-0.66 mu (ppm)	0.21	-0.66 mu (ppm)	-767.16 m	0.34
21/07/2023 09:44:14	Sample 36	Cr (425.433 nm)	-0.07 u (ppm)	0.46	-0.07 u (ppm)	-1527.71	0.46
21/07/2023 09:46:30	Sample 37	As (193.695 nm)	14.17 mo (ppm)	0.67	14.17 mo (ppm)	8679.80 m	0.09
21/07/2023 09:46:30	Sample 37	Zn (213.857 nm)	-0.15 u (ppm)	1.69	-0.15 u (ppm)	-2786.22	1.69
21/07/2023 09:46:30	Sample 37	Cd (226.502 nm)	4.35 m (ppm)	1.56	4.35 m (ppm)	7011.22 m	1.11
21/07/2023 09:46:30	Sample 37	Cu (324.754 nm)	0.05 m (ppm)	0.51	0.05 m (ppm)	5366.75 m	0.50
21/07/2023 09:46:30	Sample 37	Ni (352.454 nm)	-0.10 u (ppm)	0.25	-0.10 u (ppm)	-2116.15	0.20
21/07/2023 09:46:30	Sample 37	Pb (405.781 nm)	-0.60 mu (ppm)	0.55	-0.60 mu (ppm)	-657.20 m	0.95
21/07/2023 09:46:30	Sample 37	Cr (425.433 nm)	-0.06 u (ppm)	2.27	-0.06 u (ppm)	-1358.93	2.27
21/07/2023 09:48:37	Sample 38	As (193.695 nm)	5.18 m (ppm)	2.48	5.18 m (ppm)	7601.72 m	0.45
21/07/2023 09:48:37	Sample 38	Zn (213.857 nm)	-0.12 u (ppm)	1.53	-0.12 u (ppm)	-2294.18	1.53
21/07/2023 09:48:37	Sample 38	Cd (226.502 nm)	3.61 m (ppm)	1.14	3.61 m (ppm)	6113.89 m	0.86

Date Time	Label	Element Label (nm)	Conc	%RSD	Unadjusted Conc	Intensity	%RSD
21/07/2023 09:48:37	Sample 38	Cu (324.754 nm)	0.02 m (ppm)	0.56	0.02 m (ppm)	2675.47 m	0.55
21/07/2023 09:48:37	Sample 38	Ni (352.454 nm)	-0.07 u (ppm)	1.27	-0.07 u (ppm)	-1659.13	0.93
21/07/2023 09:48:37	Sample 38	Pb (405.781 nm)	-0.77 mu (ppm)	0.42	-0.77 mu (ppm)	-960.33 m	0.63
21/07/2023 09:48:37	Sample 38	Cr (425.433 nm)	-0.08 u (ppm)	1.13	-0.08 u (ppm)	-1704.96	1.13
21/07/2023 09:50:39	Sample 39	As (193.695 nm)	15.51 mo (ppm)	1.75	15.51 mo (ppm)	8793.92 m	0.26
21/07/2023 09:50:39	Sample 39	Zn (213.857 nm)	1.01 m (ppm)	3.90	1.01 m (ppm)	17409.68 m	3.62
21/07/2023 09:50:39	Sample 39	Cd (226.502 nm)	4.00 m (ppm)	1.64	4.00 m (ppm)	6592.83 m	1.20
21/07/2023 09:50:39	Sample 39	Cu (324.754 nm)	0.06 m (ppm)	0.20	0.06 m (ppm)	7560.65 m	0.20
21/07/2023 09:50:39	Sample 39	Ni (352.454 nm)	-0.14 mu (ppm)	0.75	-0.14 mu (ppm)	-2845.61 m	0.64
21/07/2023 09:50:39	Sample 39	Pb (405.781 nm)	-0.54 u (ppm)	1.76	-0.54 u (ppm)	-540.93	3.29
21/07/2023 09:50:39	Sample 39	Cr (425.433 nm)	-0.06 u (ppm)	0.92	-0.06 u (ppm)	-1336.62	0.92
21/07/2023 09:52:43	Sample 40	As (193.695 nm)	15.92 mo (ppm)	0.34	15.92 mo (ppm)	8828.40 m	0.05
21/07/2023 09:52:43	Sample 40	Zn (213.857 nm)	-0.11 u (ppm)	3.27	-0.11 u (ppm)	-2091.72	3.27
21/07/2023 09:52:43	Sample 40	Cd (226.502 nm)	3.94 m (ppm)	2.05	3.94 m (ppm)	6522.95 m	1.51
21/07/2023 09:52:43	Sample 40	Cu (324.754 nm)	0.03 m (ppm)	0.34	0.03 m (ppm)	3643.42 m	0.34
21/07/2023 09:52:43	Sample 40	Ni (352.454 nm)	-0.10 u (ppm)	1.00	-0.10 u (ppm)	-2122.08	0.80
21/07/2023 09:52:43	Sample 40	Pb (405.781 nm)	-0.68 mu (ppm)	0.37	-0.68 mu (ppm)	-804.22 m	0.58
21/07/2023 09:52:43	Sample 40	Cr (425.433 nm)	-0.07 u (ppm)	0.52	-0.07 u (ppm)	-1607.98	0.52
21/07/2023 09:54:51	Sample 41	As (193.695 nm)	4.12 m (ppm)	0.61	4.12 m (ppm)	7264.17 m	0.13
21/07/2023 09:54:51	Sample 41	Zn (213.857 nm)	-0.10 u (ppm)	5.46	-0.10 u (ppm)	-1861.63	5.45
21/07/2023 09:54:51	Sample 41	Cd (226.502 nm)	3.24 m (ppm)	1.73	3.24 m (ppm)	5633.83 m	1.33
21/07/2023 09:54:51	Sample 41	Cu (324.754 nm)	0.01 m (ppm)	0.27	0.01 m (ppm)	1652.48 m	0.27
21/07/2023 09:54:51	Sample 41	Ni (352.454 nm)	-0.06 u (ppm)	0.71	-0.06 u (ppm)	-1425.16	0.50
21/07/2023 09:54:51	Sample 41	Pb (405.781 nm)	-1.20 mu (ppm)	0.46	-1.20 mu (ppm)	-1774.78 m	0.59
21/07/2023 09:54:51	Sample 41	Cr (425.433 nm)	-0.10 u (ppm)	0.30	-0.10 u (ppm)	-2208.28	0.30
21/07/2023 09:56:57	Sample 42	As (193.695 nm)	7.72 m (ppm)	3.02	7.72 m (ppm)	8080.15 m	0.38
21/07/2023 09:56:57	Sample 42	Zn (213.857 nm)	-0.15 u (ppm)	2.83	-0.15 u (ppm)	-2841.94	2.82
21/07/2023 09:56:57	Sample 42	Cd (226.502 nm)	3.81 m (ppm)	1.78	3.81 m (ppm)	6360.03 m	1.32
21/07/2023 09:56:57	Sample 42	Cu (324.754 nm)	0.05 m (ppm)	0.53	0.05 m (ppm)	5908.43 m	0.53
21/07/2023 09:56:57	Sample 42	Ni (352.454 nm)	-0.10 u (ppm)	0.61	-0.10 u (ppm)	-2116.23	0.48
21/07/2023 09:56:57	Sample 42	Pb (405.781 nm)	-0.68 mu (ppm)	0.54	-0.68 mu (ppm)	-790.64 m	0.86
21/07/2023 09:56:57	Sample 42	Cr (425.433 nm)	-0.07 u (ppm)	1.07	-0.07 u (ppm)	-1606.17	1.07
21/07/2023 09:59:01	Sample 43	As (193.695 nm)	11.10 mo (ppm)	5.39	11.10 mo (ppm)	8418.57 m	0.60
21/07/2023 09:59:01	Sample 43	Zn (213.857 nm)	-0.12 u (ppm)	2.09	-0.12 u (ppm)	-2308.72	2.08
21/07/2023 09:59:01	Sample 43	Cd (226.502 nm)	3.79 m (ppm)	2.02	3.79 m (ppm)	6340.97 m	1.50
21/07/2023 09:59:01	Sample 43	Cu (324.754 nm)	0.03 m (ppm)	0.21	0.03 m (ppm)	3065.52 m	0.21
21/07/2023 09:59:01	Sample 43	Ni (352.454 nm)	-0.07 u (ppm)	0.60	-0.07 u (ppm)	-1647.15	0.44
21/07/2023 09:59:01	Sample 43	Pb (405.781 nm)	-0.82 mu (ppm)	0.85	-0.82 mu (ppm)	-1059.04 m	1.23
21/07/2023 09:59:01	Sample 43	Cr (425.433 nm)	-0.08 u (ppm)	0.47	-0.08 u (ppm)	-1721.09	0.47
21/07/2023 10:01:31	Sample 44	As (193.695 nm)	12.00 mo (ppm)	0.69	12.00 mo (ppm)	8494.84 m	0.08
21/07/2023 10:01:31	Sample 44	Zn (213.857 nm)	-0.10 u (ppm)	5.30	-0.10 u (ppm)	-1836.96	5.28
21/07/2023 10:01:31	Sample 44	Cd (226.502 nm)	4.29 m (ppm)	1.19	4.29 m (ppm)	6941.32 m	0.86
21/07/2023 10:01:31	Sample 44	Cu (324.754 nm)	0.05 m (ppm)	0.41	0.05 m (ppm)	5964.43 m	0.41
21/07/2023 10:01:31	Sample 44	Ni (352.454 nm)	-0.08 u (ppm)	1.25	-0.08 u (ppm)	-1888.68	0.96
21/07/2023 10:01:31	Sample 44	Pb (405.781 nm)	-0.66 mu (ppm)	0.25	-0.66 mu (ppm)	-768.49 m	0.41
21/07/2023 10:01:31	Sample 44	Cr (425.433 nm)	-0.07 u (ppm)	0.84	-0.07 u (ppm)	-1517.26	0.84
21/07/2023 10:03:36	Sample 45	As (193.695 nm)	8.77 m (ppm)	0.25	8.77 m (ppm)	8206.65 m	0.03
21/07/2023 10:03:36	Sample 45	Zn (213.857 nm)	0.41 (ppm)	3.37	0.41 (ppm)	7474.05	3.27
21/07/2023 10:03:36	Sample 45	Cd (226.502 nm)	3.90 m (ppm)	1.42	3.90 m (ppm)	6482.20 m	1.05
21/07/2023 10:03:36	Sample 45	Cu (324.754 nm)	0.08 m (ppm)	0.86	0.08 m (ppm)	9456.82 m	0.86

Date Time	Label	Element Label (nm)	Conc	%RSD	Unadjusted Conc	Intensity	%RSD
21/07/2023 10:03:36	Sample 45	Ni (352.454 nm)	-0.11 u (ppm)	1.29	-0.11 u (ppm)	-2304.19	1.05
21/07/2023 10:03:36	Sample 45	Pb (405.781 nm)	-0.60 mu (ppm)	3.04	-0.60 mu (ppm)	-648.19 m	5.25
21/07/2023 10:03:36	Sample 45	Cr (425.433 nm)	-0.07 u (ppm)	0.50	-0.07 u (ppm)	-1477.08	0.50
21/07/2023 10:05:38	Sample 46	As (193.695 nm)	6.08 m (ppm)	2.77	6.08 m (ppm)	7808.17 m	0.43
21/07/2023 10:05:38	Sample 46	Zn (213.857 nm)	-0.13 u (ppm)	3.13	-0.13 u (ppm)	-2355.18	3.12
21/07/2023 10:05:38	Sample 46	Cd (226.502 nm)	3.87 m (ppm)	1.92	3.87 m (ppm)	6440.54 m	1.42
21/07/2023 10:05:38	Sample 46	Cu (324.754 nm)	0.03 m (ppm)	0.35	0.03 m (ppm)	3536.02 m	0.34
21/07/2023 10:05:38	Sample 46	Ni (352.454 nm)	-0.07 u (ppm)	0.98	-0.07 u (ppm)	-1688.12	0.73
21/07/2023 10:05:38	Sample 46	Pb (405.781 nm)	-0.82 mu (ppm)	0.38	-0.82 mu (ppm)	-1065.81 m	0.55
21/07/2023 10:05:38	Sample 46	Cr (425.433 nm)	-0.09 u (ppm)	0.86	-0.09 u (ppm)	-1885.20	0.86
21/07/2023 10:07:39	Sample 47	As (193.695 nm)	8.92 m (ppm)	0.71	8.92 m (ppm)	8222.95 m	0.08
21/07/2023 10:07:39	Sample 47	Zn (213.857 nm)	-0.11 u (ppm)	2.77	-0.11 u (ppm)	-2019.08	2.76
21/07/2023 10:07:39	Sample 47	Cd (226.502 nm)	4.20 m (ppm)	1.91	4.20 m (ppm)	6834.65 m	1.38
21/07/2023 10:07:39	Sample 47	Cu (324.754 nm)	0.10 m (ppm)	0.70	0.10 m (ppm)	11331.78 m	0.70
21/07/2023 10:07:39	Sample 47	Ni (352.454 nm)	-0.18 mu (ppm)	1.31	-0.18 mu (ppm)	-3531.77 m	1.15
21/07/2023 10:07:39	Sample 47	Pb (405.781 nm)	-0.48 mu (ppm)	0.60	-0.48 mu (ppm)	-418.60 m	1.27
21/07/2023 10:07:39	Sample 47	Cr (425.433 nm)	-0.12 mu (ppm)	0.10	-0.12 mu (ppm)	-2629.89 m	0.10
21/07/2023 10:09:40	Sample 48	As (193.695 nm)	6.41 m (ppm)	2.97	6.41 m (ppm)	7873.45 m	0.45
21/07/2023 10:09:40	Sample 48	Zn (213.857 nm)	-0.11 u (ppm)	4.35	-0.11 u (ppm)	-2131.82	4.34
21/07/2023 10:09:40	Sample 48	Cd (226.502 nm)	3.66 m (ppm)	2.63	3.66 m (ppm)	6183.01 m	1.97
21/07/2023 10:09:40	Sample 48	Cu (324.754 nm)	0.02 m (ppm)	0.19	0.02 m (ppm)	2273.90 m	0.18
21/07/2023 10:09:40	Sample 48	Ni (352.454 nm)	-0.07 u (ppm)	1.72	-0.07 u (ppm)	-1714.52	1.28
21/07/2023 10:09:40	Sample 48	Pb (405.781 nm)	-0.85 mu (ppm)	0.33	-0.85 mu (ppm)	-1108.48 m	0.47
21/07/2023 10:09:40	Sample 48	Cr (425.433 nm)	-0.09 u (ppm)	2.17	-0.09 u (ppm)	-1887.74	2.17

Path: C:\Users\University Of Malta\Documents\Agilent\MP Expert\My Results\New HM-NS-01.mpws

Date created: 30/10/2023 09:43:41

Instrument used: AU12200193 Current software: Version 1.6.2.12109

Enable EGCM for monochromator purge: Off

Notes:

Calibration Correlation Coefficient Limit: 0.999

Standard addition: Off QC Active: Off

Reagent Blank: Off IEC: Off

Blank Subtraction: On

Reslope: Off

Common Conditions

Replicates: 3 Sample introduction: Manual

Pump Speed (rpm): 15

Sample Uptake Time (s): 15 Sample uptake fast pump: On

AVS 4 delay (s): N/A

SVS 1 delay (s): N/A Rinse time fast pump: N/A

Rinse time (s): N/A

Stabilization time (s): 15

Air Injection Mode: Off

Isomist Temperature (°C): N/A

Settings per element:

Element	Label (Wavelength nm)	Type	Background Correction	Calibration Fit	Read Time (s)	Viewing position
Al	Al (396.152)	Analyte	Auto	Linear Weighted	3	0
Ba	Ba (455.403)	Analyte	Auto	Rational Weighted	3	0
Mn	Mn (403.076)	Analyte	Auto	Linear Weighted	3	0
Tl	Tl (535.046)	Analyte	Auto	Linear Weighted	3	0
V	V (437.923)	Analyte	Auto	Linear Weighted	3	0

Element	Label (Wavelength nm)	Type	Nebulizer Pressure (kPa)
Al	Al (396.152)	Analyte	240
Ba	Ba (455.403)	Analyte	240
Mn	Mn (403.076)	Analyte	240
Tl	Tl (535.046)	Analyte	240
V	V (437.923)	Analyte	240

Calibration parameters:

Label (Wavelength nm)	Minimum Concentration	Maximum Concentration	Calibration Error
Al (396.152)	0 ppm	11 ppm	5 %
Ba (455.403)	0 ppm	11 ppm	5 %
Mn (403.076)	0 ppm	5.5 ppm	5 %
Tl (535.046)	0 ppm	5.5 ppm	5 %
V (437.923)	0 ppm	11 ppm	5 %

Calibration Curves:

Al (396.152 nm)
Intensity = 7248.42636383 * Concentration + 2.51910921
Correlation coefficient: 0.99993

Standards	Intensity	Method Concentration	Calculated Concentration	% Error
Blank	0.02	0.00	0.00	N/A
NS 0.3125	2307.48	0.31	0.32	1.76
NS 0.625	4605.64	0.63	0.64	1.61
NS 1.25	9041.22	1.25	1.25	0.24
NS 2.5	17906.70	2.50	2.47	1.20
NS 5	36408.94	5.00	5.02	0.45
NS 10	74296.00	10.00	10.25	2.50

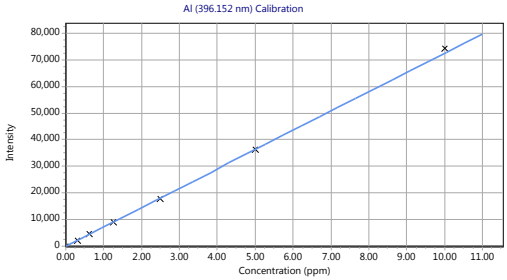

Ba (455.403 nm)
Intensity = (24831.77169030 * Concentration - 10.38465824) / (1 - 0.02523110 * Concentration)
Correlation coefficient: 0.99978

Standards	Intensity	Method Concentration	Calculated Concentration	% Error
Blank	-0.01	0.00	0.00	N/A
NS 0.3125	7799.88	0.31	0.31	0.14
NS 0.625	15695.33	0.63	0.62	0.39
NS 1.25	32218.18	1.25	1.26	0.54
NS 2.5	66784.17	2.50	2.52	0.76
NS 5	147092.13	5.00	5.15	3.07
NS 10	326727.10	10.00	9.88	1.21

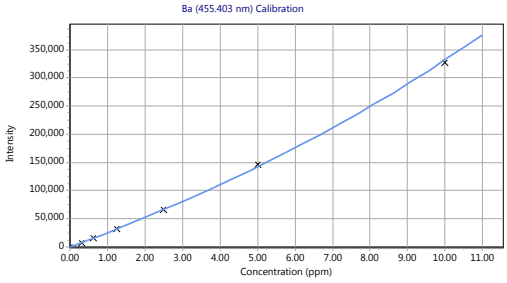

Mn (403.076 nm)
Intensity = 13638.44310454 * Concentration - 11.44248947
Correlation coefficient: 0.99992

Standards	Intensity	Method Concentration	Calculated Concentration	% Error
Blank	0.01	0.00	0.00	N/A
NS 0.3125	4168.79	0.31	0.31	1.92
NS 0.625	8316.16	0.63	0.61	2.30
NS 1.25	17106.88	1.25	1.26	0.41
NS 2.5	34554.41	2.50	2.53	1.38
NS 5	70719.02	5.00	5.19	3.72

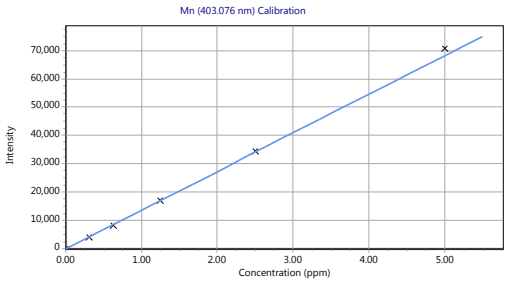

Tl (535.046 nm)
Intensity = 1397.31283281 * Concentration - 2.11658632
Correlation coefficient: 0.99982

Standards	Intensity	Method Concentration	Calculated Concentration	% Error
Blank	0.03	0.00	0.00	N/A
NS 0.3125	418.45	0.31	0.30	3.69
NS 0.625	856.98	0.63	0.61	1.63
NS 1.25	1712.32	1.25	1.23	1.84
NS 2.5	3493.24	2.50	2.50	0.06
NS 5	7240.32	5.00	5.18	3.66

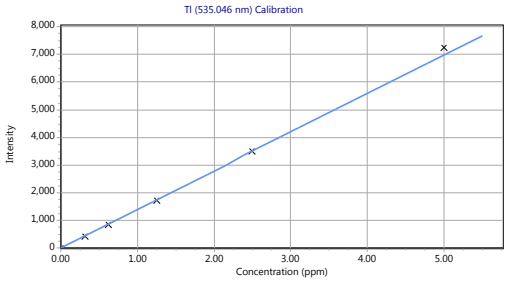

V (437.923 nm)
Intensity = 6807.19900686 * Concentration + 9.74431452
Correlation coefficient: 0.99998

Standards	Intensity	Method Concentration	Calculated Concentration	% Error
Blank	0.17	0.00	0.00	N/A
NS 0.3125	2166.36	0.31	0.32	1.38
NS 0.625	4285.18	0.63	0.63	0.49
NS 1.25	8733.70	1.25	1.28	2.53
NS 2.5	17049.87	2.50	2.50	0.13
NS 5	33697.75	5.00	4.95	1.02
NS 10	66808.91	10.00	9.81	1.87

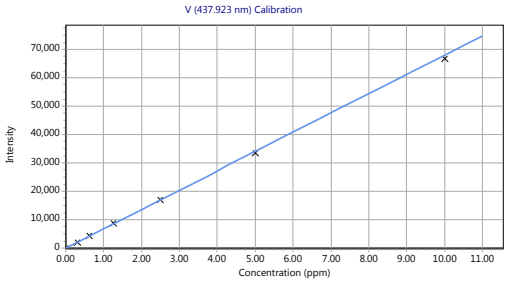

Sample Name: Blank

Date: 30/10/2023 10:01:35 Rack:Tube:

Weight (g): 1 Volume (mL): 1 Dilution: 1

Analyte Results

Label	Solution Concentration	Unit	SD	%RSD	Intensity	Calculated Concentration
Al (396.152 nm)	0.00 !	ppm	N/A	N/A	0.02 !	0.00 ! (ppm)
Mn (403.076 nm)	0.00 !	ppm	N/A	N/A	0.01 !	0.00 ! (ppm)
V (437.923 nm)	0.00 !	ppm	N/A	N/A	0.17 !	0.00 ! (ppm)
Ba (455.403 nm)	0.00 !	ppm	N/A	N/A	-0.01 !	0.00 ! (ppm)
Tl (535.046 nm)	0.00 !	ppm	N/A	N/A	0.03 !	0.00 ! (ppm)

Replicates Concentration

Label	Replicate 1	Replicate 2	Replicate 3	Units
Al (396.152 nm)	0.00	0.00	0.00	ppm
Mn (403.076 nm)	0.00	0.00	0.00	ppm
V (437.923 nm)	0.00	0.00	0.00	ppm
Ba (455.403 nm)	0.00	0.00	0.00	ppm
Tl (535.046 nm)	0.00	0.00	0.00	ppm

Replicates Intensity

Label	Replicate 1 (c/s)	Replicate 2 (c/s)	Replicate 3 (c/s)
Al (396.152 nm)	-0.60	3.90	-3.25
Mn (403.076 nm)	3.01	-6.28	3.31
V (437.923 nm)	-6.38	4.20	2.70
Ba (455.403 nm)	-7.67	9.46	-1.83
Tl (535.046 nm)	0.78	-1.53	0.82

Sample Name: NS 0.3125

Date: 30/10/2023 10:03:06 Rack:Tube:

Weight (g): 1 Volume (mL): 1 Dilution: 1

Analyte Results

Label	Solution Concentration	Unit	SD	%RSD	Intensity	Calculated Concentration
Al (396.152 nm)	0.31 !	ppm	N/A	N/A	2307.48 !	0.31 ! (ppm)
Mn (403.076 nm)	0.31 !	ppm	N/A	N/A	4168.79 !	0.31 ! (ppm)
V (437.923 nm)	0.31 !	ppm	N/A	N/A	2166.36 !	0.31 ! (ppm)
Ba (455.403 nm)	0.31 !	ppm	N/A	N/A	7799.88 !	0.31 ! (ppm)
Tl (535.046 nm)	0.31 !	ppm	N/A	N/A	418.45 !	0.31 ! (ppm)

Replicates Concentration

Label	Replicate 1	Replicate 2	Replicate 3	Units
Al (396.152 nm)	0.31	0.31	0.31	ppm
Mn (403.076 nm)	0.31	0.31	0.31	ppm
V (437.923 nm)	0.31	0.31	0.31	ppm
Ba (455.403 nm)	0.31	0.31	0.31	ppm
Tl (535.046 nm)	0.31	0.31	0.31	ppm

Replicates Intensity

Label	Replicate 1 (c/s)	Replicate 2 (c/s)	Replicate 3 (c/s)
Al (396.152 nm)	2291.26	2312.94	2318.26
Mn (403.076 nm)	4130.46	4142.65	4233.25
V (437.923 nm)	2153.90	2172.42	2172.78
Ba (455.403 nm)	7800.73	7790.93	7807.99
Tl (535.046 nm)	421.89	412.51	420.94

Sample Name: NS 0.625

Date: 30/10/2023 10:04:44 Rack:Tube:

Weight (g): 1 Volume (mL): 1 Dilution: 1

Analyte Results

Label	Solution Concentration	Unit	SD	%RSD	Intensity	Calculated Concentration
Al (396.152 nm)	0.63 !	ppm	N/A	N/A	4605.64 !	0.63 ! (ppm)
Mn (403.076 nm)	0.63 !	ppm	N/A	N/A	8316.16 !	0.63 ! (ppm)
V (437.923 nm)	0.63 !	ppm	N/A	N/A	4285.18 !	0.63 ! (ppm)
Ba (455.403 nm)	0.63 !	ppm	N/A	N/A	15695.33 !	0.63 ! (ppm)
Tl (535.046 nm)	0.63 !	ppm	N/A	N/A	856.98 !	0.63 ! (ppm)

Replicates Concentration

Label	Replicate 1	Replicate 2	Replicate 3	Units
Al (396.152 nm)	0.63	0.63	0.63	ppm
Mn (403.076 nm)	0.63	0.63	0.63	ppm
V (437.923 nm)	0.63	0.63	0.63	ppm
Ba (455.403 nm)	0.63	0.63	0.63	ppm
Tl (535.046 nm)	0.63	0.63	0.63	ppm

Replicates Intensity

Label	Replicate 1 (c/s)	Replicate 2 (c/s)	Replicate 3 (c/s)
Al (396.152 nm)	4617.22	4625.20	4574.51
Mn (403.076 nm)	8337.00	8294.52	8316.94
V (437.923 nm)	4273.40	4267.58	4314.57
Ba (455.403 nm)	15870.46	15538.95	15676.56
Tl (535.046 nm)	862.78	853.92	854.23

Sample Name: NS 1.25

Date: 30/10/2023 10:06:19 Rack:Tube:

Weight (g): 1 Volume (mL): 1 Dilution: 1

Analyte Results

Label	Solution Concentration	Unit	SD	%RSD	Intensity	Calculated Concentration
Al (396.152 nm)	1.25 !	ppm	N/A	N/A	9041.22 !	1.25 ! (ppm)
Mn (403.076 nm)	1.25 !	ppm	N/A	N/A	17106.88 !	1.25 ! (ppm)
V (437.923 nm)	1.25 !	ppm	N/A	N/A	8733.70 !	1.25 ! (ppm)
Ba (455.403 nm)	1.25 !	ppm	N/A	N/A	32218.18 !	1.25 ! (ppm)
Tl (535.046 nm)	1.25 !	ppm	N/A	N/A	1712.32 !	1.25 ! (ppm)

Replicates Concentration

Label	Replicate 1	Replicate 2	Replicate 3	Units
Al (396.152 nm)	1.25	1.25	1.25	ppm
Mn (403.076 nm)	1.25	1.25	1.25	ppm
V (437.923 nm)	1.25	1.25	1.25	ppm
Ba (455.403 nm)	1.25	1.25	1.25	ppm
Tl (535.046 nm)	1.25	1.25	1.25	ppm

Replicates Intensity

Label	Replicate 1 (c/s)	Replicate 2 (c/s)	Replicate 3 (c/s)
Al (396.152 nm)	9063.63	9070.41	8989.60
Mn (403.076 nm)	17202.39	17184.13	16934.11
V (437.923 nm)	8615.42	8796.33	8789.35
Ba (455.403 nm)	32096.74	32170.70	32387.10
Tl (535.046 nm)	1706.38	1704.42	1726.16

Sample Name: NS 2.5

Date: 30/10/2023 10:07:52 Rack:Tube:

Weight (g): 1 Volume (mL): 1 Dilution: 1

Analyte Results

Label	Solution Concentration	Unit	SD	%RSD	Intensity	Calculated Concentration
Al (396.152 nm)	2.50 !	ppm	N/A	N/A	17906.70 !	2.50 ! (ppm)
Mn (403.076 nm)	2.50 !	ppm	N/A	N/A	34554.41 !	2.50 ! (ppm)
V (437.923 nm)	2.50 !	ppm	N/A	N/A	17049.87 !	2.50 ! (ppm)
Ba (455.403 nm)	2.50 !	ppm	N/A	N/A	66784.17 !	2.50 ! (ppm)
Tl (535.046 nm)	2.50 !	ppm	N/A	N/A	3493.24 !	2.50 ! (ppm)

Replicates Concentration

Label	Replicate 1	Replicate 2	Replicate 3	Units
Al (396.152 nm)	2.50	2.50	2.50	ppm
Mn (403.076 nm)	2.50	2.50	2.50	ppm
V (437.923 nm)	2.50	2.50	2.50	ppm
Ba (455.403 nm)	2.50	2.50	2.50	ppm
Tl (535.046 nm)	2.50	2.50	2.50	ppm

Replicates Intensity

Label	Replicate 1 (c/s)	Replicate 2 (c/s)	Replicate 3 (c/s)
Al (396.152 nm)	17956.99	17891.23	17871.87
Mn (403.076 nm)	34504.70	34689.85	34468.68
V (437.923 nm)	16934.63	17057.74	17157.26
Ba (455.403 nm)	66143.53	67310.53	66898.43
Tl (535.046 nm)	3488.94	3492.42	3498.35

Sample Name: NS 5

Date: 30/10/2023 10:09:26 Rack:Tube:

Weight (g): 1 Volume (mL): 1 Dilution: 1

Analyte Results

Label	Solution Concentration	Unit	SD	%RSD	Intensity	Calculated Concentration
Al (396.152 nm)	5.00 !	ppm	N/A	N/A	36408.94 !	5.00 ! (ppm)
Mn (403.076 nm)	5.00 !	ppm	N/A	N/A	70719.02 !	5.00 ! (ppm)
V (437.923 nm)	5.00 !	ppm	N/A	N/A	33697.75 !	5.00 ! (ppm)
Ba (455.403 nm)	5.00 !	ppm	N/A	N/A	147092.13 !	5.00 ! (ppm)
Tl (535.046 nm)	5.00 !	ppm	N/A	N/A	7240.32 !	5.00 ! (ppm)

Replicates Concentration

Label	Replicate 1	Replicate 2	Replicate 3	Units
Al (396.152 nm)	5.00	5.00	5.00	ppm
Mn (403.076 nm)	5.00	5.00	5.00	ppm
V (437.923 nm)	5.00	5.00	5.00	ppm
Ba (455.403 nm)	5.00	5.00	5.00	ppm
Tl (535.046 nm)	5.00	5.00	5.00	ppm

Replicates Intensity

Label	Replicate 1 (c/s)	Replicate 2 (c/s)	Replicate 3 (c/s)
Al (396.152 nm)	36664.10	36268.06	36294.65
Mn (403.076 nm)	70671.83	70995.99	70489.26
V (437.923 nm)	33315.70	33808.79	33968.76
Ba (455.403 nm)	147691.81	146420.42	147164.17
Tl (535.046 nm)	7189.76	7249.74	7281.46

Sample Name: NS 10

Date: 30/10/2023 10:10:59 Rack:Tube:

Weight (g): 1 Volume (mL): 1 Dilution: 1

Analyte Results

Label	Solution Concentration	Unit	SD	%RSD	Intensity	Calculated Concentration
Al (396.152 nm)	10.00 !	ppm	N/A	N/A	74296.00 !	10.00 ! (ppm)
Mn (403.076 nm)		ppm	N/A	N/A	147263.11 !	
V (437.923 nm)	10.00 !	ppm	N/A	N/A	66808.91 !	10.00 ! (ppm)
Ba (455.403 nm)	10.00 !	ppm	N/A	N/A	326727.10 !	10.00 ! (ppm)
Tl (535.046 nm)		ppm	N/A	N/A	14968.45 !	

Replicates Concentration

Label	Replicate 1	Replicate 2	Replicate 3	Units
Al (396.152 nm)	10.00	10.00	10.00	ppm
Mn (403.076 nm)				ppm
V (437.923 nm)	10.00	10.00	10.00	ppm
Ba (455.403 nm)	10.00	10.00	10.00	ppm
Tl (535.046 nm)				ppm

Replicates Intensity

Label	Replicate 1 (c/s)	Replicate 2 (c/s)	Replicate 3 (c/s)
Al (396.152 nm)	74419.15	74568.57	73900.27
Mn (403.076 nm)	147674.80	146579.17	147535.35
V (437.923 nm)	66424.56	67034.77	66967.41
Ba (455.403 nm)	326990.95	325183.85	328006.50
Tl (535.046 nm)	15062.32	14969.23	14873.80

Sample Name: Sample 1

Date: 02/11/2023 09:14:02 Rack:Tube:

Weight (g): 1 Volume (mL): 1 Dilution: 1

Analyte Results

Label	Solution Concentration	Unit	SD	%RSD	Intensity	Calculated Concentration
Al (396.152 nm)	0.46 !	ppm	0.00	0.62	3362.45 !	0.46 ! (ppm)
Mn (403.076 nm)	0.09 !	ppm	0.00	1.49	1214.58 !	0.09 ! (ppm)
V (437.923 nm)	-0.01 !u	ppm	0.00	13.85	-25.40 !	-0.01 !u (ppm)

Label	Solution Concentration	Unit	SD	%RSD	Intensity	Calculated Concentration
Ba (455.403 nm)	0.62 !	ppm	0.00	0.27	15613.91 !	0.62 ! (ppm)
Tl (535.046 nm)	-0.60 !mu	ppm	0.00	0.76	-844.23 !m	-0.60 !mu (ppm)

Replicates Concentration

Label	Replicate 1	Replicate 2	Replicate 3	Units
Al (396.152 nm)	0.47	0.46	0.46	ppm
Mn (403.076 nm)	0.09	0.09	0.09	ppm
V (437.923 nm)	-0.01 u	0.00 u	-0.01 u	ppm
Ba (455.403 nm)	0.62	0.62	0.62	ppm
Tl (535.046 nm)	-0.60 mu	-0.60 mu	-0.61 mu	ppm

Replicates Intensity

Label	Replicate 1 (c/s)	Replicate 2 (c/s)	Replicate 3 (c/s)
Al (396.152 nm)	3386.36	3353.33	3347.68
Mn (403.076 nm)	1214.81	1232.69	1196.23
V (437.923 nm)	-25.32	-20.58	-30.31
Ba (455.403 nm)	15658.74	15608.87	15574.10
Tl (535.046 nm)	-839.12 m	-842.21 m	-851.36 m

Sample Name: Sample 2

Date: 02/11/2023 09:15:39 Rack:Tube:

Weight (g): 1 Volume (mL): 1 Dilution: 1

Analyte Results

Label	Solution Concentration	Unit	SD	%RSD	Intensity	Calculated Concentration
Al (396.152 nm)	0.21 !	ppm	0.01	4.46	1528.29 !	0.21 ! (ppm)
Mn (403.076 nm)	0.45 !	ppm	0.00	0.24	6071.71 !	0.45 ! (ppm)
V (437.923 nm)	-0.01 !u	ppm	0.00	6.04	-52.66 !	-0.01 !u (ppm)
Ba (455.403 nm)	10.40 !	ppm	0.05	0.48	349726.06 !	10.40 ! (ppm)
Tl (535.046 nm)	-1.91 !mu	ppm	0.02	1.21	-2674.10 !m	-1.91 !mu (ppm)

Replicates Concentration

Label	Replicate 1	Replicate 2	Replicate 3	Units
Al (396.152 nm)	0.22	0.21	0.20	ppm
Mn (403.076 nm)	0.44	0.45	0.45	ppm
V (437.923 nm)	-0.01 u	-0.01 u	-0.01 u	ppm

Label	Replicate 1	Replicate 2	Replicate 3	Units
Ba (455.403 nm)	10.34	10.44	10.41	ppm
Tl (535.046 nm)	-1.89 mu	-1.91 mu	-1.94 mu	ppm

Replicates Intensity

Label	Replicate 1 (c/s)	Replicate 2 (c/s)	Replicate 3 (c/s)
Al (396.152 nm)	1590.52	1538.79	1455.56
Mn (403.076 nm)	6054.65	6080.14	6080.34
V (437.923 nm)	-51.71	-49.45	-56.81
Ba (455.403 nm)	347316.11	351727.72	350134.34
Tl (535.046 nm)	-2647.88 m	-2664.28 m	-2710.13 m

Sample Name: Sample 3

Date: 02/11/2023 09:17:20 Rack:Tube:

Weight (g): 1 Volume (mL): 1 Dilution: 1

Analyte Results

Label	Solution Concentration	Unit	SD	%RSD	Intensity	Calculated Concentration
Al (396.152 nm)	0.63 !	ppm	0.00	0.49	4599.56 !	0.63 ! (ppm)
Mn (403.076 nm)	0.38 !	ppm	0.00	0.43	5184.14 !	0.38 ! (ppm)
V (437.923 nm)	-0.01 !u	ppm	0.00	11.41	-43.73 !	-0.01 !u (ppm)
Ba (455.403 nm)	6.91 !	ppm	0.01	0.15	207977.26 !	6.91 ! (ppm)
Tl (535.046 nm)	-2.44 !mu	ppm	0.02	0.66	-3411.67 !m	-2.44 !mu (ppm)

Replicates Concentration

Label	Replicate 1	Replicate 2	Replicate 3	Units
Al (396.152 nm)	0.63	0.64	0.64	ppm
Mn (403.076 nm)	0.38	0.38	0.38	ppm
V (437.923 nm)	-0.01 u	-0.01 u	-0.01 u	ppm
Ba (455.403 nm)	6.92	6.90	6.92	ppm
Tl (535.046 nm)	-2.42 mu	-2.45 mu	-2.45 mu	ppm

Replicates Intensity

Label	Replicate 1 (c/s)	Replicate 2 (c/s)	Replicate 3 (c/s)
Al (396.152 nm)	4574.86	4618.32	4605.50
Mn (403.076 nm)	5191.01	5202.42	5158.99

Label	Replicate 1 (c/s)	Replicate 2 (c/s)	Replicate 3 (c/s)
V (437.923 nm)	-45.09	-37.06	-49.04
Ba (455.403 nm)	208280.30	207559.84	208091.64
Tl (535.046 nm)	-3385.59 m	-3423.52 m	-3425.89 m

Sample Name: Sample 4

Date: 02/11/2023 07:45:44 Rack:Tube:

Weight (g): 1 Volume (mL): 1 Dilution: 1

Analyte Results

Label	Solution Concentration	Unit	SD	%RSD	Intensity	Calculated Concentration
Al (396.152 nm)	1.44	ppm	0.02	1.52	10409.14	1.44 (ppm)
Mn (403.076 nm)	1.39	ppm	0.01	0.89	18993.74	1.39 (ppm)
V (437.923 nm)	0.00 u	ppm	0.00	> 100.00	8.74	0.00 u (ppm)
Ba (455.403 nm)	11.92 o	ppm	0.07	0.55	417195.18	11.92 o (ppm)
Tl (535.046 nm)	-1.85 u	ppm	0.00	0.24	-2582.03	-1.85 u (ppm)

Replicates Concentration

Label	Replicate 1	Replicate 2	Replicate 3	Units
Al (396.152 nm)	1.45	1.41	1.45	ppm
Mn (403.076 nm)	1.41	1.38	1.39	ppm
V (437.923 nm)	0.00 u	0.00	0.00	ppm
Ba (455.403 nm)	11.84 o	11.95 o	11.96 o	ppm
Tl (535.046 nm)	-1.85 u	-1.84 u	-1.85 u	ppm

Replicates Intensity

Label	Replicate 1 (c/s)	Replicate 2 (c/s)	Replicate 3 (c/s)
Al (396.152 nm)	10512.94	10227.28	10487.22
Mn (403.076 nm)	19185.98	18868.99	18926.25
V (437.923 nm)	4.06	10.20	11.95
Ba (455.403 nm)	413845.14	418522.19	419218.20
Tl (535.046 nm)	-2583.09	-2575.43	-2587.57

Sample Name: Sample 5

Date: 02/11/2023 07:47:32 Rack:Tube:

Weight (g): 1 Volume (mL): 1 Dilution: 1

Analyte Results

Label	Solution Concentration	Unit	SD	%RSD	Intensity	Calculated Concentration
Al (396.152 nm)	1.17	ppm	0.01	0.95	8474.88	1.17 (ppm)
Mn (403.076 nm)	0.21	ppm	0.00	0.94	2904.18	0.21 (ppm)
V (437.923 nm)	0.00	ppm	0.00	26.73	15.00	0.00 (ppm)
Ba (455.403 nm)	0.88	ppm	0.01	0.62	22221.39	0.88 (ppm)
Tl (535.046 nm)	-1.52 u	ppm	0.01	0.70	-2126.81	-1.52 u (ppm)

Replicates Concentration

Label	Replicate 1	Replicate 2	Replicate 3	Units
Al (396.152 nm)	1.18	1.16	1.16	ppm
Mn (403.076 nm)	0.22	0.21	0.21	ppm
V (437.923 nm)	0.00	0.00	0.00	ppm
Ba (455.403 nm)	0.88	0.87	0.87	ppm
Tl (535.046 nm)	-1.52 u	-1.51 u	-1.53 u	ppm

Replicates Intensity

Label	Replicate 1 (c/s)	Replicate 2 (c/s)	Replicate 3 (c/s)
Al (396.152 nm)	8566.88	8417.34	8440.43
Mn (403.076 nm)	2934.07	2880.64	2897.84
V (437.923 nm)	16.55	13.80	14.66
Ba (455.403 nm)	22381.72	22119.72	22162.74
Tl (535.046 nm)	-2121.63	-2115.22	-2143.58

Sample Name: Sample 6

Date: 02/11/2023 07:49:22 Rack:Tube:

Weight (g): 1 Volume (mL): 1 Dilution: 1

Analyte Results

Label	Solution Concentration	Unit	SD	%RSD	Intensity	Calculated Concentration
Al (396.152 nm)	2.42	ppm	0.03	1.06	17568.45	2.42 (ppm)
Mn (403.076 nm)	0.34	ppm	0.00	0.63	4669.35	0.34 (ppm)
V (437.923 nm)	-0.01 u	ppm	0.00	21.63	-24.32	-0.01 u (ppm)
Ba (455.403 nm)	5.41	ppm	0.02	0.43	155440.89	5.41 (ppm)
Tl (535.046 nm)	-1.38 u	ppm	0.01	0.83	-1930.51	-1.38 u (ppm)

Replicates Concentration

Label	Replicate 1	Replicate 2	Replicate 3	Units
Al (396.152 nm)	2.42	2.45	2.40	ppm
Mn (403.076 nm)	0.34	0.35	0.34	ppm
V (437.923 nm)	-0.01 u	0.00 u	0.00 u	ppm
Ba (455.403 nm)	5.40	5.38	5.43	ppm
Tl (535.046 nm)	-1.39 u	-1.38 u	-1.37 u	ppm

Replicates Intensity

Label	Replicate 1 (c/s)	Replicate 2 (c/s)	Replicate 3 (c/s)
Al (396.152 nm)	17547.09	17764.95	17393.31
Mn (403.076 nm)	4654.99	4703.28	4649.79
V (437.923 nm)	-32.51	-18.24	-22.19
Ba (455.403 nm)	155397.04	154698.22	156227.41
Tl (535.046 nm)	-1948.28	-1925.84	-1917.41

Sample Name: Sample 7

Date: 02/11/2023 07:51:13 Rack:Tube:

Weight (g): 1 Volume (mL): 1 Dilution: 1

Analyte Results

Label	Solution Concentration	Unit	SD	%RSD	Intensity	Calculated Concentration
Al (396.152 nm)	0.76	ppm	0.01	0.69	5478.99	0.76 (ppm)
Mn (403.076 nm)	0.56	ppm	0.01	1.09	7565.06	0.56 (ppm)
V (437.923 nm)	-0.01 u	ppm	0.00	16.89	-36.62	-0.01 u (ppm)
Ba (455.403 nm)	7.66	ppm	0.02	0.21	235682.58	7.66 (ppm)
Tl (535.046 nm)	-2.41 u	ppm	0.02	0.93	-3367.75	-2.41 u (ppm)

Replicates Concentration

Label	Replicate 1	Replicate 2	Replicate 3	Units
Al (396.152 nm)	0.75	0.76	0.75	ppm
Mn (403.076 nm)	0.56	0.56	0.55	ppm
V (437.923 nm)	-0.01 u	-0.01 u	-0.01 u	ppm
Ba (455.403 nm)	7.64	7.65	7.68	ppm
Tl (535.046 nm)	-2.43 u	-2.38 u	-2.41 u	ppm

Replicates Intensity

Label	Replicate 1 (c/s)	Replicate 2 (c/s)	Replicate 3 (c/s)
Al (396.152 nm)	5471.69	5520.04	5445.25
Mn (403.076 nm)	7616.68	7609.13	7469.37
V (437.923 nm)	-27.67	-42.25	-39.94
Ba (455.403 nm)	235143.64	235543.70	236360.39
Tl (535.046 nm)	-3394.96	-3333.31	-3374.98

Sample Name: Sample 8

Date: 02/11/2023 07:52:57 Rack:Tube:

Weight (g): 1 Volume (mL): 1 Dilution: 1

Analyte Results

Label	Solution Concentration	Unit	SD	%RSD	Intensity	Calculated Concentration
Al (396.152 nm)	2.50	ppm	0.01	0.49	18093.89	2.50 (ppm)
Mn (403.076 nm)	1.04	ppm	0.01	0.98	14232.04	1.04 (ppm)
V (437.923 nm)	-0.01 u	ppm	0.00	6.89	-50.36	-0.01 u (ppm)
Ba (455.403 nm)	16.82 o	ppm	0.06	0.39	634984.03	16.82 o (ppm)
Tl (535.046 nm)	-4.75 u	ppm	0.06	1.33	-6634.55	-4.75 u (ppm)

Replicates Concentration

Label	Replicate 1	Replicate 2	Replicate 3	Units
Al (396.152 nm)	2.51	2.49	2.48	ppm
Mn (403.076 nm)	1.04	1.06	1.04	ppm
V (437.923 nm)	-0.01 u	-0.01 u	-0.01 u	ppm
Ba (455.403 nm)	16.88 o	16.75 o	16.82 o	ppm
Tl (535.046 nm)	-4.71 u	-4.82 u	-4.71 u	ppm

Replicates Intensity

Label	Replicate 1 (c/s)	Replicate 2 (c/s)	Replicate 3 (c/s)
Al (396.152 nm)	18187.96	18079.71	18013.99
Mn (403.076 nm)	14109.44	14383.58	14203.11
V (437.923 nm)	-50.19	-54.58	-46.30
Ba (455.403 nm)	637784.59	632025.78	635141.71
Tl (535.046 nm)	-6583.36	-6736.17	-6584.12

Sample Name: Sample 9

Date: 02/11/2023 07:54:40 Rack:Tube:

Weight (g): 1 Volume (mL): 1 Dilution: 1

Analyte Results

Label	Solution Concentration	Unit	SD	%RSD	Intensity	Calculated Concentration
Al (396.152 nm)	0.57	ppm	0.01	2.15	4114.04	0.57 (ppm)
Mn (403.076 nm)	0.17	ppm	0.00	0.07	2327.23	0.17 (ppm)
V (437.923 nm)	0.00 u	ppm	0.00	24.31	-5.93	0.00 u (ppm)
Ba (455.403 nm)	0.87	ppm	0.00	0.23	22041.93	0.87 (ppm)
Tl (535.046 nm)	-0.99 mu	ppm	0.01	1.51	-1381.18 m	-0.99 mu (ppm)

Replicates Concentration

Label	Replicate 1	Replicate 2	Replicate 3	Units
Al (396.152 nm)	0.58	0.57	0.55	ppm
Mn (403.076 nm)	0.17	0.17	0.17	ppm
V (437.923 nm)	0.00 u	0.00 u	0.00 u	ppm
Ba (455.403 nm)	0.87	0.87	0.87	ppm
Tl (535.046 nm)	-0.98 mu	-0.98 mu	-1.00 mu	ppm

Replicates Intensity

Label	Replicate 1 (c/s)	Replicate 2 (c/s)	Replicate 3 (c/s)
Al (396.152 nm)	4180.51	4147.76	4013.87
Mn (403.076 nm)	2325.86	2329.13	2326.71
V (437.923 nm)	-3.15	-10.28	-4.36
Ba (455.403 nm)	22026.30	22100.63	21998.86
Tl (535.046 nm)	-1367.62 m	-1370.82 m	-1405.10 m

Sample Name: Sample 10

Date: 02/11/2023 07:56:22 Rack:Tube:

Weight (g): 1 Volume (mL): 1 Dilution: 1

Analyte Results

Label	Solution Concentration	Unit	SD	%RSD	Intensity	Calculated Concentration
Al (396.152 nm)	0.73	ppm	0.01	1.57	5273.67	0.73 (ppm)
Mn (403.076 nm)	0.40	ppm	0.00	0.68	5487.56	0.40 (ppm)
V (437.923 nm)	0.00 u	ppm	0.00	19.05	-19.78	0.00 u (ppm)
Ba (455.403 nm)	9.31	ppm	0.05	0.55	302071.05	9.31 (ppm)
Tl (535.046 nm)	-3.22 u	ppm	0.03	0.85	-4501.59	-3.22 u (ppm)

Replicates Concentration

Label	Replicate 1	Replicate 2	Replicate 3	Units
Al (396.152 nm)	0.73	0.73	0.71	ppm
Mn (403.076 nm)	0.40	0.40	0.41	ppm
V (437.923 nm)	0.00 u	0.00 u	0.00 u	ppm
Ba (455.403 nm)	9.36	9.26	9.30	ppm
Tl (535.046 nm)	-3.19 u	-3.25 u	-3.22 u	ppm

Replicates Intensity

Label	Replicate 1 (c/s)	Replicate 2 (c/s)	Replicate 3 (c/s)
Al (396.152 nm)	5316.32	5326.32	5178.36
Mn (403.076 nm)	5459.57	5472.89	5530.22
V (437.923 nm)	-23.98	-21.96	-13.39
Ba (455.403 nm)	304310.06	299999.92	301903.16
Tl (535.046 nm)	-4464.23	-4541.02	-4499.51

Sample Name: Sample 11

Date: 02/11/2023 07:58:02 Rack:Tube:

Weight (g): 1 Volume (mL): 1 Dilution: 1

Analyte Results

Label	Solution Concentration	Unit	SD	%RSD	Intensity	Calculated Concentration
Al (396.152 nm)	0.53	ppm	0.01	0.99	3859.62	0.53 (ppm)
Mn (403.076 nm)	0.42	ppm	0.00	0.73	5687.59	0.42 (ppm)
V (437.923 nm)	0.00 u	ppm	0.00	> 100.00	10.24	0.00 u (ppm)
Ba (455.403 nm)	3.95	ppm	0.04	0.91	108791.73	3.95 (ppm)
Tl (535.046 nm)	-1.21 mu	ppm	0.01	1.13	-1694.90 m	-1.21 mu (ppm)

Replicates Concentration

Label	Replicate 1	Replicate 2	Replicate 3	Units
Al (396.152 nm)	0.53	0.53	0.54	ppm
Mn (403.076 nm)	0.42	0.42	0.42	ppm
V (437.923 nm)	0.00 u	0.00	0.00	ppm
Ba (455.403 nm)	3.98	3.95	3.91	ppm
Tl (535.046 nm)	-1.20 mu	-1.22 mu	-1.22 mu	ppm

Replicates Intensity

Label	Replicate 1 (c/s)	Replicate 2 (c/s)	Replicate 3 (c/s)
Al (396.152 nm)	3842.72	3832.60	3903.54
Mn (403.076 nm)	5649.44	5731.85	5681.47
V (437.923 nm)	2.80	11.84	16.07
Ba (455.403 nm)	109820.32	108916.14	107638.72
Tl (535.046 nm)	-1672.92 m	-1704.11 m	-1707.65 m

Sample Name: Sample 12

Date: 02/11/2023 07:59:44 Rack:Tube:

Weight (g): 1 Volume (mL): 1 Dilution: 1

Analyte Results

Label	Solution Concentration	Unit	SD	%RSD	Intensity	Calculated Concentration
Al (396.152 nm)	0.21	ppm	0.00	1.67	1508.56	0.21 (ppm)
Mn (403.076 nm)	0.09	ppm	0.00	1.22	1253.27	0.09 (ppm)
V (437.923 nm)	0.00 u	ppm	0.00	28.02	-15.74	0.00 u (ppm)

Label	Solution Concentration	Unit	SD	%RSD	Intensity	Calculated Concentration
Ba (455.403 nm)	1.15	ppm	0.00	0.42	29366.04	1.15 (ppm)
Tl (535.046 nm)	-0.45 u	ppm	0.00	1.01	-632.53	-0.45 u (ppm)

Replicates Concentration

Label	Replicate 1	Replicate 2	Replicate 3	Units
Al (396.152 nm)	0.21	0.21	0.20	ppm
Mn (403.076 nm)	0.09	0.09	0.09	ppm
V (437.923 nm)	0.00 u	0.00 u	0.00 u	ppm
Ba (455.403 nm)	1.15	1.15	1.15	ppm
Tl (535.046 nm)	-0.46 u	-0.45 u	-0.45 u	ppm

Replicates Intensity

Label	Replicate 1 (c/s)	Replicate 2 (c/s)	Replicate 3 (c/s)
Al (396.152 nm)	1533.38	1509.27	1483.03
Mn (403.076 nm)	1236.06	1257.67	1266.06
V (437.923 nm)	-8.94	-23.18	-15.10
Ba (455.403 nm)	29513.98	29281.99	29302.15
Tl (535.046 nm)	-639.25	-626.64	-631.71

Sample Name: Sample 13

Date: 02/11/2023 08:01:41 Rack:Tube:

Weight (g): 1 Volume (mL): 1 Dilution: 1

Analyte Results

Label	Solution Concentration	Unit	SD	%RSD	Intensity	Calculated Concentration
Al (396.152 nm)	3.33	ppm	0.02	0.56	24165.72	3.33 (ppm)
Mn (403.076 nm)	1.32	ppm	0.00	0.18	17979.89	1.32 (ppm)
V (437.923 nm)	0.00 u	ppm	0.00	27.83	-18.66	0.00 u (ppm)
Ba (455.403 nm)	8.49	ppm	0.00	0.04	268180.46	8.49 (ppm)
Tl (535.046 nm)	-3.20 u	ppm	0.03	0.80	-4475.35	-3.20 u (ppm)

Replicates Concentration

Label	Replicate 1	Replicate 2	Replicate 3	Units
Al (396.152 nm)	3.35	3.31	3.34	ppm
Mn (403.076 nm)	1.32	1.32	1.32	ppm
V (437.923 nm)	0.00 u	-0.01 u	0.00 u	ppm

Label	Replicate 1	Replicate 2	Replicate 3	Units
Ba (455.403 nm)	8.48	8.49	8.49	ppm
Tl (535.046 nm)	-3.22 u	-3.21 u	-3.17 u	ppm

Replicates Intensity

Label	Replicate 1 (c/s)	Replicate 2 (c/s)	Replicate 3 (c/s)
Al (396.152 nm)	24291.32	24023.29	24182.56
Mn (403.076 nm)	17948.73	17978.20	18012.75
V (437.923 nm)	-10.95	-26.75	-18.27
Ba (455.403 nm)	268018.83	268299.55	268223.01
Tl (535.046 nm)	-4505.65	-4484.83	-4435.56

Sample Name: Sample 14

Date: 02/11/2023 08:03:21 Rack:Tube:

Weight (g): 1 Volume (mL): 1 Dilution: 1

Analyte Results

Label	Solution Concentration	Unit	SD	%RSD	Intensity	Calculated Concentration
Al (396.152 nm)	0.63	ppm	0.01	1.00	4601.00	0.63 (ppm)
Mn (403.076 nm)	0.26	ppm	0.00	0.88	3589.90	0.26 (ppm)
V (437.923 nm)	0.00 u	ppm	0.00	17.13	-4.87	0.00 u (ppm)
Ba (455.403 nm)	5.16	ppm	0.02	0.36	147400.87	5.16 (ppm)
Tl (535.046 nm)	-1.35 mu	ppm	0.00	0.19	-1885.86 m	-1.35 mu (ppm)

Replicates Concentration

Label	Replicate 1	Replicate 2	Replicate 3	Units
Al (396.152 nm)	0.64	0.63	0.63	ppm
Mn (403.076 nm)	0.27	0.26	0.26	ppm
V (437.923 nm)	0.00 u	0.00 u	0.00 u	ppm
Ba (455.403 nm)	5.15	5.15	5.18	ppm
Tl (535.046 nm)	-1.35 mu	-1.35 mu	-1.35 mu	ppm

Replicates Intensity

Label	Replicate 1 (c/s)	Replicate 2 (c/s)	Replicate 3 (c/s)
Al (396.152 nm)	4648.96	4557.69	4596.36
Mn (403.076 nm)	3623.32	3560.32	3586.04

Label	Replicate 1 (c/s)	Replicate 2 (c/s)	Replicate 3 (c/s)
V (437.923 nm)	-2.90	-7.69	-4.02
Ba (455.403 nm)	146996.95	147094.00	148111.65
Tl (535.046 nm)	-1887.73 m	-1888.10 m	-1881.75 m

Sample Name: Sample 15

Date: 02/11/2023 08:05:03 Rack:Tube:

Weight (g): 1 Volume (mL): 1 Dilution: 1

Analyte Results

Label	Solution Concentration	Unit	SD	%RSD	Intensity	Calculated Concentration
Al (396.152 nm)	1.35	ppm	0.00	0.26	9781.63	1.35 (ppm)
Mn (403.076 nm)	0.24	ppm	0.00	0.40	3274.36	0.24 (ppm)
V (437.923 nm)	0.00	ppm	0.00	20.87	20.73	0.00 (ppm)
Ba (455.403 nm)	0.97	ppm	0.00	0.16	24562.69	0.97 (ppm)
Tl (535.046 nm)	-1.09 mu	ppm	0.01	0.79	-1522.56 m	-1.09 mu (ppm)

Replicates Concentration

Label	Replicate 1	Replicate 2	Replicate 3	Units
Al (396.152 nm)	1.35	1.35	1.35	ppm
Mn (403.076 nm)	0.24	0.24	0.24	ppm
V (437.923 nm)	0.00	0.00	0.00	ppm
Ba (455.403 nm)	0.97	0.97	0.96	ppm
Tl (535.046 nm)	-1.09 mu	-1.08 mu	-1.10 mu	ppm

Replicates Intensity

Label	Replicate 1 (c/s)	Replicate 2 (c/s)	Replicate 3 (c/s)
Al (396.152 nm)	9782.65	9755.89	9806.36
Mn (403.076 nm)	3263.27	3271.13	3288.68
V (437.923 nm)	18.24	22.75	21.18
Ba (455.403 nm)	24550.38	24608.44	24529.24
Tl (535.046 nm)	-1521.47 m	-1511.07 m	-1535.13 m

Sample Name: Sample 16

Date: 02/11/2023 08:06:45 Rack:Tube:

Weight (g): 1 Volume (mL): 1 Dilution: 1

Analyte Results

Label	Solution Concentration	Unit	SD	%RSD	Intensity	Calculated Concentration
Al (396.152 nm)	2.04	ppm	0.01	0.51	14792.19	2.04 (ppm)
Mn (403.076 nm)	0.25	ppm	0.00	0.99	3338.80	0.25 (ppm)
V (437.923 nm)	0.00	ppm	0.00	48.87	22.86	0.00 (ppm)
Ba (455.403 nm)	1.27	ppm	0.00	0.38	32589.45	1.27 (ppm)
Tl (535.046 nm)	-1.12 mu	ppm	0.00	0.24	-1564.44 m	-1.12 mu (ppm)

Replicates Concentration

Label	Replicate 1	Replicate 2	Replicate 3	Units
Al (396.152 nm)	2.03	2.05	2.04	ppm
Mn (403.076 nm)	0.24	0.25	0.24	ppm
V (437.923 nm)	0.00	0.00	0.00	ppm
Ba (455.403 nm)	1.27	1.28	1.27	ppm
Tl (535.046 nm)	-1.12 mu	-1.12 mu	-1.12 mu	ppm

Replicates Intensity

Label	Replicate 1 (c/s)	Replicate 2 (c/s)	Replicate 3 (c/s)
Al (396.152 nm)	14734.84	14877.53	14764.20
Mn (403.076 nm)	3327.40	3376.21	3312.79
V (437.923 nm)	29.54	22.28	16.76
Ba (455.403 nm)	32535.15	32736.54	32496.67
Tl (535.046 nm)	-1560.25 m	-1567.14 m	-1565.94 m

Sample Name: Sample 17

Date: 02/11/2023 08:08:25 Rack:Tube:

Weight (g): 1 Volume (mL): 1 Dilution: 1

Analyte Results

Label	Solution Concentration	Unit	SD	%RSD	Intensity	Calculated Concentration
Al (396.152 nm)	1.70	ppm	0.01	0.46	12295.71	1.70 (ppm)
Mn (403.076 nm)	0.79	ppm	0.00	0.61	10786.89	0.79 (ppm)
V (437.923 nm)	0.00 u	ppm	0.00	> 100.00	8.22	0.00 u (ppm)
Ba (455.403 nm)	3.84	ppm	0.03	0.88	105519.63	3.84 (ppm)
Tl (535.046 nm)	-4.58 u	ppm	0.03	0.75	-6398.39	-4.58 u (ppm)

Replicates Concentration

Label	Replicate 1	Replicate 2	Replicate 3	Units
Al (396.152 nm)	1.70	1.69	1.70	ppm
Mn (403.076 nm)	0.79	0.79	0.80	ppm
V (437.923 nm)	0.00	0.00 u	0.00 u	ppm
Ba (455.403 nm)	3.82	3.88	3.82	ppm
Tl (535.046 nm)	-4.54 u	-4.61 u	-4.57 u	ppm

Replicates Intensity

Label	Replicate 1 (c/s)	Replicate 2 (c/s)	Replicate 3 (c/s)
Al (396.152 nm)	12340.02	12231.36	12315.75
Mn (403.076 nm)	10717.96	10793.86	10848.84
V (437.923 nm)	14.36	7.77	2.54
Ba (455.403 nm)	104812.90	106695.50	105050.49
Tl (535.046 nm)	-6352.87	-6448.80	-6393.52

Sample Name: Sample 18

Date: 02/11/2023 08:10:06 Rack:Tube:

Weight (g): 1 Volume (mL): 1 Dilution: 1

Analyte Results

Label	Solution Concentration	Unit	SD	%RSD	Intensity	Calculated Concentration
Al (396.152 nm)	0.99	ppm	0.00	0.45	7204.59	0.99 (ppm)
Mn (403.076 nm)	0.40	ppm	0.00	0.57	5491.86	0.40 (ppm)
V (437.923 nm)	-0.01 u	ppm	0.00	6.97	-55.93	-0.01 u (ppm)
Ba (455.403 nm)	1.63	ppm	0.01	0.44	42230.09	1.63 (ppm)
Tl (535.046 nm)	-8.19 u	ppm	0.02	0.22	-11448.59	-8.19 u (ppm)

Replicates Concentration

Label	Replicate 1	Replicate 2	Replicate 3	Units
Al (396.152 nm)	0.99	0.99	1.00	ppm
Mn (403.076 nm)	0.40	0.40	0.41	ppm
V (437.923 nm)	-0.01 u	-0.01 u	-0.01 u	ppm
Ba (455.403 nm)	1.64	1.63	1.62	ppm
Tl (535.046 nm)	-8.20 u	-8.20 u	-8.17 u	ppm

Replicates Intensity

Label	Replicate 1 (c/s)	Replicate 2 (c/s)	Replicate 3 (c/s)
Al (396.152 nm)	7211.64	7169.45	7232.69
Mn (403.076 nm)	5477.22	5470.27	5528.09
V (437.923 nm)	-50.65	-58.37	-58.78
Ba (455.403 nm)	42431.04	42216.22	42043.03
Tl (535.046 nm)	-11464.33	-11462.45	-11418.98

Sample Name: Sample 19

Date: 02/11/2023 08:11:48 Rack:Tube:

Weight (g): 1 Volume (mL): 1 Dilution: 1

Analyte Results

Label	Solution Concentration	Unit	SD	%RSD	Intensity	Calculated Concentration
Al (396.152 nm)	1.45	ppm	0.02	1.08	10499.76	1.45 (ppm)
Mn (403.076 nm)	0.53	ppm	0.01	0.98	7226.99	0.53 (ppm)
V (437.923 nm)	0.00 u	ppm	0.00	41.79	-0.25	0.00 u (ppm)
Ba (455.403 nm)	1.16	ppm	0.01	1.06	29680.65	1.16 (ppm)
Tl (535.046 nm)	-1.36 mu	ppm	0.01	0.66	-1905.56 m	-1.36 mu (ppm)

Replicates Concentration

Label	Replicate 1	Replicate 2	Replicate 3	Units
Al (396.152 nm)	1.45	1.43	1.47	ppm
Mn (403.076 nm)	0.54	0.53	0.53	ppm
V (437.923 nm)	0.00 u	0.00 u	0.00 u	ppm
Ba (455.403 nm)	1.17	1.17	1.15	ppm
Tl (535.046 nm)	-1.36 mu	-1.36 mu	-1.37 mu	ppm

Replicates Intensity

Label	Replicate 1 (c/s)	Replicate 2 (c/s)	Replicate 3 (c/s)
Al (396.152 nm)	10479.84	10397.36	10622.08
Mn (403.076 nm)	7294.09	7233.72	7153.15
V (437.923 nm)	3.56	-4.71	0.40
Ba (455.403 nm)	29916.23	29815.69	29310.03
Tl (535.046 nm)	-1899.68 m	-1896.98 m	-1920.01 m

Sample Name: Sample 20

Date: 02/11/2023 08:13:36 Rack:Tube:

Weight (g): 1 Volume (mL): 1 Dilution: 1

Analyte Results

Label	Solution Concentration	Unit	SD	%RSD	Intensity	Calculated Concentration
Al (396.152 nm)	1.71	ppm	0.02	1.39	12370.27	1.71 (ppm)
Mn (403.076 nm)	0.33	ppm	0.00	0.73	4548.55	0.33 (ppm)
V (437.923 nm)	0.00	ppm	0.00	86.37	12.02	0.00 (ppm)
Ba (455.403 nm)	1.32	ppm	0.00	0.16	33847.73	1.32 (ppm)
Tl (535.046 nm)	-1.02 mu	ppm	0.05	4.65	-1422.65 m	-1.02 mu (ppm)

Replicates Concentration

Label	Replicate 1	Replicate 2	Replicate 3	Units
Al (396.152 nm)	1.73	1.69	1.70	ppm
Mn (403.076 nm)	0.33	0.33	0.34	ppm
V (437.923 nm)	0.00	0.00	0.00	ppm
Ba (455.403 nm)	1.32	1.32	1.32	ppm
Tl (535.046 nm)	-0.97 u	-1.02 u	-1.06 mu	ppm

Replicates Intensity

Label	Replicate 1 (c/s)	Replicate 2 (c/s)	Replicate 3 (c/s)
Al (396.152 nm)	12562.53	12231.81	12316.48
Mn (403.076 nm)	4550.11	4514.65	4580.87
V (437.923 nm)	9.89	12.39	13.77
Ba (455.403 nm)	33828.40	33911.56	33803.23
Tl (535.046 nm)	-1357.07	-1421.83	-1489.06 m

Sample Name: Sample 21

Date: 02/11/2023 08:15:16 Rack:Tube:

Weight (g): 1 Volume (mL): 1 Dilution: 1

Analyte Results

Label	Solution Concentration	Unit	SD	%RSD	Intensity	Calculated Concentration
Al (396.152 nm)	0.52	ppm	0.01	1.73	3788.38	0.52 (ppm)
Mn (403.076 nm)	0.65	ppm	0.01	1.10	8788.23	0.65 (ppm)
V (437.923 nm)	0.00 u	ppm	0.00	25.89	-19.51	0.00 u (ppm)
Ba (455.403 nm)	12.76 o	ppm	0.07	0.53	454646.92	12.76 o (ppm)
Tl (535.046 nm)	-2.16 u	ppm	0.04	1.82	-3017.35	-2.16 u (ppm)

Replicates Concentration

Label	Replicate 1	Replicate 2	Replicate 3	Units
Al (396.152 nm)	0.51	0.53	0.53	ppm
Mn (403.076 nm)	0.65	0.65	0.64	ppm
V (437.923 nm)	0.00 u	-0.01 u	0.00 u	ppm
Ba (455.403 nm)	12.82 o	12.77 o	12.69 o	ppm
Tl (535.046 nm)	-2.19 u	-2.17 u	-2.11 u	ppm

Replicates Intensity

Label	Replicate 1 (c/s)	Replicate 2 (c/s)	Replicate 3 (c/s)
Al (396.152 nm)	3712.89	3826.63	3825.62
Mn (403.076 nm)	8816.98	8867.23	8680.48
V (437.923 nm)	-11.10	-25.79	-21.63
Ba (455.403 nm)	457308.69	455220.76	451411.30
Tl (535.046 nm)	-3060.71	-3035.51	-2955.85

Sample Name: Sample 22

Date: 02/11/2023 08:16:58 Rack:Tube:

Weight (g): 1 Volume (mL): 1 Dilution: 1

Analyte Results

Label	Solution Concentration	Unit	SD	%RSD	Intensity	Calculated Concentration
Al (396.152 nm)	0.24	ppm	0.00	1.77	1777.33	0.24 (ppm)
Mn (403.076 nm)	0.29	ppm	0.00	1.37	3877.69	0.29 (ppm)
V (437.923 nm)	-0.01 u	ppm	0.00	3.53	-55.82	-0.01 u (ppm)
Ba (455.403 nm)	2.87	ppm	0.02	0.82	76774.13	2.87 (ppm)
Tl (535.046 nm)	-1.60 mu	ppm	0.02	0.97	-2232.64 m	-1.60 mu (ppm)

Replicates Concentration

Label	Replicate 1	Replicate 2	Replicate 3	Units
Al (396.152 nm)	0.24	0.25	0.24	ppm
Mn (403.076 nm)	0.28	0.29	0.28	ppm
V (437.923 nm)	-0.01 u	-0.01 u	-0.01 u	ppm
Ba (455.403 nm)	2.85	2.89	2.87	ppm
Tl (535.046 nm)	-1.58 mu	-1.61 mu	-1.60 mu	ppm

Replicates Intensity

Label	Replicate 1 (c/s)	Replicate 2 (c/s)	Replicate 3 (c/s)
Al (396.152 nm)	1753.79	1812.95	1765.24
Mn (403.076 nm)	3834.19	3936.93	3861.96
V (437.923 nm)	-54.54	-58.49	-54.42
Ba (455.403 nm)	76131.48	77486.02	76704.89
Tl (535.046 nm)	-2209.51 m	-2252.56 m	-2235.84 m

Sample Name: Sample 23

Date: 02/11/2023 08:18:38 Rack:Tube:

Weight (g): 1 Volume (mL): 1 Dilution: 1

Analyte Results

Label	Solution Concentration	Unit	SD	%RSD	Intensity	Calculated Concentration
Al (396.152 nm)	0.29	ppm	0.01	2.90	2110.14	0.29 (ppm)
Mn (403.076 nm)	0.14	ppm	0.00	0.41	1928.67	0.14 (ppm)
V (437.923 nm)	-0.01 u	ppm	0.00	5.45	-60.80	-0.01 u (ppm)

Label	Solution Concentration	Unit	SD	%RSD	Intensity	Calculated Concentration
Ba (455.403 nm)	5.00	ppm	0.02	0.44	142084.39	5.00 (ppm)
Tl (535.046 nm)	-2.03 mu	ppm	0.10	4.82	-2843.43 m	-2.03 mu (ppm)

Replicates Concentration

Label	Replicate 1	Replicate 2	Replicate 3	Units
Al (396.152 nm)	0.30	0.28	0.29	ppm
Mn (403.076 nm)	0.14	0.14	0.14	ppm
V (437.923 nm)	-0.01 u	-0.01 u	-0.01 u	ppm
Ba (455.403 nm)	5.01	4.98	5.01	ppm
Tl (535.046 nm)	-1.92 mu	-2.09 u	-2.09 u	ppm

Replicates Intensity

Label	Replicate 1 (c/s)	Replicate 2 (c/s)	Replicate 3 (c/s)
Al (396.152 nm)	2167.52	2045.87	2117.03
Mn (403.076 nm)	1933.34	1919.53	1933.15
V (437.923 nm)	-59.60	-65.10	-57.70
Ba (455.403 nm)	142498.34	141267.85	142486.98
Tl (535.046 nm)	-2685.37 m	-2925.71	-2919.20

Sample Name: Sample 24

Date: 02/11/2023 08:20:22 Rack:Tube:

Weight (g): 1 Volume (mL): 1 Dilution: 1

Analyte Results

Label	Solution Concentration	Unit	SD	%RSD	Intensity	Calculated Concentration
Al (396.152 nm)	0.82	ppm	0.01	1.63	5922.65	0.82 (ppm)
Mn (403.076 nm)	0.16	ppm	0.00	0.73	2156.35	0.16 (ppm)
V (437.923 nm)	0.00 u	ppm	0.00	> 100.00	7.69	0.00 u (ppm)
Ba (455.403 nm)	0.87	ppm	0.00	0.29	22030.44	0.87 (ppm)
Tl (535.046 nm)	-0.77 u	ppm	0.02	2.65	-1078.97	-0.77 u (ppm)

Replicates Concentration

Label	Replicate 1	Replicate 2	Replicate 3	Units
Al (396.152 nm)	0.81	0.83	0.81	ppm
Mn (403.076 nm)	0.16	0.16	0.16	ppm
V (437.923 nm)	0.00 u	0.00	0.00 u	ppm

Label	Replicate 1	Replicate 2	Replicate 3	Units
Ba (455.403 nm)	0.87	0.87	0.87	ppm
Tl (535.046 nm)	-0.75 u	-0.78 u	-0.79 u	ppm

Replicates Intensity

Label	Replicate 1 (c/s)	Replicate 2 (c/s)	Replicate 3 (c/s)
Al (396.152 nm)	5882.80	6032.71	5852.45
Mn (403.076 nm)	2174.64	2147.81	2146.60
V (437.923 nm)	6.29	11.65	5.14
Ba (455.403 nm)	21997.73	22105.76	21987.83
Tl (535.046 nm)	-1046.70	-1089.22	-1100.97

Sample Name: Sample 25

Date: 02/11/2023 08:22:04 Rack:Tube:

Weight (g): 1 Volume (mL): 1 Dilution: 1

Analyte Results

Label	Solution Concentration	Unit	SD	%RSD	Intensity	Calculated Concentration
Al (396.152 nm)	1.85	ppm	0.02	1.26	13435.01	1.85 (ppm)
Mn (403.076 nm)	0.19	ppm	0.00	0.90	2575.89	0.19 (ppm)
V (437.923 nm)	0.03 m	ppm	0.00	16.10	211.75 m	0.03 m (ppm)
Ba (455.403 nm)	2.63	ppm	0.01	0.25	69909.20	2.63 (ppm)
Tl (535.046 nm)	-103.07 u	ppm	0.43	0.42	-144025.97	-103.07 u (ppm)

Replicates Concentration

Label	Replicate 1	Replicate 2	Replicate 3	Units
Al (396.152 nm)	1.83	1.88	1.85	ppm
Mn (403.076 nm)	0.19	0.19	0.19	ppm
V (437.923 nm)	0.04 m	0.03 m	0.03 m	ppm
Ba (455.403 nm)	2.63	2.62	2.64	ppm
Tl (535.046 nm)	-103.13 u	-102.62 u	-103.47 u	ppm

Replicates Intensity

Label	Replicate 1 (c/s)	Replicate 2 (c/s)	Replicate 3 (c/s)
Al (396.152 nm)	13278.65	13615.22	13411.15
Mn (403.076 nm)	2561.27	2602.84	2563.55

Label	Replicate 1 (c/s)	Replicate 2 (c/s)	Replicate 3 (c/s)
V (437.923 nm)	249.01 m	197.18 m	189.06 m
Ba (455.403 nm)	69892.43	69734.26	70100.92
Tl (535.046 nm)	-144107.18	-143388.67	-144582.08

Sample Name: Sample 26

Date: 02/11/2023 08:23:49 Rack:Tube:

Weight (g): 1 Volume (mL): 1 Dilution: 1

Analyte Results

Label	Solution Concentration	Unit	SD	%RSD	Intensity	Calculated Concentration
Al (396.152 nm)	0.64 m	ppm	0.01	1.36	4676.07 m	0.64 m (ppm)
Mn (403.076 nm)	0.19	ppm	0.00	0.66	2542.31	0.19 (ppm)
V (437.923 nm)	0.03 m	ppm	0.01	17.85	230.31 m	0.03 m (ppm)
Ba (455.403 nm)	2.23	ppm	0.01	0.31	58630.29	2.23 (ppm)
Tl (535.046 nm)	-107.85 u	ppm	1.11	1.03	-150704.83	-107.85 u (ppm)

Replicates Concentration

Label	Replicate 1	Replicate 2	Replicate 3	Units
Al (396.152 nm)	0.64	0.65	0.65 m	ppm
Mn (403.076 nm)	0.19	0.19	0.19	ppm
V (437.923 nm)	0.04 m	0.03 m	0.03 m	ppm
Ba (455.403 nm)	2.22	2.24	2.22	ppm
Tl (535.046 nm)	-108.83 u	-108.08 u	-106.65 u	ppm

Replicates Intensity

Label	Replicate 1 (c/s)	Replicate 2 (c/s)	Replicate 3 (c/s)
Al (396.152 nm)	4609.01	4735.03	4684.18 m
Mn (403.076 nm)	2522.99	2553.70	2550.24
V (437.923 nm)	275.75 m	208.89 m	206.28 m
Ba (455.403 nm)	58511.17	58855.46	58524.24
Tl (535.046 nm)	-152074.03	-151016.95	-149023.53

Sample Name: Sample 27

Date: 02/11/2023 08:25:31 Rack:Tube:

Weight (g): 1 Volume (mL): 1 Dilution: 1

Analyte Results

Label	Solution Concentration	Unit	SD	%RSD	Intensity	Calculated Concentration
Al (396.152 nm)	2.56	ppm	0.02	0.60	18592.06	2.56 (ppm)
Mn (403.076 nm)	0.26	ppm	0.00	0.81	3503.88	0.26 (ppm)
V (437.923 nm)	0.04 m	ppm	0.01	15.06	288.57 m	0.04 m (ppm)
Ba (455.403 nm)	1.72	ppm	0.01	0.35	44640.14	1.72 (ppm)
Tl (535.046 nm)	-120.88 u	ppm	0.38	0.31	-168913.43	-120.88 u (ppm)

Replicates Concentration

Label	Replicate 1	Replicate 2	Replicate 3	Units
Al (396.152 nm)	2.55	2.57	2.58	ppm
Mn (403.076 nm)	0.26	0.26	0.26	ppm
V (437.923 nm)	0.05 m	0.04 m	0.04 m	ppm
Ba (455.403 nm)	1.72	1.71	1.73	ppm
Tl (535.046 nm)	-121.32 u	-120.64 u	-120.69 u	ppm

Replicates Intensity

Label	Replicate 1 (c/s)	Replicate 2 (c/s)	Replicate 3 (c/s)
Al (396.152 nm)	18467.35	18623.98	18684.86
Mn (403.076 nm)	3499.06	3534.59	3477.98
V (437.923 nm)	335.18 m	276.84 m	253.69 m
Ba (455.403 nm)	44636.36	44477.99	44806.07
Tl (535.046 nm)	-169526.17	-168574.41	-168639.73

Sample Name: Sample 28

Date: 02/11/2023 08:27:14 Rack:Tube:

Weight (g): 1 Volume (mL): 1 Dilution: 1

Analyte Results

Label	Solution Concentration	Unit	SD	%RSD	Intensity	Calculated Concentration
Al (396.152 nm)	1.66	ppm	0.01	0.51	12037.84	1.66 (ppm)
Mn (403.076 nm)	0.42	ppm	0.00	0.27	5727.28	0.42 (ppm)
V (437.923 nm)	0.04 m	ppm	0.01	12.23	313.11 m	0.04 m (ppm)
Ba (455.403 nm)	1.36	ppm	0.01	0.39	34915.56	1.36 (ppm)
Tl (535.046 nm)	-145.02 u	ppm	0.41	0.28	-202639.25	-145.02 u (ppm)

Replicates Concentration

Label	Replicate 1	Replicate 2	Replicate 3	Units
Al (396.152 nm)	1.66	1.67	1.66	ppm
Mn (403.076 nm)	0.42	0.42	0.42	ppm
V (437.923 nm)	0.05 m	0.04 m	0.04 m	ppm
Ba (455.403 nm)	1.36	1.35	1.36	ppm
Tl (535.046 nm)	-144.58 u	-145.08 u	-145.39 u	ppm

Replicates Intensity

Label	Replicate 1 (c/s)	Replicate 2 (c/s)	Replicate 3 (c/s)
Al (396.152 nm)	11999.77	12108.53	12005.22
Mn (403.076 nm)	5721.05	5715.63	5745.16
V (437.923 nm)	355.82 m	288.75 m	294.75 m
Ba (455.403 nm)	34891.77	34787.42	35067.48
Tl (535.046 nm)	-202024.68	-202730.17	-203162.89

Sample Name: Sample 29

Date: 02/11/2023 08:28:55 Rack:Tube:

Weight (g): 1 Volume (mL): 1 Dilution: 1

Analyte Results

Label	Solution Concentration	Unit	SD	%RSD	Intensity	Calculated Concentration
Al (396.152 nm)	7.12	ppm	0.07	1.03	51583.13	7.12 (ppm)
Mn (403.076 nm)	0.63	ppm	0.00	0.66	8644.80	0.63 (ppm)
V (437.923 nm)	0.06 m	ppm	0.01	11.52	388.55 m	0.06 m (ppm)
Ba (455.403 nm)	1.46	ppm	0.01	0.45	37648.82	1.46 (ppm)
Tl (535.046 nm)	-172.84 u	ppm	0.91	0.53	-241510.50	-172.84 u (ppm)

Replicates Concentration

Label	Replicate 1	Replicate 2	Replicate 3	Units
Al (396.152 nm)	7.11	7.19	7.05	ppm
Mn (403.076 nm)	0.63	0.63	0.64	ppm
V (437.923 nm)	0.06 m	0.05 m	0.05 m	ppm
Ba (455.403 nm)	1.47	1.46	1.45	ppm
Tl (535.046 nm)	-173.88 u	-172.18 u	-172.45 u	ppm

Replicates Intensity

Label	Replicate 1 (c/s)	Replicate 2 (c/s)	Replicate 3 (c/s)
Al (396.152 nm)	51510.95	52147.31	51091.13
Mn (403.076 nm)	8591.50	8637.65	8705.26
V (437.923 nm)	438.29 m	370.77 m	356.60 m
Ba (455.403 nm)	37798.05	37692.38	37456.03
Tl (535.046 nm)	-242966.28	-240593.61	-240971.60

Sample Name: Sample 30

Date: 02/11/2023 08:30:36 Rack:Tube:

Weight (g): 1 Volume (mL): 1 Dilution: 1

Analyte Results

Label	Solution Concentration	Unit	SD	%RSD	Intensity	Calculated Concentration
Al (396.152 nm)	0.07 m	ppm	0.01	12.19	511.04 m	0.07 m (ppm)
Mn (403.076 nm)	0.32	ppm	0.00	0.44	4360.90	0.32 (ppm)
V (437.923 nm)	0.03 m	ppm	0.00	9.01	210.30 m	0.03 m (ppm)
Ba (455.403 nm)	0.82	ppm	0.00	0.56	20847.07	0.82 (ppm)
Tl (535.046 nm)	-61.46 u	ppm	0.41	0.66	-85874.74	-61.46 u (ppm)

Replicates Concentration

Label	Replicate 1	Replicate 2	Replicate 3	Units
Al (396.152 nm)	0.08 m	0.07 m	0.06 m	ppm
Mn (403.076 nm)	0.32	0.32	0.32	ppm
V (437.923 nm)	0.03 m	0.03 m	0.03 m	ppm
Ba (455.403 nm)	0.82	0.83	0.82	ppm
Tl (535.046 nm)	-61.02 u	-61.83 u	-61.52 u	ppm

Replicates Intensity

Label	Replicate 1 (c/s)	Replicate 2 (c/s)	Replicate 3 (c/s)
Al (396.152 nm)	581.58 m	486.22 m	465.33 m
Mn (403.076 nm)	4339.13	4374.98	4368.60
V (437.923 nm)	230.97 m	202.42 m	197.50 m
Ba (455.403 nm)	20880.44	20945.04	20715.73
Tl (535.046 nm)	-85270.05	-86391.68	-85962.49

Sample Name: Sample 31

Date: 02/11/2023 08:32:31 Rack:Tube:

Weight (g): 1 Volume (mL): 1 Dilution: 1

Analyte Results

Label	Solution Concentration	Unit	SD	%RSD	Intensity	Calculated Concentration
Al (396.152 nm)	3.60	ppm	0.03	0.71	26070.70	3.60 (ppm)
Mn (403.076 nm)	0.68	ppm	0.00	0.53	9240.24	0.68 (ppm)
V (437.923 nm)	0.08 m	ppm	0.01	16.52	524.67 m	0.08 m (ppm)
Ba (455.403 nm)	2.14	ppm	0.00	0.10	56288.51	2.14 (ppm)
Tl (535.046 nm)	-298.88 u	ppm	0.94	0.31	-417635.35	-298.88 u (ppm)

Replicates Concentration

Label	Replicate 1	Replicate 2	Replicate 3	Units
Al (396.152 nm)	3.59	3.57	3.62	ppm
Mn (403.076 nm)	0.67	0.68	0.68	ppm
V (437.923 nm)	0.09 m	0.07 m	0.07 m	ppm
Ba (455.403 nm)	2.15	2.15	2.14	ppm
Tl (535.046 nm)	-299.90 u	-298.06 u	-298.69 u	ppm

Replicates Intensity

Label	Replicate 1 (c/s)	Replicate 2 (c/s)	Replicate 3 (c/s)
Al (396.152 nm)	26060.41	25891.35	26260.34
Mn (403.076 nm)	9193.99	9235.44	9291.27
V (437.923 nm)	621.10 m	492.55 m	460.37 m
Ba (455.403 nm)	56329.14	56313.82	56222.57
Tl (535.046 nm)	-419058.08	-416486.44	-417361.53

Sample Name: Sample 32

Date: 02/11/2023 08:35:13 Rack:Tube:

Weight (g): 1 Volume (mL): 1 Dilution: 1

Analyte Results

Label	Solution Concentration	Unit	SD	%RSD	Intensity	Calculated Concentration
Al (396.152 nm)	14.40 o	ppm	0.03	0.21	104381.04	14.40 o (ppm)
Mn (403.076 nm)	1.95	ppm	0.01	0.75	26583.79	1.95 (ppm)
V (437.923 nm)	0.09 m	ppm	0.01	8.98	628.65 m	0.09 m (ppm)
Ba (455.403 nm)	2.23	ppm	0.00	0.12	58608.79	2.23 (ppm)
Tl (535.046 nm)	-227.44 u	ppm	1.25	0.55	-317801.51	-227.44 u (ppm)

Replicates Concentration

Label	Replicate 1	Replicate 2	Replicate 3	Units
Al (396.152 nm)	14.37 o	14.40 o	14.43 o	ppm
Mn (403.076 nm)	1.94	1.94	1.97	ppm
V (437.923 nm)	0.10 m	0.09 m	0.08 m	ppm
Ba (455.403 nm)	2.23	2.23	2.23	ppm
Tl (535.046 nm)	-228.23 u	-228.08 u	-226.00 u	ppm

Replicates Intensity

Label	Replicate 1 (c/s)	Replicate 2 (c/s)	Replicate 3 (c/s)
Al (396.152 nm)	104164.20	104373.58	104605.35
Mn (403.076 nm)	26449.31	26489.78	26812.30
V (437.923 nm)	692.05 m	605.71 m	588.20 m
Ba (455.403 nm)	58554.00	58575.81	58696.55
Tl (535.046 nm)	-318904.63	-318706.15	-315793.76

Sample Name: Sample 33

Date: 02/11/2023 08:36:55 Rack:Tube:

Weight (g): 1 Volume (mL): 1 Dilution: 1

Analyte Results

Label	Solution Concentration	Unit	SD	%RSD	Intensity	Calculated Concentration
Al (396.152 nm)	1.26	ppm	0.00	0.19	9143.59	1.26 (ppm)
Mn (403.076 nm)	0.15	ppm	0.00	1.10	2014.22	0.15 (ppm)
V (437.923 nm)	0.04 m	ppm	0.01	18.32	259.67 m	0.04 m (ppm)
Ba (455.403 nm)	1.52	ppm	0.00	0.28	39137.60	1.52 (ppm)
Tl (535.046 nm)	-72.50 u	ppm	0.41	0.56	-101307.76	-72.50 u (ppm)

Replicates Concentration

Label	Replicate 1	Replicate 2	Replicate 3	Units
Al (396.152 nm)	1.26	1.26	1.26	ppm
Mn (403.076 nm)	0.15	0.15	0.15	ppm
V (437.923 nm)	0.04 m	0.03 m	0.03 m	ppm
Ba (455.403 nm)	1.52	1.51	1.52	ppm
Tl (535.046 nm)	-72.55 u	-72.88 u	-72.07 u	ppm

Replicates Intensity

Label	Replicate 1 (c/s)	Replicate 2 (c/s)	Replicate 3 (c/s)
Al (396.152 nm)	9151.90	9155.23	9123.63
Mn (403.076 nm)	1989.33	2021.15	2032.17
V (437.923 nm)	310.69 m	246.19 m	222.13 m
Ba (455.403 nm)	39213.51	39007.18	39192.10
Tl (535.046 nm)	-101375.90	-101836.55	-100710.82

Sample Name: Sample 34

Date: 02/11/2023 08:38:32 Rack:Tube:

Weight (g): 1 Volume (mL): 1 Dilution: 1

Analyte Results

Label	Solution Concentration	Unit	SD	%RSD	Intensity	Calculated Concentration
Al (396.152 nm)	5.20	ppm	0.02	0.46	37720.78	5.20 (ppm)
Mn (403.076 nm)	0.30	ppm	0.00	0.73	4021.93	0.30 (ppm)
V (437.923 nm)	0.06 m	ppm	0.01	13.20	442.45 m	0.06 m (ppm)

Label	Solution Concentration	Unit	SD	%RSD	Intensity	Calculated Concentration
Ba (455.403 nm)	2.57	ppm	0.01	0.25	68297.81	2.57 (ppm)
Tl (535.046 nm)	-160.15 u	ppm	1.02	0.64	-223777.05	-160.15 u (ppm)

Replicates Concentration

Label	Replicate 1	Replicate 2	Replicate 3	Units
Al (396.152 nm)	5.23	5.18	5.20	ppm
Mn (403.076 nm)	0.29	0.30	0.29	ppm
V (437.923 nm)	0.07 m	0.06 m	0.06 m	ppm
Ba (455.403 nm)	2.58	2.57	2.56	ppm
Tl (535.046 nm)	-159.74 u	-161.30 u	-159.39 u	ppm

Replicates Intensity

Label	Replicate 1 (c/s)	Replicate 2 (c/s)	Replicate 3 (c/s)
Al (396.152 nm)	37911.27	37569.94	37681.12
Mn (403.076 nm)	4000.17	4055.69	4009.94
V (437.923 nm)	507.49 m	419.29 m	400.57 m
Ba (455.403 nm)	68443.28	68361.17	68088.96
Tl (535.046 nm)	-223212.70	-225393.93	-222724.53

Sample Name: Sample 35

Date: 02/11/2023 08:40:20 Rack:Tube:

Weight (g): 1 Volume (mL): 1 Dilution: 1

Analyte Results

Label	Solution Concentration	Unit	SD	%RSD	Intensity	Calculated Concentration
Al (396.152 nm)	4.08	ppm	0.02	0.53	29600.53	4.08 (ppm)
Mn (403.076 nm)	0.48	ppm	0.00	0.28	6568.88	0.48 (ppm)
V (437.923 nm)	0.07 m	ppm	0.01	8.43	472.93 m	0.07 m (ppm)
Ba (455.403 nm)	1.68	ppm	0.00	0.29	43582.30	1.68 (ppm)
Tl (535.046 nm)	-176.56 u	ppm	1.23	0.70	-246711.82	-176.56 u (ppm)

Replicates Concentration

Label	Replicate 1	Replicate 2	Replicate 3	Units
Al (396.152 nm)	4.06	4.10	4.09	ppm
Mn (403.076 nm)	0.48	0.48	0.48	ppm
V (437.923 nm)	0.07 m	0.06 m	0.07 m	ppm

Label	Replicate 1	Replicate 2	Replicate 3	Units
Ba (455.403 nm)	1.68	1.68	1.68	ppm
Tl (535.046 nm)	-177.02 u	-175.17 u	-177.49 u	ppm

Replicates Intensity

Label	Replicate 1 (c/s)	Replicate 2 (c/s)	Replicate 3 (c/s)
Al (396.152 nm)	29429.50	29736.39	29635.70
Mn (403.076 nm)	6584.87	6549.22	6572.55
V (437.923 nm)	517.91 m	447.91 m	452.97 m
Ba (455.403 nm)	43641.91	43431.94	43673.05
Tl (535.046 nm)	-247349.94	-244767.43	-248018.09

Sample Name: Sample 36

Date: 02/11/2023 08:42:10 Rack:Tube:

Weight (g): 1 Volume (mL): 1 Dilution: 1

Analyte Results

Label	Solution Concentration	Unit	SD	%RSD	Intensity	Calculated Concentration
Al (396.152 nm)	4.39	ppm	0.03	0.78	31845.63	4.39 (ppm)
Mn (403.076 nm)	0.36	ppm	0.00	0.52	4897.41	0.36 (ppm)
V (437.923 nm)	0.06 m	ppm	0.00	6.78	398.44 m	0.06 m (ppm)
Ba (455.403 nm)	1.80	ppm	0.01	0.47	46680.93	1.80 (ppm)
Tl (535.046 nm)	-133.42 u	ppm	0.25	0.18	-186437.97	-133.42 u (ppm)

Replicates Concentration

Label	Replicate 1	Replicate 2	Replicate 3	Units
Al (396.152 nm)	4.37	4.38	4.43	ppm
Mn (403.076 nm)	0.36	0.36	0.36	ppm
V (437.923 nm)	0.06 m	0.06 m	0.05 m	ppm
Ba (455.403 nm)	1.79	1.80	1.79	ppm
Tl (535.046 nm)	-133.59 u	-133.54 u	-133.14 u	ppm

Replicates Intensity

Label	Replicate 1 (c/s)	Replicate 2 (c/s)	Replicate 3 (c/s)
Al (396.152 nm)	31647.81	31765.29	32123.80
Mn (403.076 nm)	4924.92	4875.13	4892.19

Label	Replicate 1 (c/s)	Replicate 2 (c/s)	Replicate 3 (c/s)
V (437.923 nm)	427.47 m	391.77 m	376.08 m
Ba (455.403 nm)	46542.28	46948.29	46552.21
Tl (535.046 nm)	-186666.73	-186603.25	-186043.91

Sample Name: Sample 37

Date: 02/11/2023 08:43:56 Rack:Tube:

Weight (g): 1 Volume (mL): 1 Dilution: 1

Analyte Results

Label	Solution Concentration	Unit	SD	%RSD	Intensity	Calculated Concentration
Al (396.152 nm)	1.71	ppm	0.02	0.94	12363.18	1.71 (ppm)
Mn (403.076 nm)	0.20	ppm	0.00	0.37	2771.38	0.20 (ppm)
V (437.923 nm)	0.04 m	ppm	0.00	10.47	299.83 m	0.04 m (ppm)
Ba (455.403 nm)	2.67	ppm	0.02	0.68	70942.37	2.67 (ppm)
Tl (535.046 nm)	-105.91 u	ppm	0.37	0.35	-147993.91	-105.91 u (ppm)

Replicates Concentration

Label	Replicate 1	Replicate 2	Replicate 3	Units
Al (396.152 nm)	1.71	1.69	1.72	ppm
Mn (403.076 nm)	0.20	0.20	0.20	ppm
V (437.923 nm)	0.05 m	0.04 m	0.04 m	ppm
Ba (455.403 nm)	2.64	2.67	2.68	ppm
Tl (535.046 nm)	-106.01 u	-106.23 u	-105.50 u	ppm

Replicates Intensity

Label	Replicate 1 (c/s)	Replicate 2 (c/s)	Replicate 3 (c/s)
Al (396.152 nm)	12413.32	12230.40	12445.80
Mn (403.076 nm)	2781.94	2761.68	2770.53
V (437.923 nm)	334.77 m	284.99 m	279.74 m
Ba (455.403 nm)	70352.57	71177.60	71296.94
Tl (535.046 nm)	-148129.27	-148436.92	-147415.53

Sample Name: Sample 38

Date: 02/11/2023 08:45:38 Rack:Tube:

Weight (g): 1 Volume (mL): 1 Dilution: 1

Analyte Results

Label	Solution Concentration	Unit	SD	%RSD	Intensity	Calculated Concentration
Al (396.152 nm)	2.40	ppm	0.02	1.00	17367.97	2.40 (ppm)
Mn (403.076 nm)	0.41	ppm	0.00	0.75	5514.92	0.41 (ppm)
V (437.923 nm)	0.06 m	ppm	0.01	11.31	414.17 m	0.06 m (ppm)
Ba (455.403 nm)	1.93	ppm	0.00	0.25	50365.25	1.93 (ppm)
Tl (535.046 nm)	-147.22 u	ppm	1.53	1.04	-205710.34	-147.22 u (ppm)

Replicates Concentration

Label	Replicate 1	Replicate 2	Replicate 3	Units
Al (396.152 nm)	2.37	2.42	2.39	ppm
Mn (403.076 nm)	0.41	0.41	0.40	ppm
V (437.923 nm)	0.07 m	0.06 m	0.06 m	ppm
Ba (455.403 nm)	1.93	1.94	1.93	ppm
Tl (535.046 nm)	-146.64 u	-146.06 u	-148.95 u	ppm

Replicates Intensity

Label	Replicate 1 (c/s)	Replicate 2 (c/s)	Replicate 3 (c/s)
Al (396.152 nm)	17201.51	17548.84	17353.56
Mn (403.076 nm)	5535.63	5541.92	5467.20
V (437.923 nm)	466.84 m	384.55 m	391.12 m
Ba (455.403 nm)	50326.24	50511.64	50257.85
Tl (535.046 nm)	-204904.64	-204094.78	-208131.60

Sample Name: Sample 39

Date: 02/11/2023 08:47:52 Rack:Tube:

Weight (g): 1 Volume (mL): 1 Dilution: 1

Analyte Results

Label	Solution Concentration	Unit	SD	%RSD	Intensity	Calculated Concentration
Al (396.152 nm)	1.83	ppm	0.00	0.16	13231.52	1.83 (ppm)
Mn (403.076 nm)	0.41	ppm	0.00	0.10	5568.62	0.41 (ppm)
V (437.923 nm)	0.04 m	ppm	0.01	11.96	313.79 m	0.04 m (ppm)
Ba (455.403 nm)	2.47	ppm	0.01	0.49	65477.71	2.47 (ppm)
Tl (535.046 nm)	-88.47 u	ppm	0.53	0.60	-123617.75	-88.47 u (ppm)

Replicates Concentration

Label	Replicate 1	Replicate 2	Replicate 3	Units
Al (396.152 nm)	1.83	1.83	1.82	ppm
Mn (403.076 nm)	0.41	0.41	0.41	ppm
V (437.923 nm)	0.05 m	0.04 m	0.04 m	ppm
Ba (455.403 nm)	2.48	2.46	2.47	ppm
Tl (535.046 nm)	-88.06 u	-89.07 u	-88.27 u	ppm

Replicates Intensity

Label	Replicate 1 (c/s)	Replicate 2 (c/s)	Replicate 3 (c/s)
Al (396.152 nm)	13251.28	13233.43	13209.86
Mn (403.076 nm)	5571.60	5572.34	5561.92
V (437.923 nm)	352.77 m	280.75 m	307.83 m
Ba (455.403 nm)	65813.52	65129.40	65490.21
Tl (535.046 nm)	-123048.68	-124460.48	-123344.09

Sample Name: Sample 40

Date: 02/11/2023 08:49:31 Rack:Tube:

Weight (g): 1 Volume (mL): 1 Dilution: 1

Analyte Results

Label	Solution Concentration	Unit	SD	%RSD	Intensity	Calculated Concentration
Al (396.152 nm)	1.49	ppm	0.01	0.81	10833.45	1.49 (ppm)
Mn (403.076 nm)	0.38	ppm	0.00	0.38	5195.76	0.38 (ppm)
V (437.923 nm)	0.06 m	ppm	0.01	8.82	426.71 m	0.06 m (ppm)
Ba (455.403 nm)	1.92	ppm	0.01	0.52	50013.43	1.92 (ppm)
Tl (535.046 nm)	-117.29 u	ppm	1.16	0.99	-163886.84	-117.29 u (ppm)

Replicates Concentration

Label	Replicate 1	Replicate 2	Replicate 3	Units
Al (396.152 nm)	1.50	1.50	1.48	ppm
Mn (403.076 nm)	0.38	0.38	0.38	ppm
V (437.923 nm)	0.07 m	0.06 m	0.06 m	ppm
Ba (455.403 nm)	1.92	1.92	1.91	ppm
Tl (535.046 nm)	-118.16 u	-117.74 u	-115.96 u	ppm

Replicates Intensity

Label	Replicate 1 (c/s)	Replicate 2 (c/s)	Replicate 3 (c/s)
Al (396.152 nm)	10866.91	10899.08	10734.35
Mn (403.076 nm)	5189.05	5218.28	5179.96
V (437.923 nm)	469.14 m	407.33 m	403.66 m
Ba (455.403 nm)	50195.57	50146.55	49698.16
Tl (535.046 nm)	-165104.43	-164515.16	-162040.91

Sample Name: Sample 41

Date: 02/11/2023 08:51:14 Rack:Tube:

Weight (g): 1 Volume (mL): 1 Dilution: 1

Analyte Results

Label	Solution Concentration	Unit	SD	%RSD	Intensity	Calculated Concentration
Al (396.152 nm)	2.08	ppm	0.01	0.28	15063.18	2.08 (ppm)
Mn (403.076 nm)	0.50	ppm	0.00	0.89	6762.86	0.50 (ppm)
V (437.923 nm)	0.08 m	ppm	0.01	10.93	535.03 m	0.08 m (ppm)
Ba (455.403 nm)	1.50	ppm	0.00	0.08	38620.28	1.50 (ppm)
Tl (535.046 nm)	-229.17 u	ppm	3.00	1.31	-320218.71	-229.17 u (ppm)

Replicates Concentration

Label	Replicate 1	Replicate 2	Replicate 3	Units
Al (396.152 nm)	2.07	2.08	2.08	ppm
Mn (403.076 nm)	0.50	0.49	0.49	ppm
V (437.923 nm)	0.09 m	0.07 m	0.07 m	ppm
Ba (455.403 nm)	1.50	1.50	1.50	ppm
Tl (535.046 nm)	-231.82 u	-225.91 u	-229.77 u	ppm

Replicates Intensity

Label	Replicate 1 (c/s)	Replicate 2 (c/s)	Replicate 3 (c/s)
Al (396.152 nm)	15014.73	15088.44	15086.37
Mn (403.076 nm)	6831.89	6723.78	6732.91
V (437.923 nm)	600.89 m	508.63 m	495.56 m
Ba (455.403 nm)	38582.15	38644.97	38633.72
Tl (535.046 nm)	-323923.45	-315669.12	-321063.57

Sample Name: Sample 42

Date: 02/11/2023 08:52:55 Rack:Tube:

Weight (g): 1 Volume (mL): 1 Dilution: 1

Analyte Results

Label	Solution Concentration	Unit	SD	%RSD	Intensity	Calculated Concentration
Al (396.152 nm)	5.55	ppm	0.04	0.66	40246.98	5.55 (ppm)
Mn (403.076 nm)	0.70	ppm	0.00	0.54	9497.04	0.70 (ppm)
V (437.923 nm)	0.06 m	ppm	0.00	8.86	385.96 m	0.06 m (ppm)
Ba (455.403 nm)	1.24	ppm	0.00	0.12	31744.92	1.24 (ppm)
Tl (535.046 nm)	-112.25 u	ppm	0.73	0.65	-156844.82	-112.25 u (ppm)

Replicates Concentration

Label	Replicate 1	Replicate 2	Replicate 3	Units
Al (396.152 nm)	5.56	5.59	5.51	ppm
Mn (403.076 nm)	0.69	0.70	0.70	ppm
V (437.923 nm)	0.06 m	0.05 m	0.05 m	ppm
Ba (455.403 nm)	1.24	1.24	1.24	ppm
Tl (535.046 nm)	-112.28 u	-112.96 u	-111.50 u	ppm

Replicates Intensity

Label	Replicate 1 (c/s)	Replicate 2 (c/s)	Replicate 3 (c/s)
Al (396.152 nm)	40268.91	40500.59	39971.43
Mn (403.076 nm)	9437.85	9531.99	9521.29
V (437.923 nm)	421.40 m	381.18 m	355.29 m
Ba (455.403 nm)	31710.18	31737.61	31786.96
Tl (535.046 nm)	-156889.97	-157843.03	-155801.47

Sample Name: Sample 43

Date: 02/11/2023 08:54:32 Rack:Tube:

Weight (g): 1 Volume (mL): 1 Dilution: 1

Analyte Results

Label	Solution Concentration	Unit	SD	%RSD	Intensity	Calculated Concentration
Al (396.152 nm)	2.18	ppm	0.00	0.11	15773.95	2.18 (ppm)
Mn (403.076 nm)	0.45	ppm	0.00	0.61	6141.15	0.45 (ppm)
V (437.923 nm)	0.07 m	ppm	0.01	10.65	466.77 m	0.07 m (ppm)
Ba (455.403 nm)	1.10	ppm	0.00	0.37	28124.63	1.10 (ppm)
Tl (535.046 nm)	-153.35 u	ppm	1.31	0.86	-214279.75	-153.35 u (ppm)

Replicates Concentration

Label	Replicate 1	Replicate 2	Replicate 3	Units
Al (396.152 nm)	2.18	2.17	2.18	ppm
Mn (403.076 nm)	0.45	0.45	0.45	ppm
V (437.923 nm)	0.08 m	0.06 m	0.06 m	ppm
Ba (455.403 nm)	1.10	1.10	1.10	ppm
Tl (535.046 nm)	-154.47 u	-153.68 u	-151.90 u	ppm

Replicates Intensity

Label	Replicate 1 (c/s)	Replicate 2 (c/s)	Replicate 3 (c/s)
Al (396.152 nm)	15788.53	15753.77	15779.55
Mn (403.076 nm)	6133.55	6108.20	6181.71
V (437.923 nm)	522.88 m	435.97 m	441.45 m
Ba (455.403 nm)	28196.96	28176.62	28000.31
Tl (535.046 nm)	-215844.76	-214737.35	-212257.15

Sample Name: Sample 44

Date: 02/11/2023 08:56:16 Rack:Tube:

Weight (g): 1 Volume (mL): 1 Dilution: 1

Analyte Results

Label	Solution Concentration	Unit	SD	%RSD	Intensity	Calculated Concentration
Al (396.152 nm)	2.06	ppm	0.01	0.67	14905.75	2.06 (ppm)
Mn (403.076 nm)	0.26	ppm	0.00	0.71	3530.12	0.26 (ppm)
V (437.923 nm)	0.05 m	ppm	0.00	8.84	373.80 m	0.05 m (ppm)
Ba (455.403 nm)	1.91	ppm	0.01	0.42	49880.15	1.91 (ppm)
Tl (535.046 nm)	-117.22 u	ppm	0.97	0.83	-163795.00	-117.22 u (ppm)

Replicates Concentration

Label	Replicate 1	Replicate 2	Replicate 3	Units
Al (396.152 nm)	2.05	2.07	2.04	ppm
Mn (403.076 nm)	0.26	0.26	0.26	ppm
V (437.923 nm)	0.06 m	0.05 m	0.05 m	ppm
Ba (455.403 nm)	1.92	1.92	1.90	ppm
Tl (535.046 nm)	-117.85 u	-117.71 u	-116.10 u	ppm

Replicates Intensity

Label	Replicate 1 (c/s)	Replicate 2 (c/s)	Replicate 3 (c/s)
Al (396.152 nm)	14881.50	15014.75	14821.01
Mn (403.076 nm)	3558.71	3521.03	3510.63
V (437.923 nm)	409.31 m	365.54 m	346.55 m
Ba (455.403 nm)	50001.00	50013.81	49625.64
Tl (535.046 nm)	-164682.13	-164474.40	-162228.48

Sample Name: Sample 45

Date: 02/11/2023 08:57:56 Rack:Tube:

Weight (g): 1 Volume (mL): 1 Dilution: 1

Analyte Results

Label	Solution Concentration	Unit	SD	%RSD	Intensity	Calculated Concentration
Al (396.152 nm)	1.88	ppm	0.02	1.23	13633.12	1.88 (ppm)
Mn (403.076 nm)	0.41	ppm	0.00	0.80	5631.05	0.41 (ppm)
V (437.923 nm)	0.06 m	ppm	0.00	8.61	397.90 m	0.06 m (ppm)

Label	Solution Concentration	Unit	SD	%RSD	Intensity	Calculated Concentration
Ba (455.403 nm)	1.63	ppm	0.01	0.33	42139.65	1.63 (ppm)
Tl (535.046 nm)	-97.54 u	ppm	1.07	1.10	-136301.87	-97.54 u (ppm)

Replicates Concentration

Label	Replicate 1	Replicate 2	Replicate 3	Units
Al (396.152 nm)	1.86	1.88	1.91	ppm
Mn (403.076 nm)	0.42	0.41	0.41	ppm
V (437.923 nm)	0.06 m	0.05 m	0.05 m	ppm
Ba (455.403 nm)	1.63	1.62	1.63	ppm
Tl (535.046 nm)	-97.07 u	-98.77 u	-96.79 u	ppm

Replicates Intensity

Label	Replicate 1 (c/s)	Replicate 2 (c/s)	Replicate 3 (c/s)
Al (396.152 nm)	13480.84	13605.15	13813.37
Mn (403.076 nm)	5668.88	5580.87	5643.38
V (437.923 nm)	436.07 m	374.00 m	383.62 m
Ba (455.403 nm)	42282.56	41996.24	42140.16
Tl (535.046 nm)	-135640.75	-138018.70	-135246.16

Sample Name: Sample 46

Date: 02/11/2023 08:59:37 Rack:Tube:

Weight (g): 1 Volume (mL): 1 Dilution: 1

Analyte Results

Label	Solution Concentration	Unit	SD	%RSD	Intensity	Calculated Concentration
Al (396.152 nm)	2.17	ppm	0.00	0.14	15737.89	2.17 (ppm)
Mn (403.076 nm)	0.32	ppm	0.00	0.73	4286.77	0.32 (ppm)
V (437.923 nm)	0.07 m	ppm	0.01	7.27	481.09 m	0.07 m (ppm)
Ba (455.403 nm)	2.28	ppm	0.00	0.21	60048.59	2.28 (ppm)
Tl (535.046 nm)	-151.20 u	ppm	0.71	0.47	-211278.83	-151.20 u (ppm)

Replicates Concentration

Label	Replicate 1	Replicate 2	Replicate 3	Units
Al (396.152 nm)	2.17	2.17	2.17	ppm
Mn (403.076 nm)	0.31	0.31	0.32	ppm
V (437.923 nm)	0.08 m	0.07 m	0.07 m	ppm

Label	Replicate 1	Replicate 2	Replicate 3	Units
Ba (455.403 nm)	2.28	2.28	2.28	ppm
Tl (535.046 nm)	-151.49 u	-150.39 u	-151.73 u	ppm

Replicates Intensity

Label	Replicate 1 (c/s)	Replicate 2 (c/s)	Replicate 3 (c/s)
Al (396.152 nm)	15713.88	15743.23	15756.56
Mn (403.076 nm)	4277.18	4261.48	4321.65
V (437.923 nm)	520.63 m	463.00 m	459.66 m
Ba (455.403 nm)	60200.75	59935.73	60009.30
Tl (535.046 nm)	-211677.41	-210148.46	-212010.63

Sample Name: Sample 47

Date: 02/11/2023 09:01:09 Rack:Tube:

Weight (g): 1 Volume (mL): 1 Dilution: 1

Analyte Results

Label	Solution Concentration	Unit	SD	%RSD	Intensity	Calculated Concentration
Al (396.152 nm)	0.67	ppm	0.01	1.77	4839.84	0.67 (ppm)
Mn (403.076 nm)	0.12	ppm	0.00	0.87	1668.19	0.12 (ppm)
V (437.923 nm)	0.04 m	ppm	0.00	7.60	266.25 m	0.04 m (ppm)
Ba (455.403 nm)	1.33	ppm	0.00	0.25	34041.28	1.33 (ppm)
Tl (535.046 nm)	-58.57 u	ppm	0.47	0.81	-81841.60	-58.57 u (ppm)

Replicates Concentration

Label	Replicate 1	Replicate 2	Replicate 3	Units
Al (396.152 nm)	0.66	0.68	0.67	ppm
Mn (403.076 nm)	0.12	0.12	0.12	ppm
V (437.923 nm)	0.04 m	0.04 m	0.04 m	ppm
Ba (455.403 nm)	1.32	1.33	1.33	ppm
Tl (535.046 nm)	-59.03 u	-58.58 u	-58.09 u	ppm

Replicates Intensity

Label	Replicate 1 (c/s)	Replicate 2 (c/s)	Replicate 3 (c/s)
Al (396.152 nm)	4760.56	4930.72	4828.24
Mn (403.076 nm)	1652.94	1669.52	1682.11

Label	Replicate 1 (c/s)	Replicate 2 (c/s)	Replicate 3 (c/s)
V (437.923 nm)	288.34 m	258.98 m	251.43 m
Ba (455.403 nm)	33940.99	34095.60	34087.25
Tl (535.046 nm)	-82492.33	-81861.08	-81171.41

Sample Name: Sample 48

Date: 02/11/2023 09:02:53 Rack:Tube:

Weight (g): 1 Volume (mL): 1 Dilution: 1

Analyte Results

Label	Solution Concentration	Unit	SD	%RSD	Intensity	Calculated Concentration
Al (396.152 nm)	0.65 m	ppm	0.01	1.71	4708.42 m	0.65 m (ppm)
Mn (403.076 nm)	0.49	ppm	0.00	0.45	6653.28	0.49 (ppm)
V (437.923 nm)	0.06 m	ppm	0.01	11.99	436.94 m	0.06 m (ppm)
Ba (455.403 nm)	2.83	ppm	0.01	0.24	75633.60	2.83 (ppm)
Tl (535.046 nm)	-154.02 u	ppm	2.16	1.40	-215217.60	-154.02 u (ppm)

Replicates Concentration

Label	Replicate 1	Replicate 2	Replicate 3	Units
Al (396.152 nm)	0.65 m	0.64 m	0.66 m	ppm
Mn (403.076 nm)	0.49	0.49	0.49	ppm
V (437.923 nm)	0.07 m	0.06 m	0.06 m	ppm
Ba (455.403 nm)	2.83	2.83	2.82	ppm
Tl (535.046 nm)	-151.68 u	-154.45 u	-155.93 u	ppm

Replicates Intensity

Label	Replicate 1 (c/s)	Replicate 2 (c/s)	Replicate 3 (c/s)
Al (396.152 nm)	4719.47 m	4623.18 m	4782.60 m
Mn (403.076 nm)	6679.18	6660.46	6620.22
V (437.923 nm)	495.44 m	415.31 m	400.06 m
Ba (455.403 nm)	75787.37	75701.95	75411.48
Tl (535.046 nm)	-211950.58	-215819.92	-217882.31